Reduction in Friction in Ironing of Aluminium Alloy and Stainless Steel Drawn Cups

(アルミニウム合金とステンレス鋼深絞り容器のしごき加工における摩擦の低減)

January, 2016

Doctor of Engineering

Witthaya Daodon

ウィッタヤ　ダオドン

Toyohashi University of Technology

Abstract

In Chapter 1, the general introduction for overall contents of this thesis is presented. Because of growing awareness of environmental protection, there is a requirement to reduce CO_2 emission from automobiles. The reduction in weight of automobiles and the technologies for electric and hybrid vehicles play an important role in reducing greenhouse gas emissions. The key component for electric and hybrid vehicles is batteries. Metal cups used as battery cases are produced by multi-stage stamping operations including deep drawing and ironing of stainless steel and aluminium alloy cup. Since ironing involves a high contact pressure and high speed, friction plays an important role in the success of the ironing process. Reduction in friction with low friction tool materials, lubrication and coating is presented.

In Chapter 2, a TiCN-based cermet die having low friction was applied to improve the limit in ironing of stainless steel and aluminium alloy drawn cups. In this cermet die, an additional surface coating is not required because it was made of hard TiCN having low friction without WC and Co. For all the stainless steel and aluminium alloy drawn cups, the cermet die exhibited the largest ironing limit for single ironing due to the low friction. For repeated ironing using the cermet die, the seizure was prevented up to 100 times.

In Chapter 3, the TiCN-based cermet dies having fine lubricant pockets made by lapping shot-peened surfaces were utilised to reduce friction in ironing of stainless steel and aluminium alloy drawn cups. The shape of the lubricant pockets was controlled to improve the ironing limit. The ironing limit was improved for the die having an appropriate surface shape of fine lubricant pockets. Friction was reduced by liquid lubricant squeezed out from the pockets during ironing, and the ironing load became smaller. The mechanism of the superior seizure resistance of the die having an appropriate surface shape was examined from the remaining amount of lubricant in ironed cups.

In Chapter 4, the conditions of the ironing process and lubrication for attaining low friction in ironing of stainless steel cups using the cermet die having fine lubricant pockets were investigated. The thickness of the remaining lubricant on the sidewall of the ironed cup was measured by mixing a fluorescence oil in the lubricant. When the amount of lubricant was sufficient and the ironing speed was high, the ironing load was lower than that of a die having a polished surface. In repeated ironing, the surface roughness of the ironed cup for the die having the lubricant pockets was almost constant.

In Chapter 5, the TiCN-based cermet die having fine lubricant pockets and roughening of drawn cup surface were utilised to reduce friction in ironing of stainless steel drawn cups. Sanding with emery papers, deep drawing with large clearance, and deep drawing including redrawing with a small die radius were employed to roughen the drawn cup surface. The effects of the sanding direction and the surface roughness of the cups having the roughened surface on the ironing limit were investigated. During ironing, the lubricant was trapped with the cups sanded in the circumferential direction and the ironing limit was higher than with the cup sanded in the axial direction. Friction in ironing was lowered by roughening of cup surface because the lubrication was enhanced.

In Chapter 6, the lubricants containing the fine particles were utilised to improve seizure resistance in ironing of aluminium alloy drawn cups. The effects of types and size of particles on the improvement of seizure resistance were investigated. The mixing lubricant with silica (SiO_2) particles having a size of 0.01 μm improves the seizure resistance. The good dispersion and suspension of the fine SiO_2 particles in the lubricant enhanced lubrication. The effect of different mixing quantities of fine SiO_2 particles in lubricants on the seizure resistance was examined. For a low viscosity lubricant, the fine SiO_2 particles had a little effect on increasing the ironing limit. The ironing limit was improved only with a large quantity of SiO_2. The seizure resistance was effectively improved by applying the high viscosity lubricant with the fine SiO_2 particles.

In Chapter 7, titanium nitride (TiN) and vanadium nitride (VN) coatings were deposited on high speed steel substrates by direct current magnetron sputtering to improve seizure resistance in ironing of aluminium alloy cups. Coating parameters were optimised to obtain phase compositions of TiN and VN. The coatings were characterised for phase composition using X-ray diffraction (XRD), hardness using nano-indentation and load-to-failure between the coating and substrate using scratch testing. Ring-on-disc testing was carried out to evaluate the tribological properties between aluminium alloy rings sliding against high speed steel discs with a lubricant. Finally, the coating which mainly had the superior tribological properties was further evaluated in ironing of an aluminium cup.

In Chapter 8, concluding remarks are presented and future perspectives for improving the seizure resistance are given.

Table of contents

List of figures

List of tables

Chapter 1
Introduction

1.1 Electric and hybrid vehicles

Because of growing awareness of environmental protection, there is a requirement to reduce the emission of carbon dioxide gas from automobiles. Alternative fuel vehicles play an important role in reducing greenhouse gas emissions [1]. Therefore, the demand for alternative fuel vehicles such as electric, hybrid and plug-in hybrid vehicles is increasing. In the electric vehicle, the electricity is supplied from external electric sources, stored in a battery on the vehicle and used in electric motors. The hybrid vehicle has the combination of an internal combustion engine and electric motors in its drive system, whereas the plug-in hybrid vehicles are hybrid which can be recharged from external electric sources. The structure of electric and hybrid vehicles is shown in **Fig. 1.1** [2].

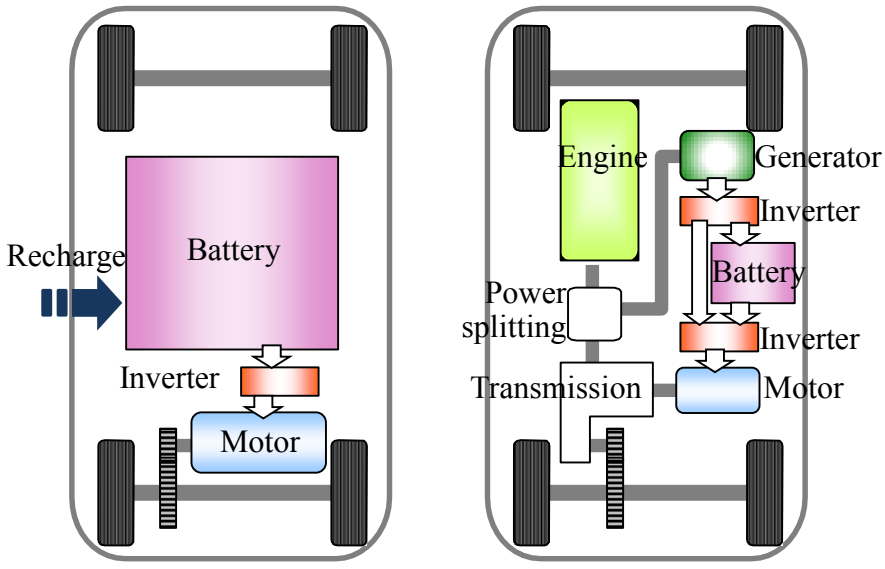

(a) Electric vehicles (b) Hybrid vehicles

Fig. 1.1 Structure of electric and hybrid vehicles [2].

The electric vehicles enable by high-efficiency electric motor and controller, and powered by alternative energy sources, provide the means for a clean, efficient and environmentally friendly urban transportation system. Electric vehicles have no emission

and therefore are capable of curbing the pollution problem in an efficient way. Consequently, electric vehicles are the only zero-emission vehicles possible. The limited range of the battery-powered electric vehicles led the researchers and auto industry players to search for alternatives. The aggressive efforts by the industry led to the rapid development of hybrid vehicles. The hybrid vehicles use both electric machines and an internal combustion engine for delivering the propulsion power. These vehicles have lower emissions compared to a similarly sized conventional internal combustion engine vehicles resulting in less environmental pollution [3]. The key component for electric and hybrid vehicles is the battery [4]. And thus batteries that have a high capacity are particularly desirable. In the battery, metal cups are used for electrolyte cases as shown in **Fig. 1.2**.

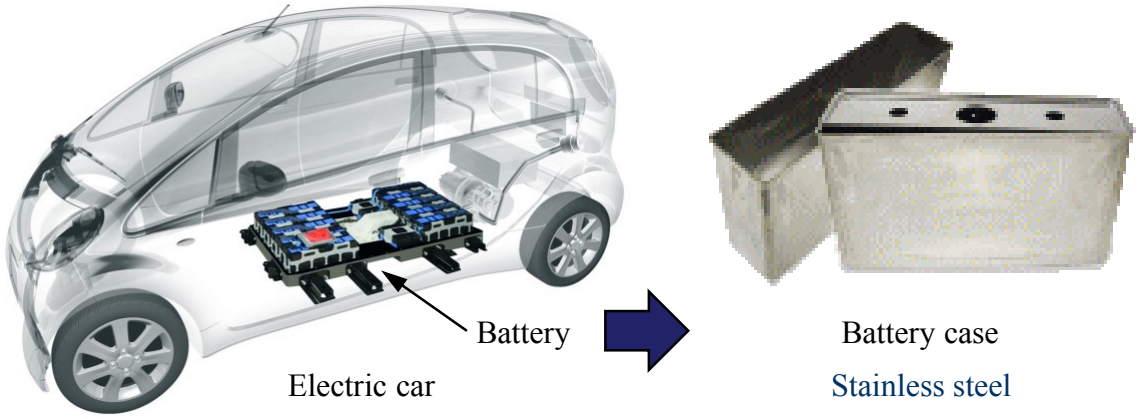

Fig. 1.2 Battery case for hybrid and electric vehicles.

1.2 Lightweight materials

For the electric car, the longer range of driving requires the larger battery size causing an increase in weight of the vehicle. Therefore the reduction in weight of battery and other parts has great influence on the energy efficiency of vehicles. Aluminium alloys and magnesium alloys offer a high potential for the reduction in weight of the automobile due to lightweight and high specific strength [5-7]. The density of the magnesium alloys is 1/4 time of the mild steels, but the specific strength of the magnesium alloys is 2.5 times more than the mild steels. Similarly, the density of the aluminium alloys is 3/8 time of the mild steels, but the specific strength of the aluminium alloys is 1.4 times more than the mild steel [8]. As the formability of aluminium and the magnesium alloys is low at room

temperature, the cold stamping process including deep drawing was developed to form magnesium alloy cups [9, 10].

1.3 Deep drawing and ironing of stainless steel and aluminium alloy sheets

Since cups with a large aspect ratio are required for battery cases, they are mainly produced by multi-stage stamping which includes the deep drawing and ironing of stainless steel and aluminium alloy sheets as shown in **Fig. 1.3**. To improve the process conditions, process modelling was applied to the deep drawing and ironing operations [11]. Aluminium alloy cups with an extreme aspect ratio are achieved by process design and a modification of the initial blank in multi-stage deep drawing [12].

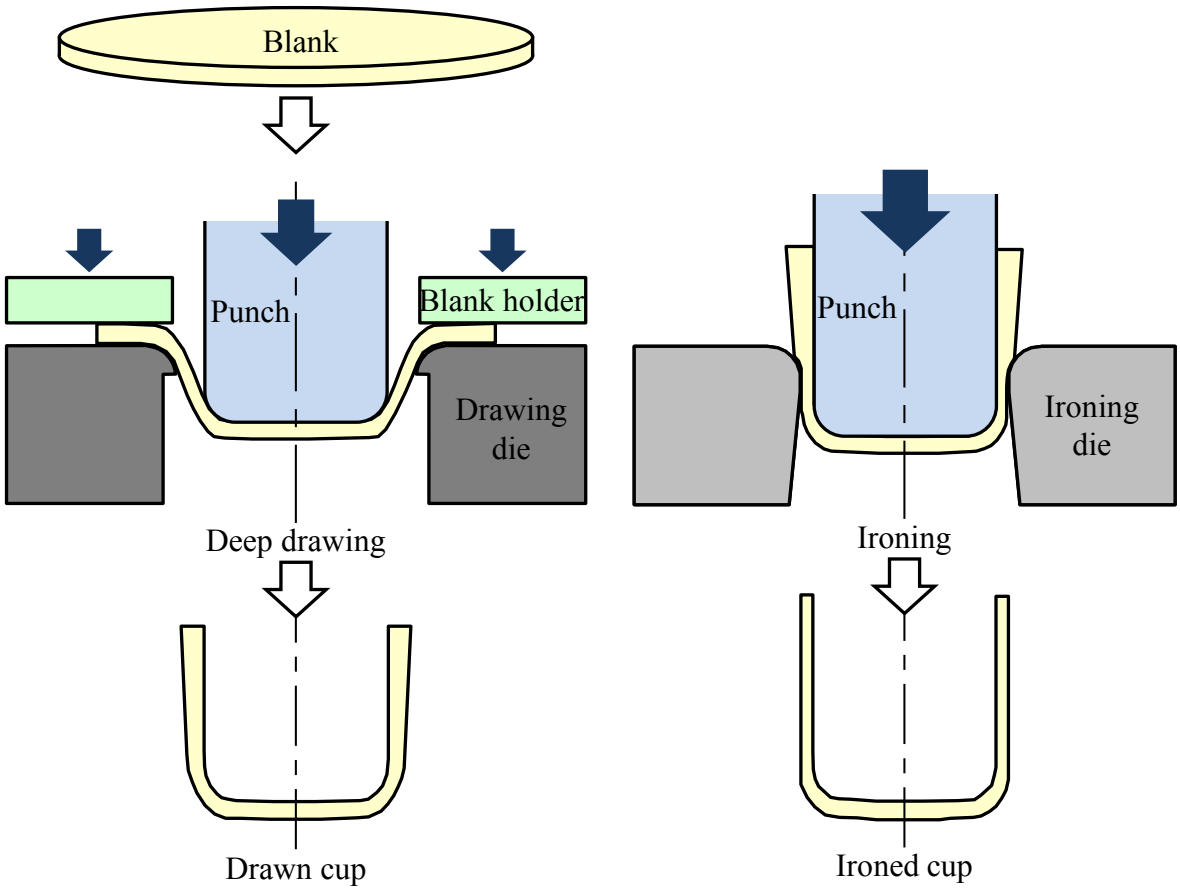

Fig. 1.3 Deep drawing and ironing processes.

Tool design for multi-stage deep drawing with ironing was carried out to obtain cups with a large aspect ratio with the aid of finite element analysis [13]. Ku et al. [14] introduced the tool design for the manufacturing of battery cases made from low-carbon steel (SPCC) sheets including an ironing process. The strength of the battery case such as its resistance to mechanical loading and accidental load is important for preventing the hazard associated with electrolyte spillage. The plasticity and fracture of the case of the lithium-ion cylindrical battery were characterised [15].

In recent years, more computational programs, based on finite element schemes, have been developed and used to study plastic deformation in sheet metal forming processes. The ironing process was analysed by taking work hardening into account in a slab method [16], and analysed with continuum elements in two dimensions in the finite element method [17]. Danckert [18] predicted the residual stress in the wall of the ironed cup. To attain high accuracy of the ironed products, the factors influencing the dimensions of the cups were analysed [19]. For the design of the ironing process with a high relative speed, the dynamic projection algorithm is more efficient and intrinsic than the penalty method [20]. Delarbre and Montmitonnet [21] discussed the maximum thickness reduction in the ironing of the stainless steel cup using a slab method and a finite element method. The geometry of the tools has an effect on the critical reduction in ironing of the stainless steel cup [22]. Therefore the basic process design of ironing has been established. However, the accuracy of the analysis for the design process is limited by the knowledge of boundary conditions, a good understanding of friction is crucial for improving the accuracy in the simulation of sheet metal forming processes.

Since ironing involves high contact normal stress and high relative speed, friction plays an important role in the success of the ironing process. A method for determining the friction coefficient in ironing was developed [23]. Due to the friction coefficient being influenced by tool geometry [24], the curved shape of the die inlet and the semi-cone angle of dies were optimised to minimise the deformation force in ironing [25]. Becker et al. [26] proposed an alternative approach to describe friction by modelling the geometric surface roughness of the tools. In the ironing of stainless steel cups, the fracture limit is affected by friction between the cup and the die [21]. Friction has a significant effect on formability in ironing.

To achieve high surface qualities in multi-stage stamping that includes deep drawing and ironing processes, the surface flattening mechanism in the ironing of aluminium cups was clarified and then the seizure is prevented by the appropriate viscosity of lubricants [27]. Mori et al. [28] utilised coloured sheets for the prevention of seizure in multi-stage deep drawing of long pure titanium cups. Furthermore, the inner surface of deep drawn stainless steel cups was improved by inner ironing [29].

1.4 Adhesive wear in deep drawing and ironing of aluminium alloy and stainless steel sheets

High friction occurring in an ironing process has a negative effect by raising the loads required for ironing. As the loads imposed on a die and cup are increased, die wear or cup fractures may increase. Since the ironing of stainless steel cups creates very severe tribological conditions due to their high strength and low thermal conductivity, adhesive wear has a tendency to occur as shown in **Fig. 1.4**. This wear is also found in the ironing of aluminium alloy cups because of their high adhesion. To optimise the ironing process, a substantial understanding of the occurrence of adhesive wear is essential [30, 31]. Groche and Nitzsche [32] investigated the influence of temperature on the initiation of adhesive wear in the deep drawing of aluminium alloy sheets. Adhesive wear is preferably initiated at the areas of highest mechanical and thermal stress. The initiation of adhesive wear is also a function of mechanical loads acting on local asperities.

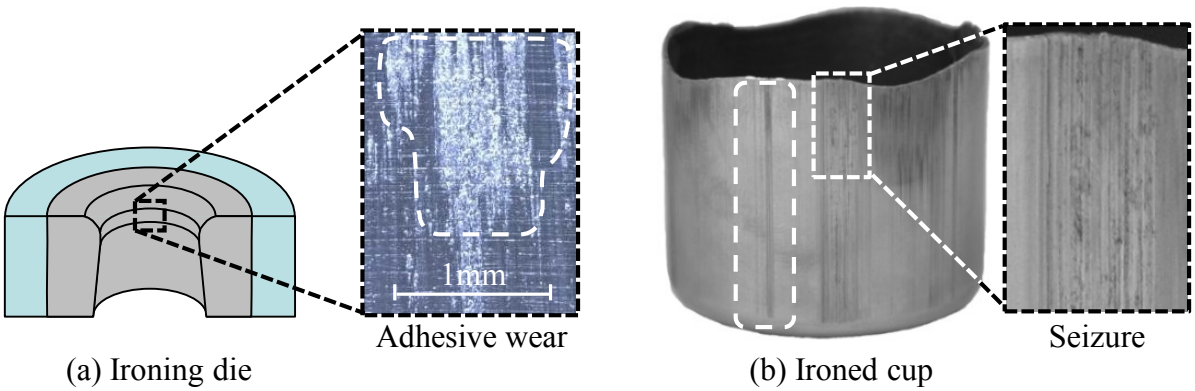

Fig. 1.4 Seizure in ironing of stainless steel cups.

Stainless steel and aluminium alloy develop a thin, hard adherent film of oxide on their surface that protects the metal from corrosion. In the deep drawing of aluminium, the oxide layers of sheets are cracked by local plastic deformation, which have been caused by high normal and shear stresses. Thus, the generating metallic contact determines local micro-welding. Due to the progressive relative movement between the sheet and die, the bonding is torn apart. The separation occurs inside the volume of the sheet material and thus initiates adhesive wear [33]. In more severe conditions, such as ironing with high loads and strongly bounded asperities, adhesive wear is described as scuffing, smearing, tearing, galling, or seizure. Since the proper use of lubricant is important for preventing seizure in ironing, a strip reduction test has been used to emulate the tribological conditions for screening the lubricant in ironing of stainless steel sheets [34]. Seizure is quantified by surface roughness measurements across the strip after testing. With increasing sliding length the tool becomes heated due to workpiece deformation and friction implying eventual breakdown of the lubricant film. Pre-heating of the tool results in earlier breakdown of the lubricant film [35]. An oil containing chlorinated paraffin is effective for the prevention of seizure in the forming of stainless steel sheets. The good lubrication performance of the oil containing chlorinated paraffin is attributed to the chemical activity of the chlorinated paraffin with all the main components of stainless steel. The oil containing chlorinated paraffin enforces the formation of a thick oxide layer [36]. However, chlorinated paraffin oils are not perceived to be environmentally friendly lubricants. Therefore, there has been increasing effort to develop environmentally benign lubricants suitable for metal forming and dry film solid lubricants is one of them. Various types of dry film solid lubricants were evaluated using deep drawing tests with increasing blank holding force. Dry film lubricants performed better than oil-based lubricants in the tests [37]. Kim et al. [38] reported that polymeric lubricants containing EP additives performed better than water emulsion and straight oil lubricants in deep drawing and ironing tests.

In an ironing operation, the reduction of friction has a beneficial effect by lowering the loads required for ironing. Because the loads acting on a die and cup are decreased, the occurrence of seizure on the die or the cup can be lowered. Friction can be reduced by selecting die materials that exhibit low friction (such as carbides, ceramics and cermets), by improving lubrication and applying coatings [39].

1.5 Reduction in friction with low friction die materials

Since tool wear in deep drawing and ironing is problematic in mass production, high friction, which causes seizure in these processes, needs to be reduced. The tendency to develop a seizure can be reduced by selecting dissimilar die-cup material structures, for example between non-metallic and metallic materials [40]. Therefore, low friction tool materials such as ceramics and cermets are applied.

Ceramics are compounds of metallic and non-metallic elements. Because they possess high hardness, good wear resistance, low thermal conductivity and low friction, ceramics have become increasingly important in tool and die materials [39]. Ceramic dies were applied to dry deep drawing for various sheet materials. For stainless steel SUS304 sheets, the limit drawing ratio was slightly improved with silicon carbide (SiC) and silicon nitride (Si_3N_4) ceramic dies. Whereas, an alumina (Al_2O_3) ceramic die gave very good results. The punch load was significantly reduced with the number of drawn cups [41]. Tamaoki et al. [42] proposed electro conductive ceramics which can be fabricated by using electric discharge machining (EDM) for dry deep drawing dies. Although mild steel sheets were deep drawn in a dry condition, the limiting drawing ratio (LDR) with a zirconia-based ceramic die reached the same level as lubricated deep drawing with a conventional tool steel die. The zirconia-based ceramic die showed a low tendency to galling and then the cups were successfully deep drawn over 10,000 times [43]. For the purpose of finding the most suitable die material for the lubricated deep drawing of stainless steel AISI 304 sheets, three different silicon nitride ceramics were evaluated with pin-on-disk tests as compared to hard coatings such as TiCN, WC/C and TiAlN coatings. The silicon nitride ceramic Si_3N_4 performed well [44]. However, it is not easy to apply the brittle ceramic die to the ironing of stainless steel cups.

Cermets are combinations of a ceramic phase bonded with a metallic phase. They combine the high-temperature oxidation resistance of ceramics with the toughness, thermal-shock resistance, and ductility of metals [39]. Advances in the synthesis of ultrafine/nano TiCN powders and the preparation of TiCN-based cermets enhance their hardness, toughness and wear resistance [45]. The fracture toughness and hardness of ultrafine grade TiCN-based cermets are considerably better than conventional coarse TiCN-based materials [46]. To develop materials having both a good hardness and a good toughness, the effects of the TiN addition and binder contents on the microstructure and

the properties of the TiC based cermets elaborated by pressureless sintering have been investigated. Toughness can be improved by the addition of a metallic binder. The rupture strength and the toughness increase with the addition of nickel. Consequently, cermets having both a good hardness and a good toughness can be produced [47]. The relationship between hardness and toughness of various tool materials is shown in **Fig. 1.5** [48]. In addition, a TiC-based cermet containing titanium nitride exhibits good tribological properties with a low friction coefficient [49]. A common application of cermets is in cutting tools. Bellosi et al. [50] evaluated the performance of developed TiCN-based tools used in the machining of carbon and quenched-tempered steel. The developed TiCN-based tools showed an improvement in machining performance compared to commercial tools. The TiCN-based cermet becomes more attractive for cutting tools because the cermet has excellent wear resistance [51, 52]. As the main component of the cermet is made of the low friction TiCN, an additional surface coating is not required. Therefore, the TiCN-based cermet is expected to be effective for improving the formability in the ironing of stainless steel and aluminium alloy drawn cups.

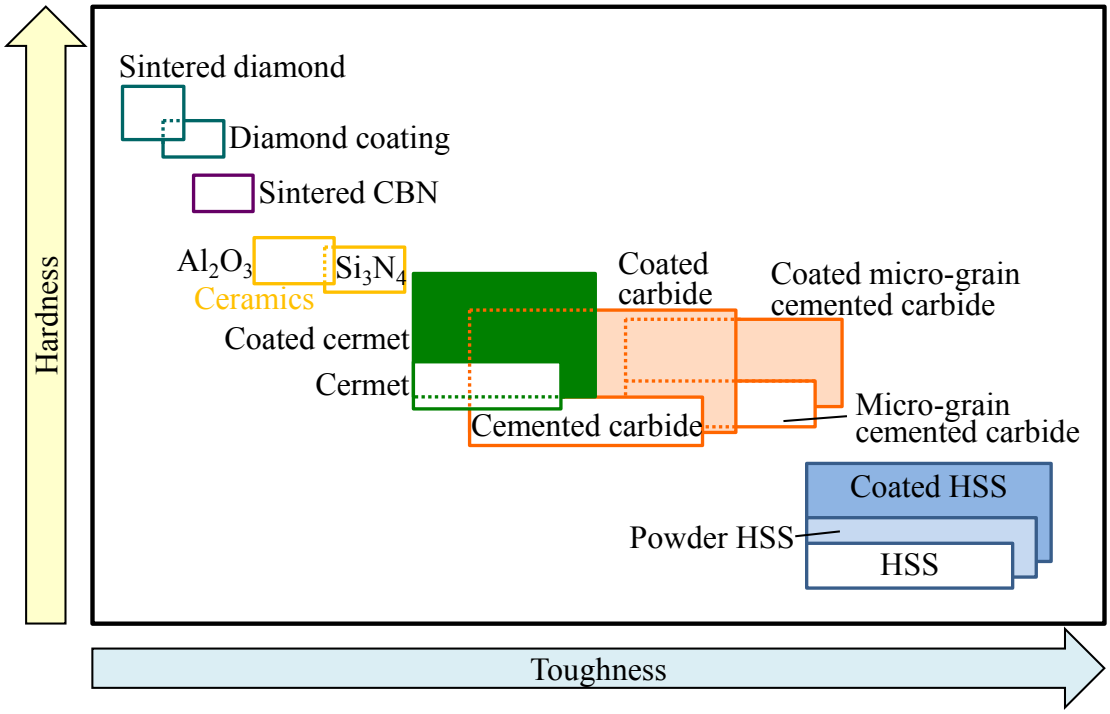

Fig. 1.5 Relationship between hardness and toughness of various tool materials [48].

1.6 Reduction in friction by improving lubrication

1.6.1 Reduction in friction by improving lubrication with roughening of sheet surface

Effective lubrication systems bring about lower friction levels. Liquid lubricants interpose an adherent film between the die and the cup. This film minimises the adhesion and interactions of the die surface with the other which increases die life by reducing wear and improves product quality by reducing the incidence of seizure and other surface defects [53]. Therefore, lubrication is vitally important in an ironing process.

The lubrication of interfacial surfaces during deformation is conventionally employed in ironing operations to reduce friction and to prevent the occurrence of seizure. Bay et al. [54] reviewed lubrication mechanisms in with ironing in sheet metal forming processes. In hydrostatic lubrication, a part of the normal contact load between the tool and workpiece is supported by the hydrostatic pressure of the trapped lubricant generated in fine pockets. In hydrodynamic lubrication, although the liquid pressure in the pockets is smaller than the sealing pressure on the surrounding asperities in contact with the tool, the hydrodynamic permeation of the trapped lubricant into the tool-workpiece interface develops the thin lubricant film as shown in **Fig. 1.6**. During forming, not only hydrostatic but also hydrodynamic lubrication occurs [55]. The occurrence of hydrodynamic lubrication in cold sheet drawing is influenced by the drawing speed, lubricant viscosity and die angle [56]. Micro-hydrodynamic lubrication, induced by the escape of the lubricant from the pockets, was directly observed through a transparent die in strip drawing. The degree of reduction, drawing speed and lubricant viscosity have an influence on the escape of lubricant from the pockets [57, 58]. Utilising the same direct observation technique, the effect of pocket geometry, lubricant viscosity, drawing speed and reduction on the entrapment and escape of liquid lubrication were investigated [59, 60]. The escape of trapped lubricants from pockets during strip drawing has an influence on drawing load [61].

Applying liquid lubricants, the workpiece surface topography has an influence on the improvement of the lubrication. Because a rough surface is able to provide small pits, the transporting of the trapped lubricant with plastic deformation of the workpiece to the tool-workpiece interface develops the thin lubricant film and then facilitates lubrication in the forming processes.

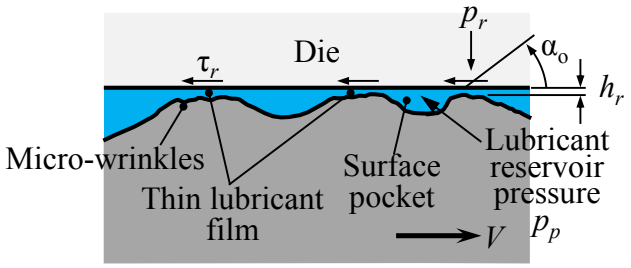

(a) Model of micro-plasto-hydrodynamic lubrication

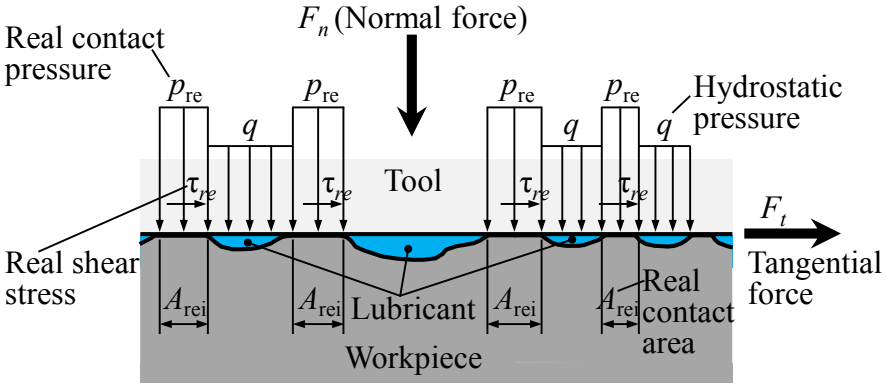

(b) Local pressure distribution

Fig. 1.6 Schematic outline of micro-plasto-hydrostatic lubrication and local pressure distribution [57].

Hence the sheet-surface structures providing a surface topography with lubricant pockets have been developed to improve the tribological conditions for sheet forming processes [62]. A rolling process with high productivity is generally utilised. The sheet-surface structure is transferred from a roll-surface structure in cold-rolling processes. The roll-surface texturing processes were discussed [63]. The structured sheet surface produced by the transferring of roller surfaces prepared by electron beam texturing in skin pass rolling was introduced to the deep drawing process. Because the lubrication is assisted during the process, the friction decreases with increases in drawing speed [64]. To clearly obtain the defined surface structure of the sheet in cold-rolling processes, the finite-element model was developed to simulate the transfer characteristics of the roll surface textured by electron-beam texturing [65]. The 3D surface parameters were developed to characterise the structured sheet surfaces with respect to their functional behaviour [66]. The structured stainless steel sheet significantly improved the lubrication performance with no sign of lubricant film breakdown in strip ironing and in deep drawing [67]. However,

the structured sheet surface does not function when it is completely flattened in a large deformation.

1.6.2 Reduction in friction by improving lubrication with die having lubricant pockets

On the other hand, the tool surface seldom changes. Applying texturing on the tool surface facilitates the forming process even after long-running use. Excimer laser radiation has been introduced to texture the surface of a TiN-coated punch for cold forging [68]. The pressurization of the entrapped lubricant in the well-designed micro pockets as shown in **Fig. 1.7** improves tool life [69]. During the process, tool wear is reduced by the lubricant wiped from micro pockets. In addition, tool life of the cold forging tool surface, locally structured by laser surface texturing, was enhanced because the tribological state is improved [70, 71]. Vilhena et al. [72] employed laser surface texturing to hardened bearing steel and the parameters of the laser surface texturing process were optimised. Well defined micro-dimples improved tribological behaviour [73]. In the drawing of stainless steel strip, the orientation of grooves on the die surface patterned by photochemical etching has effects on lubrication. Due to the presence of lubricant reservoirs and the encouragement of the micro-plasto hydrodynamic lubrication, probably caused by textured surface, lubrication is enhanced. Therefore, friction force is considerably reduced with grooves oriented perpendicularly to the drawing direction [74]. Meng et al. [75] exhibited friction can be reduced by using the laser textured tool having micro rectangle dimples with a flat bottom. Aramaki et al. [76] showed the die treated by the combination of shot-peening and nitriding improves seizure resistance in the drawing test of high strength steel sheets because of its lubricating effect. In addition, the die life in the drawing test of high strength steel sheets is improved by the combination of shot-peening and solid lubricant [77]. The seizure resistance of tool surfaces prepared by turning, grinding, polishing, shot-peening, and laser surface texturing were investigated. Polishing to remove sharp peaks on the bearing surface giving a plateau-like topography improves the seizure resistance of the forming tool [78].

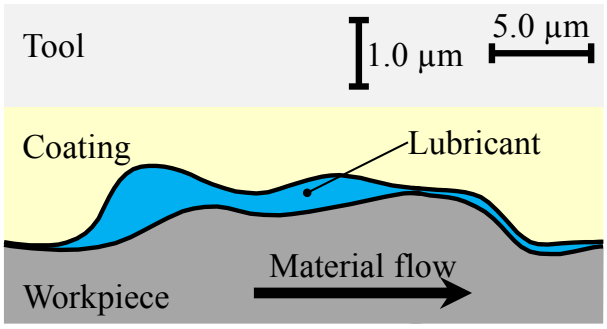

Fig. 1.7 Tool pocket profile and suggested lubrication mechanism [69].

With regard to reducing in friction by assisting in lubrication, the dies having fine lubricant pockets and the cups having a roughening surface being capable of retaining lubricant are able to minimise seizure.

1.6.3 Measurement of lubricant film

In ironing, liquid lubricants interpose an adherent film between the die and cup. This film minimises the adhesion and the interactions of the die surface with the other, thus reducing friction and preventing the direct die-to-cup contact. However, this lubricant film can break down. The sliding surfaces then may wear and score severely. Thus the behaviour of the liquid lubricant at the interfaces during ironing is important. For monitoring the state of lubrication in the machine elements, the transmission and reflection of ultrasonic waves were used to monitor the oil-films in shaft seals [79]. Ultrasonic reflection coefficient measurements were applied to monitor the oil-film thickness in a range of bearings [80-83]. Next, an apparatus incorporating an ultrasonic array was developed in which the accuracy of the measurement of the oil-film thickness distribution can be assessed [84]. However, this approach is still difficult to apply to forming processes with complex-shaped dies. Azushima et al. [85] developed the direct observation using a transparent die and fluorescence measurement method. The effect of the surface topography of a workpiece on the pressure dependence of the coefficient of friction in sheet metal forming was examined. This method was also employed to measure the oil film thickness at the interface between the tool and the workpiece in lubricated upsetting [86, 87].

1.7 Lubricant containing fine particles for improving seizure resistance

Effective lubrication systems result in low friction levels which reduce the load imposed on tooling and workpieces. Since the addition of nanoparticles into lubricating oil as lubricant additives significantly reduces the friction coefficient and increases the load-bearing capacity of the frictional parts in mechanical systems, the application of nanoparticles has attracted more attention. The use of titanium dioxide (TiO_2) nanoparticles as an oil additive in liquid paraffin exhibits good performance in friction and wear reduction as well as in load-carrying capacity. A boundary film mainly composed of TiO_2 and titanates is formed on the rubbed surfaces [88]. Suspensions of copper (Cu), copper oxide (CuO), zinc oxide (ZnO) or zirconium dioxide (ZrO_2) nanoparticles in the lubricants exhibits a reduction in friction and wear compared to the base oil. The anti-wear mechanism of nanoparticles is produced by the tribo-sintering of nanoparticles on the wear surfaces, reducing metal-to-metal contact and acting as load-bearing areas [89-91].

Nanoparticles such as silicon dioxide, also known as silica (SiO_2), are sphere-like in shape, are chemically stable, and have high temperature resistance and are of low cost. The nano-SiO_2 particles can evidently increase anti-wear ability and reduce the friction coefficient of lubricant [92]. The use of alumina/silica (Al_2O_3/SiO_2) composite nanoparticles as lubricating oil additives also shows the reduction in the amount of wear and the increase in seizure resistance. The modified composite nanoparticles can adsorb onto the friction surfaces, which results in rolling friction. Therefore, the friction coefficient is reduced [93]. Nanoparticles have been widely used as additives to improve the tribological performance of some lubricants in load-bearing processes such as in metal cutting [94, 95], and sliding bearings [96]. A category of mechanisms have been proposed to explain the lubrication enhancement of the nanoparticles suspended in lubricating oil, including the rolling effect [97], protective film [98], mending effect [99] and polishing effect [100]. These mechanisms can be mainly classified into two groups [101].

The first is the direct effect of the nanoparticles on lubrication enhancement. The nanoparticles suspended in lubricating oil play the role of ball bearings between the friction surfaces. In addition, they also make a protective film to some extent by coating the rough friction surfaces. The other is the secondary effect of the presence of nanoparticles on surface enhancement. The nanoparticles deposit on the friction surface and compensate for the loss of mass, which is known as mending effect [99]. And also the

roughness of the lubricating surface is reduced by nanoparticle-assisted abrasion, which is known as a polishing effect [100]. Therefore, the application of lubricants containing nanoparticles in sheet metal forming processes, particularly in the ironing process, is expected to be effective in reducing friction and improving seizure resistance.

1.8 Reduction in friction by using die coating

Coatings deposited on forming tools are used to increase tool life by minimising tool wear. The low friction coefficient of the coatings is an important factor against adhesive wear. In addition, a high hardness is decisive for abrasive wear resistance as the tribological in the ironing of stainless steel and aluminium alloy cups are severe. The hardness and friction coefficient of coatings at dry friction against steel are shown in **Fig. 1.8** [102].

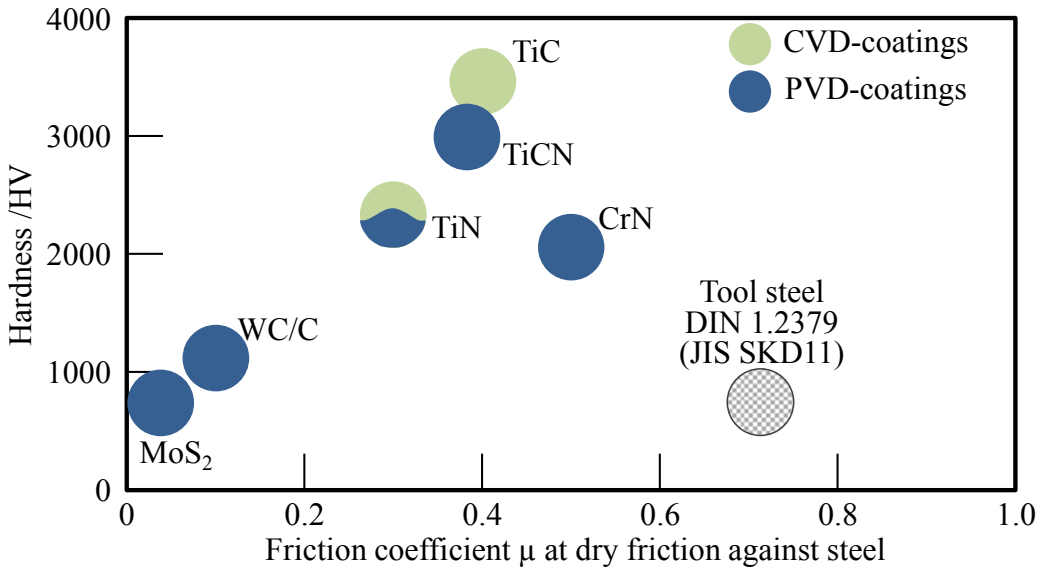

Fig. 1.8 Hardness and friction coefficient of coatings at dry friction against steel [102].

Because of the tribological loads in ironing of stainless steel and aluminium alloy cups are severe. When the lubricant film breaks down, sliding surfaces may wear and score severely and thus, the application of low-friction coatings on dies by chemical vapour deposition (CVD) and physical vapour deposition (PVD) are generally used to improve seizure resistance. Sato and Besshi [103] evaluated the anti-seizure performance of tools

used in the forming of aluminium sheets and the MoB-based cermet, cemented carbide and coated tools exhibited better seizure resistance than an uncoated tool steel die.

When treating the die surface with coating, the chemical junctions between the tool surface and the workpiece can be reduced and then the tendency to seizure is lowered. Podgonik et al. [104] indicated that seizure resistance could be improved by using suitably-coated forming tools for each type of working material. In the deep drawing of aluminium sheets without lubricant, diamond-like carbon (DLC) coating is effective in preventing the adhesion of aluminium to the die [105]. However, application of DLC coating has presented problems such as a peeling off due to the insufficient adhesion strength on the substrate tool material at high loads. A TiCN PVD coating was effective in reducing seizure in the forming of galvanised advanced high strength steel sheets [106]. In the forming of high strength steel sheets, however, nitriding combined with a CrN-coated tool showed better performance than a TiCN PVD coating and a DLC coating. The DLC and TiN coatings did not provide satisfactory results because of their low adhesion strength and wear resistance. Both coatings peeled off after 500 forming strikes. [107]

For an ironing die, the adhesion strength of the DLC coating to the tool surface was improved by adding silicon and using the preliminary nitrided and ion etched tool surface. DLC-Si coating presents possibilities for application in the dry ironing of high strength steel sheets [108]. In the ironing of aluminium alloy cups, the TiN coating by PVD with a direct current magnetron sputtering technique improves the seizure resistance of the high-speed steel die [109]. Abe et al. [110] utilised a VC-coated die in the deep drawing of ultra-high strength steel sheets and then seizure was prevented. The TiCN, AlTiN and CrN PVD coatings showed high anti-adhesion performance for the deep drawing of high strength steel [111]. The coatings with a low coefficient of friction are very effective in improving seizure resistance.

The performance for resisting the seizure of a coated forming tool greatly depends on the type of work material. Podgonik et al. [104] suggested that in the case of stainless steel, carbon-based coatings provide the best protection against work material transfer. The forming of aluminium and aluminium alloys requires nitride type coatings, such as titanium nitride (TiN) while titanium and titanium alloys require vanadium nitride (VN) coatings to show improvement in seizure resistance performance. Amongst the nitride-based coatings, VN was shown to be less prone to initiate seizure as compared to TiN, for

stainless steel [112]. In addition, the surface roughness of the coated tool has a crucial influence on seizure resistance behaviour [113]. The tendency of seizure increases with rough tool surfaces and the hardness of the coating does not correlate to the seizure tendency [114]. Therefore, a proper coating selection for forming tools with low friction and a suitable coating process with low surface defects and low surface roughness are very effective to enhance adhesive wear resistance.

1.9 Research objectives

1.9.1 Reduction in friction in ironing of aluminium alloy and stainless steel drawn cups

The aim of this dissertation is to improve the ironing limit in ironing of aluminium alloy and stainless steel drawn cups by reducing friction between the die-cup interfaces. The low friction TiCN-based cermet die is utilised and then the cermet dies having fine lubricant pockets made by lapping of shot-peened surfaces are employed and next the conditions of the ironing process and lubrication for attaining low friction with the die having lubricant pockets are determined by the measurement of thickness of remaining lubricant on the sidewall of the ironed cup. In addition, friction is lowered with the improvement of lubrication by roughening of cup surface and seizure resistance is improved by the lubricant containing fine particles. Moreover, the vanadium and titanium nitride coatings are utilised to improve seizure resistance in ironing.

1.10 Outline of dissertation

This dissertation discusses about the reduction in friction in ironing of aluminium alloy and stainless steel drawn cups. First, the friction is reduced by using the TiCN-based cermet die, followed by utilising the die having the lubricant pockets, and the investigation of the lubrication behaviours in ironing with the die having lubricant pockets. And then the improvement of lubrication by roughening of cup surface in ironing of stainless steel cups as well as the lubricant containing fine particles for improving seizure resistance in ironing of aluminium alloy cups are exhibited. Finally, the coatings for improving seizure resistance in ironing of aluminium alloy cups are presented.

This dissertation consists of eight chapters:

Chapter 1 presents the general introduction for the overall contents of the thesis.

Chapter 2 presents the reduction in friction in ironing of stainless steel and aluminium alloy drawn cups using the TiCN-based die. In the cermet die, an additional surface coating is not required because it is made of hard TiCN having low friction. For comparison, TiC-coated WC-Co, non-coated WC-Co and tool steel dies are employed. The ironing load is lowered by the cermet die. The effect of Young's modulus of the die materials on the dimension of the ironed cups is investigated. The performance of the cermet die in repeated ironing is examined.

Chapter 3 presents the reduction in friction in ironing of stainless steel and aluminium alloy drawn cups with die having fine lubricant pockets. Due to fine pockets on the die surface can retain the lubricant, consequently, can help transporting of the trapped lubricant to the die-cup interface for reducing friction. Therefore, the shape of fine lubricant pockets is optimised. The ironing limit is improved with the die having fine lubricant pockets. The mechanism of the improvement of the ironing limit with the die having an appropriate surface shape is examined from the remaining amount of lubricant in the ironed cups.

Chapter 4 presents the lubrication behaviours in ironing of the stainless steel cup with the die having lubricant pockets. The conditions of the ironing process and lubrication for attaining low friction are investigated by the measurement of the thickness of the remaining lubricant on the sidewall of the ironed cup. By mixing a fluorescence oil in the lubricant and using ultraviolet rays, the thickness of the remaining lubricant on the ironed cup is able to be measured. Furthermore, the situation of seizure growth and surface roughness of the ironed cups in repeated ironing is examined.

Chapter 5 presents the improvement of lubrication in ironing of the stainless steel cups by roughening of the drawn cup surface. The drawn cup surface roughened by sanding process with emery papers, deep drawing with large clearance, and deep drawing including redrawing with a small die radius are utilised to improve lubrication. For roughening by sanding, the cup is sanded in an axial or circumferential direction. Effects of sanding directions and surface roughness of the cups having the roughened surface on the improvement of the ironing limit are investigated. Friction is lowered with the cups having

the roughened surface. The reduction in friction is examined by the measurement of thickness of remaining lubricant on the sidewall of the ironed cup.

Chapter 6 presents the lubricant containing fine particles for improving seizure resistance in ironing of aluminium alloy cups. The lubricants applying for ironing are mixed with fine particles. The effects of the types and size of particles on the improvement of seizure resistance are investigated. Only a mixing lubricant with silica (SiO_2) particles having a ten nanometre size exhibits improvement in seizure resistance. Then, the effect of different mixing quantities of fine SiO_2 particles in paraffin oils on the improvement of seizure resistance is examined. The mechanism of the improvement of seizure resistance with the lubricant containing fine SiO_2 particles is investigated.

Chapter 7 presents the vanadium and titanium nitride coatings for improving seizure resistance in ironing of aluminium alloy cups. Titanium nitride (TiN) and vanadium nitride (VN) coatings are deposited on high speed steel substrates by direct current magnetron sputtering. Coating parameters are optimised to obtain phase compositions of TiN and VN. The coatings are characterised for phase composition using X-ray diffraction (XRD), hardness using nano-indentation and load-to-failure between the coating and substrate using scratch testing. Ring-on-disc testing is conducted to evaluate the tribological properties between aluminium alloy rings sliding against high speed steel discs under a lubricating condition. Finally, the coating which mainly has the superior tribological properties was further evaluated in an aluminium cup ironing process.

Finally concluding remarks and future prospective are given in Chapter 8.

Chapter 2

Ironing of stainless steel and aluminium alloy drawn cup using TiCN-based cermet die

2.1 Introduction

Because of the growing awareness of environmental protection, it is necessary to reduce the emission of carbon dioxide gas from automobiles. Therefore, the demand for hybrid and electric vehicles increases, and thus lithium-ion batteries having high capacity are required. In the battery, the metal cups are used as electrolyte cases. The cases with a large aspect ratio are desirable in the industry. The aluminium alloy cups with an extreme aspect ratio were achieved by process design and a modification of the initial blank in multi-stage deep drawing [12]. Schünemann et al. [11] illustrated the application of process modelling to deep drawing and ironing operations, then the cases are mainly produced by multi-stage stamping that includes deep drawing and ironing of stainless steel and aluminium alloy sheets. In ironing of stainless steel drawn cups, the fracture and seizure tend to occur. The fracture limit in ironing is affected by the friction between a cup and die [21].

To reduce friction and to prevent the occurrence of seizure in ironing, liquid lubricants are conventionally used. Bay et al. [54] reviewed lubrication mechanisms in ironing of sheet metal forming processes. Kawai et al. [27] showed that the seizure was prevented by appropriate viscosity of lubricants in ironing of aluminium cups. Ironing operations in the stainless steel cups are severe due to high flow stress and low thermal conductivity, and thus low friction coating of dies by the CVD and PVD treatments is generally used. The TiCN, AlTiN and CrN PVD coatings showed high anti-adhesion performance for deep drawing of high strength steel [107]. Although wear resistance of the coating is desirable to improve die life, the wear resistance of coating by PVD and CVD is insufficient.

Since tool wear in deep drawing and ironing is problematic in the mass production, low friction tool materials such as ceramics and cermets are applied. Sato and Besshi [103] evaluated anti-galling performance of tools in forming of aluminium sheets and the MoB-based cermet tool exhibited better anti-galling performance than cemented carbide and

coated tools. For deep drawing of stainless steel using an alumina ceramic die, the drawing load was significantly reduced [41]. Tamaoki et al. [42] proposed electro conductive ceramic dies for deep drawing, and then the cups were successfully deep drawn over 10,000 times [43]. However, it is not easy to apply the brittle ceramic die to ironing of stainless steel cups.

Peng et al. [45] reviewed the development of TiCN-based cermets. The advances in the synthesis of ultrafine/nano TiCN powders and preparation of TiCN-based cermets enhance their hardness, toughness and wear resistance. Jeon et al. [46] showed the fracture toughness and hardness of the ultrafine grade TiCN-based cermets are considerably improved compared to conventional coarse TiCN-based materials. Bellosi et al. [50] evaluated the performance of developed TiCN-based tools in machining of carbon steel and quenched-tempered steel. The developed TiCN-based tools showed the improvement of machining performance compared to commercial tools. The TiCN-based cermet becomes more attractive for cutting tools because the cermet has excellent wear resistance [51, 52]. Therefore, the TiCN-based cermet is expected to be effective for improving the formability by reducing friction in ironing of stainless steel and aluminium alloy drawn cups.

In the present study, a TiCN-based cermet die was utilised to reduce friction in the ironing of stainless steel and aluminium alloy drawn cups. For comparison, TiC-coated WC-Co, non-coated WC-Co and tool steel dies were employed. The influence of the die materials on the ironing limit was studied. The effect of Young's modulus of the die materials on the dimension of the ironed cups was investigated. In addition, the performance of the cermet die in repeated ironing was examined.

2.2 Ironing conditions

The sheet materials were austenitic stainless steel SUS304, ferritic stainless steel SUS430 and aluminium alloy A3003 sheets having a thickness of 0.6 mm. The mechanical properties of sheets obtained from the tensile test are shown in **Table 2.1**. The diameters of the stainless steel and aluminium alloy sheets for deep drawing were 66 and 64 mm, respectively.

Table 2.1 Mechanical properties of sheets used for ironing.

Sheet	Tensile strength /MPa	Elongation /%	*n*-value	*r*-value
SUS304	710	59.3	0.40	1.01
SUS430	547	25.7	0.20	1.17
A3003	106	26.8	0.21	0.42

The ironing conditions of cylindrical drawn cups are shown in **Fig. 2.1**. To change the ironing ratio, the punch diameter d is changed while the inside diameter of the die is fixed at 34 mm. The ironing limit is defined by the largest ironing ratio which the die is able to iron without the occurrence of seizure on the die or the fracture of the cup. The ironing ratio is given by

$$r = \frac{t_0 - t_m}{t_0}, \tag{1}$$

where t_0 is the initial thickness of a blank and t_m is the average of the wall thickness of the ironed cup.

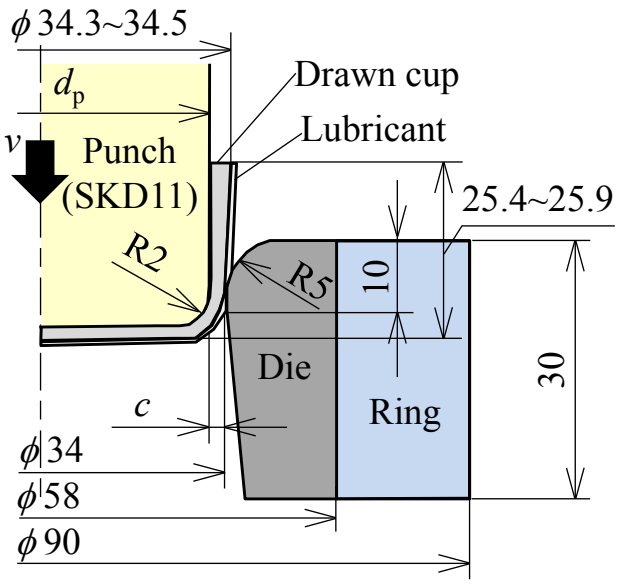

Fig. 2.1 Ironing conditions of drawn cup.

The surface in the die land for the different tool materials is shown in **Fig. 2.2.** The dies made of the tool steel SKD11, non-coated WC-Co, CVD-coated WC-Co with TiC coating and TiCN-based cermet were utilised. The WC-Co is a V20 code in accordance

with the Japanese Industrial Standard B 4053. The TiCN-based cermet was obtained by sintering of main TiCN powders with a nickel binder without tungsten carbide and cobalt in its composition. Because the main component of the cermet is made from low friction TiCN, an additional surface coating is not required. To prevent the fracture of the dies, each die except the tool steel one was fixed into a steel ring by press fitting. The tool steel die was made into one part with the inside and outside diameters of 34 and 90 mm, respectively.

The surface roughness and micro-Vickers hardness of the dies are shown in **Table 2.2.** All the die surfaces were finished by lapping hence their surfaces are very fine with surface roughness in an axial direction about 0.02 μmRa. The maximum hardness is obtained from the TiC-coated WC-Co die, while the tool steel die exhibits minimum hardness. Lubricants were oils. For the SUS304 cup, a lubricant containing a chlorine-based extreme-pressure additive with a kinematic viscosity η = 513 mm^2/s (40 °C) was employed. For the SUS430 cup, the lubricants containing the chlorine additive with η = 513 and 3.0 mm^2/s were applied. A lubricant without the extreme-pressure additive with the kinematic viscosity η = 562 mm^2/s was used for the A3003 cup. The cup was attached to the punch and then a lubricant was applied to the die and the outside of the cup sidewall. The ironing was performed by using a universal testing machine with an ironing speed v = 8.0 mm/s. To maintain the same surface condition, the die surface was lapped by diamond paste having a size of 1 μm and cleaned thoroughly after each ironing condition.

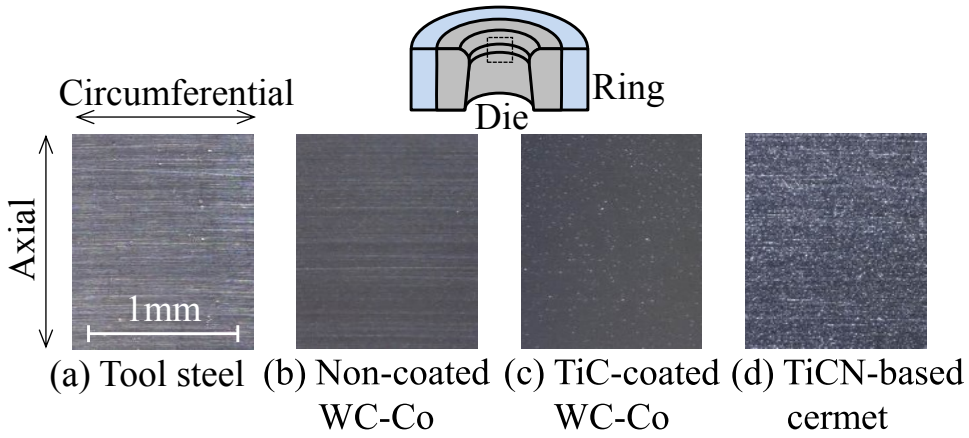

Fig. 2.2 Surface in die land for different tool materials.

Table 2.2 Surface roughness and Vickers hardness of dies.

Die material	Surface roughness in die land		Vickers hardness /HV50
	Arithmetic mean /μmRa	Maximum height /μmRz	
Tool steel SKD11	0.02	0.28	750
Non-coated WC-Co V20	0.02	0.21	1650
TiC-coated WC-Co V20	0.02	0.14	1650, 3000 (TiC)
TiCN-based cermet	0.02	0.20	1550

2.3 Ironing of stainless steel cups

2.3.1 Ironing limit

The ironed SUS304 cups with the non-coated WC-Co die are shown in **Fig. 2.3.** Although the ironed cup was obtained without the defect at r = 11%. At the ironing ratios r = 15% and 21%, the seizure and the fracture take place, respectively.

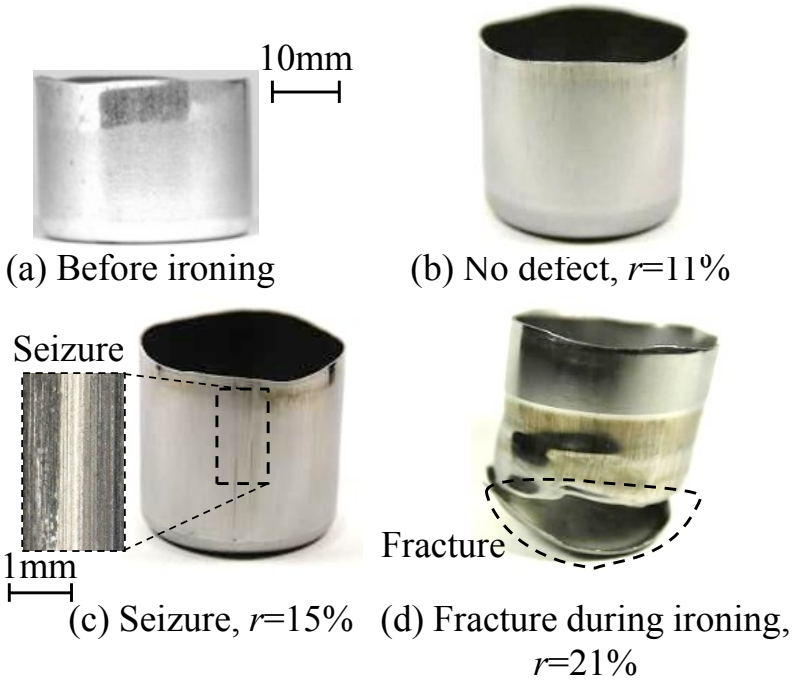

Fig. 2.3 Ironed SUS304 cups with non-coated WC-Co die.

The wall thickness distribution in the sidewall of the ironed cups for SUS304 with the different tool materials and d = 33.16 mm is shown in **Fig. 2.4.** The wall thickness was measured every 3 mm. As shown in Fig. 2.3, the height of the ironed cups became wavy. Therefore, the measurement was performed till the uniform height in a circumferential direction. By using the same punch diameter, the obtained wall thickness of the cups is differed with different die materials. Using the tool steel die shows the largest wall thickness of the ironed cup because of large elastic deformation of the die. The wall thickness becomes closer to the clearance between the punch and die with the TiCN-based cermet, TiC-coated WC-Co and non-coated WC-Co dies, respectively.

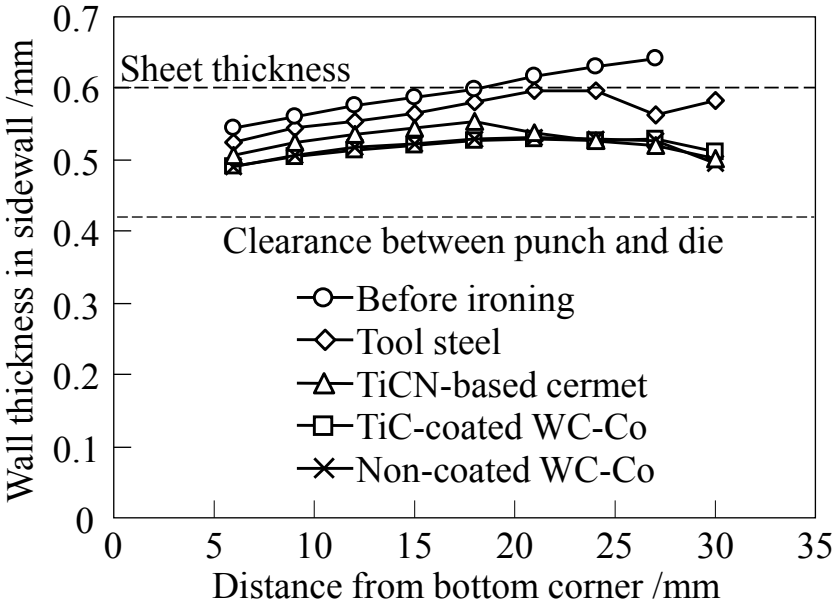

Fig. 2.4 Wall thickness distribution in sidewall of ironed cups for SUS304 with different tool materials and d = 33.16 mm.

The ironing limit and the surface of the die land for the SUS304 cup with the different tool materials are shown in **Fig. 2.5.** At a high ironing ratio, the seizure occurs for the non-coated WC-Co and the tool steel dies, whereas for the TiC-coated WC-Co and TiCN-based cermet dies, the seizure is prevented. The TiCN-based cermet die exhibits the largest ironing limit, and then no seizure occurs on the surface of the die.

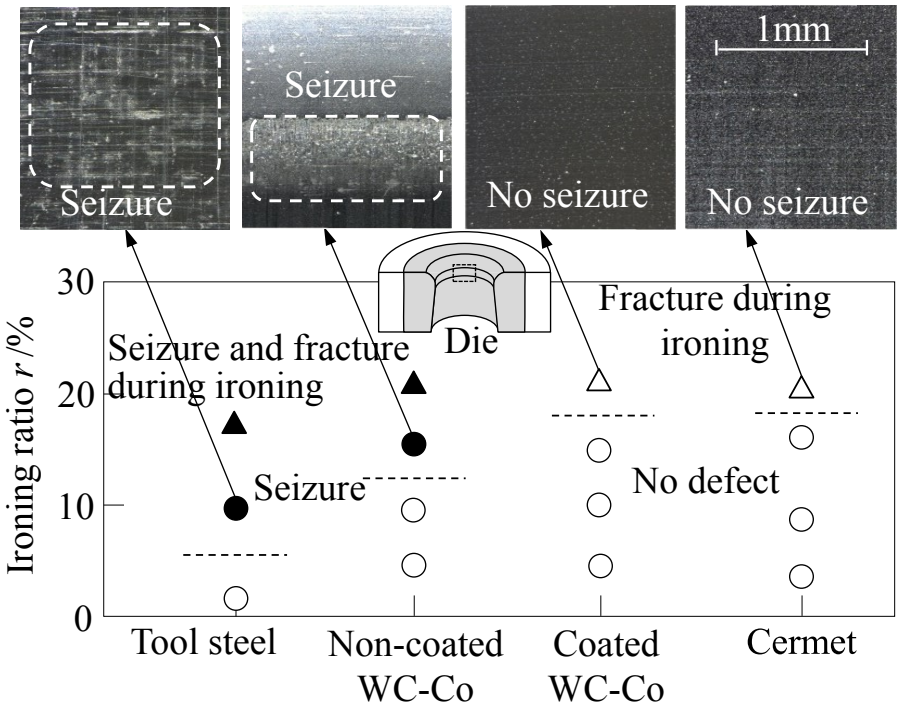

Fig. 2.5 Ironing limit and surface of die land for SUS304 cup with different tool materials.

The ironing load-stroke curves and the ironing energy for the SUS304 cup with the different tool materials and d = 33.16 mm are shown in **Fig. 2.6.** The ironing load-stroke curves and the ironing energy with the different tool materials were compared at the same ironing ratio about 15%. The ironing energy is calculated from the area of the ironing load-stroke curve. The ironing energy obtained from the non-coated WC-Co die is the largest. While the ironing energy obtained from the TiC-coated WC-Co and the TiCN-based cermet dies are same. Since the ironing ratio of the TiCN-based cermet die was higher than that of the TiC-coated WC-Co die. This suggests that the TiCN-based cermet die has lower friction.

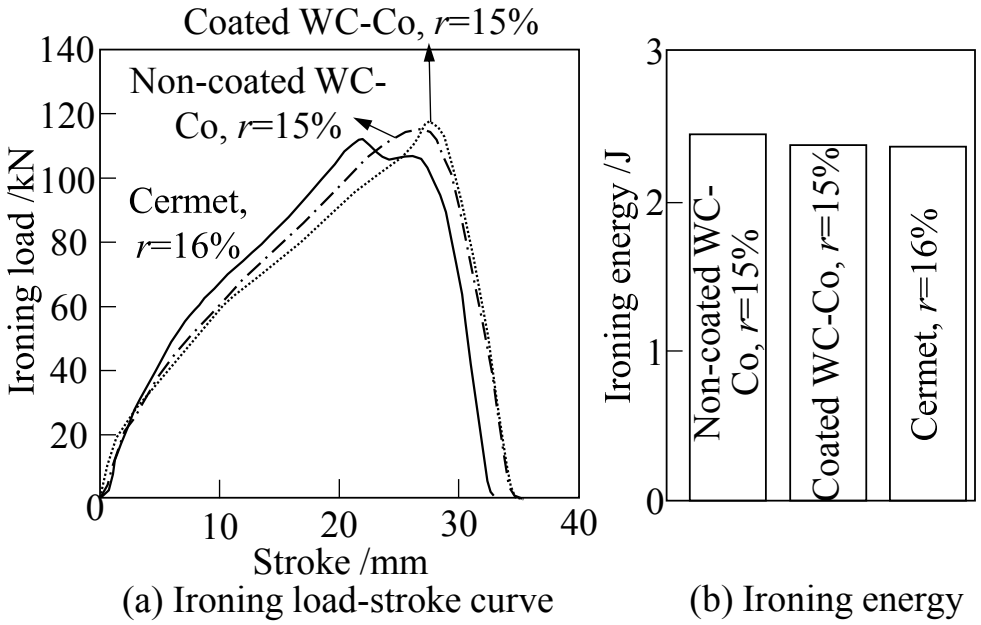

Fig. 2.6 Ironing load-stroke curves and ironing energy for SUS304 cup with different tool materials and d = 33.16 mm.

The ironing limit and the surface of the die land for the SUS430 cup with the different tool materials are shown in **Fig. 2.7.** By applying the lubricant having the viscosity η = 3.0 mm^2/s, the ironing limit of each die is slightly different. However, by applying the lubricant having the viscosity η = 513 mm^2/s, all dies except the tool steel die are able to iron until r = 20% without the occurrence of seizure. By increasing the viscosity of the lubricant, the ironing limit is significantly improved.

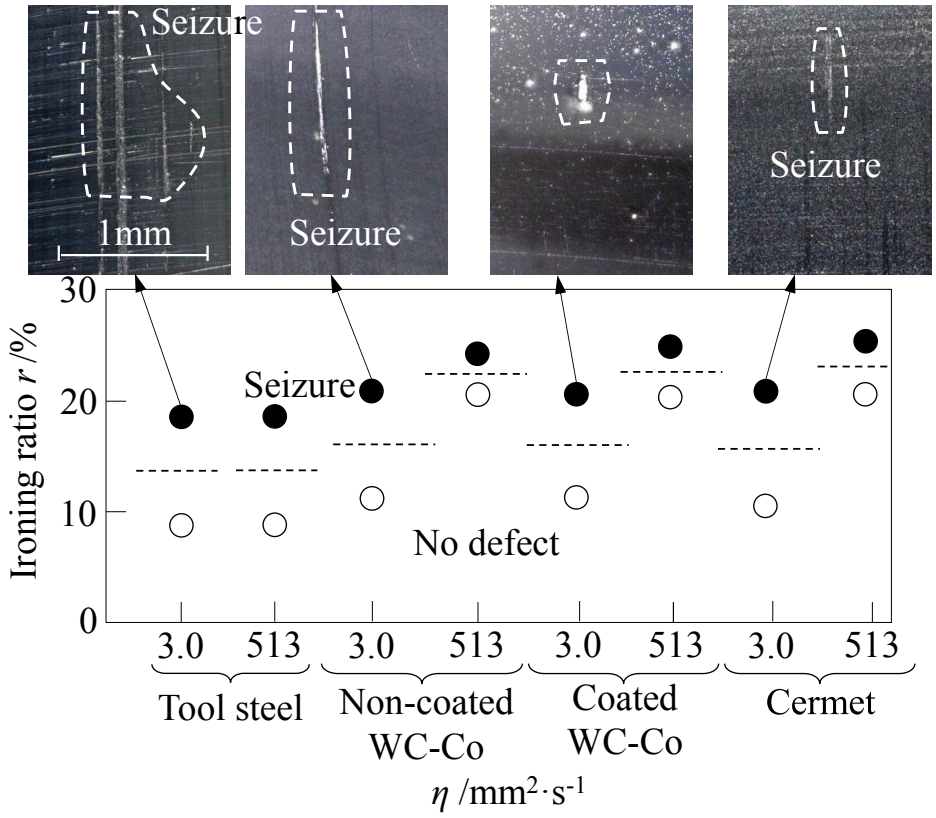

Fig. 2.7 Ironing limit and surface of die land for SUS430 cup with different tool materials.

Since the cermet die shows a high ironing limit, this die was chosen for the investigation of an effect of the ironing speed on the ironing limit. The effect of the ironing speed on the ironing limit for stainless steel cups with the TiCN-based cermet die is shown in **Fig. 2.8.** In addition, the distribution of the temperature on the sidewall of the ironed cup is also illustrated. The distribution of the temperature was measured by a thermographic camera at 0.1 s after ironing. For SUS304 and all ironing speeds at r = 20%, the fracture of the cups takes place. Although at r = 17% the temperature of the upper portion of the ironed cup becomes high, no seizure occurs. The ironing speed has no significant effect on the occurrence of seizure. On the other hand, for SUS430 at r = 21% and the ironing speed above v = 25 mm/s, the seizure and the delayed fracture take place.

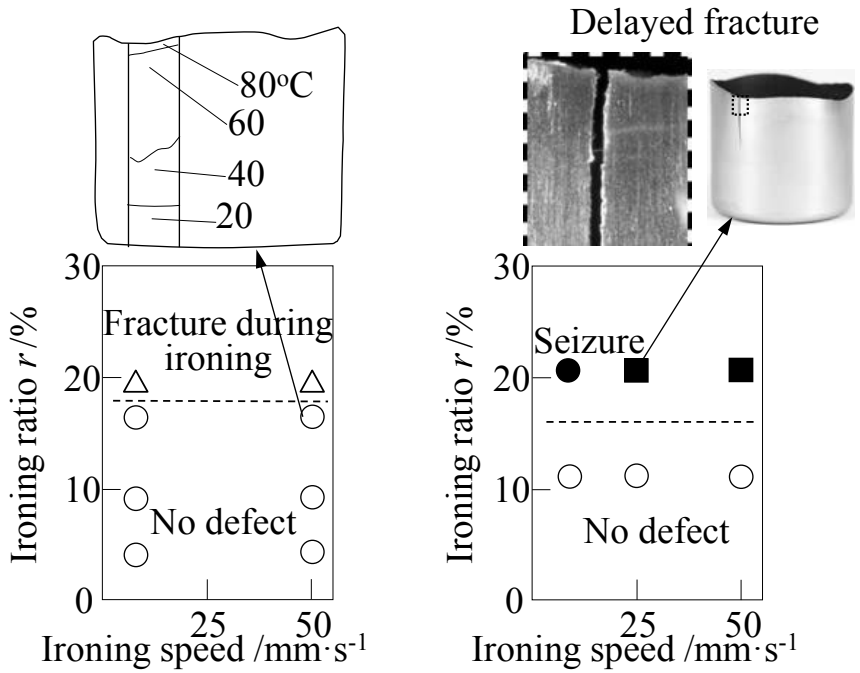

(a) SUS304, η =513 /mm^2·s^{-1} (b) SUS430, η =3.0 /mm^2·s^{-1}

Fig. 2.8 Effect of ironing speed on ironing limit for stainless steel cups with TiCN-based cermet die.

2.3.2 Effect of die materials on dimension of ironed cups

The ironed SUS304 cups and the average sidewall thickness of the ironed cups with the different tool materials and d = 33.16 mm are shown in **Fig. 2.9.** For comparison, the calculation of the average wall thickness with the finite element simulation was carried out using the commercial finite element method software LS-DYNA. In the simulation, the die was assumed as an elastic body and the cup was assumed as an elastic-plastic body, while the others were assumed to be rigid. The Young's modulus of tool steel, cermet and non-coated WC-Co dies are 210, 410 and 600 GPa, respectively. The flow stress curves of the SUS304 and SUS430 sheets obtained from the tensile test are $\sigma = 1262\varepsilon^{0.4}$ MPa and $\sigma = 864\varepsilon^{0.2}$ MPa, respectively. Where σ is the flow stress and ε is the true strain. Coulomb friction was defined. The coefficient of friction at an interface between the punch and cup as well as at an interface between the cup and die were assumed to be 0.2 and 0.1, respectively. The cup ironed by the TiC-coated WC-Co die has the tallest height. The second is the cup obtained from the cermet die. With the tool steel one shows the lowest height of the cup. The average sidewall thickness of the ironed cup with the TiC-coated

WC-Co, non-coated WC-Co and cermet dies are closer to the punch-die clearance than with the tool steel one. For the ironed SUS304 cup having large flow stress, the discrepancy between the average sidewall thickness and the punch-die clearance is markedly noticed. Although the average sidewall thickness obtained from the calculation is smaller than the experiment, they show the same tendency.

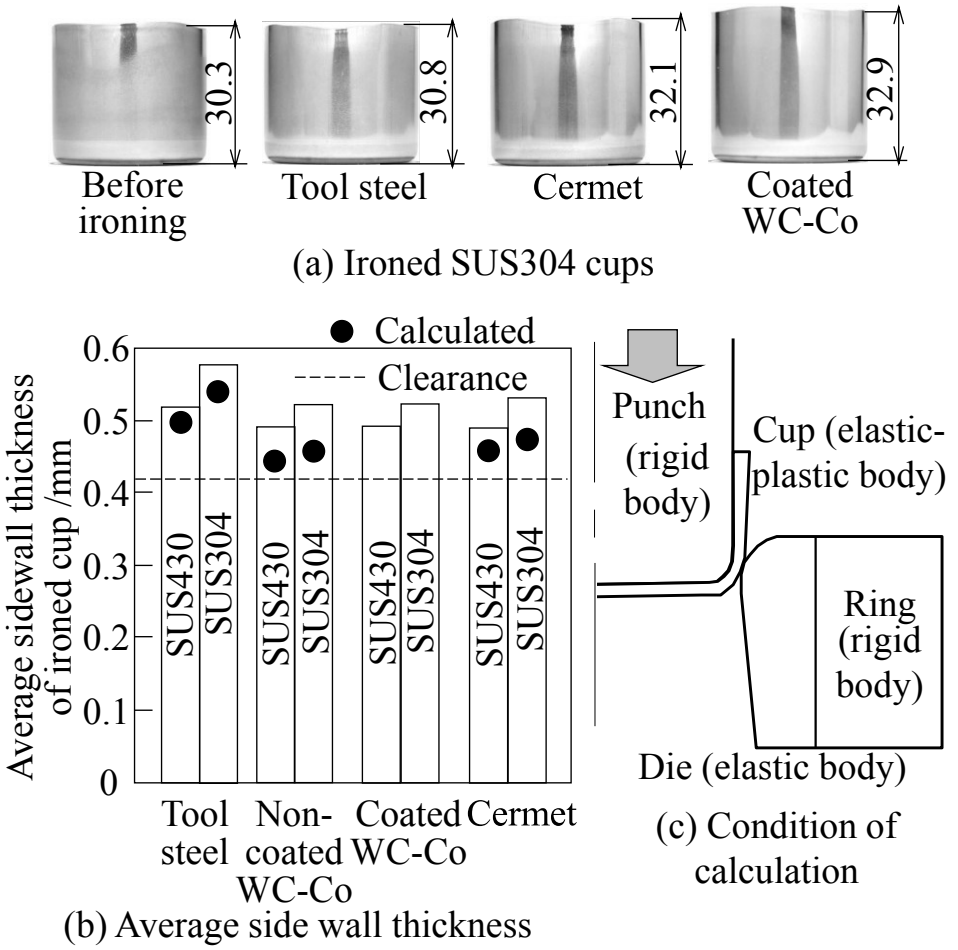

Fig. 2.9 Ironed SUS304 cups and average sidewall thickness of ironed cup with different tool materials and d = 33.16 mm.

The effect of the Young's modulus of the die on the sidewall thickness and the height of the ironed cup is shown in **Fig. 2.10**. Due to a high contact pressure generated during ironing causes the expansion of the inside diameter of the die. When the inside diameter of the die expands, the reduction in the sidewall thickness of the ironed cup is small, consequently the increase in the height of the cup becomes small. The Young's modulus of

the die materials has an influence on the expansion of the die. As shown in Fig. 2.9, the height of the ironed cup increases when the Young's modulus of the die is high. Since the flow stress of the SUS304 cup is greater than the SUS430 cup, the expansion of the die is large. Thus the wall thickness of the ironed cup becomes thick. The ironing of high precision parts is able to gain the benefit from the high Young's modulus of the tungsten carbide die.

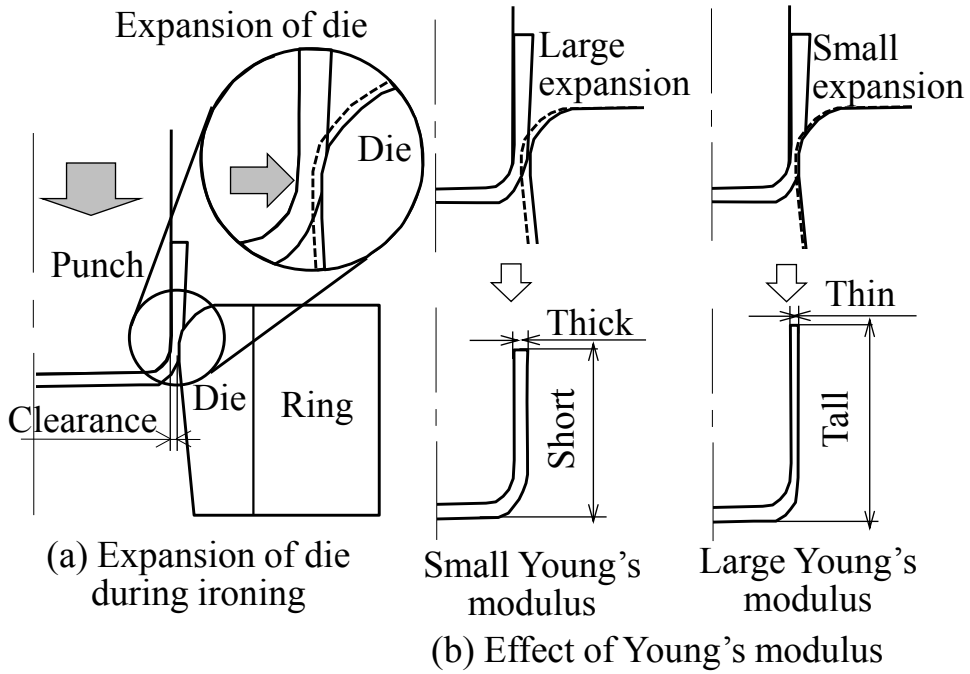

Fig. 2.10 Effect of Young's modulus of die on sidewall thickness and height of ironed cup.

2.4 Ironing of aluminium alloy cups

The ironing limit for the A3003 cup with the different tool materials is shown in **Fig. 2.11**. For the lubricant without the additive with $\eta = 562$ mm^2/s and $r = 37\%$, the seizure occurs for the TiC-coated WC-Co die, whereas the seizure is prevented for the cermet one. There are the fractures of the cup edge for both dies. For the lubricant containing the chlorine additive with $\eta = 513$ mm^2/s, the ironing limit also exhibits the same tendency which the seizure is prevented for the cermet die.

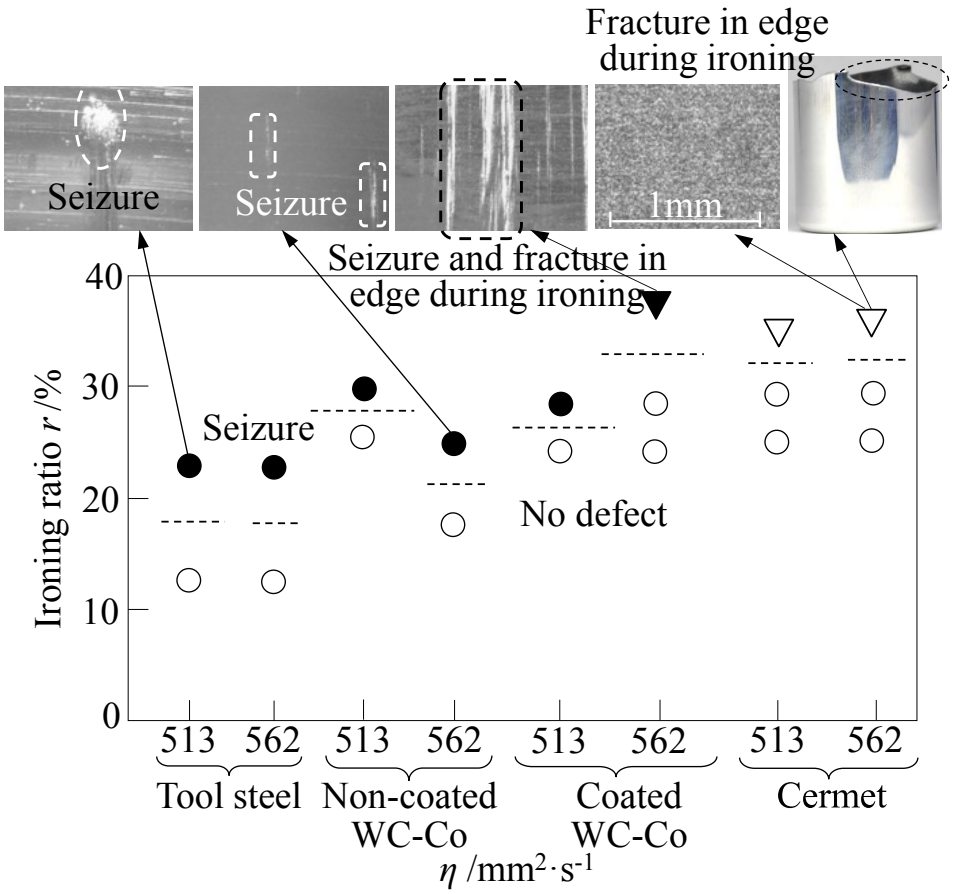

Fig. 2.11 Ironing limit for A3003 cup with different tool materials.

The effect of the ironing speed on the ironing limit and the temperature distribution of the ironed A3003 cup with the cermet die are shown in **Fig. 2.12.** The ironing limit does not change with the increasing in the ironing speed. Furthermore, the temperature of the cup rises slightly because the aluminium alloy has low flow stress and high thermal conductivity. With the lubricant without the additive, the ironing limit becomes high.

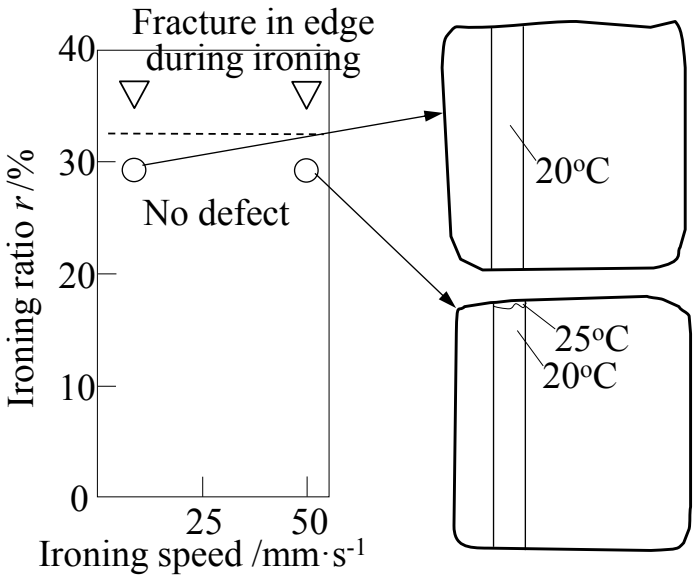

Fig. 2.12 Effect of ironing speed on ironing limit and temperature distribution of ironed A3003 cup with cermet die.

The average sidewall thickness of the ironed A3003 cups with the different tool materials and d = 33.16 mm is shown in **Fig. 2.13.** The sidewall thickness of the ironed cup from each die becomes larger than the punch-die clearance. The sidewall thickness of the obtained cup from difference die materials is slightly different, because the flow stress of A3003 is small compared to the Young's modulus of the die.

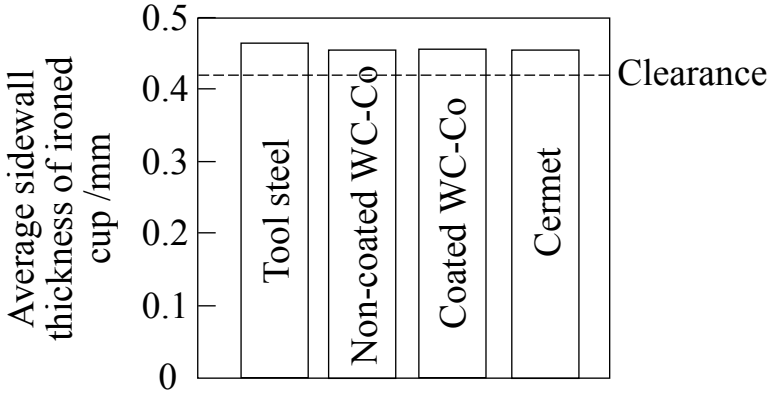

Fig. 2.13 Average sidewall thickness of ironed A3003 cup for d = 33.16 mm.

2.5 Performance of cermet die in repeated ironing

The repeated ironing of the SUS430 and A3003 cups were conducted by using the cermet die. In addition, the TiC-coated WC-Co die was used as a comparison. The ironing ratio for the SUS430 and A3003 cups were about 6% and 25%, respectively. The total number of strikes for the SUS430 and A3003 cups were n = 100 and 50, respectively. The deep drawing and ironing dies were arranged vertically, two processes were performed in one strike. The repeated ironing was performed by using a mechanical servo press with an ironing speed of 75 mm/s. Because the blanks were manually fed into the die, the number of strikes per minute of the process was about 5. For SUS430, the lubricant containing the chlorine additive having the viscosity η = 3.0 mm^2/s was applied. For A3003, the lubricant without the additive with η = 562 mm^2/s was employed. The lubricant was applied to the dies and the blank. The repeated ironing was performed continuously until the maximum number of strikes without polishing of the die during ironing.

The surfaces in the die land after repeated ironing are shown in **Fig. 2.14.** The results of the TiC-coated WC-Co die are also shown as a comparison. For SUS430 cups, using the cermet die, the cups are successfully formed up to 100 strikes without the occurrence of seizure, whereas using the TiC-coated WC-Co die, the seizure takes place. For A3003 cups, the cermet die is able to perform ironing until n = 50 without seizure, while tiny seizure occurs in the TiC-coated WC-Co one.

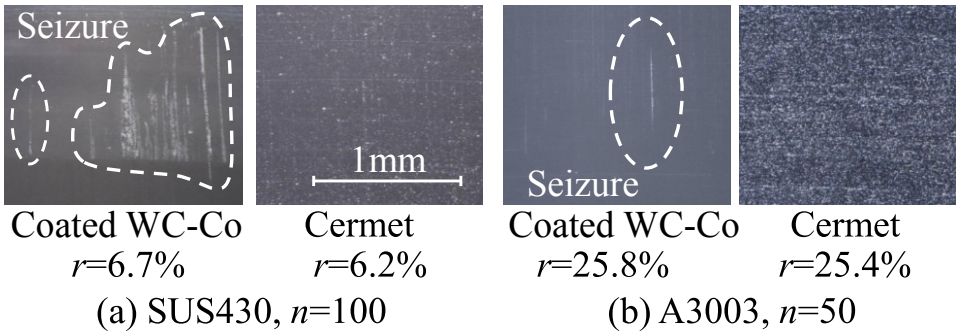

Fig. 2.14 Surfaces in die land after repeated ironing.

The histories of the ironing load and the die temperature for SUS430 cups with the different tool materials are shown in **Fig. 2.15.** The die temperature is the maximum temperature of the die land taken by a thermographic camera at 2 s after the end of ironing.

There is no change in the ironing load with the number of strikes. By using the cermet die, the ironing load is lower than the TiC-coated WC-Co die. The die temperature increases with the number of strikes. Although the thermal conductivity of WC-Co is superior to that of the TiCN-based cermet [115], the temperature of the cermet die is lower than the TiC-coated WC-Co die. Because of the ironing load by the TiC-coated WC-Co die is high.

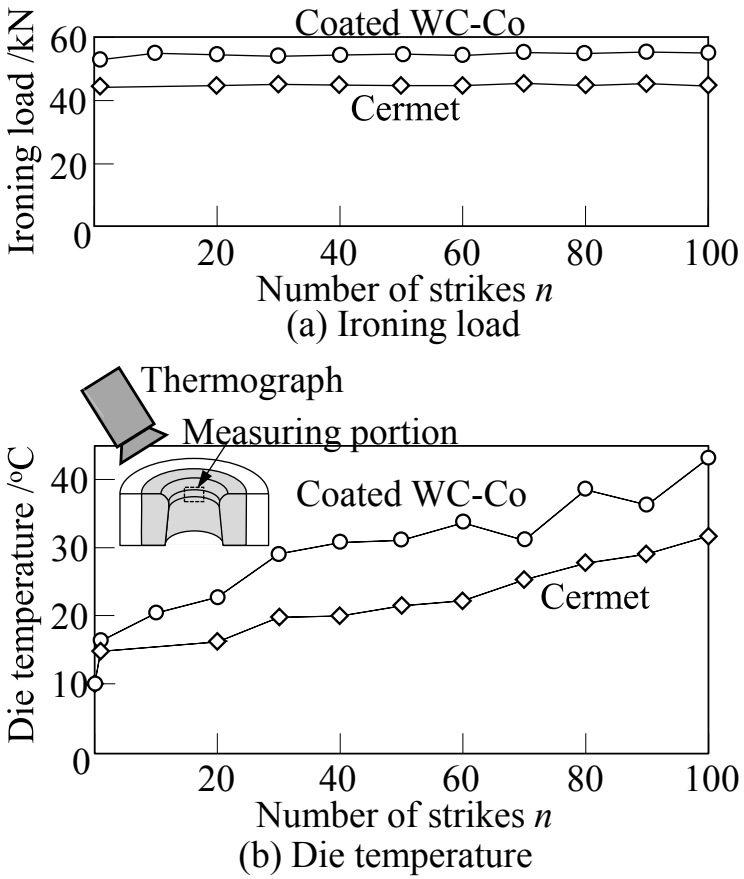

Fig. 2.15 Histories of ironing load and die temperature for SUS430 cups with different tool materials.

The histories of the ironing load and the die temperature for A3003 cups with the different tool materials are shown in **Fig. 2.16**. After the first strike, there is no change in the ironing load and the die temperature with the number of strikes. The temperature of the TiC-coated WC-Co die is equivalent to that of the cermet die.

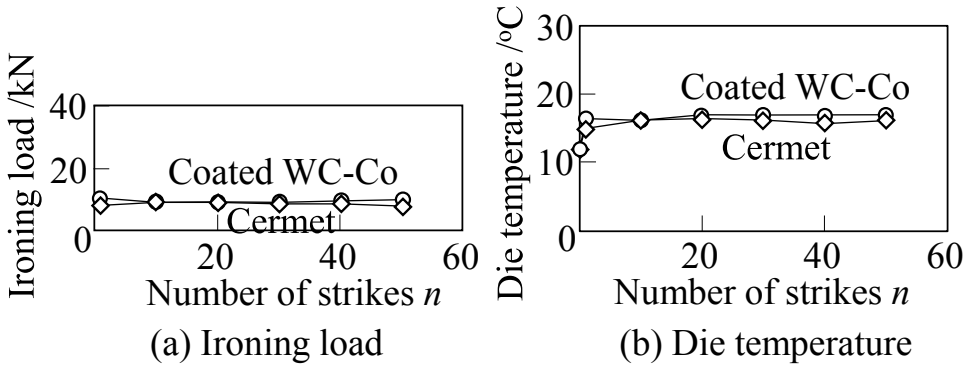

Fig. 2.16 Histories of ironing load and die temperature for A3003 cups with different tool materials.

The variation of surface roughness in the sidewall of ironed SUS430 and A3003 cups in repeated ironing is shown in **Fig. 2.17**. The surface roughness was measured in the circumferential direction at the distance of 25 mm from the bottom of the ironed cup. For SUS430 cups, the surface roughness of the cups produced by the cermet die remains almost constant up to 100 strikes, whereas the surface roughness of the cups produced by the TiC-coated WC-Co die has a tendency to increase after 70 strikes. For A3003 cups, the surface roughness of the cups produced by the cermet die is lower than that by the TiC-coated WC-Co one. The cermet die has high seizure resistance in ironing of stainless steel and aluminium alloy cups.

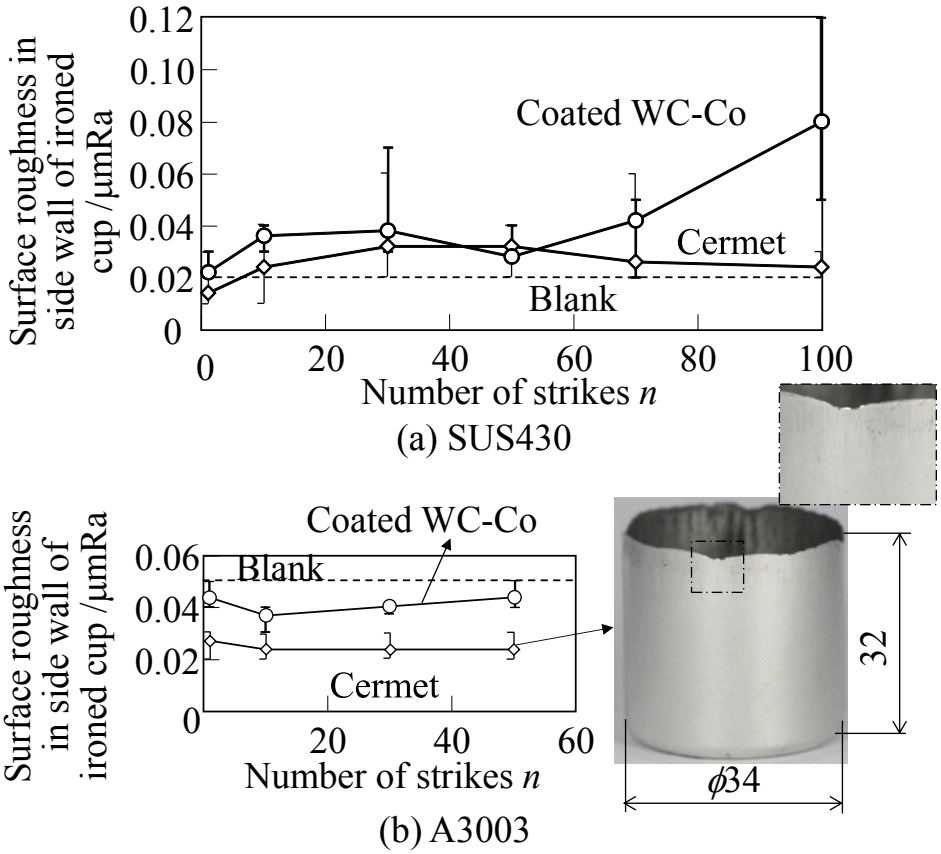

Fig. 2.17 Variation of surface roughness in sidewall of ironed cup in repeated ironing.

2.6 Conclusions

The TiCN-based cermet die was utilised to reduce friction in ironing of stainless steel and aluminium alloy drawn cups. For comparison, TiC-coated WC-Co, non-coated WC-Co and tool steel dies were employed. The influence of the die materials on the ironing limit was studied. The effect of Young's modulus of the die materials on the dimension of the ironed cups was investigated. In addition, the performance of the cermet die in repeated ironing was examined, and the following results were obtained:

1. For ironing of stainless steel cups, the ironing limit of the TiCN-based cermet and TiC-coated WC-Co dies were the highest and then followed by the non-coated WC-Co die. The ironing limit of the tool steel die was the lowest. For ironing of aluminium alloy cups, the ironing limit of the TiCN-based cermet die was the highest and then followed by TiC-coated WC-Co and the non-coated WC-Co dies, respectively. The ironing limit of the tool steel die exhibited the lowest.

2. For repeated ironing of the ferritic stainless steel SUS430 and aluminium alloy A3003 cups using the TiCN-based cermet die, the SUS430 and A3003 cups were successfully formed up to 100 and 50 strikes, respectively, without the occurrence of seizure.
3. The height of ironed stainless steel cups with the TiC-coated WC-Co die was the highest and followed by the TiCN-based cermet die and the tool steel one, respectively. The height of the cup increased as the elastic modulus of the die was large. For the austenitic stainless steel SUS304 cup having large strength, the tendency of the discrepancy between the average sidewall thickness and the punch-die clearance was more remarkable than for the ferritic stainless steel SUS430 cup.

Chapter 3

Reduction in friction in ironing of stainless steel and aluminium alloy drawn cup using die having lubricant pockets

3.1 Introduction

The metal cups are widely used as beverage cans, food containers, electrical parts and mechanical parts. Since the cups with a large aspect ratio are required for electrolyte cases in the battery, the cases are mainly produced by multi-stage stamping which includes deep drawing and ironing of stainless steel and aluminium alloy sheets. To improve the process conditions, process modelling is applied to deep drawing and ironing operations [11]. The aluminium alloy cups with an extreme aspect ratio were achieved by process design and a modification of the initial blank in multi-stage deep drawing [12].

Sheet stamping operations in the stainless steel are severe due to their high flow stress and low thermal conductivity. The fracture and seizure tend to occur. The fracture limit is affected by friction between the cup and the die [21]. To reduce friction and to prevent the occurrence of seizure in ironing, liquid lubricants are conventionally used. Applying liquid lubricants, the workpiece surface topography has an influence on the improvement of lubrication. Because a rough surface is able to provide small pits, consequently, the transporting of the trapped lubricant with plastic deformation of the workpiece to the tool-workpiece interface develops the thin lubricant film. This mechanism was named micro-plasto-hydrodynamic lubrication [55]. In a cold sheet drawing test, the mechanism of micro-plasto-hydrodynamic lubrication was elucidated [56]. The mechanism was verified by direct observation of the tool-workpiece interface through a transparent die. The degree of reduction, drawing speed and lubricant viscosity have an influence on the escaping lubricant from the pockets [57, 58]. Utilising the same direct observation technique, the effects of pocket geometry, lubricant viscosity, drawing speed and reduction on the

entrapment and escape of liquid lubrication were investigated [59, 60]. The escape of trapped lubricants from pockets during strip drawing has an influence on drawing load [61]

Since the use of structured sheet surfaces providing surface topography with lubricant pockets facilitates the lubrication in the forming processes. The sheet-surface structures have been developed to improve the tribological conditions of sheet forming processes [62]. The structured sheet surface produced by transferring of roller surfaces prepared by electron beam texturing in skin pass rolling was introduced to the deep drawing process. Because the lubrication is assisted during the process, the friction decreases with increasing in drawing speed [64]. To clearly obtain a defined surface structure of the sheet in cold-rolling processes, the finite-element model was developed to simulate the transfer characteristics of the roll surface textured by electron-beam texturing [65]. The 3D surface parameters were developed to characterise the structured sheet surfaces with respect to their functional behaviour [66]. The structured stainless steel sheet significantly improved the lubrication performance with no sign of lubricant film breakdown in strip ironing and in deep drawing [67]. However, the structured sheet surface does not function when it is completely flattened in the large deformation.

On the other hand, the tool surface seldom changes. Applying the texturing on the tool surface facilitates the forming process even after long-running use. Geiger et al. [68] introduced the texturing using an excimer laser radiation to the surface of a TiN-coated punch for cold forging. Popp and Engel [69] showed the pressurization of the entrapped lubricant in the well-designed micro pockets improved the tool life. During the process, tool wear was reduced by the wiped lubricant from micro pockets [71]. Vilhena et al. [72] employed laser surface texturing to hardened bearing steel and parameters of the laser surface texturing process were optimised. Well defined micro-dimples improved tribological behaviour [73]. Meng et al. [75] exhibited friction can be reduced by using the laser textured tool having micro rectangle dimples with a flat bottom. Aramaki et al. [76] showed the die treated by the combination of shot-peening and nitriding improves seizure resistance in the drawing test of high strength steel sheets because of its lubricating effect. To assist in lubricating in ironing of stainless steel cups, the dies textured by shot peening producing fine lubricant pockets were introduced.

In the present study, TiCN-based cermet dies having fine lubricant pockets made by the lapping of shot-peened surfaces was utilised to reduce friction in the ironing of

stainless steel and aluminium alloy drawn cups. The effect of dies having fine lubricant pockets with different surface roughness on the ironing limit was investigated. The lubrication mechanism for improving the ironing limit with the die having the lubricant pockets was determined.

3.2 Ironing conditions using die having lubricant pockets

The ironing conditions using the die having the lubricant pockets are shown in **Fig. 3.1**. The cup obtained from deep drawing as shown in Fig. 3.1 (a), was attached to the punch and then was ironed as shown in Fig. 3.1 (b). The obtained cups were drawn from circular sheets of the ferritic stainless steel SUS430 having 0.6 and 66 mm in thickness and diameter, respectively. For comparison, austenitic stainless steel SUS304 and aluminium alloy A3003 sheets were employed. The mechanical properties of the sheets used for ironing are shown in **Table 3.1**. The ironing ratio r was changed by changing the punch diameter d_p while the inside diameter of ironing dies was fixed at 34 mm. The ironing ratio r was determined by a difference between the initial thickness of the blank and the average wall thickness of the ironed cup divided by the initial thickness. The ironing speed v was 100 mm/s. The lubricant for the stainless steel cups was a mineral oil containing a chlorine-based extreme-pressure additive with a kinematic viscosity of 2.99 mm^2/s at 40 °C. The lubricant for the aluminium alloy cups was a mineral oil without the additive with a kinematic viscosity of 562 mm^2/s at 40 °C. The lubricant was applied to the cup and die surfaces. In the experiment, seizure was examined every ironing. The ironing ratio was increased until the seizure had occurred.

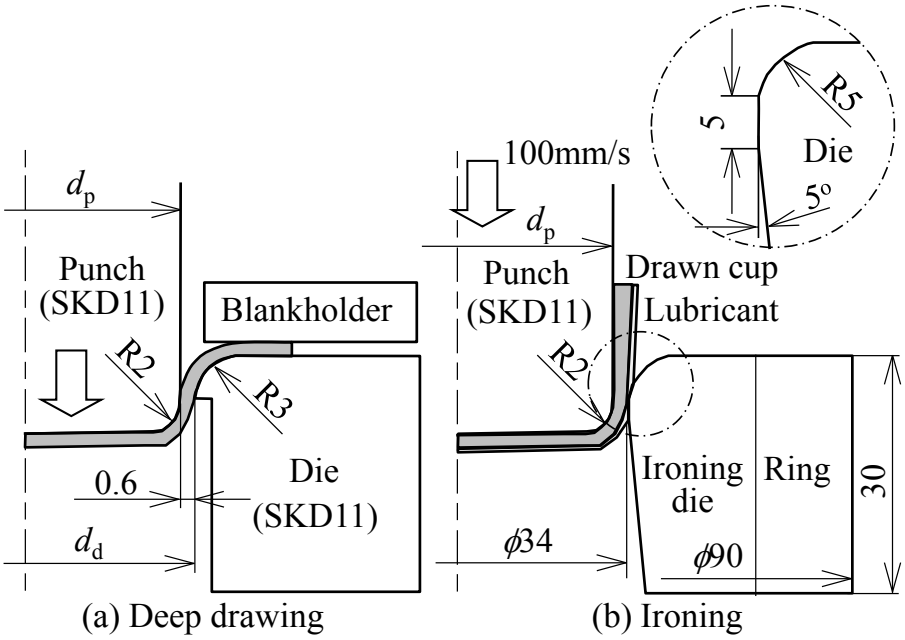

Fig. 3.1 Ironing conditions using die having lubricant pockets.

Table 3.1 Mechanical properties of sheets used for ironing.

Sheet	SUS430	SUS304	A3003-O
Tensile strength /MPa	547	710	200
Elongation /%	25.7	59.3	26.8
n-value	0.20	0.40	0.22
r-value	1.17	1.01	0.79
Surface roughness /μmRa	0.02	0.06	0.22

In the previous study, as the TiCN-based cermet die showed a high ironing limit in ironing of stainless steel, the TiCN-based cermet die was utilised. The TiCN-based cermet was obtained by sintering of main TiCN powders with a nickel binder. Because the main component of the cermet is made of low friction TiCN, an additional surface coating is not required. The modulus of elasticity and hardness of the TiCN-based cermet are 410GPa and 1550HV50, respectively. To prevent the fracture of the dies, each die was fixed into a steel ring by press fitting. The outside diameter of the dies was 58.23 mm, while the steel rings had the inside diameter of 58.00 mm.

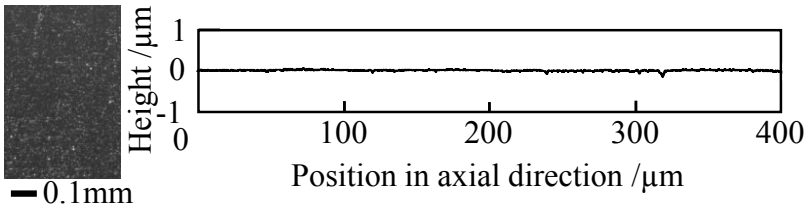

(a) Polished surface, 0.02μmRa, 0.01μmRpk, 0.06μmRvk

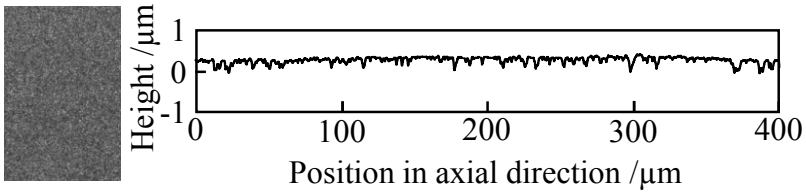

(b) Shot-peened surface, 0.05μmRa, 0.02μmRpk, 0.18μmRvk

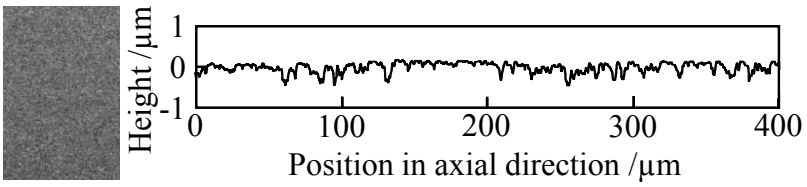

(c) Shot-peened surface, 0.11μmRa, 0.07μmRpk, 0.20μmRvk

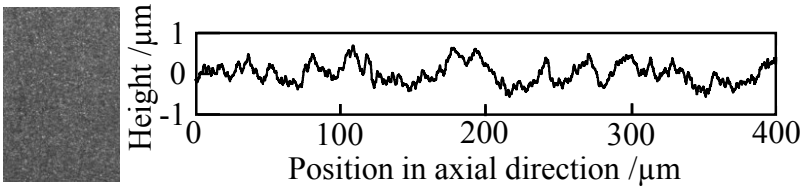

(d) Shot-peened surface, 0.17μmRa, 0.19μmRpk, 0.14μmRvk

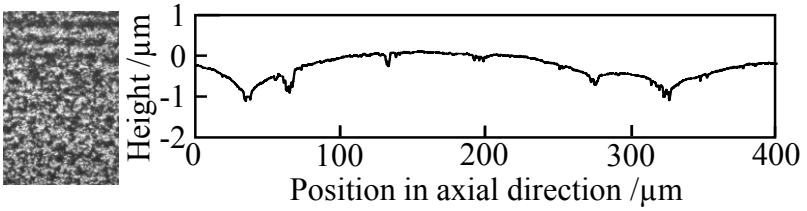

(e) Surface having lubricant pockets, 0.06μmRa, 0.01μmRpk, 0.43μmRvk

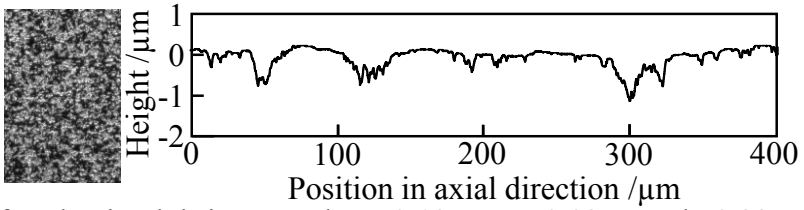

(f) Surface having lubricant pockets, 0.12μmRa, 0.02μmRpk, 0.23μmRvk

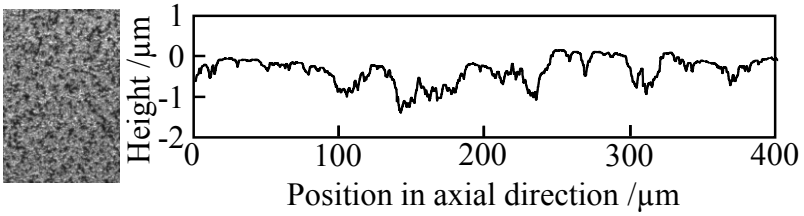

(g) Surface having lubricant pockets, 0.15μmRa, 0.11μmRpk, 0.50μmRvk

Fig. 3.2 Surface shapes of die land.

The pockets for retaining the lubricant on a smooth surface were obtained by shot peening and polishing. In a comparison, the die having a polished surface and shot-peened surfaces were also used. In the shot peening process, first, the uneven surface was formed, and then two steps of removal of protrusion were performed. Alumina, glass, and hard carbide particles with the size about ten micrometres were used as shot-peening materials in each step, respectively. Various surfaces were obtained by changing the shot-peening time and polishing time with micro-size diamond particles. The surface shapes of the die land of each die are shown in **Fig. 3.2**. Surface roughness of the dies was measured at the die land in an axial direction by using a mechanical stylus profiler. The evaluation length was 0.8 mm (ten times as cut-off length) with the cut-off length of 0.08 mm. The arithmetic mean surface roughness Ra, reduced peak height Rpk and reduced valley depth Rvk were examined. The polished surface is very smooth. The shot-peened surface has a large number of irregular shapes with fine diameter and depth. The surface having lubricant pockets has both a flat smooth surface and concave shape pockets.

The surface roughness parameters are shown in **Fig. 3.3**. The core roughness depth Rk is the depth of the roughness core profile. The reduced peak height Rpk is the average height of the protruding peaks above the roughness core profile. The reduced valley depth Rvk is the average depth of the profile valleys projecting through the roughness core profile.

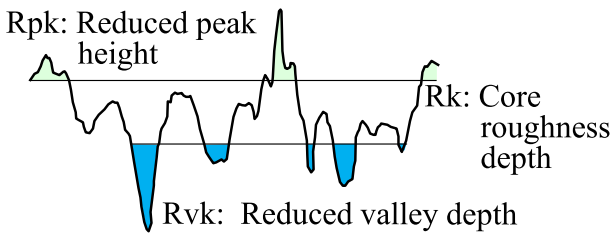

Fig. 3.3 Surface roughness parameters.

The reduced peak height and reduced valley depth in the die land are shown in **Fig. 3.4**. For the shot-peened surface, although the reduced valley depth for retaining the lubricant was large, the reduced peak height being the protrusion was also large with increasing in the arithmetic mean surface roughness. For the surface having the lubricant pockets, the reduced valley depth for trapping the lubricant was large whereas the reduced peak height maintained the same level as that of the polished surface for the arithmetic

mean surface roughness until 0.12μm. And then above that the reduced peak height also increased.

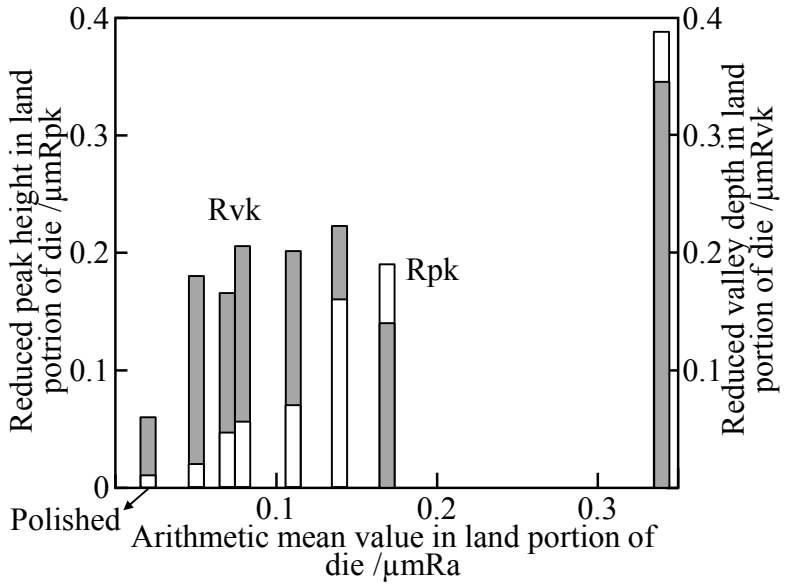

(a) Shot-peened die

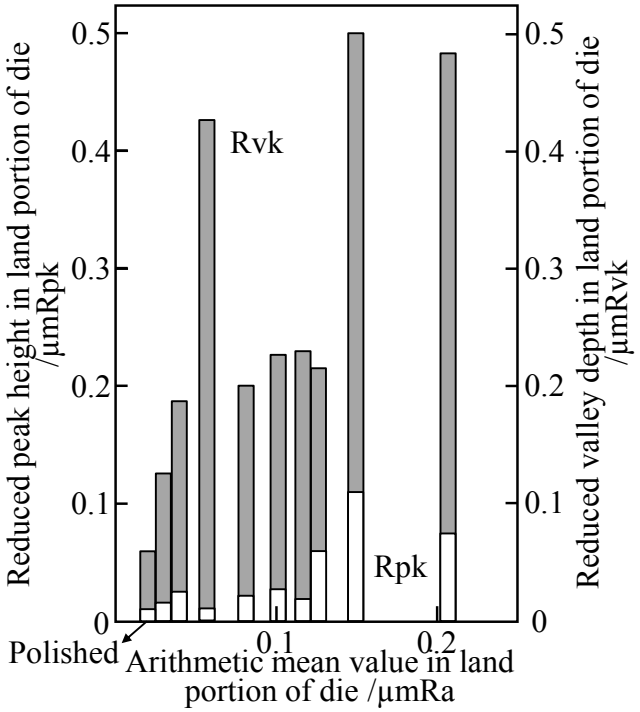

(b) Surface having lubricant pockets

Fig. 3.4 Reduced peak height and reduced valley depth in die land.

The surface shapes of the sidewall of the drawn cup are shown in **Fig. 3.5**. The surface was taken about 20 mm from the bottom corner of the cup. Due to plastic deformation in the deep drawing process, the surface of the cup is roughened and then has a large number of irregularities.

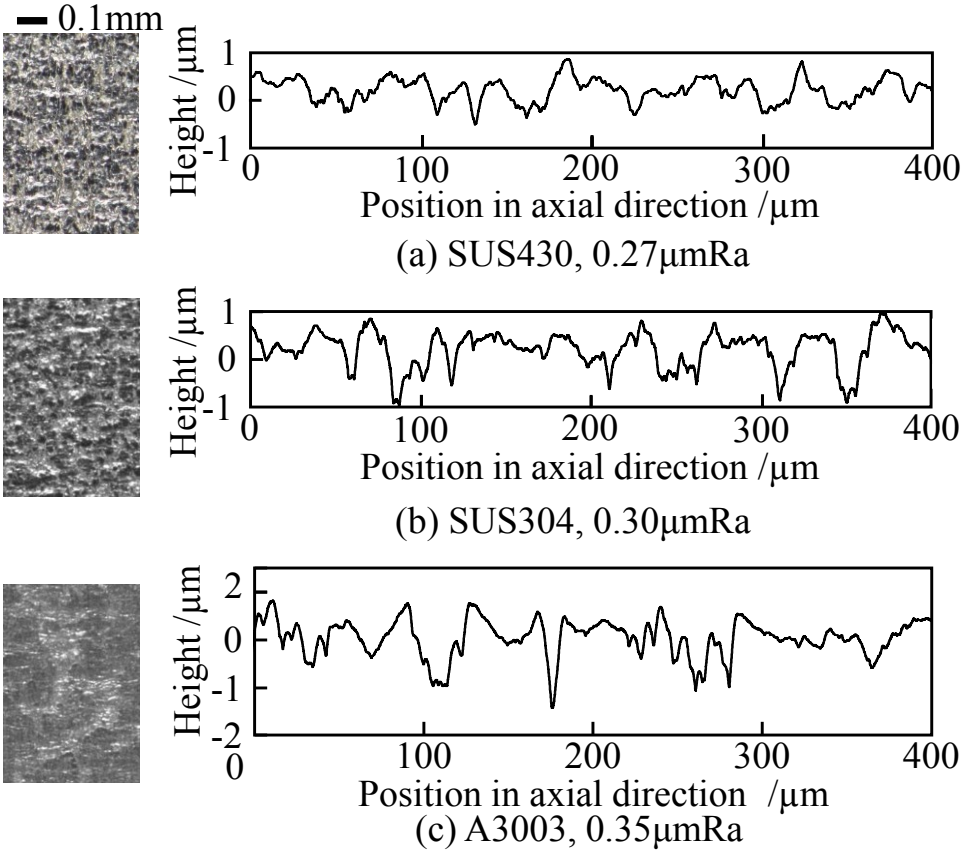

Fig. 3.5 Surface shapes of sidewall of drawn cup.

3.3 Effect of die having lubricant pockets on ironing limit and ironing load

3.3.1 Improvement of ironing limit

The SUS430 cup before ironing and the defects of ironed cups are shown in **Fig. 3.6**. Fig. 3.6 (a) shows the cup before ironing. Fig 3.6 (b) is the ironed cup without the defect. For Fig. 3.6 (c) and (d) there were vertical scratches caused by seizure occurring on the sidewall of the ironed cup. For Fig. 3.6 (d) the fracture of the upper sidewall of the cup also occurred.

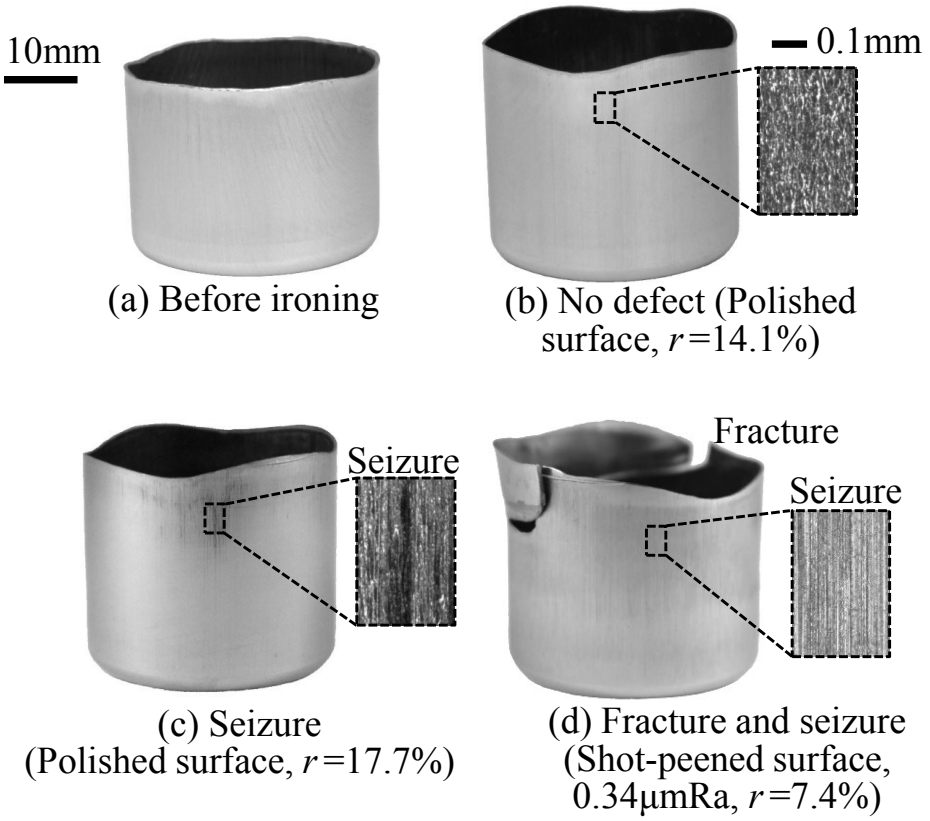

Fig. 3.6 SUS430 cup before ironing and defects of ironed cups.

The ironing limit for the die having the shot-peened surface and the surface having lubricant pockets for SUS430 cups is shown in **Fig. 3.7**. When the ironing ratio increases, the fracture of the cup and the seizure occur for each die surface. The seizure is adhesion of the stainless steel occurring at the die land. For the shot-peened surface with the reduced valley depth about 0.18 μm, the ironing limit was the same as that for the polished surface. With further increasing in the reduced valley depth, the ironing limit cannot be improved, because the reduced peak height also increases. For the surface having the lubricant pockets, when the reduced valley depth was in the range of 0.22 μm to 0.42 μm, the surfaces are composed of concave shaped pockets and the flat smooth surface. The limits of the ironing ratio became high. It is two times as large as the polished surface. In each surface of die, when the reduced peak is higher than about 0.06 μm, the defects are prone to early occur and then the limits of the ironing ratio become low. The surface having the reduced valley depth without protrusions is effective for retaining the lubricant.

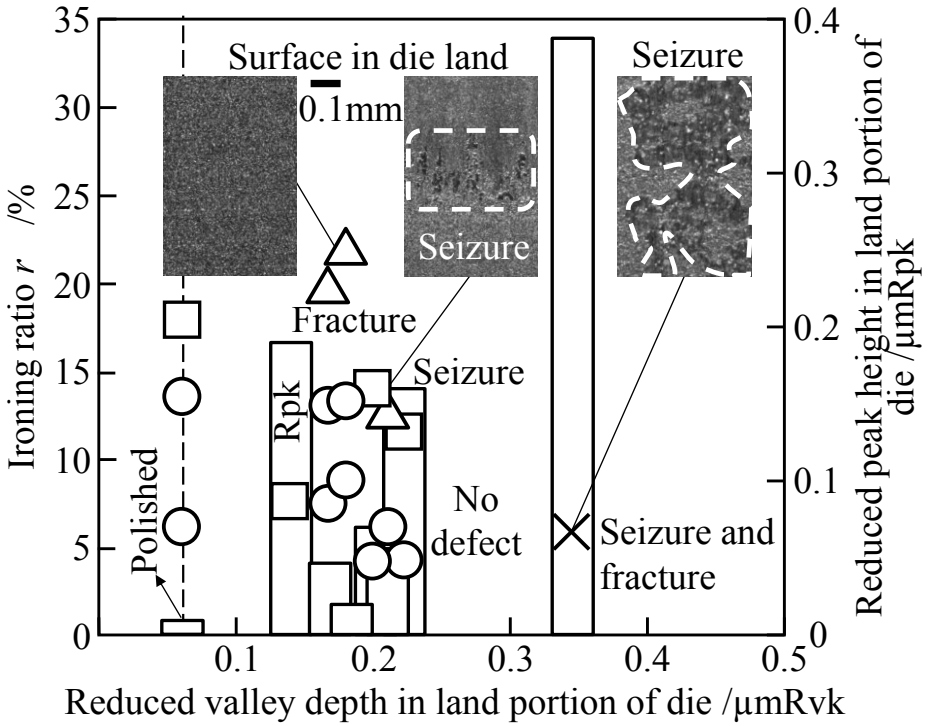

(a) Shot-peened surface

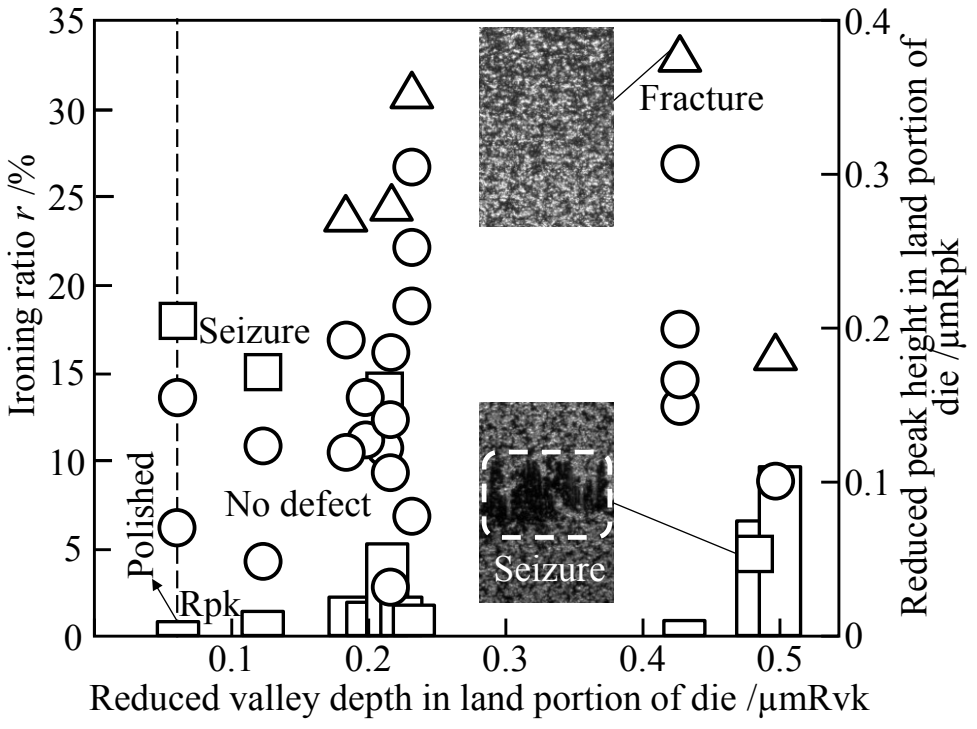

(b) Surface having lubricant pockets

Fig. 3.7 Ironing limit for die having shot-peened surface and surface having lubricant pockets for SUS430 cups.

The ironing limit for the die having the lubricant pockets and A3003 cups is shown in **Fig. 3.8**. Because aluminium alloy possesses low flow stress, the TiCN-based cermet die showed a high ironing limit for A3003 in the previous study, the ironing limit for the A3003 cup is higher than that for the SUS430 cup. For each surface roughness of die, when the ironing ratio increases, the fracture of the cup and the seizure occur. The same as the SUS430 cup, when the reduced valley depth of the surface having the lubricant pockets was about 0.22 μm to 0.42 μm, the ironing limit was improved about 1.2 times larger than the polished surface.

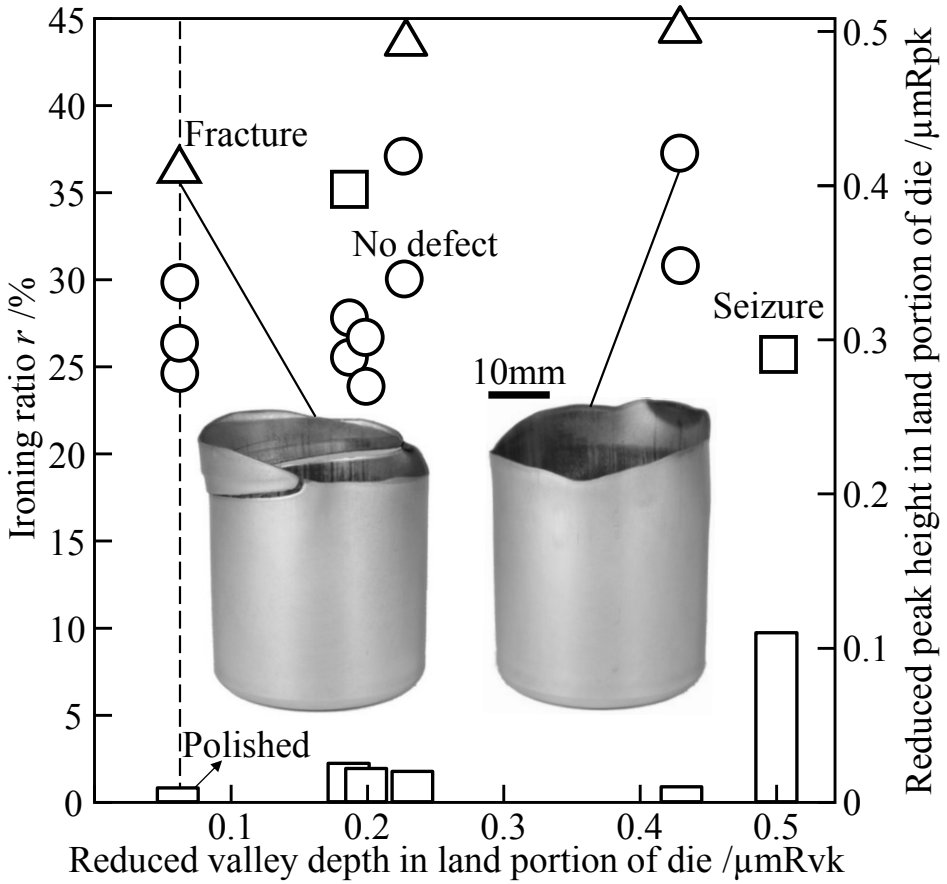

Fig. 3.8 Ironing limit for die having lubricant pockets and A3003 cups.

The ironing limit for the die having the lubricant pockets and the SUS304 cups is shown in **Fig. 3.9**. Due to high strength and high work hardening of SUS304, the ironing limit was lower than that of SUS430 cup as shown in Fig. 3.7. However, with the die

having the lubricant pockets, the forming limit was improved about 1.8 times larger than the polished surface.

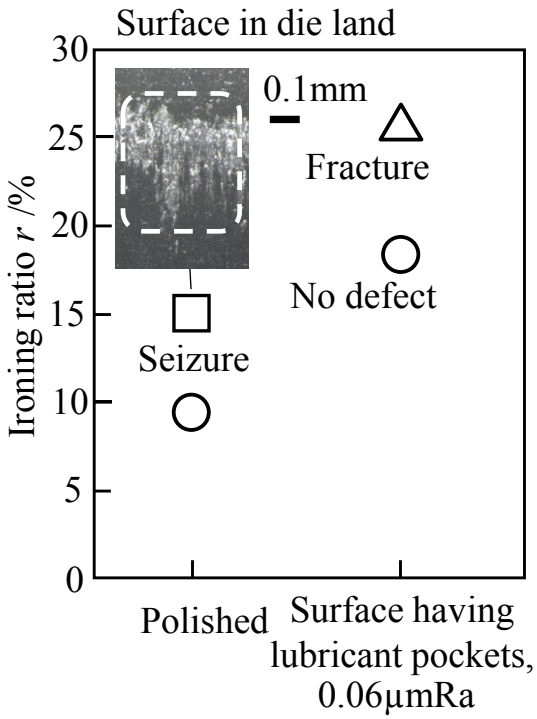

Fig. 3.9 Ironing limit for die having lubricant pockets and SUS304 cups.

3.3.2 Reduction of ironing load

The ironing load-stroke curve for the polished surface and the surface having the lubricant pockets and the SUS430 cups is shown in **Fig. 3.10**. Although the die having the lubricant pockets performed cup ironing at a higher ratio than the polished surface die, the ironing load for the die having the lubricant pockets was slightly lower than that for the polished surface.

The relationship between the average ironing load and the ironing ratio for the SUS430 cups is shown in **Fig. 3.11**. In each surface, the average ironing load increases with the ironing ratio. The average ironing load for the die having the lubricant pockets shows the lowest, for the polished surface die exhibits the largest. By comparison with the polished surface die, with the die having the lubricant pockets the average ironing load is decreased about 20%.

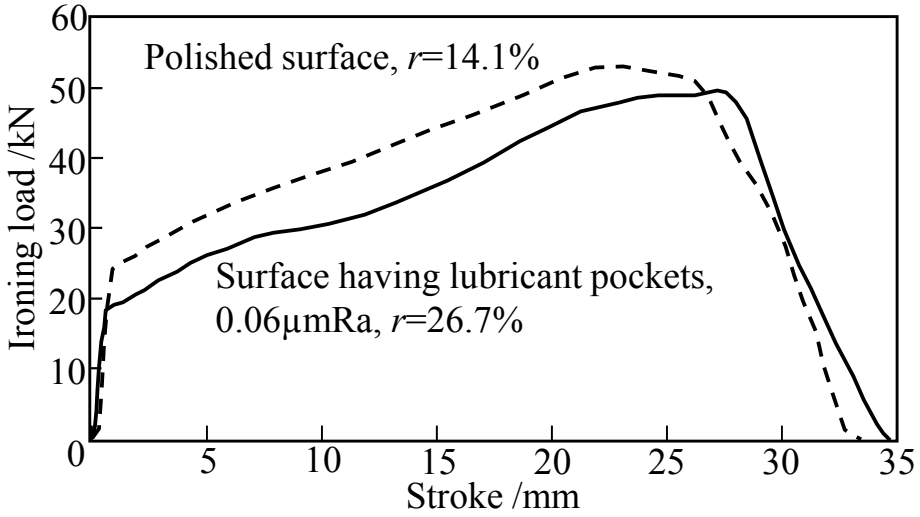

Fig. 3.10 Ironing load-stroke curve for polished surface and surface having lubricant pockets and SUS430 cups.

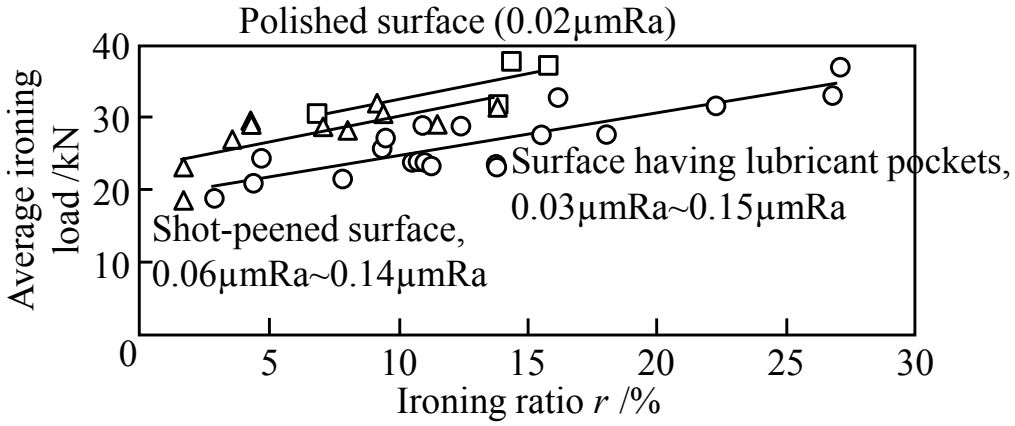

Fig. 3.11 Relationship between average ironing load and ironing ratio for SUS430 cups.

The relationship between the coefficient of friction and the ironing ratio for SUS430 cups is shown in **Fig. 3.12**. The coefficient of friction μ between a die and a cup was calculated by the following equation:

$$\mu = \frac{P_{ave} \tan \alpha}{1.15 \sigma A_f ln\left(\frac{A_0}{A_f}\right)} - \tan \alpha, \quad (1)$$

where, P_{ave} is the average ironing load, α is the semi-cone angle of a die, σ is the tensile strength of the sheet, A_0, A_f are cross-sectional area of cup before and after ironing, respectively [120]. The coefficient of friction increased with the ironing ratio. The coefficient for the die having the lubricant pockets was the smallest because escaping of the lubricant from the pockets reduced friction. Since the lubricant on the polished surface die squeezed out easily, this die exhibits the largest coefficient of friction.

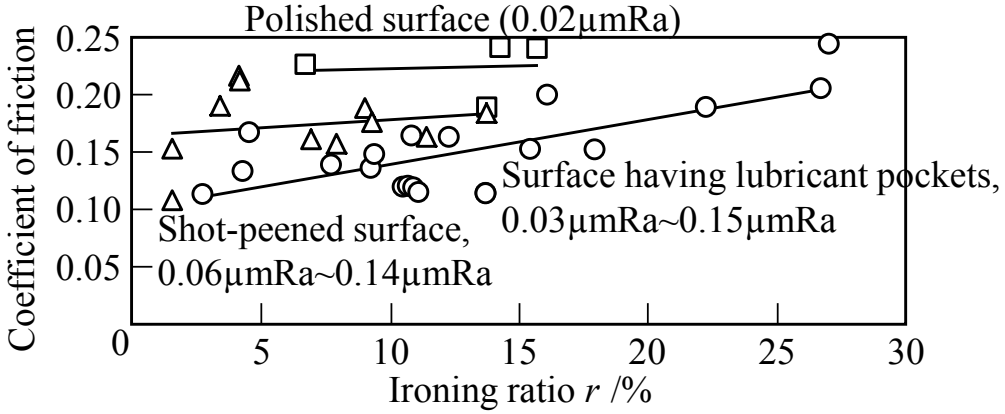

Fig. 3.12 Relationship between coefficient of friction and ironing ratio for SUS430 cups.

3.4 Lubrication mechanism of die having lubricant pockets

3.4.1 Remaining lubricant on sidewall of ironed cup

Since the friction is reduced by the occurring of a thick lubricating film induced by a large number of the lubricant pockets of the die surfaces, the average ironing load with the shot-peened surface and the surface having the lubricant pockets decreases as shown in Fig. 3.11. However, the friction is slightly lowered for the surface that was only shot-peened because of its large local asperities. The friction with the surface having the lubricant pockets without the asperities is significantly decreased. Consequently, the seizure is prevented. Therefore, the remaining lubricant on the cup sidewall and the die land after ironing was investigated by mixing fluorescence powders in the lubricant and using ultraviolet rays [87].

The observation of the remaining lubricant on the ironed cup surface by fluorescence powders and ultraviolet rays is shown in **Fig. 3.13**. The lubricant mixed with fluorescence

powders irradiating to ultraviolet rays was applied to the cup sidewall. After ironing, the cup and the punch was pushed through the die and then dropped onto the die plate. The surface of the dropped cup irradiated with ultraviolet rays having the peak wave length of 375 nm, and then the exposure of the remaining fluorescence powder-mixed lubricant was photographed by a camera. The mixing ratio of fluorescence powders having an average particle size of 5 μm in the lubricant was 5wt%.

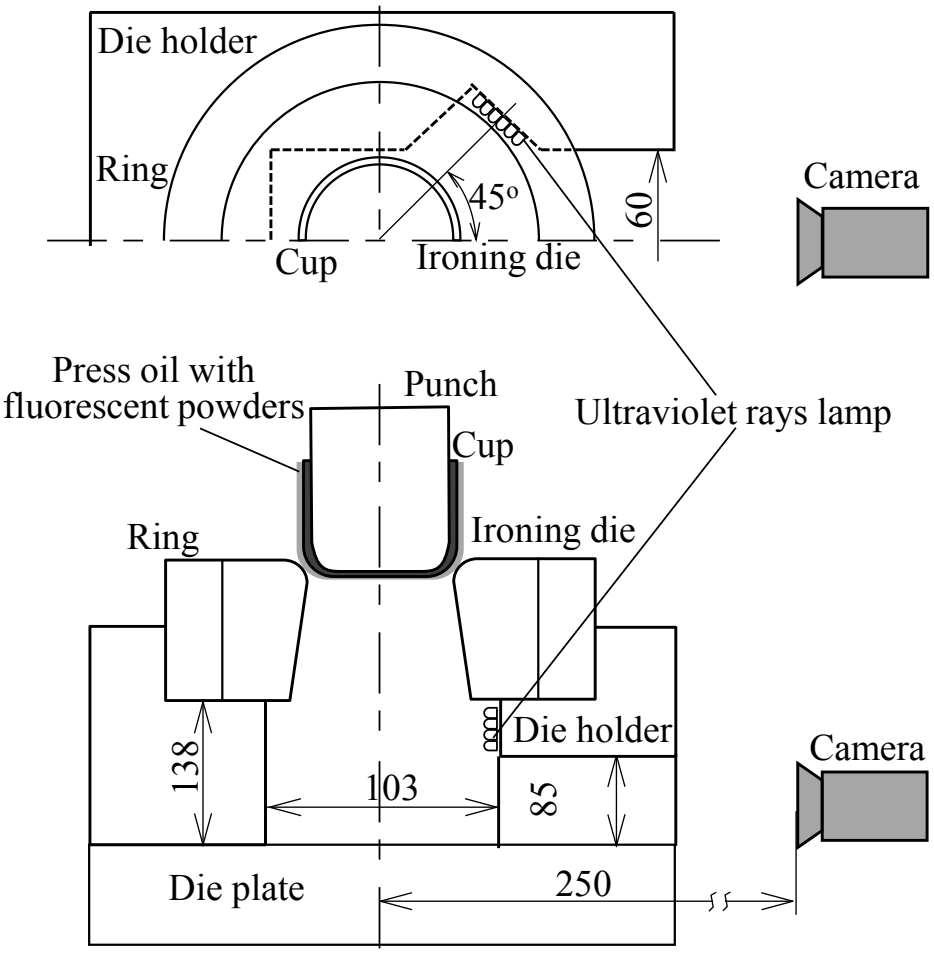

Fig. 3.13 Observation of remaining lubricant on ironed cup surface by fluorescence powders and ultraviolet rays.

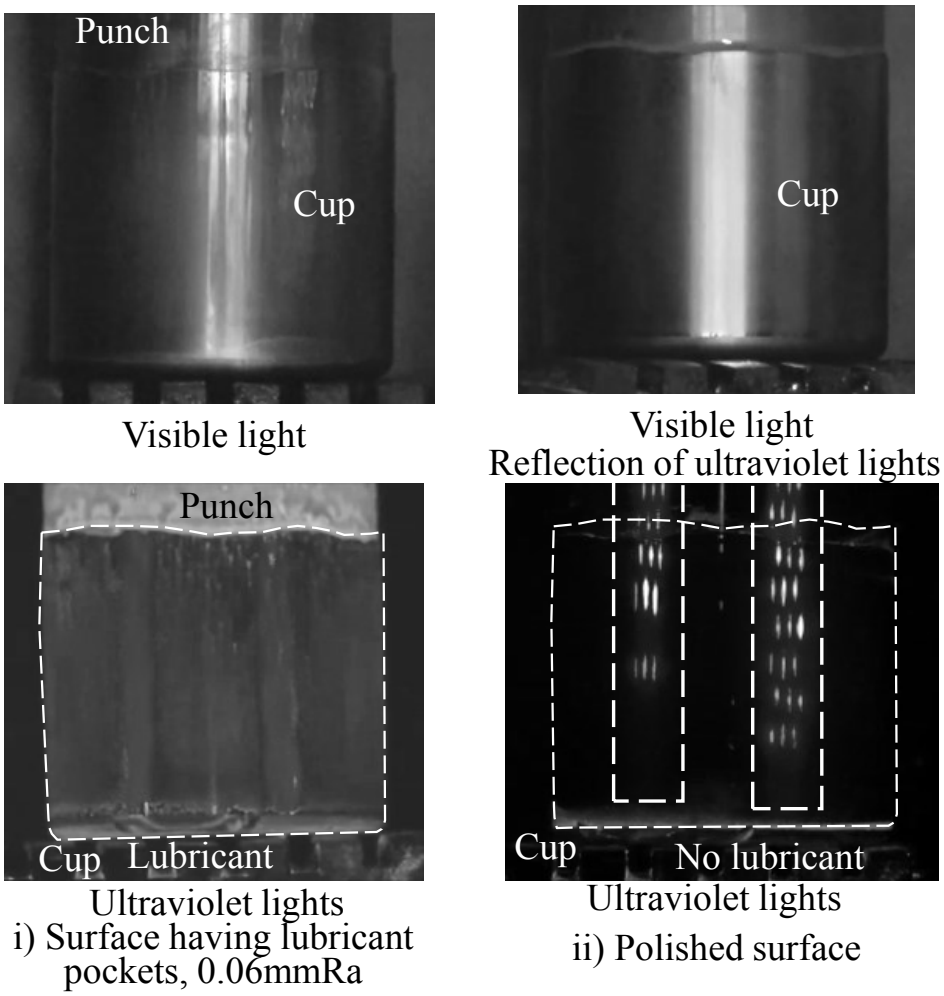

Fig. 3.14 Remaining lubricant on SUS430 cups and die surfaces after ironing.

The remaining lubricant on the SUS430 cups and die surfaces after ironing are shown in **Fig. 3.14**. After ironing, the die was taken out from the die set and then the die surface was observed by irradiation with ultraviolet rays. At the surfaces of the cup and die with the surface having the lubricant pockets, the bright white luminous area of the remaining

fluorescence powder-mixed lubricant was observed. On the other hand, on the cup sidewall with the polished surface, there was almost no the bright white luminous area of the remaining lubricant apart from the reflection of the ultraviolet lights. From the observation of the remaining lubricant on the cup sidewall, with the surface having the lubricant pockets showed the large amount of the lubricant retained.

The SUS430 cups and die surfaces after ironing without the lubricant are shown in **Fig. 3.15**. Before ironing, the surfaces of the cup and die were degreased by acetone. Seizure occurs severely in the die land of both the polished surface and the surface having the lubricant pockets as well as in the sidewall the ironed cup. From this, even with the lubricant pockets, high lubrication cannot occur if there is no any lubricant.

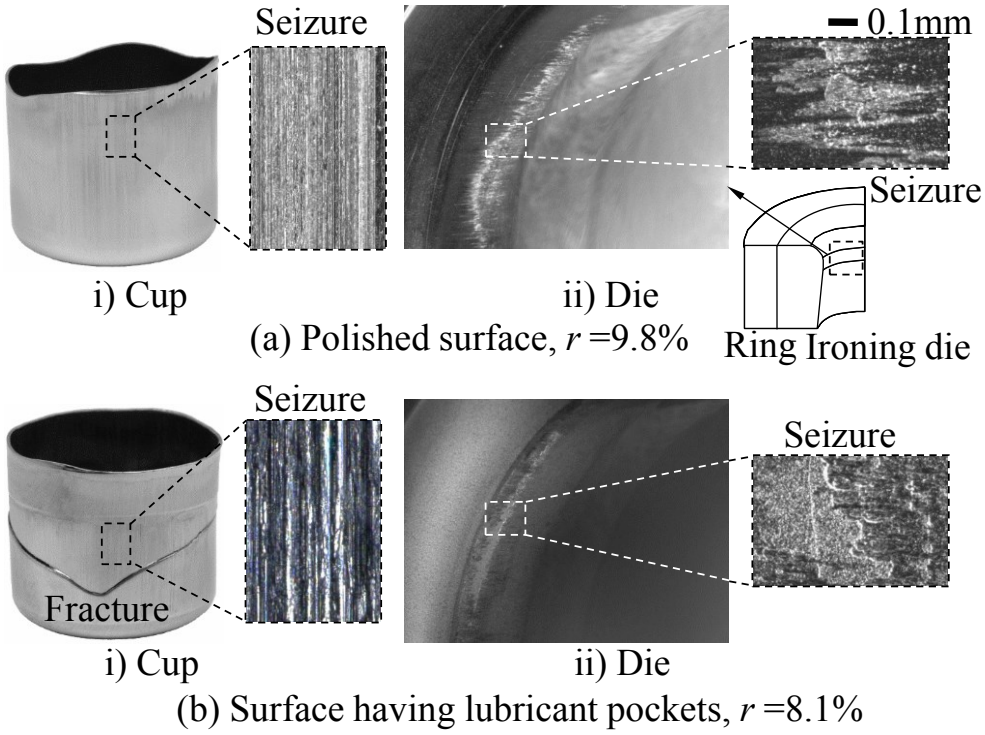

Fig. 3.15 SUS430 cups and die surfaces after ironing without lubricant.

3.4.2 Repeated ironing

Deep drawing and ironing of the SUS430 sheets in the same strike using the die having the lubricant pockets was repeatedly conducted with the die set as shown in **Fig. 3.16**. The effectiveness of the surface having the lubricant pockets was verified. Pre-

lubricating oil was applied to the sheet and then the process was repeatedly performed until the number n = 100 without polishing of the die surface. Two TiCN-based cermet dies with the polished surface and with the surface having the lubricant pockets with 0.06 μmRa were employed. The ironing ratio was set at r = 9%. The forming was performed with a speed of 150 mm/s.

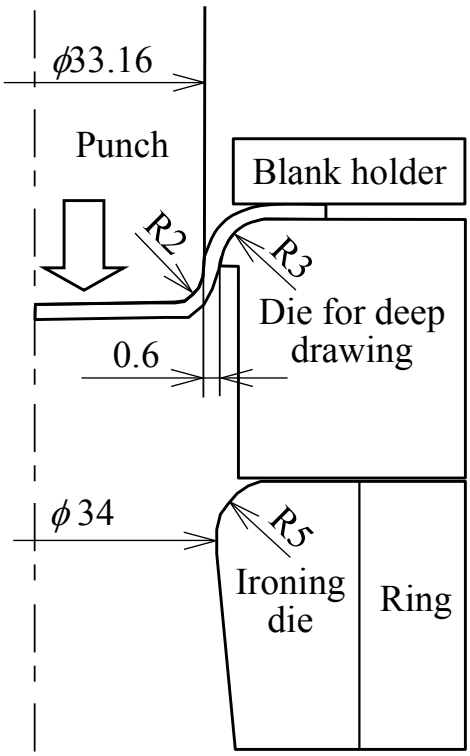

Fig. 3.16 Repeated ironing condition for SUS430 blank and r=9%.

The die surfaces and cups after repeated ironing are shown in **Fig. 3.17**. For the polished surface at n=100, seizure slightly occurred on the die land and the upper sidewall of the cup. But for the surface having the lubricant pockets, seizure was prevented.

The history of the maximum ironing loads in repeated ironing is shown in **Fig. 3.18**. Although there are some variations for each surface, the maximum ironing load with the die having the lubricant pockets is lower than that with the polished surface. It is due to the surface having the lubricant pockets can improve the lubrication in repeated ironing of 100 times. Thus friction is lowered.

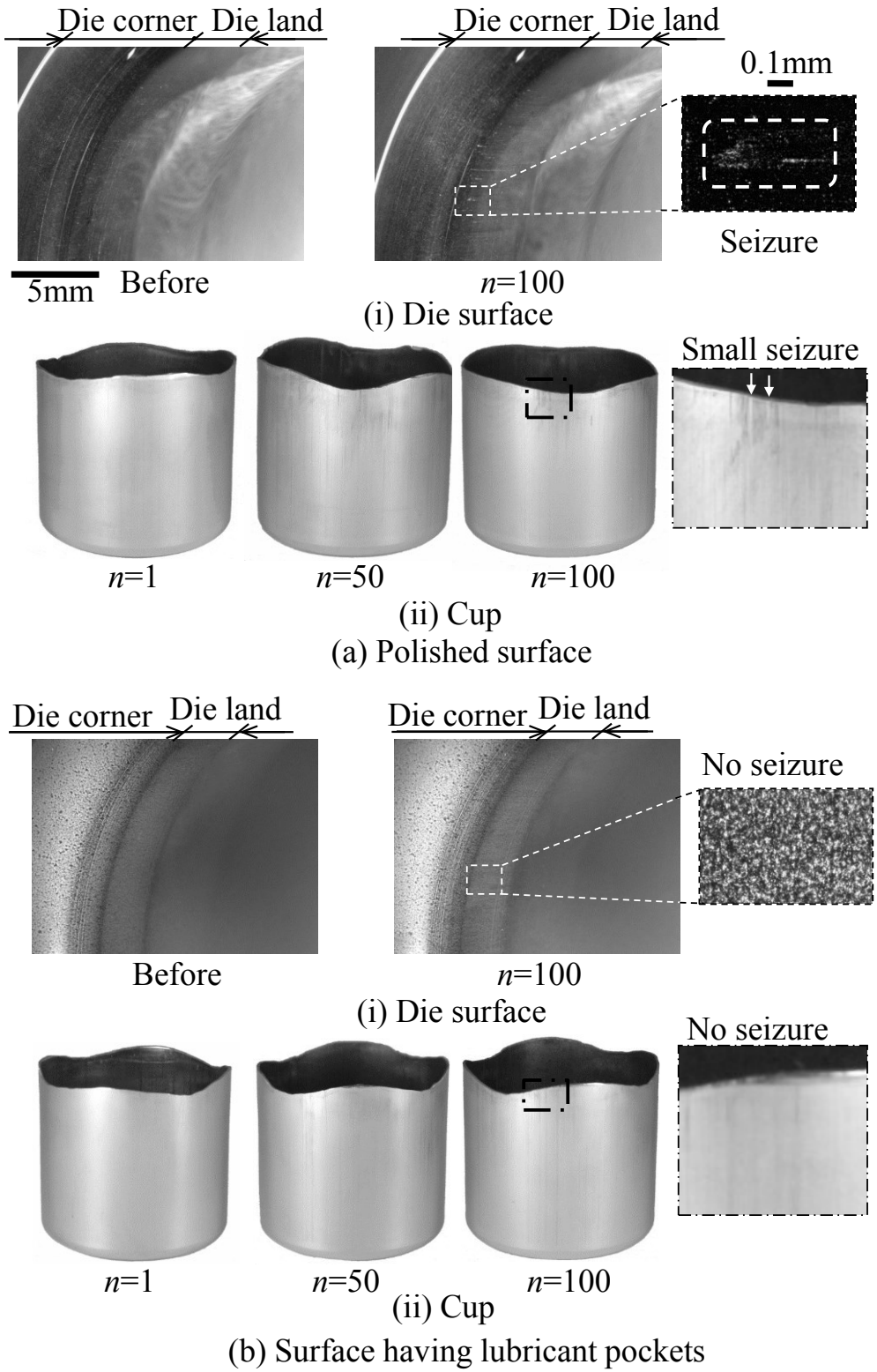

Fig. 3.17 Die surfaces and cups after repeated ironing.

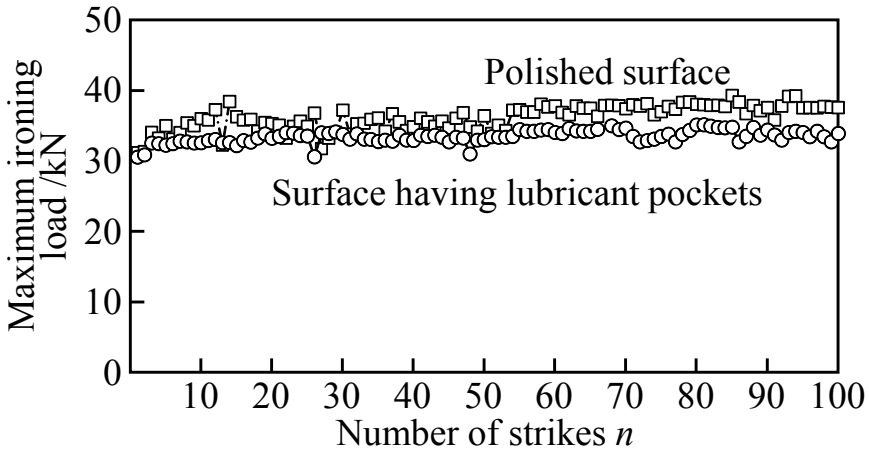

Fig. 3.18 History of maximum ironing loads in repeated ironing.

3.5 Conclusions

The TiCN-based cermet dies having fine lubricant pockets made by lapping of shot-peened surfaces was utilised to reduce friction in ironing of stainless steel and aluminium alloy drawn cups. The effect of dies having fine lubricant pockets with different surface roughness on the ironing limit was investigated. The lubrication mechanism for improving the ironing limit with the die having the lubricant pockets was determined, and the following results were obtained:

1. Either with the shot-peened surface or with the surface having the lubricant pockets, the defect early occurred at a low ironing ratio when the reduced peak height was more than about 0.06 μm. With the surface having the lubricant pockets for the reduced valley depth in the range of 0.22 μm to 0.42 μm, the ironing limit was improved about 2 times larger than the polished surface.
2. The average ironing load for the surface having the lubricant pockets was the lowest, whereas for the polished surface was the highest. The average ironing load in ironing of SUS430 cup with the surface having the lubricant pockets was reduced about 20% compared to the polished surface.
3. The remaining lubricant on the sidewall of the ironed cup with the surface having the lubricant pockets became greater than that with the polished surface. For the die having the lubricant pockets, the large amount of the lubricant was able to be retained during the process.

4. In repeated ironing at the strike number of 100, for the polished surface, seizure slightly occurred on the die land and the upper sidewall of the cup. But for the surface having the lubricant pockets, seizure was prevented and the ironing load was also lower than for the polished surface.

Chapter 4

Lubrication behaviours in ironing of stainless steel cup with die having lubricant pockets

4.1 Introduction

Effective lubrication systems bring about low friction levels. Liquid lubricants interpose an adherent film between the die and cup. This film minimises adhesion and interactions of die surface with the other which increases die life by reducing wear and improves product quality by reducing the incidence of seizure and other surface defects. Therefore, lubrication is vitally important in an ironing process. To reduce friction and to prevent the occurrence of seizure in ironing, liquid lubricants are conventionally used. Bay et al. [54] reviewed lubrication mechanisms in ironing of sheet metal forming processes. In hydrostatic lubrication, a part of the normal contact load between the tool and workpiece is supported by the hydrostatic pressure of the trapped lubricant generated in the pockets. In hydrodynamic lubrication, the permeation of the trapped lubricant into the tool-workpiece interface develops the thin lubricant film. Mizuno and Okamoto [55] demonstrated during forming, not only the hydrostatic but also hydrodynamic lubrication occurs. Kudo et al. [56] exhibited the occurrence of the hydrodynamic lubrication in cold sheet drawing is influenced by the drawing speed, the lubricant viscosity and the die angle. The micro-hydrodynamic lubrication induced by the escape of the lubricant from the pockets was directly observed through a transparent die in strip drawing. The degree of reduction, drawing speed and lubricant viscosity have an influence on the escaping lubricant from the pockets [57, 58]. Although Kawai et al. [27] showed that the seizure is prevented by the appropriate viscosity of lubricants in ironing of aluminium cups, it is not easy for stainless steel cups to be ironed.

Since the use of structured sheet surfaces providing surface topography with lubricant pockets facilitates the lubrication in the forming processes. The sheet-surface structures have been developed to improve the tribological conditions of sheet forming processes [62]. The structured sheet surface produced by transferring of roller surfaces prepared by

electron beam texturing in skin pass rolling was introduced to the deep drawing process. Because the lubrication is assisted during the process, the friction decreases with increasing in drawing speed [64]. Furthermore, the tool surface seldom changes. Applying the texturing on the tool surface facilitates the forming process even after long-running use. Geiger et al. [68] introduced the texturing using an excimer laser radiation to the surface of TiN-coated punch for cold forging. Popp and Engel [69] showed the pressurization of the entrapped lubricant in the well-designed micro pockets improved the tool life. During the process, tool wear was reduced by the wiped lubricant from micro pockets [71]. Aramaki et al. [76] showed the die treated by the combination of shot-peening and nitriding improves seizure resistance in the drawing test of high strength steel sheets because of its lubricating effect. In the aspect of reduction in friction by assisting in lubrication, the dies having fine lubricant pockets and the cups having roughening surface that can retain the lubricant are able to minimise seizure.

In ironing, the presence of an effective lubricant film minimises adhesion and interactions of die surface with the cup surface, thus reduces friction and prevents the direct die-to-cup contact. However, this lubricant film can break down. The sliding surfaces then may wear and score severely. The behaviour of the liquid lubricant at the interfaces during ironing is important. For monitoring the state of lubrication in the machine elements, Anderson et al. [79] used the transmission and reflection of ultrasonic waves to monitor the oil-films in shaft seals. Zhang et al. [82] applied ultrasonic reflection coefficient measurements to monitor the oil-film thickness in a range of bearings. However, this approach is still difficult to apply to the forming processes with complex-shaped dies. Azushima et al. [85] developed the direct observation using a transparent die and a fluorescence measurement. The effect of the surface topography of workpiece on the pressure dependence of the coefficient of friction in sheet metal forming was examined. This method was also employed to measure the oil film thickness at the interface between the tool and the workpiece in lubricated upsetting [86, 87].

In previous work, the ironing limit of stainless steel drawn cups was improved by using the TiCN-based cermet die and then a TiCN-based cermet die with a surface having lubricant pockets consisting of the smooth flat and pocket portions, brought about a high ironing limit. However, the state of lubrication between the die-cup interfaces in ironing with the die having lubricant pockets is not clarified. The condition for reducing friction is

still unclear. Therefore, in the present study, the measurement of the film thickness of the remaining lubricant on the sidewall of the ironed cup was employed to clarify the lubrication behaviours in ironing with the die having lubricant pockets. The effects of conditions of the ironing process and lubrication on the thickness of the remaining lubricant were examined. Moreover, the situation of seizure growth in repeated ironing with the die having lubricant pockets was investigated.

4.2 Ironing conditions with die having lubricant pockets and measurement method of thickness of remaining lubricant on sidewall of ironed cup

4.2.1 Ironing conditions and surface having lubricant pockets

The sheets used for drawing and ironing processes are ferritic stainless steel SUS430 having 0.6 and 66 mm in thickness and diameter, respectively. The mechanical properties of sheets obtained from the tensile test are shown in **Table 4.1**.

Table 4.1 Mechanical properties of stainless steel SUS430 sheets.

Sheet	Tensile strength /MPa	Elongation /%	*n*-value	*r*-value
SUS430	547	25.7	0.20	1.17

To investigate the effect of process conditions on the ironing limit in ironing with the die having the lubricant pockets, single ironing was performed as shown in **Fig. 4.1.** The drawn cup was mounted to the punch and then was ironed through the die. The inside diameter of ironing dies is 34 mm. To change the ironing ratio, the clearance between the die and punch is changed by the punch diameter d_p. The outer diameter and height of the drawn cup were between 34.3 and 34.5 mm and between 25.4 and 25.9 mm, respectively. The ironing ratio r was determined by a difference between the initial thickness of the blank and the average wall thickness of the ironed cup divided by the initial thickness.

A mineral oil containing a chlorine-based extreme-pressure additive having high seizure resistance in forming of the stainless steel sheet with a kinematic viscosity of 2.99 mm^2/s at 40 °C was applied [36]. In addition, a mineral oil containing a sulphur-based extreme-pressure additive having less environmental effects with a kinematic viscosity of

95.74 mm^2/s was used [54]. The amount of the lubricant which was about 370 $\mu g/mm^2$ was applied on the cup and die surfaces. The ironing speed v of 100 mm/s was used as a reference speed and the ironing speed v of 10 and 150 mm/s was utilised for comparison.

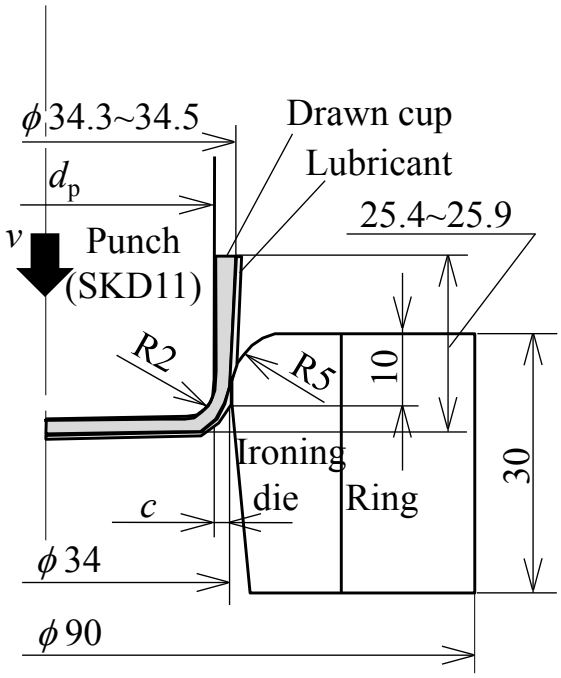

Fig. 4.1 Single ironing conditions.

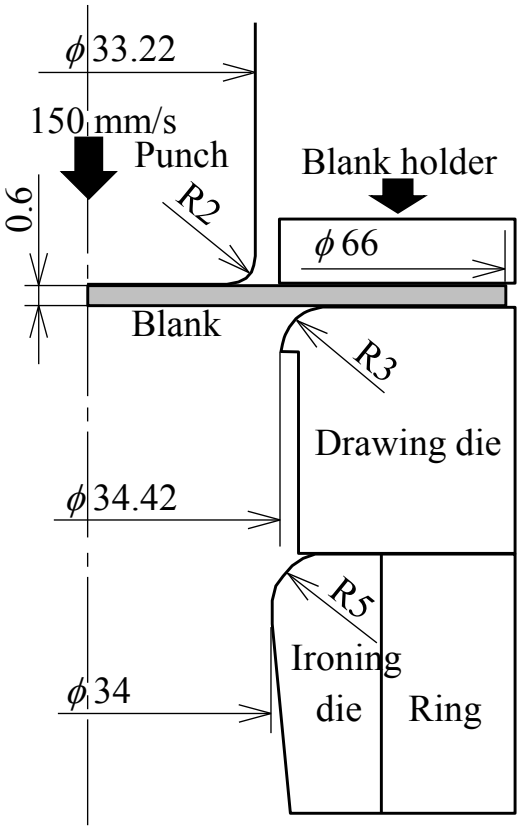

Fig. 4.2 Repeated ironing conditions.

The repeated ironing conditions are shown in **Fig. 4.2**. In an operation, the blank was deep drawn, ironed and then was taken out by the stripper in the same strike. Because the blanks were manually fed into the die, the number of strikes per minute of the process was about 3. The repeated ironing process was continuously performed until the maximum number of strikes without polishing of the die during the process.

The dies were made of the TiCN-based cermet for both single ironing and repeated ironing. The main component of the cermet is the low friction TiCN powders bounded with a nickel binder by the sintering process. The Young's modulus and hardness of the TiCN-based cermet are 410GPa and 1550HV50, respectively.

To attain low friction, the surface having the lubricant pockets was introduced to a high hardness cermet die. The surface having the lubricant pockets was treated by shot peening and then by lapping. Three steps of shot peening using alumina, glass and hard carbide particles with the size about ten micrometers as shot-peening materials were employed, respectively. Finally, the surface was polished by diamond paste. The arithmetic mean surface roughness at the die land became 0.06μmRa. **Fig. 4.3** and **Table 4.2** show the surface shape of the die having the lubricant pockets. After the asperities of the shot-peened surface were removed by polishing, they became flat portions. In addition, the valleys became micro-lubricant pockets. The reduced peak height and reduced valley depth are 0.01μmRpk and 0.43μmRvk, respectively. The depth, width and edge angle of pockets are 0.4~1.0 μm, 9~15 μm and 5~15° respectively. The ratio of pocket area is about 30% of total die land area. For the polished surface die, its surface was very fine.

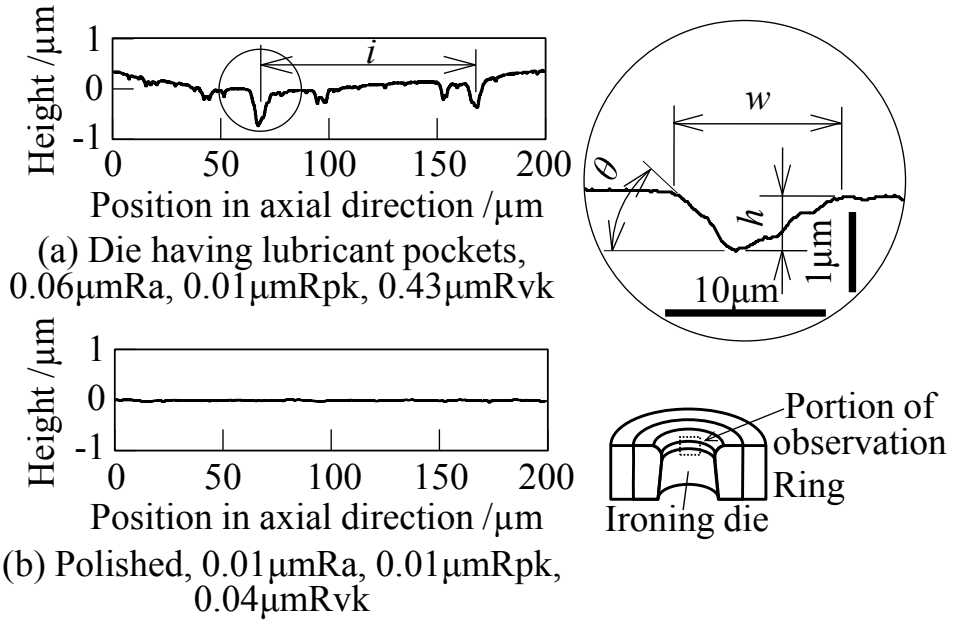

Fig. 4.3 Surface shapes and average surface roughness of die land in axial direction.

Table 4.2 Shape of lubricant pockets of die having lubricant pockets.

Parameters	Value
Pocket depth h /μm	0.4~1.0
Pocket width w /μm	9~15
Average distance between pockets i /μm	50~200
Angle of edge of pockets θ /°	5~15
Ratio of pocket area /%	25~30
Reduced peak height /μmRpk	0.01
Reduced valley depth /μmRvk	0.43

4.2.2 Measurement method of thickness of remaining lubricant on sidewall of ironed cup

A measurement method of the thickness of the remaining lubricant on the outer sidewall of the ironed cup using a fluorescence oil and ultraviolet rays is shown in **Fig. 4.4.** Before ironing the lubricant mixed with the fluorescence oil irradiating to ultraviolet rays was applied to the sidewall of the drawn cup. The cup was ironed and then dropped onto the die plate. The fluorescence oil-mixed lubricant luminesced immediately to ultraviolet rays. Thus, the thickness of the remaining lubricant on the sidewall of the ironed cup was measured by a camera. The mixing ratio of the fluorescence oil in the lubricant was 1wt%. The conditions of the camera were set at ISO400, F5.6 and shutter speed of 1/10s.

In order to quantitatively measure the film thickness of the remaining lubricant on the sidewall of the ironed cup, the method for calibrating brightness to the thickness of the luminous remaining lubricant were conducted as shown in **Fig. 4.5**. A spherical steel ball with a diameter of 38.1 mm and a planar glass slide were attached together, and next the fluorescence oil-mixed lubricant was applied between their interfaces, and then they were maintained in the same environmental conditions as the ironing process. The pictures of the luminous fluorescence oil-mixed lubricant were taken by a camera at the same distance as ironing. Where, t is the thickness of the lubricant between the glass slide and steel ball, R is a radius of the steel ball and l is the distance from the centre. The film thickness of the lubricant was calculated using the following equation:

$$t = R - \sqrt{R^2 - l^2} \tag{1}$$

The calibration curves of the lubricant containing the chlorine or sulphur additive are shown in **Fig. 4.6.** The film thickness of the lubricant at each position from the centre of the contacting interface and the brightness of the luminous lubricant were plot together. The equations for converting the brightness to the thickness for the lubricant containing the chlorine or sulphur additive are shown in equation (2) and (3), respectively.

$$t_c=0.001b^2+0.01b+0.07\ \mu m \quad (2)$$

$$t_s=0.004b^2+0.02b+0.24\ \mu m \quad (3)$$

where, t_c, t_s are the film thicknesses of the lubricant containing the chlorine or sulphur additive and b is the brightness of the luminous fluorescence oil-mixed lubricant.

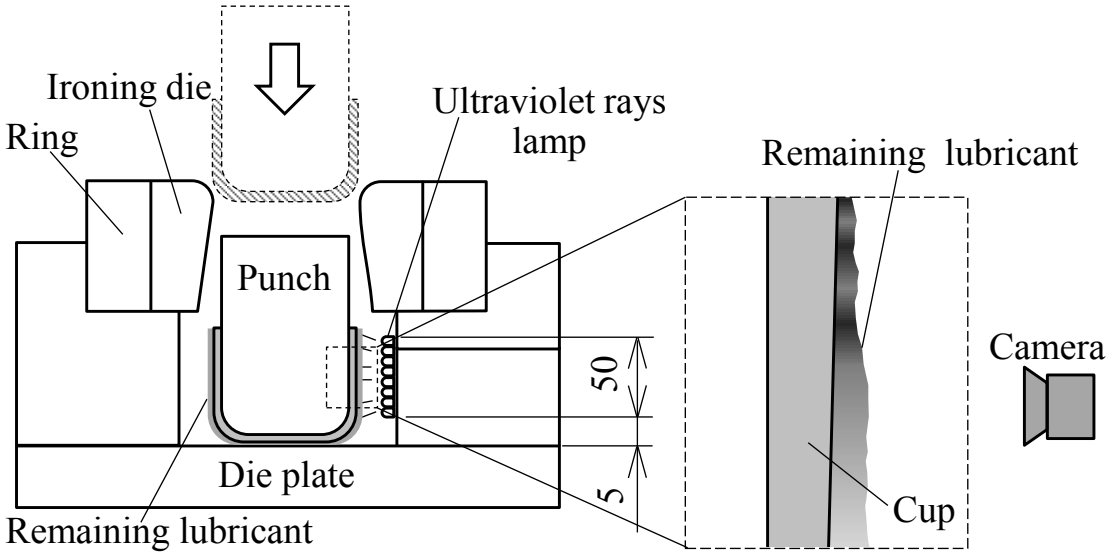

Fig. 4.4 Measurement of thickness of remaining lubricant on outer sidewall of ironed cup using fluorescence oil and ultraviolet rays.

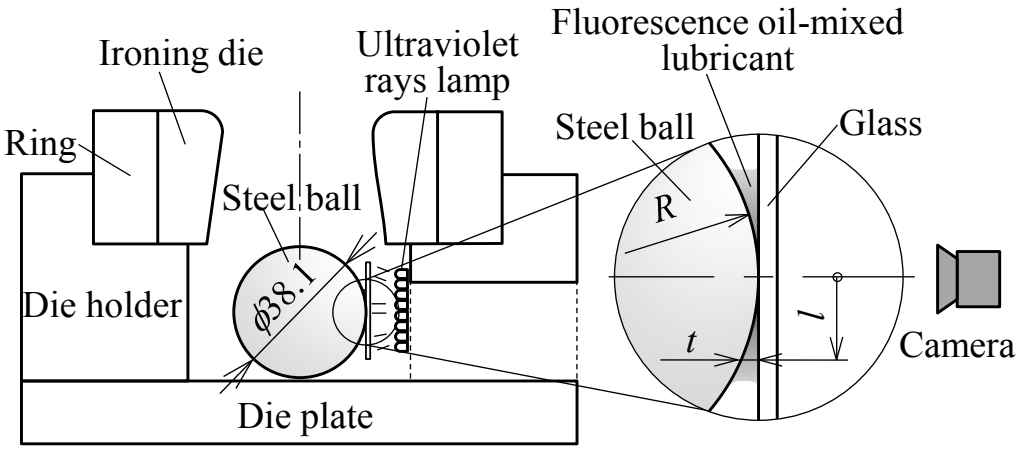

Fig. 4.5 Calibration for measuring thickness of remaining lubricant.

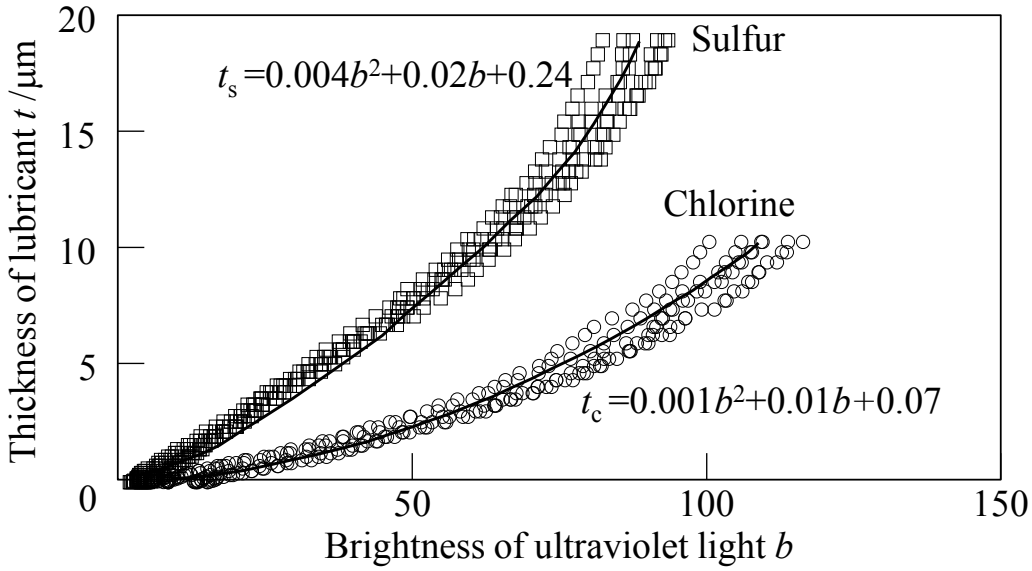

Fig. 4.6 Calibration curves of lubricant containing chlorine or sulphur additive.

4.3 Lubrication conditions

4.3.1 Effects of lubricants on ironing limit of die having lubricant pockets

The appearance of the ironed cups is shown in **Fig. 4.7**. Although no defect occurred with the die having the lubricant pockets for the lubricant containing the chlorine additive. For the lubricant containing the sulphur additive, seizure took place on the sidewall of the

ironed cup. With the die having the polished surface for each lubricant, seizure occurred on the sidewall of the ironed cups.

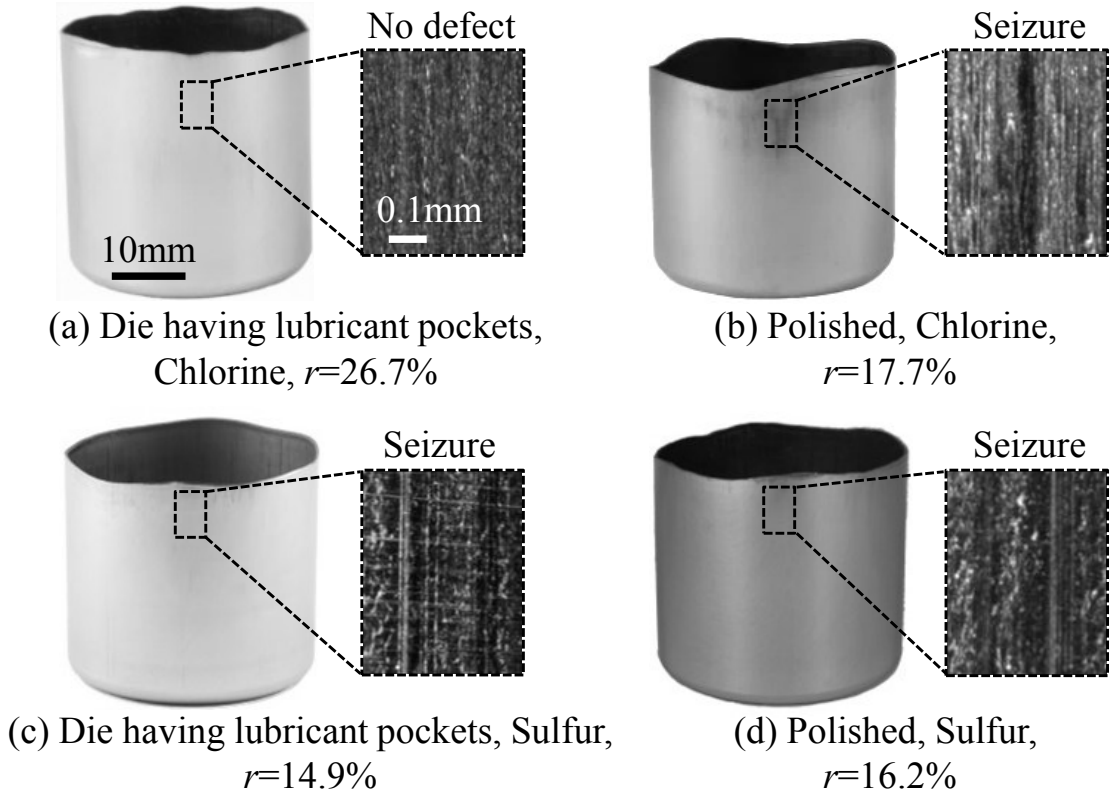

Fig. 4.7 Appearance of ironed cups.

The effect of extreme-pressure additives on the ironing limit for the ironing speed v=100mm/s is shown in **Fig. 4.8**. For the lubricant containing the sulphur additive, the ironing limit of the die having the lubricant pockets and the die having the polished surface are the same. But for the lubricant containing the chlorine additive with a high chemically active, the ironing limit of each die was higher than that in the case of the lubricant containing the sulphur one. The good lubrication performance of the lubricant containing the chlorine additive is attributed to the chemical activity of the chlorine with all the main components of stainless steel. The lubricant containing the chlorine additive enforces the formation of a thick oxide layer [36].

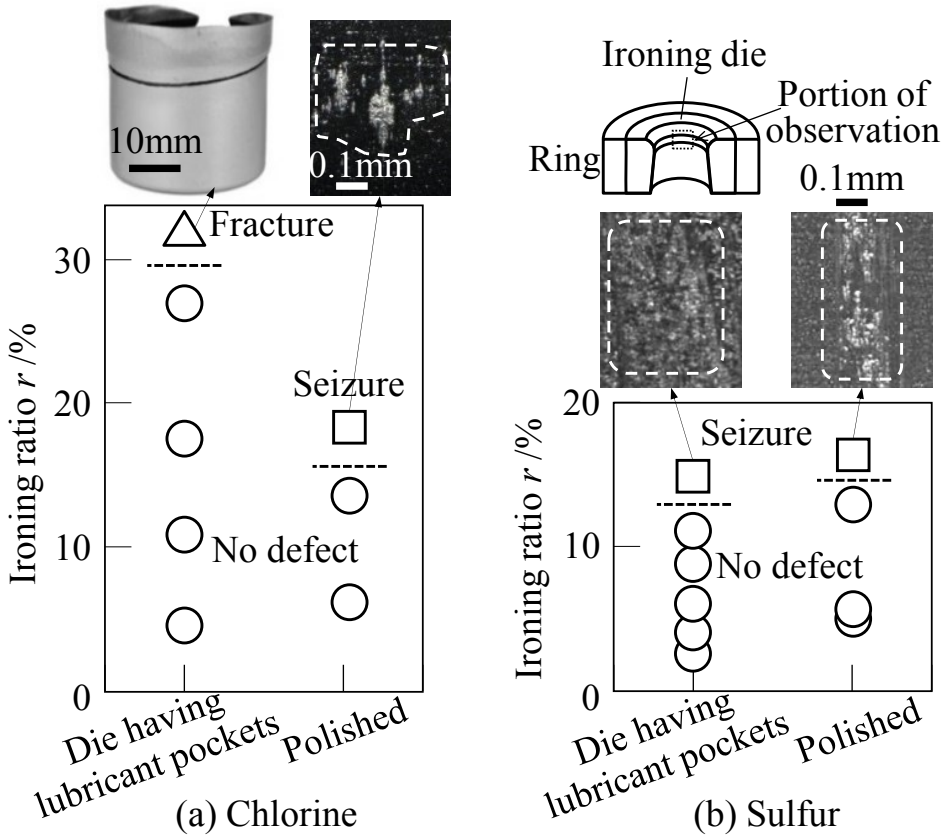

Fig. 4.8 Effect of extreme-pressure additives on ironing limit for v=100mm/s.

The distribution of the film thickness of the remaining lubricant on the sidewall of the ironed cup for v=100 mm/s is shown in **Fig. 4.9**. For each die and each lubricant, although the film thickness of the remaining lubricant near the bottom of the cup was thick, in the upper end of the cup where forming is severe, the film thickness becomes thin. Employing the lubricant containing the chlorine additive with the die having the lubricant pockets, the film thickness of 3μm distributes constantly along the upper portion of the sidewall of the ironed cup. But for other conditions, only little amount of the lubricants remained and the film thickness was less than 1 μm.

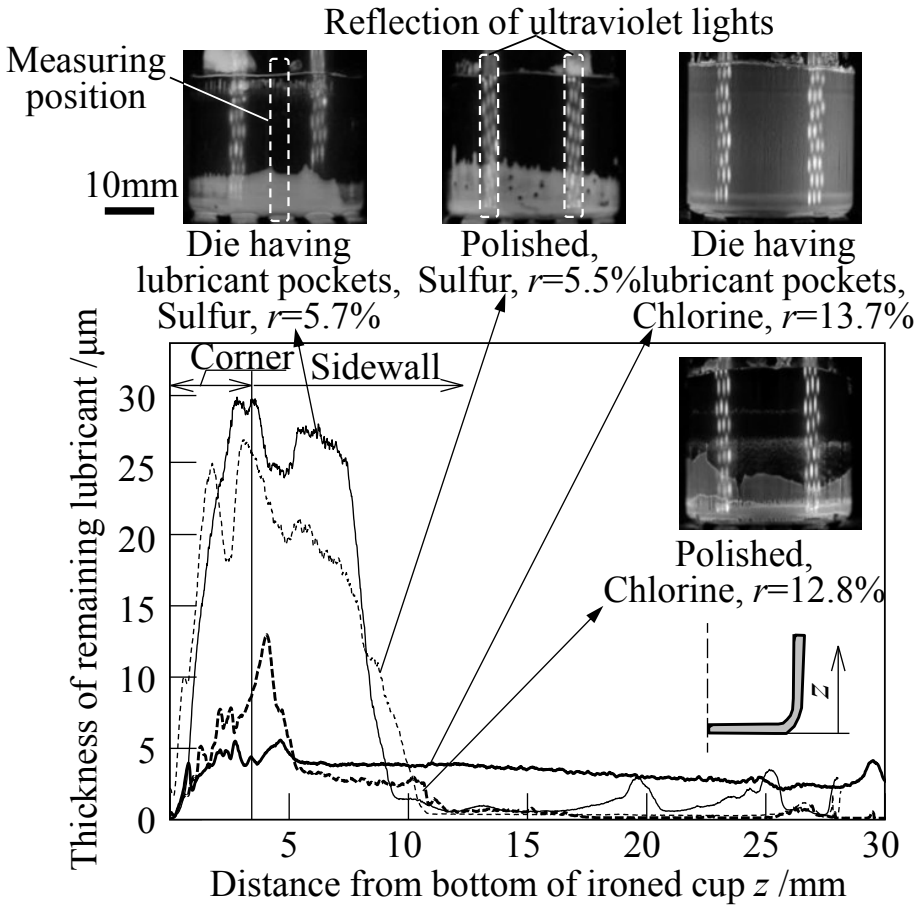

Fig. 4.9 Distribution of thickness of remaining lubricant on sidewall of ironed cup for v=100 mm/s.

The effect of the ironing ratio on the average film thickness of the remaining lubricant on the sidewall of the ironed cup with the lubricant containing the chlorine additive is shown in **Fig. 4.10**. The film thickness of the remaining lubricant was averaged from the distance of 15 to 25 mm from the bottom of the ironed cup where seizure usually occurs around this area. The average film thickness of the remaining lubricant with the die having the lubricant pockets was thicker than that with the die having the polished surface. During ironing with the die having the lubricant pockets, there is a possibility that the thick lubricating film occurs.

The relationship between the average ironing load and the ironing ratio of each die is shown in **Fig. 4.11**. This shows only the average ironing load of the conditions that no seizure occurred in Fig. 4.8. With each die and for each lubricant, the average ironing load increases with the ironing ratio. Moreover, the average ironing load with the die having the

lubricant pockets for each lubricant was lower than that with the die having the polished surface because friction is reduced by the thick lubricating film. At r= 10%, the average ironing loads were reduced about 18% and 13% for the lubricant containing the chlorine and sulphur additive, respectively.

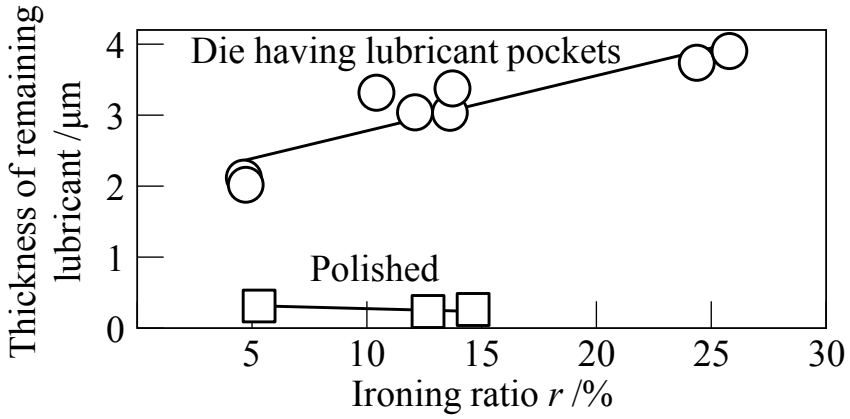

Fig. 4.10 Effect of ironing ratio on average film thickness of remaining lubricant on sidewall of ironed cup with lubricant containing chlorine additive.

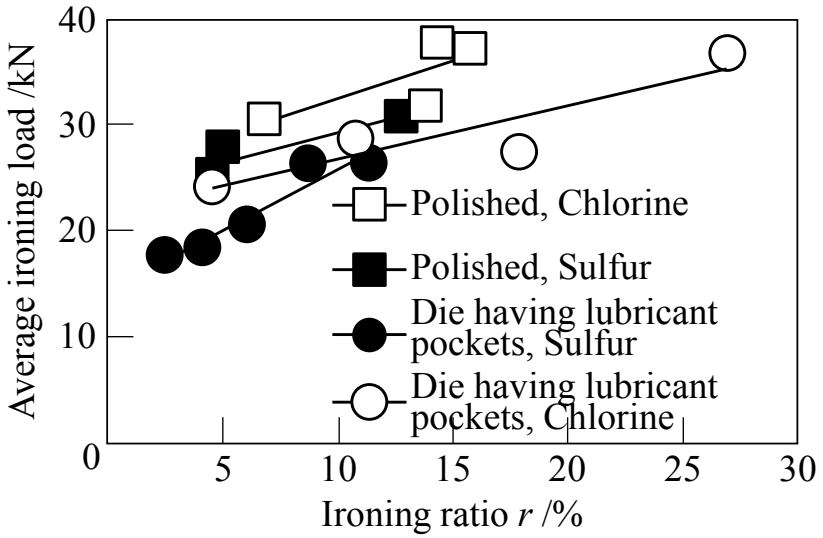

Fig. 4.11 Relationship between average ironing load and ironing ratio of each die.

The coefficient of friction was calculated by the equation (1) in Chapter 3 and determined from the ironing conditions that no seizure occurred in Fig. 4.8. The relationship between the coefficient of friction and the ironing ratio of each die is shown in

Fig. 4.12. The coefficient of friction with the die having the lubricant pockets for each lubricant was lower than that with the die having the polished surface.

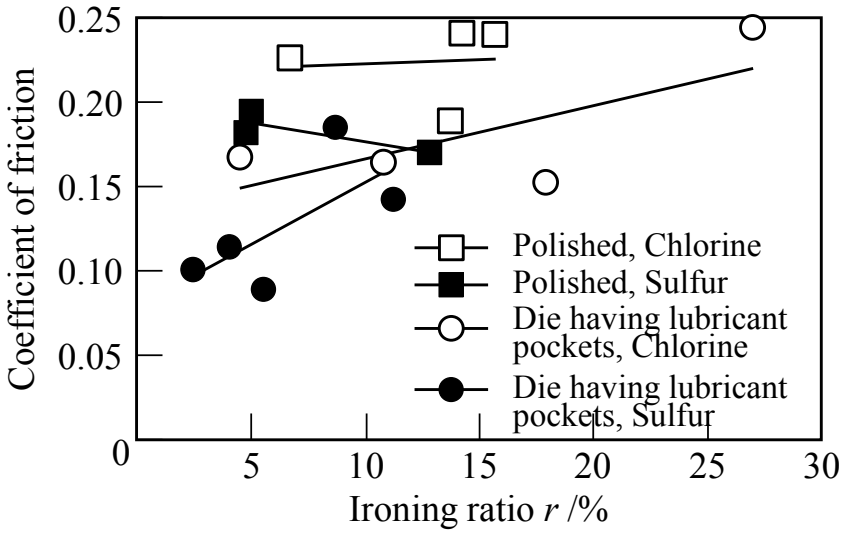

Fig. 4.12 Relationship between coefficient of friction and ironing ratio of each die.

The effect of the amount of the applied lubricant on the seizure limit with the lubricant containing the chlorine additive for v=100mm/s and r=13% is shown in **Fig. 4.13**. Since the lubricant was applied by painting on the cup with a brush. The amount of the applied lubricant was determined by a weight difference of the brush before and after applying the lubricant divided by the area of the sidewall of the drawn cup. Although the average ironing load with the die having the lubricant pockets was slightly lower than that with the die having the polished surface, the average ironing load increases with the reduction in the amount of the applied lubricant and then seizure occurred at the amount of the applied lubricant of 15μg/mm^2.

The effect of the amount of the applied lubricant on the average film thickness of the remaining lubricant with the lubricant containing the chlorine additive and the die having the lubricant pockets for v=100mm/s and r=13% is shown in **Fig. 4.14**. The average film thickness with the die having the lubricant pockets is greater than that with the die having the polished surface. However the average film thickness with the die having the lubricant pockets becomes thin with the reduction in the amount of the applied lubricant and then the lubricity decreases.

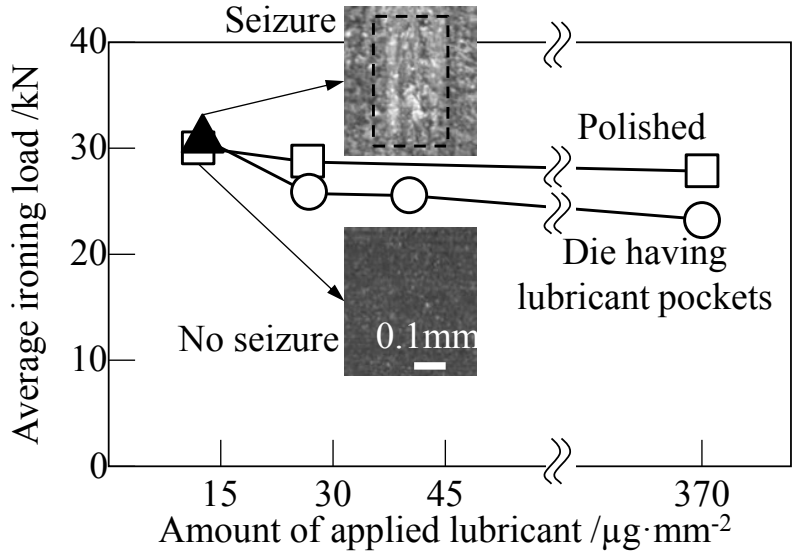

Fig. 4.13 Effect of amount of applied lubricant on seizure limit with lubricant containing chlorine additive for v=100mm/s and r=13%.

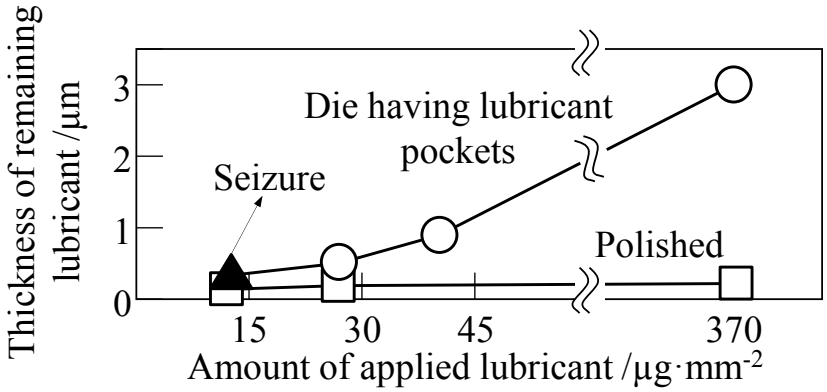

Fig. 4.14 Effect of amount of applied lubricant on average film thickness of remaining lubricant with lubricant containing chlorine additive and die having lubricant pockets for v=100mm/s and r=13%.

4.3.2 Effects of ironing speed on ironing limit of die having lubricant pockets

The effect of the ironing speed on the ironing limit in each die with the lubricant containing the chlorine additive is shown in **Fig. 4.15.** The ironing limits with the die having the lubricant pockets for each ironing speed show that there are the fracture of cups at r around 30%. Although the ironing limit with the die having the polished surface

slightly increases with the ironing speed, the ironing limit with this die is lower than that with the die having the lubricant pockets.

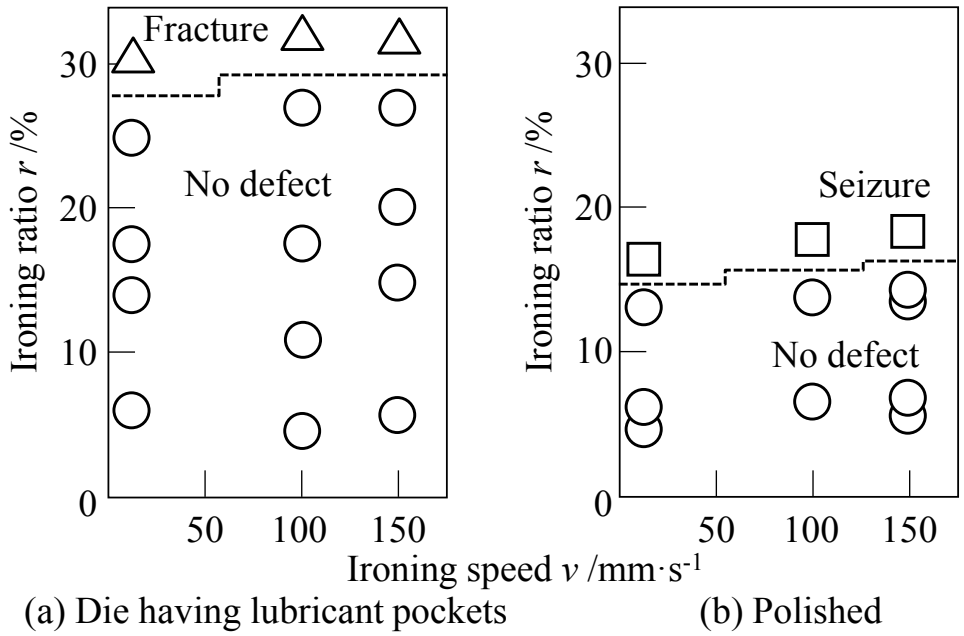

Fig. 4.15 Effect of ironing speed on ironing limit in each die with lubricant containing chlorine additive.

The effect of the ironing speed on the film thickness of the remaining lubricant on the sidewall of the ironed cup with the lubricant containing the chlorine additive is shown in **Fig. 4.16.** The film thickness of the remaining lubricant with the die having the polished surface is almost constant regardless of the ironing speed. But the film thickness with the die having the lubricant pockets increases with the ironing speed. Mizuno and Okamoto [55] showed that with the high speed, lubricant flowing out of the pockets to the flat portions was considerable, accompanying microscopic plastic deformations of the surface caused by the hydrodynamic shear stress. Therefore, the film thickness of the lubricant was thickened. Using the die having the lubricant pockets in the circumstance that supplies a sufficiently amount of the lubricant and performs at the high ironing speed becomes the better lubrication condition because friction is reduced by a large film thickness of the remaining lubricant.

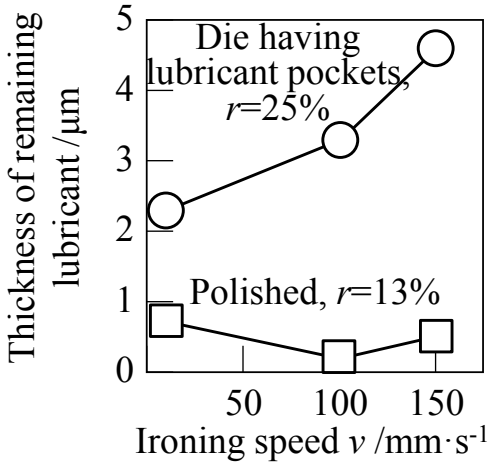

Fig. 4.16 Effect of ironing speed on thickness of remaining lubricant on sidewall of ironed cup with lubricant containing chlorine additive.

4.4 Situation of seizure growth in repeated ironing

Repeated ironing was conducted in order to verify the effectiveness of the friction reduction mechanism with using the die having the lubricant pockets. The ironing ratio was set at r=16%. As the result of single ironing, the film thickness of the lubricant was the largest at the speed of v=150mm/s. Therefore, repeated ironing with the die having the lubricant pockets was carried out at this speed.

The ironed cups in repeated ironing are shown in **Fig. 4.17**. With the die having the lubricant pockets, the repeated ironing is successfully performed until n=300 without the occurrence of any defect on the cup. Because of seizure occurred on the die and the cup at n=10 with the die having the polished surface. And then the fracture of the upper end of the cup frequently took place. Thus, repeated ironing was done up to n=150 only for this die.

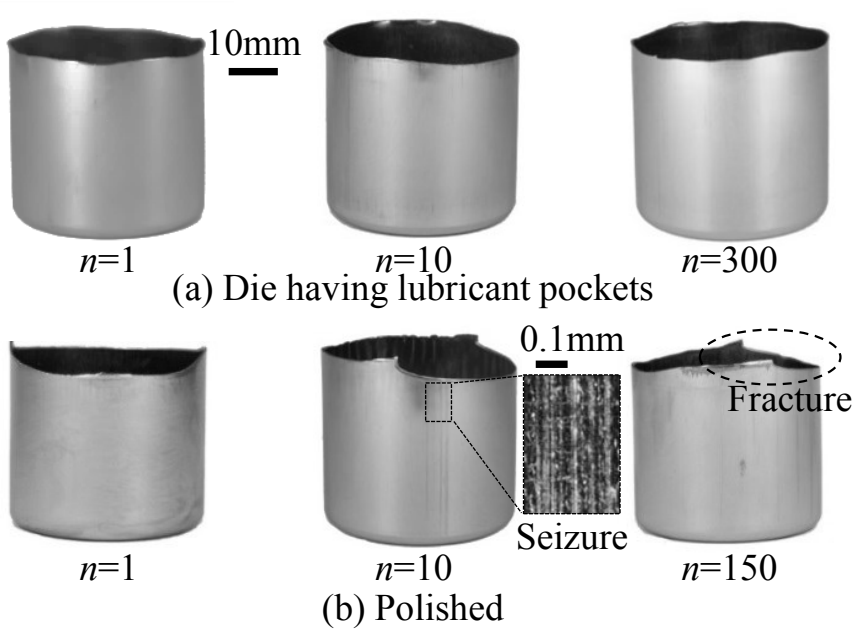

Fig. 4.17 Ironed cups in repeated ironing.

The seizure on the die surface for each number of strikes is shown in **Fig. 4.18**. With the die having the lubricant pockets the black and gray areas are the micro-pockets and the flat portion, respectively. The white area is seizure of stainless steel. Although the surface of the die having the lubricant pockets at n=0 is shown as a reference, only the surfaces from the number of strikes above n=50 were taken at the same position.

Although micro-seizure occurred at n=50 and several locations of the pockets were filled with that seizure. At n=80, some parts of seizure which occurred at n=50 were peeling off. Even in n=150, there was a part that seizure was peeling again. Adhesion and peeling-off of micro-seizure have repeatedly occurred on this die. On the other hand, with the die having the polished surface, at n=10 large seizure occurred and then seizure grows up when the number of strikes increases.

The variation of the ratio of seizure on the die surface is shown in **Fig. 4.19**. The ratio of seizure is determined by measuring of the seizure area divided by the area of observing portion. The ratio of seizure with the die having the lubricant pockets rises till n=100, after that it is almost constant. While the ratio of seizure with the die having the polished surface increases as the number of strikes increases.

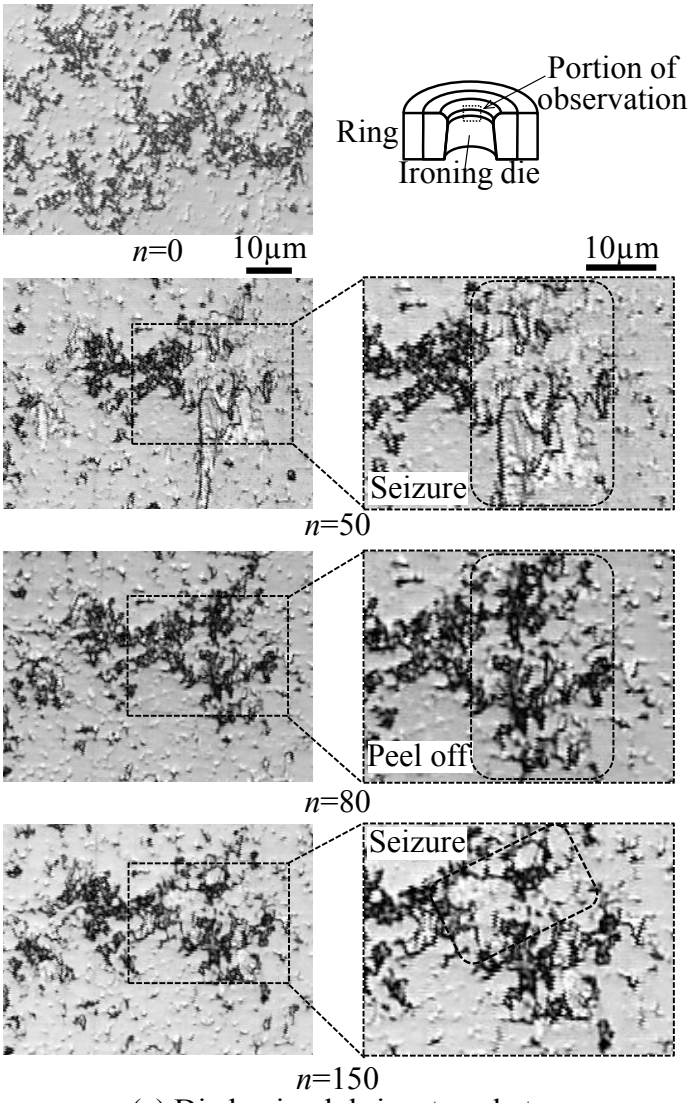

Fig. 4.18 Seizure on die surface for each number of strikes.

The variation of surface roughness of the die is shown in **Fig. 4.20**. Because of a large number of the lubricant pockets, the initial surface roughness of the die having the lubricant pockets is higher than that of the die having the polished surface. The surface roughness of the die having the lubricant pockets is almost constant, but the surface roughness of the die having polished increases with the number of strikes.

As shown in Fig. 4.19, because the ratio of seizure with the die having the polished surface becomes large after 100 strikes, the surface roughness of the die having the polished surface becomes high.

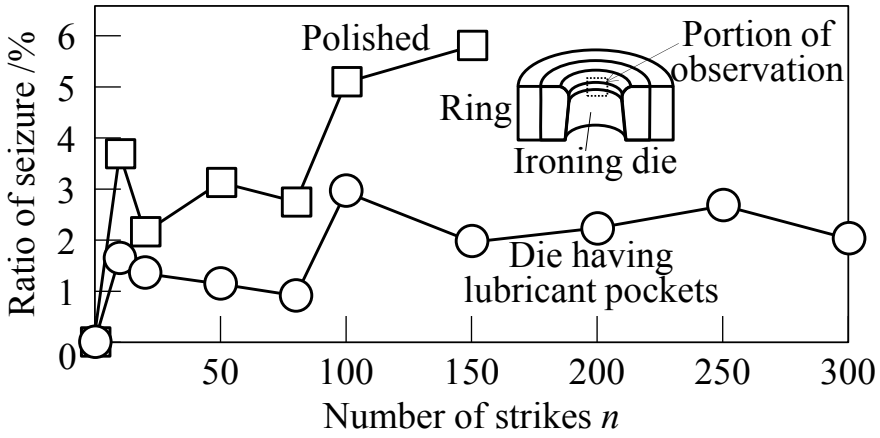

Fig. 4.19 Variation of ratio of seizure on die surface.

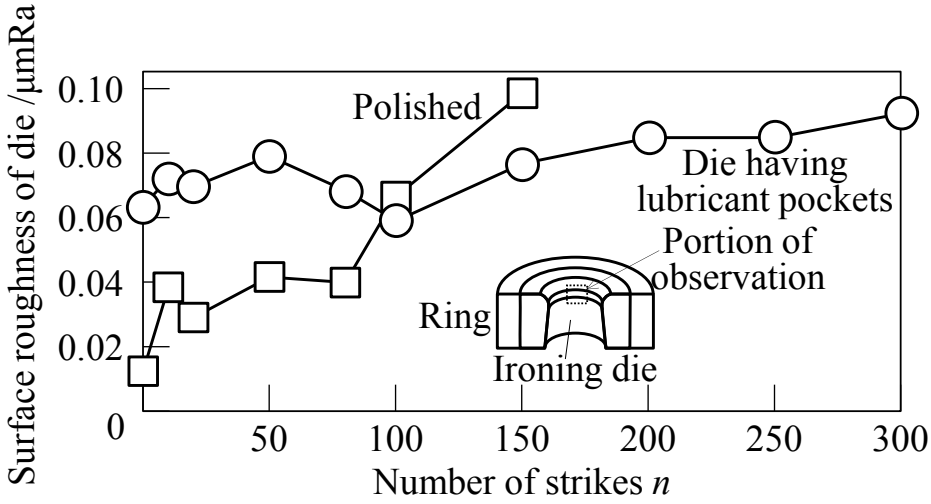

Fig. 4.20 Variation of surface roughness of die.

The surface roughness in a circumferential direction of the ironed cup is shown in **Fig. 4.21**. The measurement of the surface roughness was done in the circumferential direction

at distances of 5, 15 and 25 mm from the bottom of the ironed cup in four positions every 90°. Because of seizure occurred at n=10 with the die having the polished surface, the surface roughness of the ironed cup increases with the number of strikes. Whereas with the die having the lubricant pockets until n=300 only micro-seizure occurred. The surface roughness of the ironed cups maintains the same level irrespective to the number of strikes.

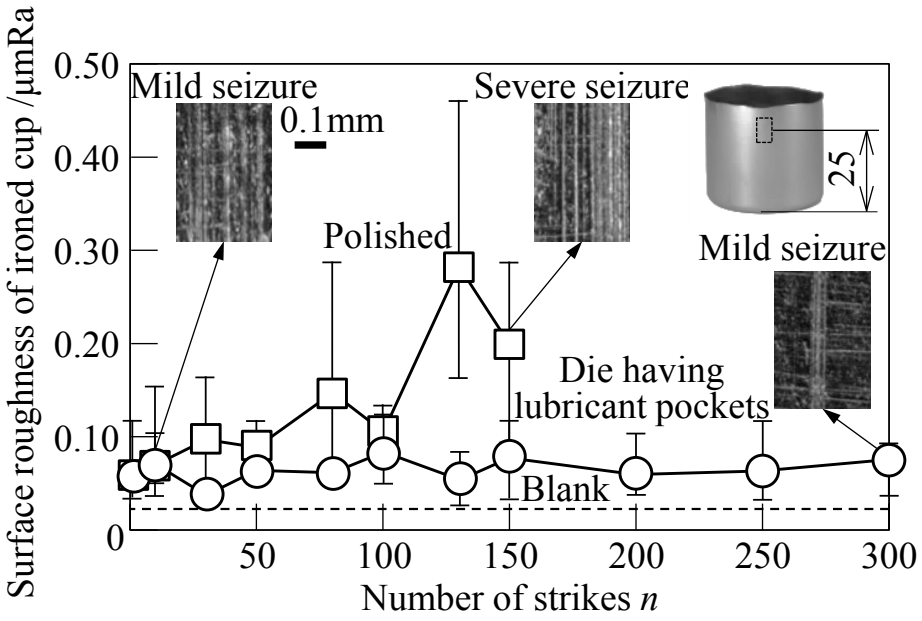

Fig. 4.21 Surface roughness in circumferential direction of ironed cup.

4.5 Conclusions

The film thickness of the remaining lubricant on the sidewall of the ironed stainless steel cup was measured in ironing with the die having the lubricant pockets. The lubrication conditions with low friction were determined. The situation of seizure growth in repeated ironing was investigated, and the following results were obtained:

1. Using the die having the lubricant pockets, the condition that supplied a sufficiently amount of the lubricant and performed at the high ironing speed was the better lubrication condition for reducing friction.
2. The film thickness of the remaining lubricant with the die having the lubricant pockets was thicker than that with the die having the polished surface. With the die having the

lubricant pockets, there is a possibility that the thick lubricating film occurs during ironing.

3. The ironing load with the die having the lubricant pockets was lower than that with the die having the polished surface because friction is reduced by the thick lubricating film. For the lubricant containing the chlorine and sulphur additive at the ironing ratio of 10%, the average ironing loads were reduced about 18% and 13%, respectively.
4. In repeated ironing, the surface roughness of the ironed cup with the die having the polished surface increases with the number of strikes because of the growth of seizure. But with the die having the lubricant pockets, adhesion and peeling-off of micro-seizure have repeatedly occurred. The surface roughness of the ironed cups maintains the same level regardless of the number of strikes.

Chapter 5
Improvement of lubrication in ironing of stainless steel cups by roughening of cup surface

5.1 Introduction

The reduction in emissions of greenhouse gases such as carbon dioxide gas from automobiles is strongly required to mitigate global warming. Consequently, the demand for alternative fuel vehicles such as hybrid and electric vehicles is increasing, and thus a lot of batteries are used for these vehicles. In the batteries, metal cups used as electrolyte cases are generally made of stainless steels and aluminium alloys. Aluminium alloy cases can be formed by either impact extrusion [116] or multi-stage stamping [12]. On the other hand, due to the high strength of the stainless steels, these cases are generally produced by multi-stage stamping processes including deep drawing and ironing [14]. In ironing, not only the thickness of the cup sidewall is uniform, but also tensile residual stress is reduced [121].

In ironing of stainless steel and aluminium alloy sheets, galling and seizure tend to occur due to severe plastic deformation, and these defects bring about severe tool wear and fracture of stamped products. Low-friction coatings of dies are generally used to prevent the occurrence of these defects. Podgonik et al. [104] indicated that the seizure resistance could be improved by using tool coatings suitable for each type of the working materials. In stamping of high strength steel sheets, diamond-like carbon (DLC) coatings presented possibilities of dry ironing [108]. The TiCN, AlTiN and CrN PVD coatings showed high anti-adhesion performance in deep drawing [111]. The seizure in deep drawing of ultra-high strength steel sheets was prevented by using the VC coating [110]. In forming of aluminium alloy sheets, the DLC coating was effective in preventing the adhesion of aluminium in deep drawing without lubricant [105]. The seizure resistance of a high-speed steel die in ironing was improved with the TiN coating [109]. The coatings with a low coefficient of friction are effective in improving seizure resistance. In addition, the surface roughness of the coated tool has a crucial influence on the seizure resistance [113]. The seizure tends to occur with increasing roughness of the coating, whereas the hardness hardly correlates [114].

The occurrence of seizure can be reduced by using low friction tool materials such as ceramics and cermets. Kataoka et al. [41] applied ceramic dies to dry deep drawing for various sheet metals, and significantly reduced the drawing load for stainless steel sheets by using an alumina ceramic die. Tamaoki et al. [42] proposed electro conductive ceramic dies for dry deep drawing of mild steel sheets, and exhibited that a zirconia-based ceramic die was effective in reducing the seizure. Repeated deep drawing with the zirconia-based ceramic die was successfully performed up to 10,000 times [43]. Abe et al. [117] heightened the seizure resistance in ironing of stainless steel and aluminium alloy cups by using a TiCN-based cermet die.

Liquid lubricants are conventionally used to reduce friction and to prevent the occurrence of seizure in ironing. The rough surface of workpieces has an influence on the improvement of lubrication by providing micro pockets for trapping the lubricant. Mizuno and Okamoto [55] named this lubrication mechanism as micro-plasto-hydrodynamic lubrication. Kudo et al. [56] elucidated the mechanism of micro-plasto-hydrodynamic lubrication in a cold sheet drawing test. The mechanism was verified by the direct observation of the tool-workpiece interface through a transparent die. The reduction in thickness, drawing speed and lubricant viscosity have influences on the escape of the lubricant from pockets [57, 58]. Utilising the same direct observation technique, the effects of the pocket geometry, lubricant viscosity, drawing speed and reduction in thickness on the entrapment and escape of liquid lubricants were investigated [59, 60]. The escape of trapped lubricants from the pockets during strip drawing has an influence on the drawing load [61].

The use of textured sheets providing a surface topography with lubricant pockets facilitates lubrication in forming processes. Therefore, the sheet-surface textures have been developed to improve the tribological conditions for sheet metal forming [62]. The textured sheet produced by transferring roller surfaces prepared by electron beam texturing in skin pass rolling was introduced to deep drawing. Because lubrication was assisted during the process, friction decreased with increasing in the drawing speed [64]. Li et al. [122] investigated the influence of texturing conditions of roll mills by the YAG laser-induced discharge process on the patterns and the shape of pockets. Both deterministic and random pockets could be obtained by the YAG laser-induced discharge texturing technique. In strip ironing and deep drawing, the textured stainless steel sheet significantly improved

the lubrication performance with no sign of lubricant film breakdown [67]. However, the textured sheet surface does not function when the surface is completely flattened by large deformation.

Since the dies undergo only elastic deformation, texturing of die surfaces facilitates forming even for long-running use. Geiger et al. [68] introduced texturing using excimer laser radiation to the surface of a TiN-coated punch for cold forging. Texturing on a silicon nitride ceramic surface, creating micro-pockets artificially exhibited substantial reduction in friction [123]. Popp and Engel [69] showed the pressurisation of the entrapped lubricant in micro-pockets for improvement of tool life. In forging, the tool wear was reduced by a lubricant run out of micro-pockets [71]. The textured surface with grooves oriented perpendicular to the sliding direction improved lubrication and gave the largest thickness of the lubricant film for the highest load in reciprocating sliding [124]. Basnyat et al. [125] produced micro-pockets filled with solid lubricants on the surface of the TiAlCN coating. The friction was significantly reduced by the textured coating because the pockets acted as reservoirs for supplying solid lubricants to the contact surfaces. Vilhena et al. [72] employed laser surface texturing to hardened bearing steel, and optimised the parameters of the laser surface texturing process. Well defined micro-pockets improved tribological behaviour [73]. Meng et al. [75] exhibited that friction could be reduced by using the laser textured tool having micro rectangle pockets with a flat bottom. Aramaki et al. [76] showed that the combination treatments of the die with shot-peening and nitriding improved seizure resistance in drawing of high strength steel sheets because of its lubricating effect. Abe et al. [126] improved seizure resistance in ironing of stainless steel cups by using a TiCN-based cermet die having fine lubricant pockets by polishing a shot-peened surface. In this die, friction is reduced by squeezing liquid lubricants from the pockets during ironing

In this study, surfaces of ferritic stainless steel drawn cups were roughened to improve the seizure resistance in ironing with a TiCN-based cermet die having lubricant pockets. The lubricant pockets on the die surface were formed by shot-peening and polishing. The sidewall of the drawn cup was roughened by sanding with emery paper and using modified deep drawing processes. The effect of the surface finish of the drawn cup on the seizure resistance in ironing using a lubricant with a sulphur additive were investigated. The

seizure resistance was increased by roughening the cup surface using modified deep drawing processes.

5.2 Ironing procedure of stainless steel cup

In ironing with a TiCN-based cermet die having lubricant pockets developed by Abe et al. [126], the seizure resistance was heightened by roughening the sidewall surfaces of ferritic stainless steel drawn cups. The ironing conditions using the die having lubricant pockets are shown in **Fig. 5.1**. A drawn cup was ironed by using a die having lubricant pockets. Ironing was carried out by using an 800 kN CNC servo press with an ironing speed of 100 mm/s. A drawn cup was attached to the punch prior to ironing, and then the cup was ironed by passing through the die. To increase the ironing ratio, the punch diameter d_p and drawn cup diameter are increased while the inner diameter of the die is fixed at 34 mm. The ironing ratio r is given by

$$r = \frac{t_0 - t_m}{t_0}, \tag{1}$$

where t_0 and t_m are the initial thickness of the blank and the average wall thickness of the ironed cup, respectively. As the ironing ratio increases, the cup undergoes severe deformation. When the ironing ratio exceeds a certain value, seizure occurs on the die or the cup fractures. The highest ironing ratio without defects such as seizure on the die or the fracture of the cup is defined as the ironing limit. The higher seizure resistance brings about the higher ironing limit.

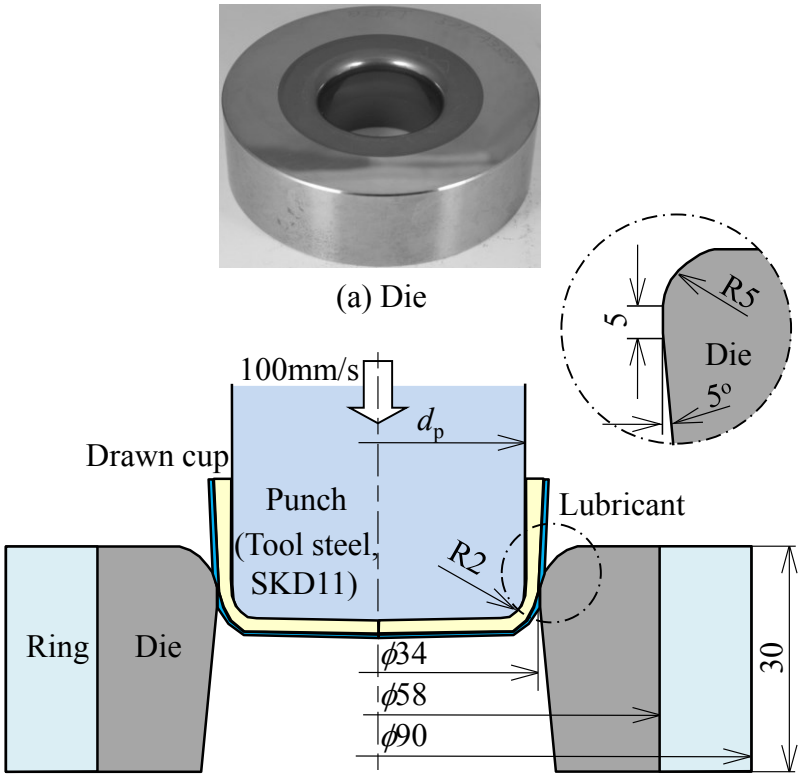

Fig. 5.1 Ironing of stainless steel cup using die having lubricant pockets.

The die is made of TiCN-based cermet, and is reinforced with a steel ring. The TiCN-based cermet was obtained by sintering main TiCN powder with a nickel binder without tungsten carbide and cobalt in its composition. Because the main component of the cermet is made of low friction TiCN having high seizure resistance in ironing [117], a re-coating is not required even for wearing of the die.

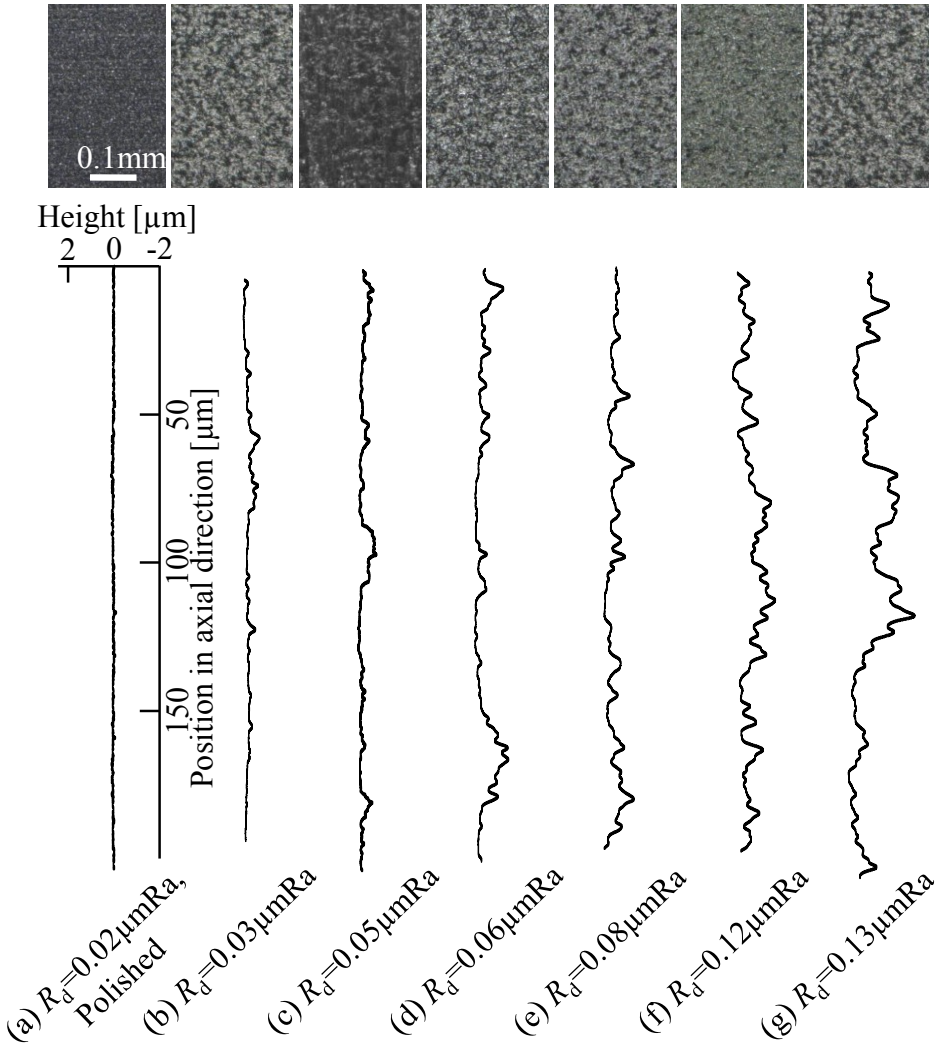

Fig. 5.2 Surface roughness profiles of die having lubricant pockets.

The lubricant pockets on the die surface are structured by shot-peening and polishing [126]. The surface roughness profiles of the die having lubricant pockets are shown in **Fig. 5.2**, where R_d is the arithmetic mean roughness in the die land. The various surface pockets are formed by using shot-peening and polishing under differing conditions. The surface roughness profiles in the die land were measured by a stylus profilometer, and then the reduced peak height Rpk, the reduced valley depth Rvk and the arithmetic mean roughness Ra were obtained. The reduced valley depth acts as lubricant pockets in ironing, whereas the reduced peak height behaves like asperities. Thus, seizure may occur due to the excessive reduced peak height. The relationship between the reduced peak height, the reduced valley depth and the arithmetic mean roughness in the die land is shown in **Fig.**

5.3. In the structured die, the reduced valley depth was greater than that in the polished die. The reduced peak height was low, for the arithmetic mean roughness in the die land was 0.12 μm and below. Thus, the die surface consisted of the flat smooth portion and lubricant pockets. Although the reduced valley depth was increased in the condition that the arithmetic mean roughness was above 0.12 μm, seizure tended to occur because of the large reduced peak height.

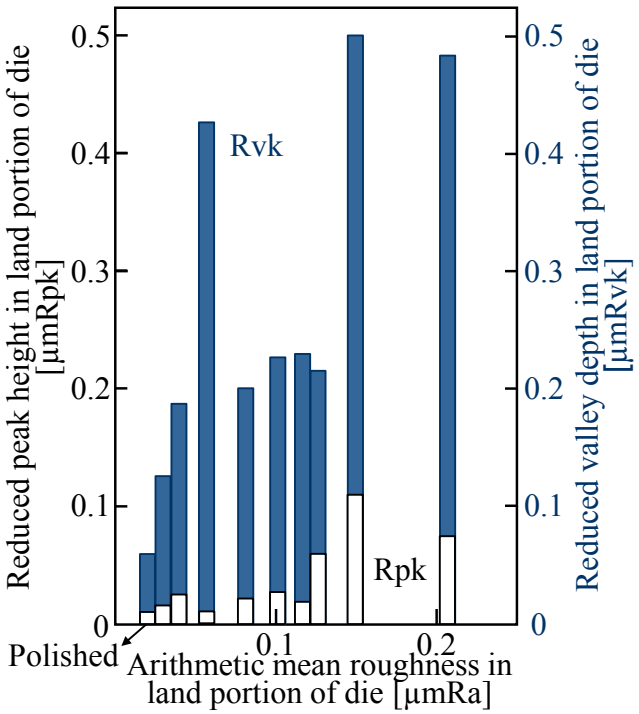

Fig. 5.3 Relationship between reduced peak height, reduced valley depth and arithmetic mean roughness in die land.

The lubricants were a mineral oil with a sulphur additive having a kinematic viscosity of 96 mm^2/s (G-3170, Nihon Kohsakuyu Co., Ltd.) and a mineral oil with a chlorine additive having a kinematic viscosity of 3.0 mm^2/s (X-2834, Nihon Kohsakuyu Co., Ltd). The properties of the oil used for the ironing of the stainless steel cup are shown in **Table 5.1**. The outer surface of the cup and the die were lubricated before ironing.

Table 5.1 Properties of oil for ironing of stainless steel cup.

Lubricant	Base oil	Additive	Kinematic viscosity at 40°C [mm^2/s]
X-2834	Mineral oil	Chlorine compound	3.0
G-3170	Mineral oil	Sulphur compound	96

Prior to the ironing process, ferritic stainless steel SUS430 circular blanks with 66 mm in diameter and 0.6 mm in thickness were drawn into cylindrical cups with a constant blankholder force of 9 kN. The mechanical properties of ferritic stainless steel SUS430 sheets are shown in **Table 5.2.**

Table 5.2 Mechanical properties of ferritic stainless steel SUS430 sheets.

Sheet	Tensile strength [MPa]	Elongation [%]	*n*-value	*r*-value
SUS430	547	25.7	0.20	1.17

The conditions for deep drawing are shown in **Fig. 5.4**. The clearance between the drawing die and punch was set to be equal to the sheet thickness. By using different sets of the diameter of the punch, d_p and die, d_d as shown in **Table 5.3**, several diameters of drawn cups were obtained for providing different ironing ratios. The die was polished before deep drawing at each forming to prevent the die from seizure.

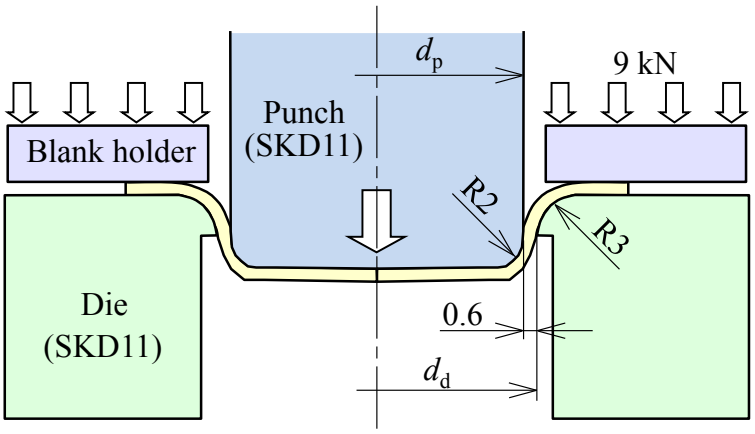

Fig. 5.4 Conditions of deep drawing.

Table 5.3 Relationship between nominal ironing ratio, punch diameter and die diameter in deep drawing.

Nominal ironing ratio [%]	Punch diameter d_p [mm]	Die diameter in deep drawing d_d [mm]
10	32.92	34.12
20	33.04	34.24
30	33.16	34.36
35	33.22	34.42
40	33.28	34.48
50	33.40	34.60

The surface roughness of the cup is effective for reducing the friction in ironing. The drawn cup was sanded with emery paper. The method of sanding was in an axial or circumferential direction. The surface and the surface roughness profile of drawn and sanded cups are shown in **Fig. 5.5**. The surface roughness of the drawn cup was about 0.3 μmRa in both the axial and circumferential directions. In the axial sanding direction with #80, the surface roughness of the circumferential direction R_c was increased, whereas the surface roughness of the axial direction R_z was decreased. By contrast, this tendency had an opposite effect with the circumferential sanding direction with #80. The surface roughness of the drawn cup sanded with #1500 was about 0.1 μmRa in both axial and circumferential directions.

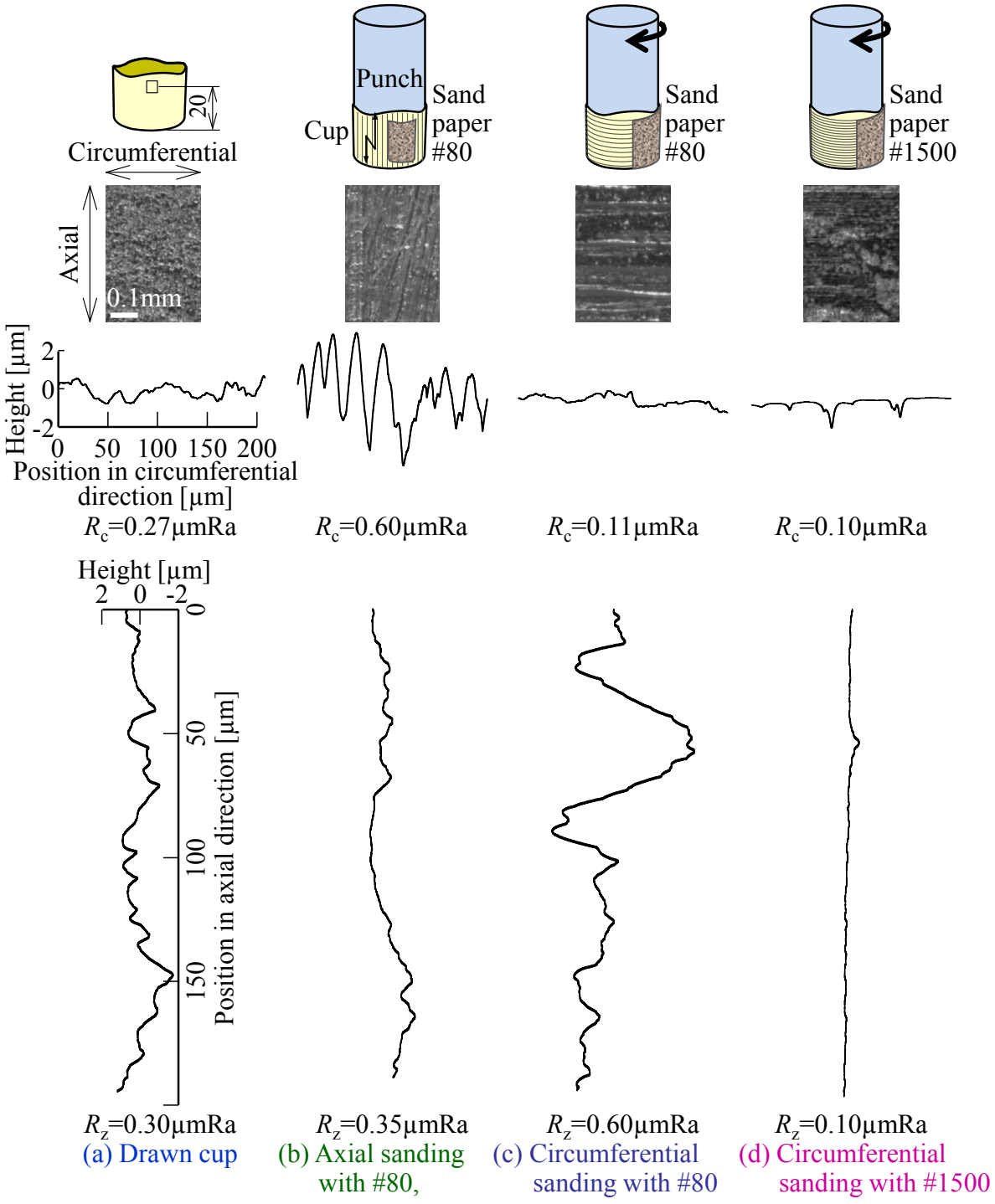

Fig. 5.5 Surface and surface roughness profile of drawn and sanded cups.

The distributions of the wall thickness and hardness of the drawn cup are shown in **Fig. 5.6,** where x is the distance from the bottom centre of the drawn cup. The wall thickness in the range of x = 32 to 41 mm was larger than the blank thickness. The hardness of the drawn cup was increased by plastic deformation.

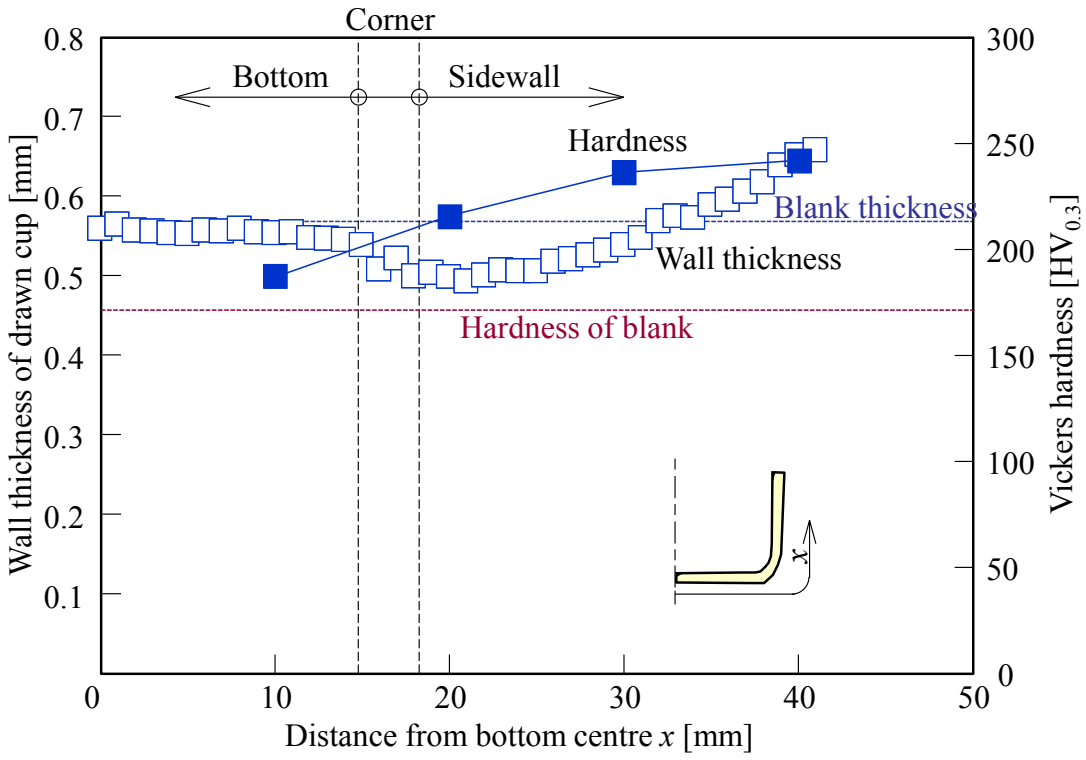

Fig. 5.6 Distributions of wall thickness and hardness of drawn cup.

5.3 Improvement of seizure resistance by roughening sidewall surface of cup with sanding

The effect of the arithmetic mean roughness of the die having lubricant pockets on the ironing limit for the drawn cup and the lubricant with the chlorine additive is shown in **Fig. 5.7**. Because ironing became more severe for a large ironing ratio, defects such as seizure and fracturing of the cup occurred. When surface roughness in the die land was in the range between R_d=0.05μmRa and 0.12μmRa, the seizure resistance of the die having lubricant pockets was higher than that of the polished die. In the large arithmetic mean roughness, not only the reduced valley depth increased, but also the reduced peak height became large, and thus the surface with the high reduced peak height was not capable of preventing seizure because of its large protruding irregularities. In this study, the die having R_d=0.06μmRa was mainly used as the die having lubricant pockets.

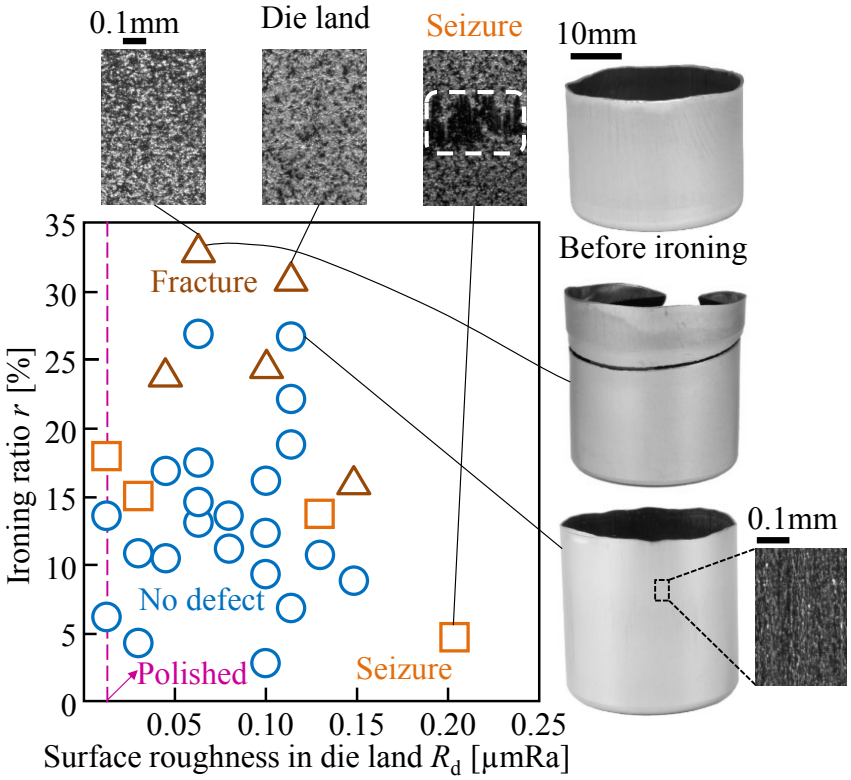

Fig. 5.7 Effect of arithmetic mean roughness of die having lubricant pockets on ironing limit for drawn cup and lubricant with chlorine additive.

The effect of the arithmetic mean roughness of the cup on the ironing limit for the lubricant with the sulphur additive, the polished die and the die having lubricant pockets is shown in **Fig. 5.8**. For the die having lubricant pockets R_d=0.06μmRa was used. In both polished die and die having lubricant pockets, seizure resistance increased with the surface roughness of the cup in the axial direction. The improvement of seizure resistance for R_d=0.06μmRa was much larger than that for the polished die. Although the seizure resistance of the lubricant with the sulphur additive was smaller than that for the drawn cup and the lubricant with a chlorine additive, using the sanded cup with R_z=0.60μmRa, the seizure resistance reached almost the same level as the drawn cup and the lubricant with the chlorine one. With the cup sanded in the circumferential direction, the ironing limit was higher than with the cup sanded in the axial direction.

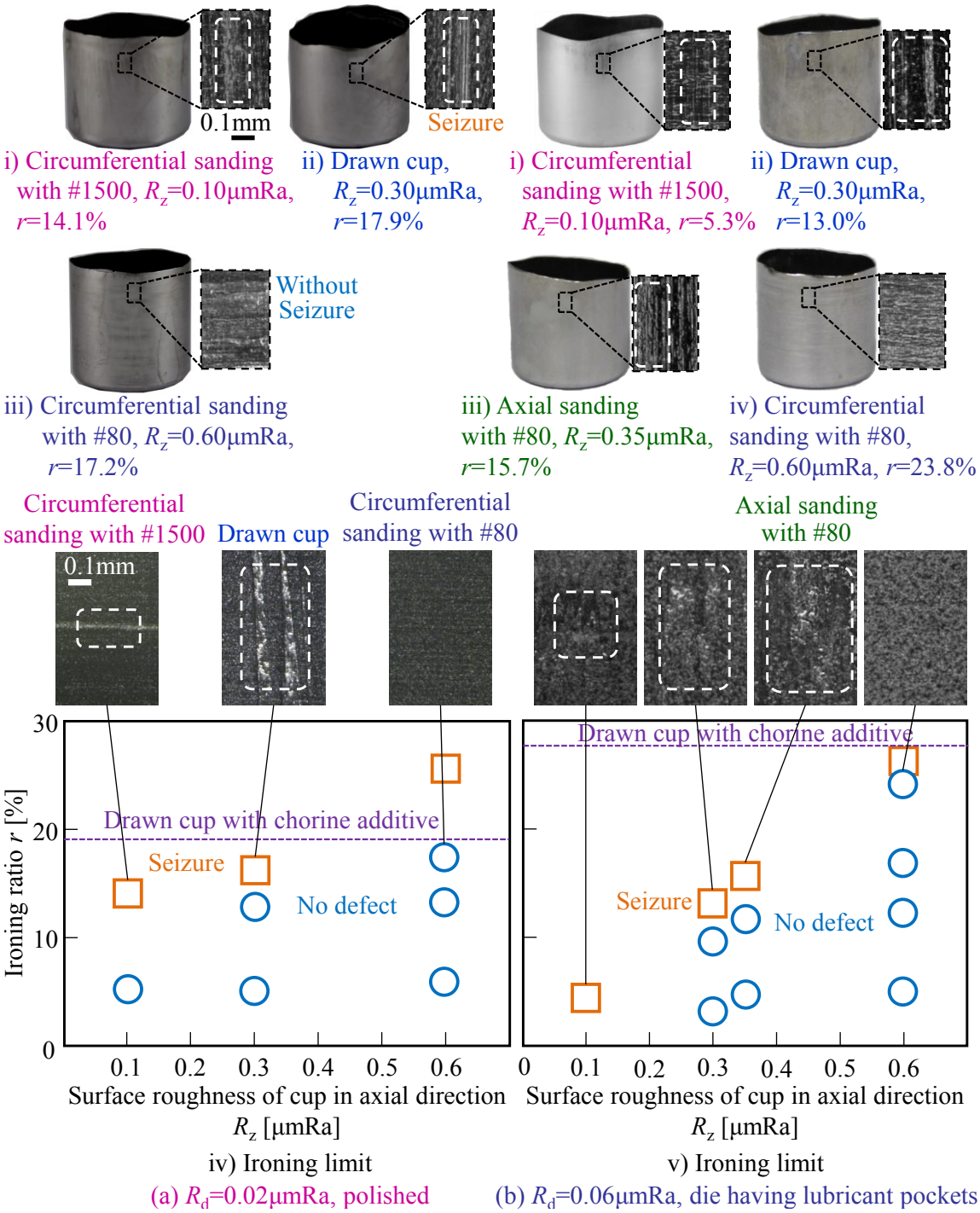

Fig. 5.8 Effect of arithmetic mean roughness of cup on ironing limit for lubricant with sulphur additive, polished die and die having lubricant pockets.

The effect of the sanding direction of the cup on the ironing load-stroke curve for the lubricant with the sulphur additive is shown in **Fig. 5.9**. The ironing limits for both dies were increased by circumferential sanding. The ironing load for circumferential sanding

was lower than that for axial sanding. Sanding parallel to the ironing direction is not effective because of flowing of the lubricant, and sanding perpendicular to the ironing direction is desirable for trapping lubricants.

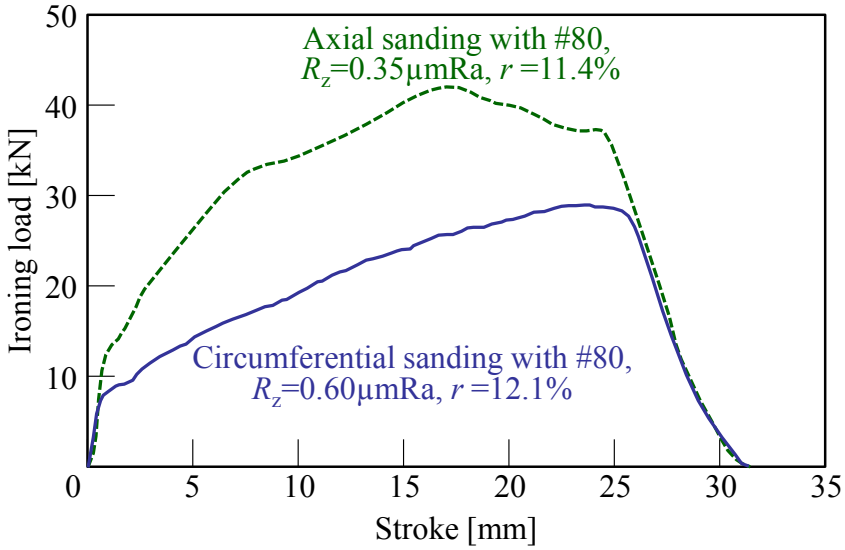

Fig. 5.9 Effect of sanding direction of cup on ironing load-stroke curve for lubricant with sulphur additive.

5.4 Improvement of seizure resistance by roughening sidewall of deeply drawn cup

5.4.1 Cups having roughened sidewall surface by deep drawing

The surface roughness in the axial direction of the cup was increased by the following two deep drawing operations. One was deep drawing with a large clearance between the punch and die, and the sidewall is stretched without contact with the die after passing through the die. The other was deep drawing and redrawing with a small die corner radius, and the surface roughness is increased by a large plastic deformation.

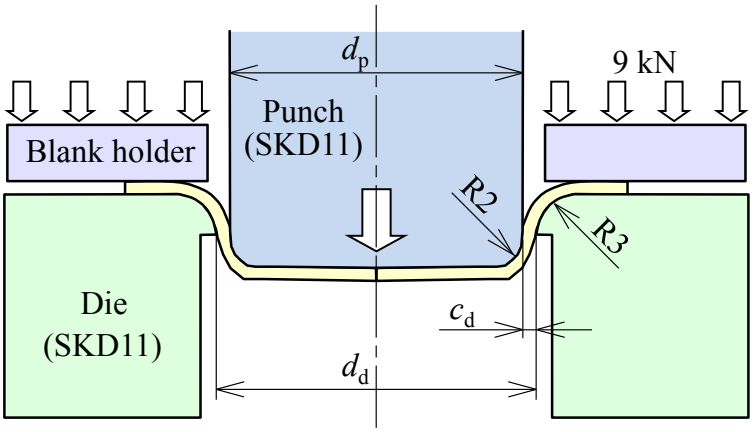

Fig. 5.10 Conditions of deep drawing with large clearance between punch and die.

The conditions of the deep drawing with a large clearance between the punch and die are shown in **Fig. 5.10** and **Table 5.4**. The ironing ratio was given by the punch diameter, and then the die diameter was increased to obtain the larger clearance in deep drawing as shown in Table 5.4. Because the excessive clearance ratio causes fracturing by the occurrence of wrinkling, the maximum clearance ratio was up to 150% in this section, whereas it was 100% in the previous section.

Table 5.4 Relationship between ironing ratio, tool geometries and clearance ratio in deep drawing with large clearance between punch and die.

Nominal ironing ratio [%]	Punch diameter d_p [mm]	Die diameter in deep drawing d_d [mm]	Clearance ratio in deep drawing c_d [%]
20	33.04	34.48	120
30	33.16	34.60	120
30	33.16	34.96	150
35	33.22	34.60	115
40	33.28	34.60	110

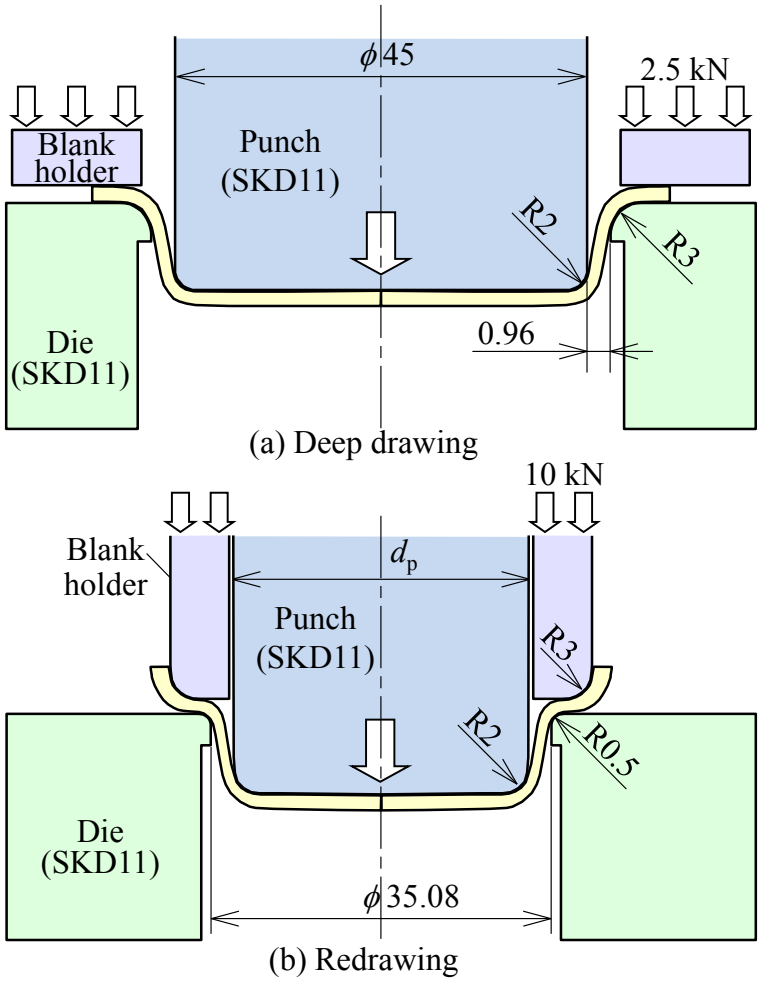

Fig. 5.11 Conditions of two-stage deep drawing composed of deep drawing and redrawing.

The conditions of two-stage deep drawing composed of deep drawing and redrawing are shown in **Fig. 5.11**. Surface roughness was increased by the large plastic deformation using the small die corner radius in drawing. Because the fracture tends to occur with the use of the small corner radius, redrawing was used. In deep drawing, the drawing ratio was reduced to 1.47 from about 2 in the previous section. In redrawing, the small die corner radius was utilised.

The surface and roughness profiles of the drawn cup with the large clearance and the redrawn cup are shown in **Fig. 5.12**. The surface roughness increased in comparison with that of the drawn cup in the previous section. In particular, the increase in surface roughness by using redrawing was larger than by using large clearance drawing.

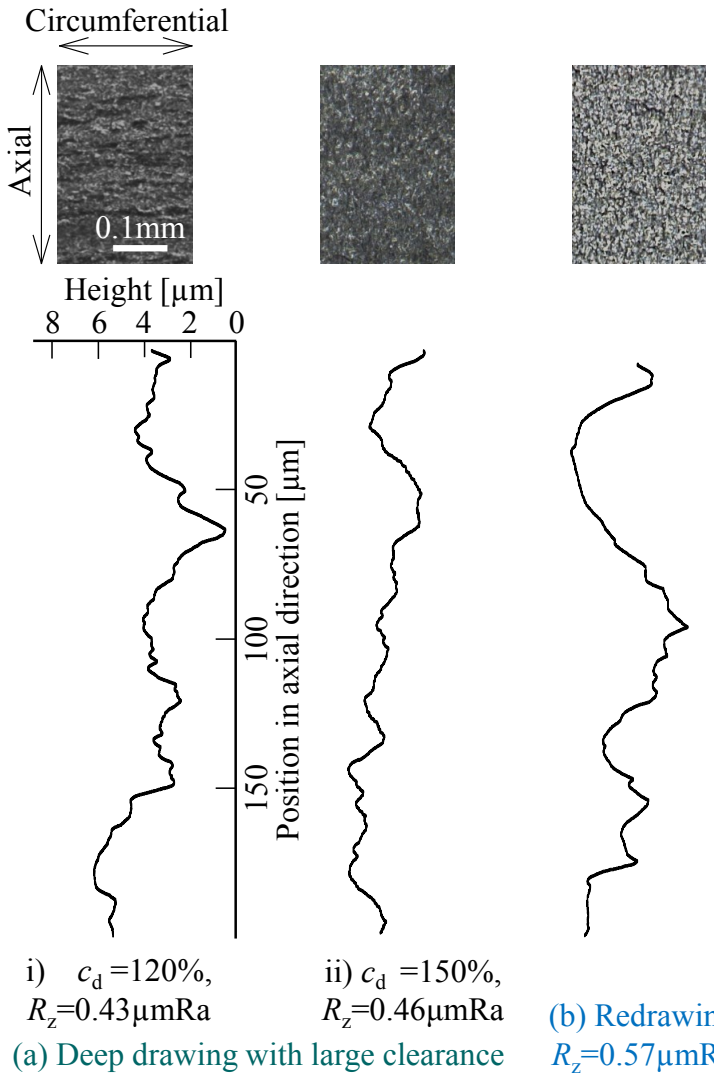

Fig. 5.12 Surface and roughness profiles of drawn cup with large clearance and redrawn cup.

The distributions of the wall thickness and hardness in cups formed by deep drawing with the large clearance and two-stage deep drawing are shown in **Fig. 5.13**. Although the tendency of the distributions of the wall thickness with the large clearance was similar to the drawn cup for c_d=100%, the wall thickness in the sidewall of the cup was increased with the clearance ratio. For the drawn cup with redrawing due to the small die corner radius causing the large plastic deformation, hardness of the cup was higher than the drawn cup for c_d=100%.

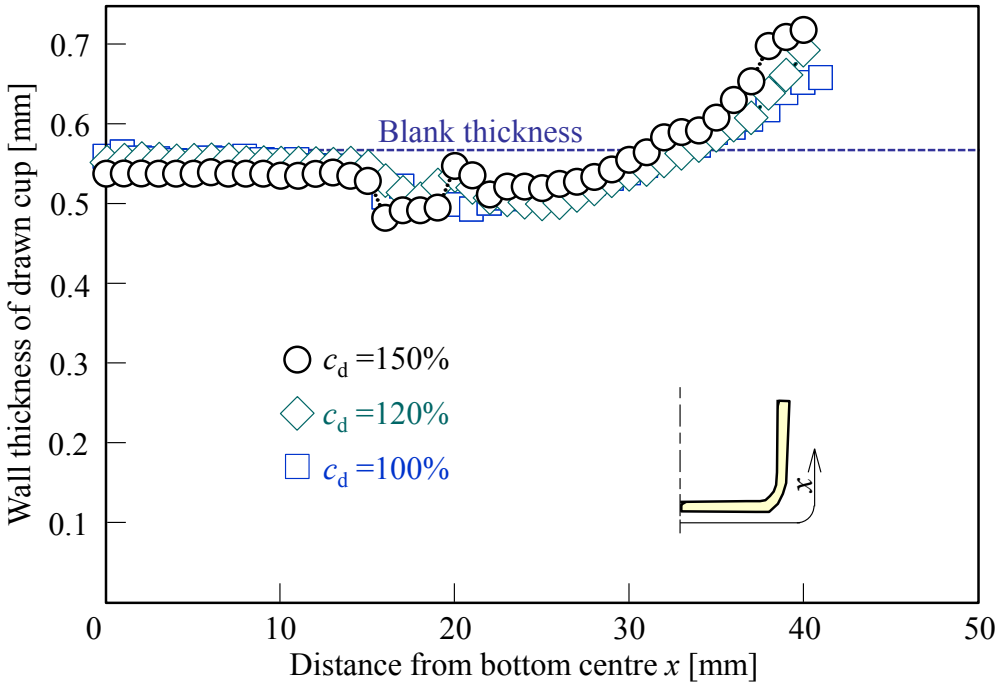

(a) Deep drawing with large clearance between punch and die

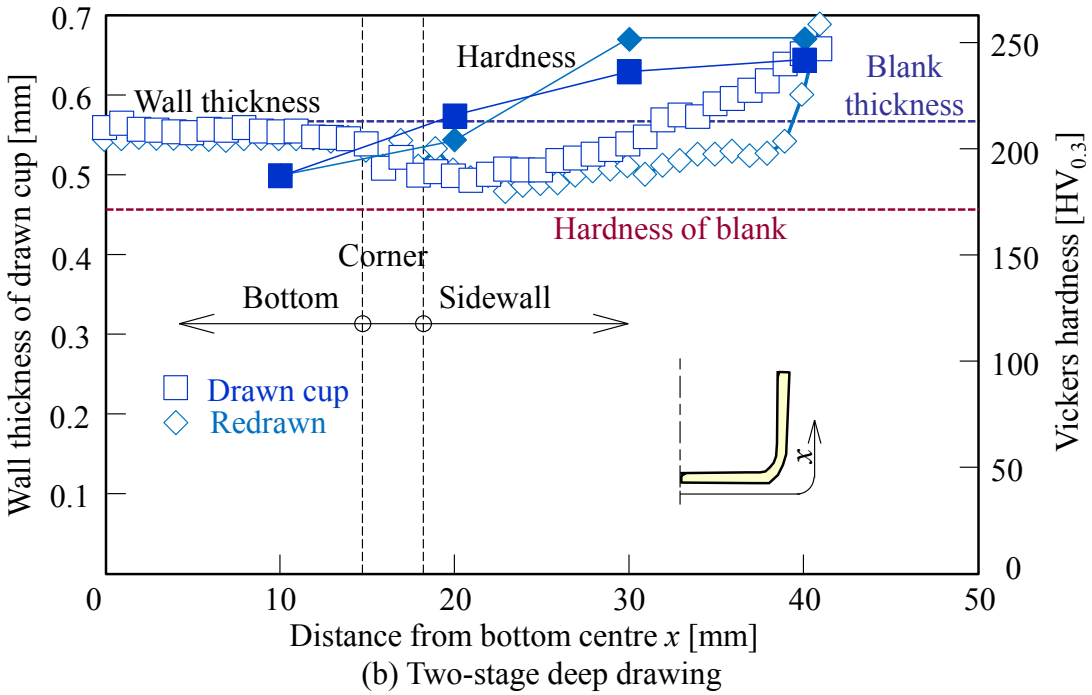

(b) Two-stage deep drawing

Fig. 5.13 Distributions of wall thickness and hardness in cups formed by deep drawing with a large clearance and two-stage deep drawing.

5.4.2 Improvement of seizure resistance

The ironing limit for cups formed by deep drawing with the large clearance and two-stage deep drawing is shown in **Fig. 5.14**. The ironing limits of both the drawn and the redrawn cups were higher than that of c_d=100%. The increments of the drawn and the redrawn cups are 84% and 89%, respectively. The ironing limit of the redrawn cup was higher than that of the drawn cup with the large clearance drawing because of its higher surface roughness causing more improvement on lubrication. However, the ironing limit does not reach the level when using the lubricant with the chlorine additive.

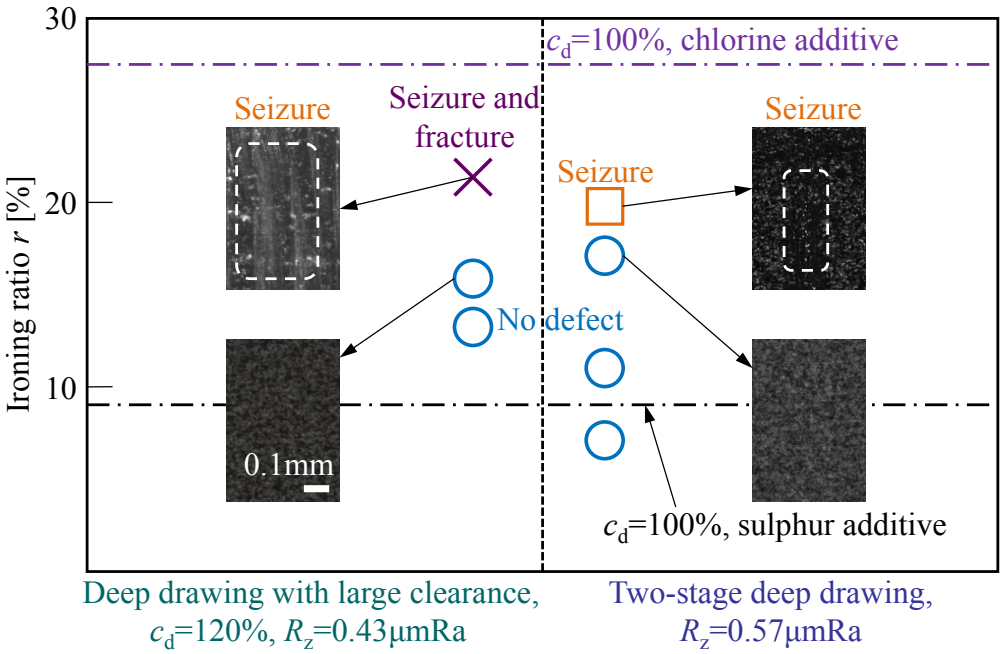

Fig. 5.14 Ironing limit for cups formed by deep drawing with a large clearance and two-stage deep drawing.

The surface and the arithmetic mean roughness of the ironing cup are shown in **Fig. 5.15**. Surface roughness was measured at about 20 mm from the bottom corner in the axial and circumferential directions. After ironing, surface roughness decreased, whereas small sanded asperities remained on the sanded cups.

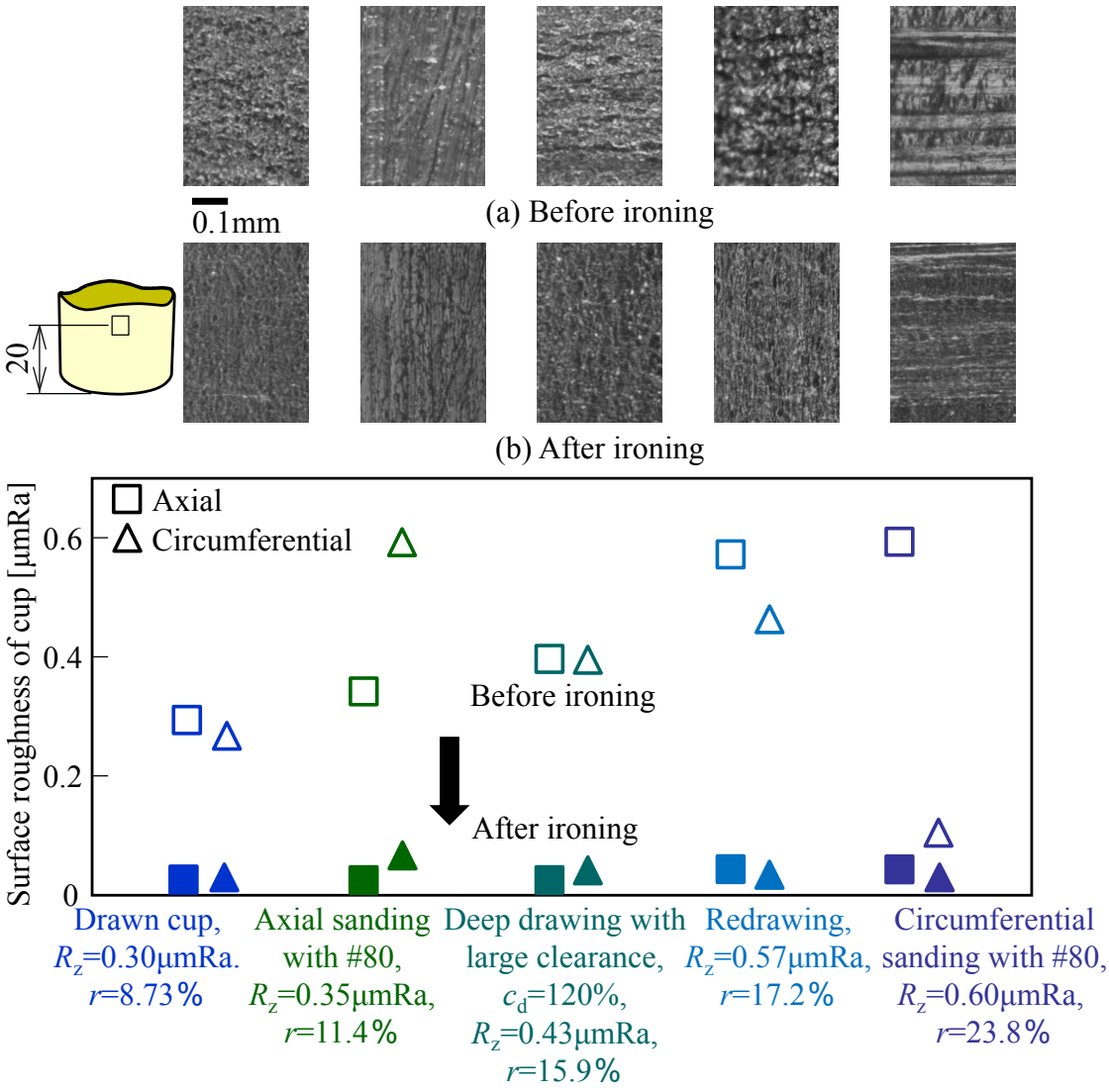

Fig. 5.15 Surface and arithmetic mean roughness of ironing cup.

The relationship between the coefficient of friction in ironing and the ironing ratio is shown in **Fig. 5.16**. The coefficient of friction between the tools and cup μ is given by:

$$\mu = \frac{P\tan\alpha}{1.15\sigma_b A_f \ln(\frac{A_0}{A_f})} - \tan\alpha, \tag{2}$$

where σ_b, A_0, A_f, α and P are the tensile strength of the sheet, the cross-sectional area of the cup before ironing, the cross-sectional area of the ironed cup, the contact angle of the die and the cup and the average ironing load, respectively [120]. The coefficient of friction increased with the ironing ratio. The coefficient of friction for the circumferential sanding

with #80 was the smallest because of the abundant lubricant in the interface caused by the large surface roughness. The coefficient of friction for the redrawn cup and the drawn cup with the large clearance ratio were smaller than that of the drawn cup.

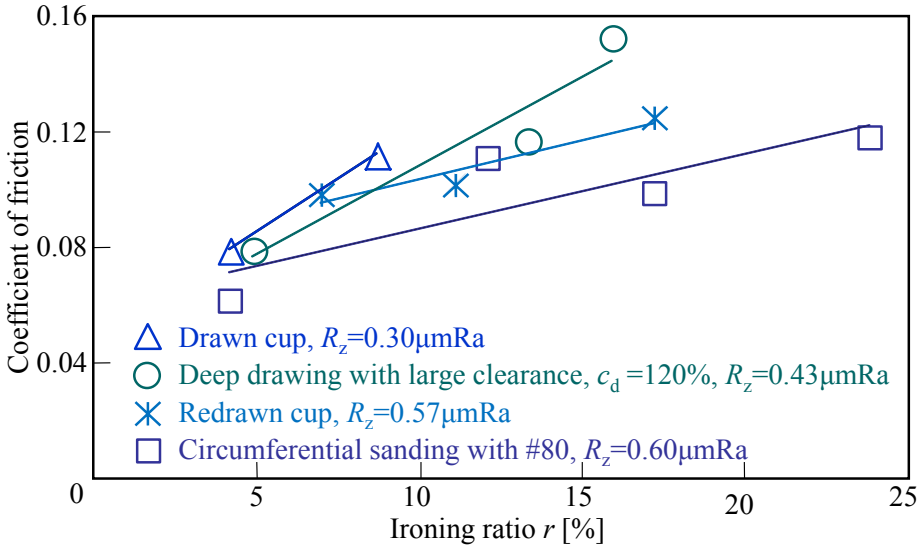

Fig. 5.16 Relationship between coefficient of friction in ironing and ironing ratio.

The measurement of the thickness of the remaining lubricant film on the sidewall of the ironed cup using fluorescence and ultraviolet rays is shown in **Fig. 5.17**. The amount of the lubricant on the sidewall of the ironed cup was measured by using fluorescence and ultraviolet rays. The drawn cup with the lubricant including fluorescence oil was ironed, and then the cup was dropped to the die plate. The ultraviolet rays were irradiated to the cup sidewall, and the exposure was observed by a camera. The relationship between the brightness of fluorescence oil and the thickness of the lubricant was calibrated with a spherical steel ball and a slide glass [127].

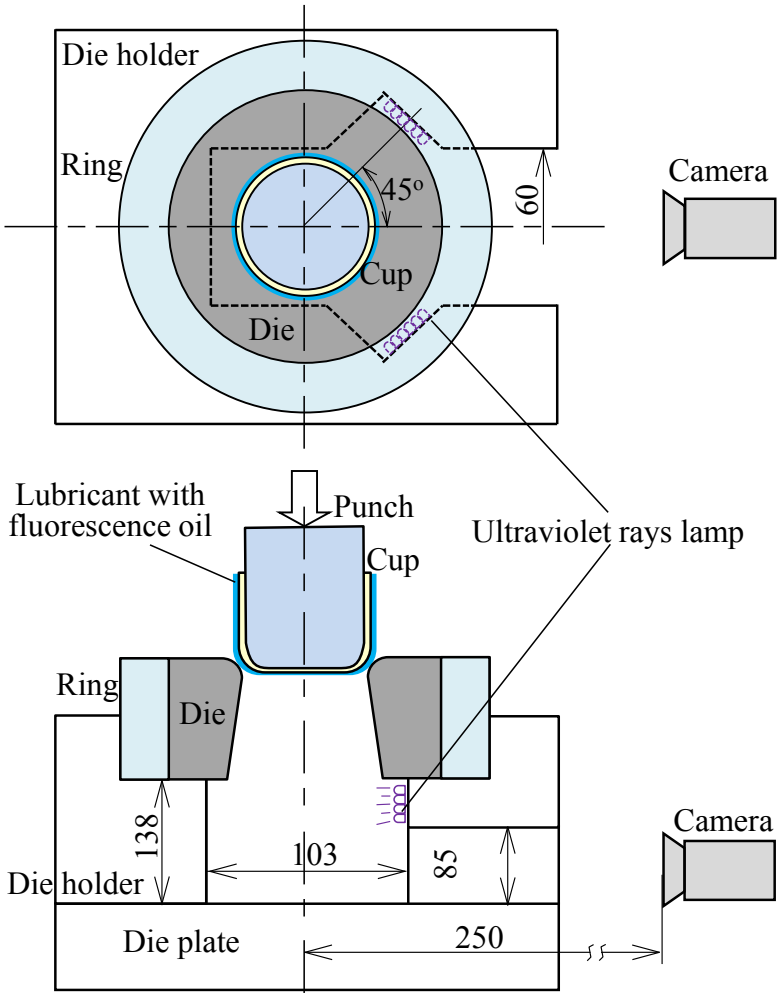

Fig. 5.17 Measurement of thickness of remaining lubricant film on sidewall of ironed cup using fluorescence and ultraviolet rays.

The distribution of the remaining lubricant film on the sidewall of the ironed cup is shown in **Fig. 5.18**. The remaining lubricant film decreased in the opening side of the cup because of large ironing caused by the larger wall thickness in the opening side of the cup before ironing as shown in Fig. 5.13.

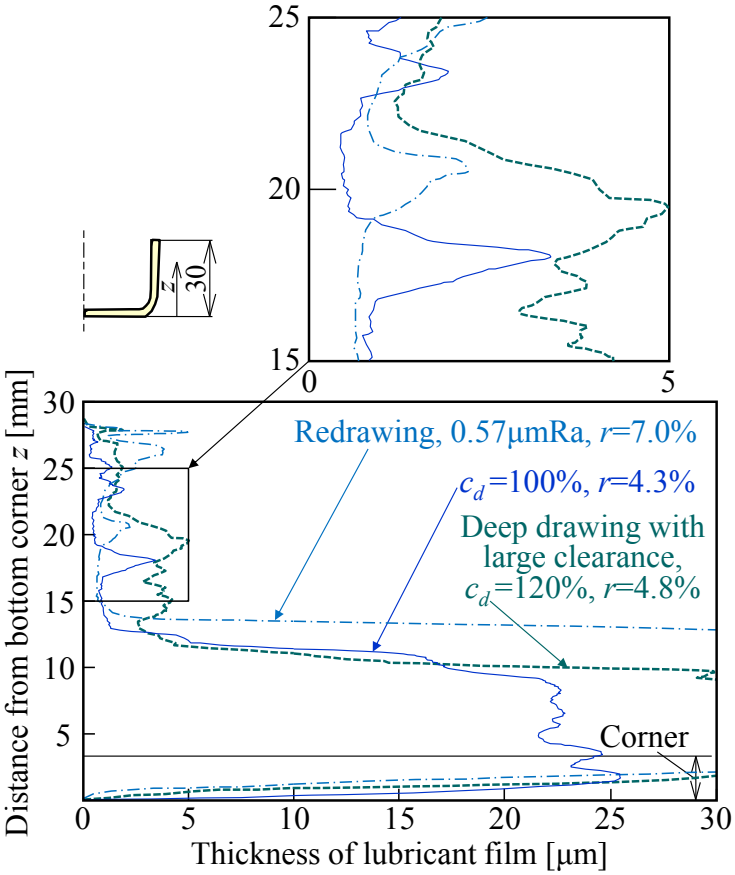

Fig. 5.18 Distribution of remaining lubricant film on sidewall of ironed cup.

The effect of surface roughness of the cup on the average thickness of the remaining lubricant film is shown in **Fig. 5.19**. Since ironing in the opening side of the cup is more severe and then seizure usually occurs around this area. The thickness of the remaining lubricant film in the sidewall from 15 mm to 30 mm of the ironed cup was averaged. The average thickness of the remaining lubricant film in the sidewall increased with surface roughness in the axial direction of the cup. Lubrication was enhanced by increasing surface roughness of the cup.

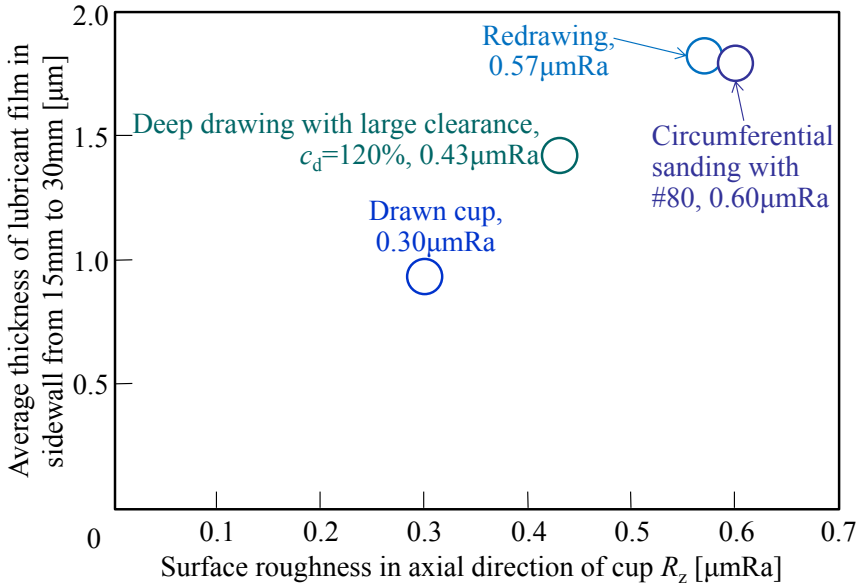

Fig. 5.19 Effect of surface roughness of cup on average thickness of remaining lubricant film.

5.5 Conclusions

The effects of the surface finish of the ferritic stainless steel cup and the die having lubricant pockets on the seizure resistance in ironing using the lubricant with the sulphur additive were investigated. In addition, the seizure resistance was improved by increasing the surface roughness of the cup using the modified deep drawing processes, and the following results were obtained:

1. The seizure resistance using the die having optimum lubricant pockets was higher than that of the polished die.
2. The seizure resistance increased with the surface roughness of the cup in the axial direction, and the increment of the die having optimum lubricant pockets was much larger than that of the polished die.
3. The ironing limits of both the drawn cup with the large clearance and the redrawing with the small die corner radius were higher than that of 100% of the clearance ratio, and the increments of the drawn and the redrawn cups were 84% and 89%, respectively.
4. The remaining lubricant film thickness in the sidewall of the ironed cup increased with surface roughness in the axial direction of the cup, thus it was found that the improvement of seizure resistance was caused by increasing the lubricant film thickness between the die and cup.

Chapter 6
Lubricant containing fine particles for improving seizure resistance in ironing of aluminium alloy cup

6.1 Introduction

Since global warming is being caused mostly by increasing concentrations of greenhouse gases and other human activities. Reducing greenhouse gas emissions such as carbon dioxide gas from automobiles is vital required. Consequently, the demand for the alternative fuel vehicles such as hybrid and electric vehicles increases, and thus batteries having high capacity are desirable. In the battery, the metal cups are used for electrolyte cases. Since the cups with a large aspect ratio are required for these parts, the cases are mainly produced by multi-stage stamping which includes deep drawing and ironing of stainless steel and aluminium alloy sheets. To improve the process conditions, process modelling was applied to deep drawing and ironing operations [11]. The aluminium alloy cups with an extreme aspect ratio are achieved by process design and a modification of the initial blank in multi-stage deep drawing [12].

In sheet stamping operations of aluminium alloy, the sheet is prone to pick-up on the die because of its high adhesion. Although aluminium alloy develops a thin, hard adherent film of oxide on their surface that protects the metal from corrosion. Seizure tends to occur when the oxide film is cracked. In deep drawing of aluminium, because of the oxide layers of sheets are cracked by local plastic deformation, caused by high normal and shear stresses. Thus, the generating metallic contact determines local micro-welding. Due to the progressive relative movement between the sheet and die, the bonding is torn apart. The separation occurs inside the volume of the sheet material and thus initiates adhesive wear [33]. In more severe conditions, such as ironing with high loads and strongly bounded asperities, adhesive wear is described as scuffing, smearing, tearing, galling, or seizure. Since proper use of the lubricant is important for preventing seizure in ironing. A strip reduction test has been used to emulate the tribological conditions for screening the lubricant in ironing of stainless steel sheets [34]. Seizure is quantified by surface roughness measurements across the strip after testing. With increasing sliding length the tool becomes

heated due to workpiece deformation and friction implying eventual breakdown of the lubricant film. Pre-heating of the tool results in earlier breakdown of the lubricant film [35]. The oil containing chlorinated paraffin is effective for the prevention of seizure in forming of stainless steel sheets. The good lubrication performance of the oil containing chlorinated paraffin is attributed to the chemical activity of the chlorinated paraffin with all the main components of stainless steel. The oil containing chlorinated paraffin enforces the formation of a thick oxide layer [36]. However, chlorinated paraffin oils are not perceived to be environmentally friendly lubricants. Therefore, there has been increasing efforts to develop environmentally benign lubricants for metal forming. Dry film solid lubricants are one of them. Various dry film solid lubricants were evaluated using deep drawing tests with increasing blank holding force. Dry film lubricants performed better than oil-based lubricants in the tests [37]. Kim et al. [38] reported that polymeric lubricants containing EP additives performed better than water emulsion and straight oil lubricants in deep drawing and ironing tests.

Since the addition of nanoparticles into lubricating oil as the lubricant additives significantly reduces the friction coefficient and increases the load-bearing capacity of the frictional parts in mechanical systems, the application of nanoparticles has attracted more attention. The use of titanium dioxide (TiO_2) nanoparticles as an oil additive in liquid paraffin exhibits good performance in friction and wear reduction as well as in load-carrying capacity. A boundary film mainly composed of TiO_2 and titanates is formed on the rubbed surfaces [88]. A suspension of each copper (Cu), copper oxide (CuO), zinc oxide (ZnO) or zirconium dioxide (ZrO_2) nanoparticles in the lubricants exhibits reduction in friction and wear compared to the base oil. The anti-wear mechanism of nanoparticles is produced by tribo-sintering of nanoparticles on the wear surfaces, reducing metal-to-metal contact and acting as load-bearing areas [89-91].

Nanoparticles such as silicon dioxide, also known as silica (SiO_2) are sphere-like in shape, are chemically stable, and have high temperature resistance and low cost. The nano-SiO_2 particles can evidently increase anti-wear ability and reduce the friction coefficient of the lubricant [92]. The use of alumina/silica (Al_2O_3/SiO_2) composite nanoparticles as lubricating oil additives also shows the reduction in the amount of wear and the increase in seizure resistance. The modified composite nanoparticles can adsorb onto the friction surfaces, which results in rolling friction. Therefore, the friction coefficient is reduced [93].

Nanoparticles have been widely used as additives to improve the tribology performance of some lubricants in load-bearing processes such as metal cutting [94, 95], and sliding bearing [96]. Therefore, the application of lubricants containing nanoparticles in the sheet metal forming processes, particularly in the ironing process, is expected to be effective in reducing friction and improving seizure resistance.

In the present study, the lubricants containing fine particles were utilised to improve seizure resistance in ironing of aluminium alloy cups. Effects of the types and size of particles on the improvement of seizure resistance were investigated. Only a mixed lubricant with silica (SiO_2) particles having ten nanometers in size exhibited a good seizure resistance performance. And then effect of different mixing quantities of fine SiO_2 particles in the lubricant on the improvement of seizure resistance was examined.

6.2 Ironing conditions using lubricant containing fine particles

The drawn cups were made of aluminium alloy A3003-O sheets having 0.6 mm in thickness and 66 mm in diameter. The mechanical properties of sheets obtained from the tensile test are shown in **Table 6.1**.

Table 6.1 Mechanical properties of aluminium alloy A3003-O sheets.

Tensile strength /MPa	Elongation /%	*n*-value	*r*-value	Hardness /HV5	Surface roughness /μmRa
200	26.8	0.22	0.79	31	0.30

The ironing conditions of drawn cups are shown in **Fig. 6.1**. The dies made of the tool steel SKD11, and TiCN-based cermet were utilised. The inside diameter of ironing dies is 34 mm. To change the ironing ratio, the clearance between the die and punch is changed by the punch diameter d_p. The drawn cups were prepared with different size corresponding to the punch diameter d_p. The outer diameter and height of the drawn cup were between 34.3 and 34.5 mm and between 25.4 and 25.9 mm, respectively. The ironing ratio r is defined as a difference between the initial thickness of the blank and the wall thickness of the ironed cup divided by the initial thickness.

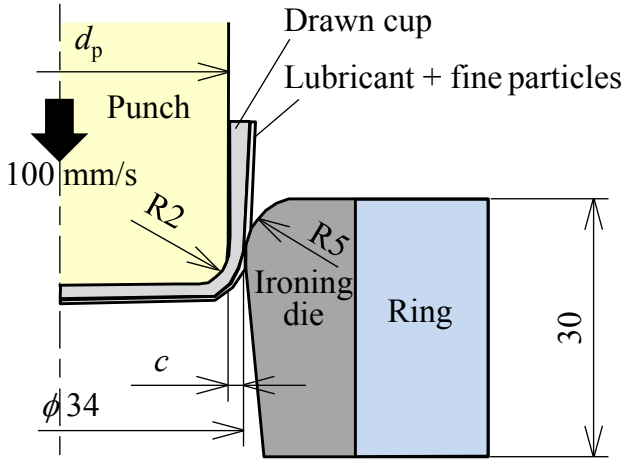

Fig. 6.1 Ironing conditions of drawn cup.

Lubricants were paraffin oils having kinematic viscosities v of 10, 170 and 500 mm^2/s at 40 °C. To investigate the effect of types of particles on the improvement of seizure resistance, silica (SiO_2), zirconium dioxide (ZrO_2) and alumina (Al_2O_3) particles were utilised as the lubricant additives. In addition, to study the effect of particle sizes, fine SiO_2 particles having the average particle size d_s of 0.01, 0.3 and 0.5 μm were used. The lubricants were ultrasonically mixed with the particles. The mixing quantity W was in the range of 0 to 5 wt% (equivalent to 0 until 2 vol%). The drawn cup was mounted to the punch, next the mixed oil was applied to the die and cup, and then the cup was ironed through the die with an ironing speed of 100 mm/s. Each ironing test was performed two times. The material properties of fine particles are given in **Table 6.2**.

Table 6.2 Material properties of fine particles.

Particles	Hardness /HV	Density /g·cm^{-3}	Average particle size d_s /nm
SiO_2	950	2.2	10 (5~15), 300 and 500
ZrO_2	1230	5.68	13 (10~15)
Al_2O_3	1570	3.95	15 (10~20)

The TEM micrograph of fine SiO_2 particles with d_s=0.01μm are shown in **Fig. 6.2**. The particles have nearly a spherical shape with the average particle size d_S=0.01μm.

Although the particles are agglomerated, after the oil was ultrasonically mixed with the particles for six hours, the particles were uniformly dispersed.

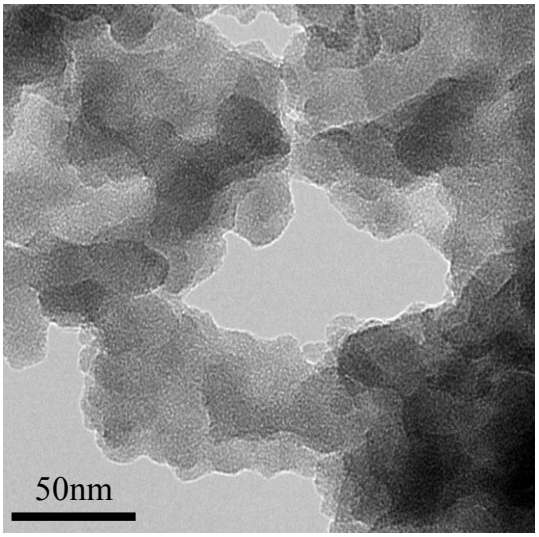

Fig. 6.2 TEM micrograph of fine SiO_2 particles with d_s =0.01μm.

The surface shapes of the die land and drawn cup are shown in **Fig. 6.3**. Both dies were finished by polishing to the fine surface with the arithmetic mean surface roughness of 0.02 μm for the TiCN-based cermet die and 0.01 μm for the tool steel one. For the drawn cup, the surface of the cup is roughened due to plastic deformation in the deep drawing process. The arithmetic mean surface roughness of the drawn cup was 0.35 μm.

The hardness of the aluminium alloy sheet, fine SiO_2 particles, the tool steel die and the cermet die are 31, 950, 750 and 1550 HV, respectively. Fine SiO_2 particles are harder than the aluminium alloy drawn cups but softer than the cermet die. Compared to the tool steel die, fine SiO_2 particles are harder than this die.

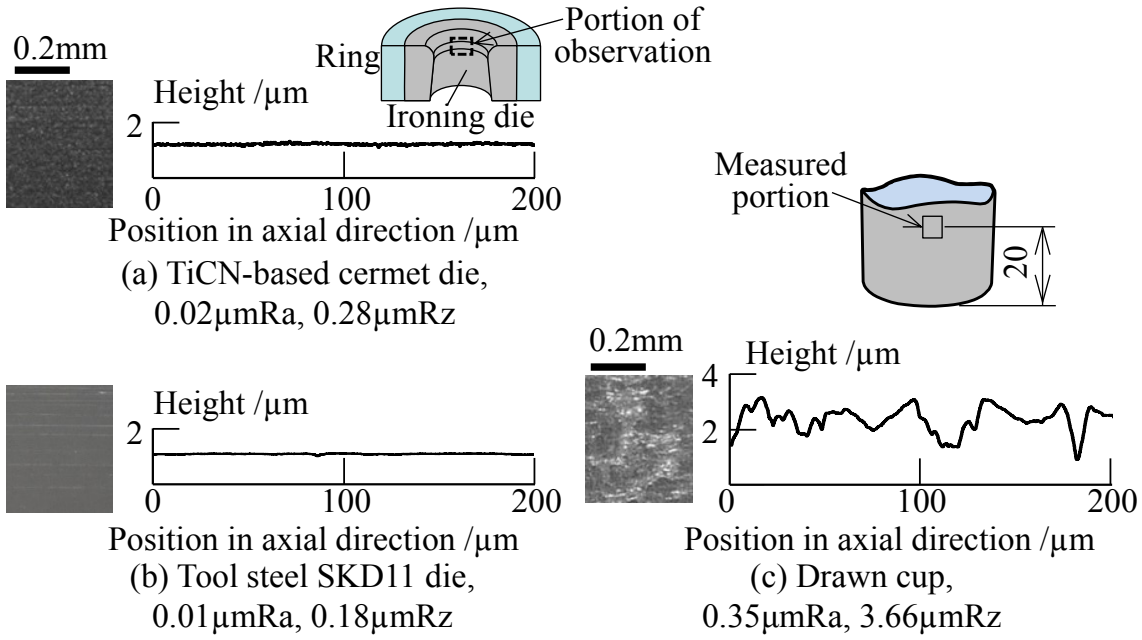

Fig. 6.3 Surface shapes of die land and drawn cup.

6.3 Improvement of seizure resistance in ironing using lubricant containing fine particles

6.3.1 Effects of types of fine particles and die materials on seizure resistance

The effect of types of fine particles mixed in the lubricant on seizure resistance for v=10 mm^2/s and W=1wt% is shown in **Fig. 6.4.** The sizes of SiO_2, ZrO_2 and Al_2O_3 particles are nearly same and their average particle sizes are in the range of 10 to 15 nm. Applying the lubricant containing fine Al_2O_3 particles, seizure early occurred and the ironing limit was inferior to that using the lubricant without particles. Rabinowicz [118] showed seizure of the sliding pair is influenced by their metallurgical compatibility. When the similar materials such as between Al_2O_3 and aluminium alloy slide against each other, seizure easily develops due to their high metallurgical compatibility. Applying the lubricant containing fine ZrO_2 particles, the ironing limit was close to that using the lubricant without particles. Another reason that there was no an improvement on seizure resistance for the lubricant containing fine Al_2O_3 or ZrO_2 particles was due to high density of these particles as shown in Table 6.2 causing sedimentation of them in few minutes after ultrasonically mixing. Thus, there was no a lubricating effect caused by the particles.

However, seizure resistance for ironing using the lubricant containing fine SiO_2 particles was improved. The good dispersion and suspension of fine SiO_2 particles in the lubricant enhanced lubrication and low metallurgical compatibility of dissimilar material structures between SiO_2 and aluminium alloy lowered the occurrence of seizure.

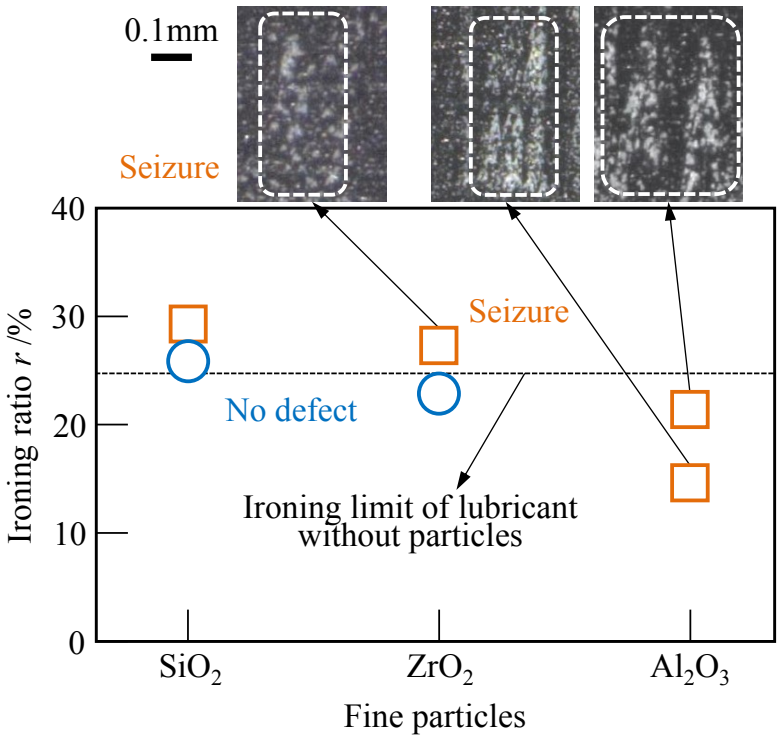

Fig. 6.4 Effect of types of fine particles mixed in lubricant on seizure resistance for v=10 mm^2/s, W=1wt%.

The effect of die materials and fine SiO_2 particles mixed in the lubricant on seizure resistance for v=10 mm^2/s, W=5wt% and d_s=0.01μm is shown in **Fig. 6.5**. For the tool steel die using the lubricant without particles, the ironing limit was low. By using the lubricant containing fine SiO_2 particles, the ironing limit of both dies was improved. The ironing limit of the cermet die was superior to the tool steel one.

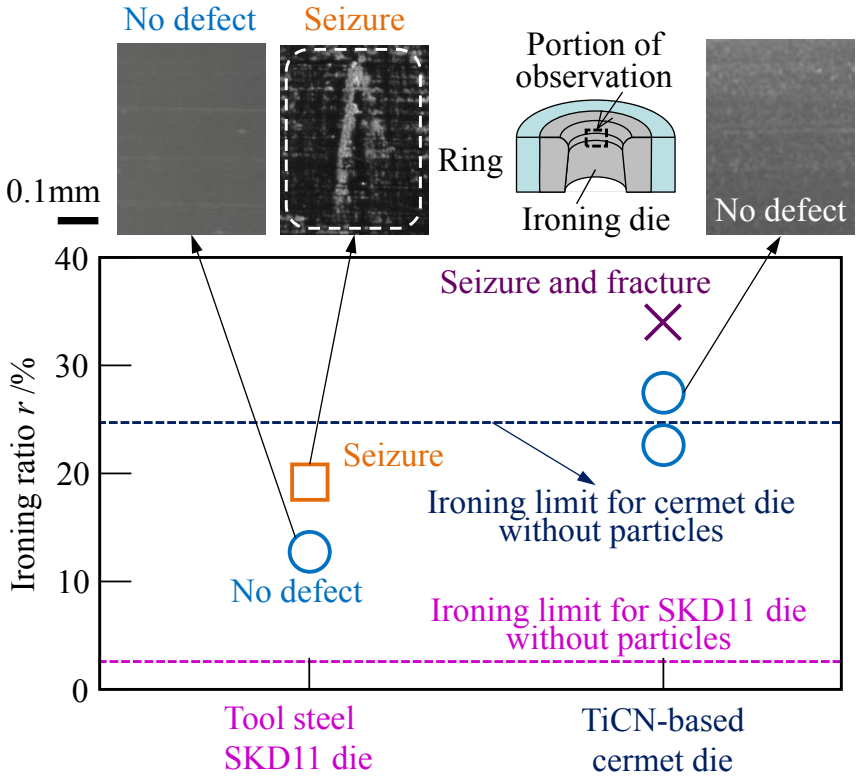

Fig. 6.5 Effect of die materials and fine SiO_2 particles mixed in lubricant on seizure resistance for v=10 mm^2/s, W=5wt%, d_s=0.01μm.

The surfaces of the die land with the lubricant containing fine SiO_2 particles for v=10 mm^2/s, W=5wt% and d_s=0.01μm are shown in **Fig. 6.6**. Although the fine and hard particles were applied, there was no damage caused by particles on the cermet die. Whereas some tiny scratches took place on the tool steel die because this die material is softer than fine SiO_2 particles.

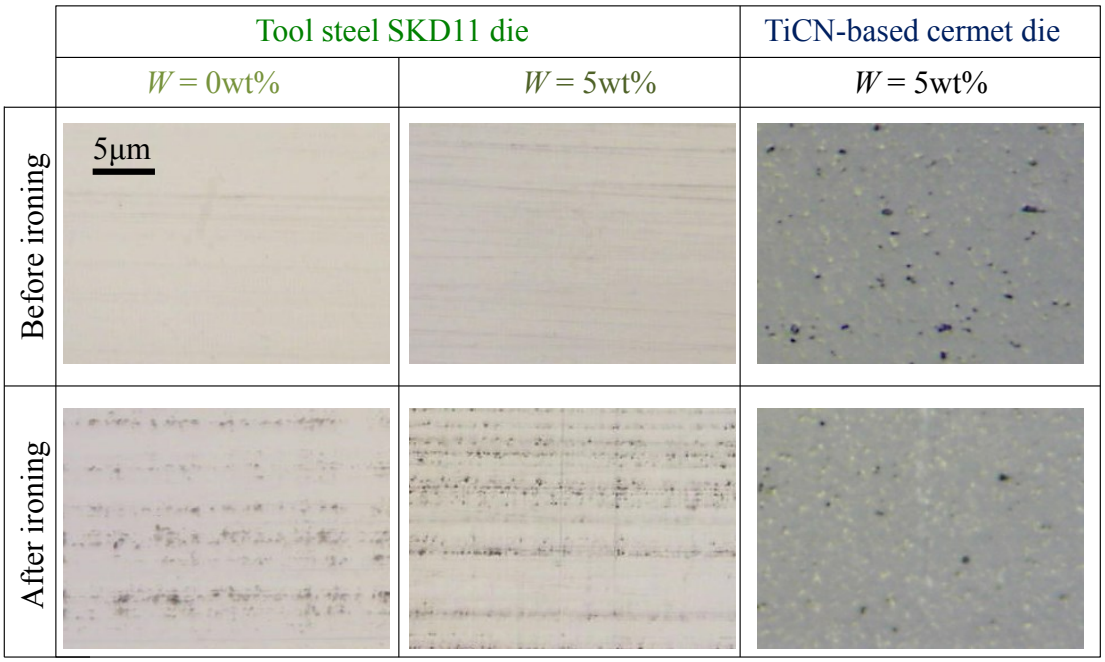

Fig. 6.6 Surfaces of die land with lubricant containing fine SiO_2 particles for v=10 mm^2/s, W=5wt% and d_s=0.01μm.

6.3.2 Effect of size of fine SiO_2 particles on seizure resistance

The ironed cups with the lubricant containing different sizes of fine SiO_2 particles and with the cermet die for v=10 mm^2/s and W=5wt% are shown in **Fig. 6.7**. Seizure was prevented when the lubricant containing fine SiO_2 particles having the size of 0.01 μm was employed. For the lubricant containing other sizes of the particles, the cups were obtained with seizure on their sidewall.

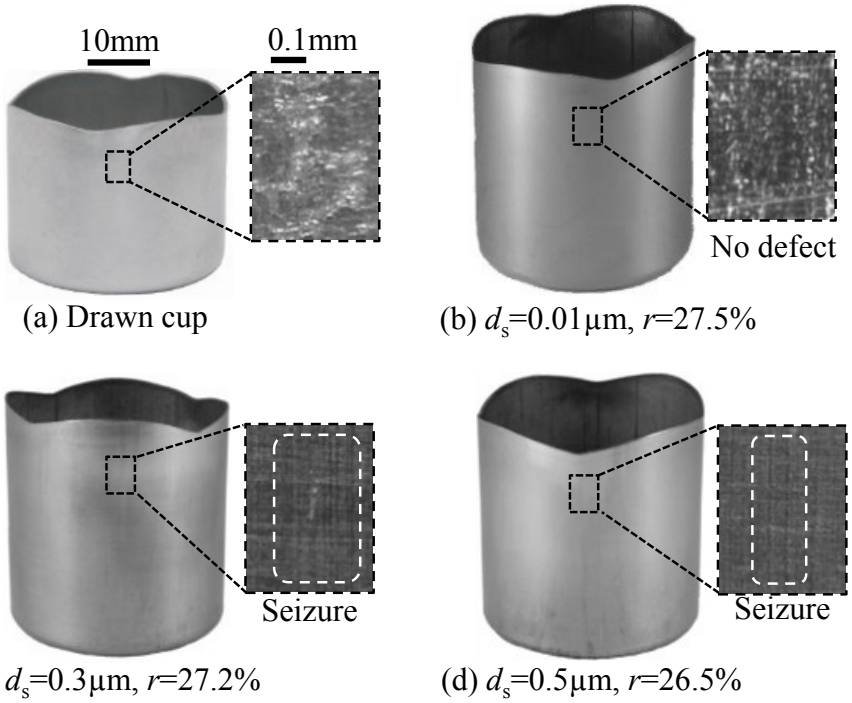

(a) Drawn cup (b) d_s=0.01μm, r=27.5%

(c) d_s=0.3μm, r=27.2% (d) d_s=0.5μm, r=26.5%

Fig. 6.7 Ironed cups with lubricant containing different sizes of fine SiO_2 particles and with cermet die for v=10 mm^2/s, W=5wt%.

The effect of the size of fine SiO_2 particles mixed in the lubricant on seizure resistance with the cermet die for v=10 mm^2/s and W=5wt% is shown in **Fig. 6.8**. With the lubricant containing large particle sizes of 0.3 or 0.5 μm, there was no an improvement. The ironing limit is nearly same as the lubricant without particles. However, with fine particles, 0.01 μm, the ironing limit was improved. Since the weight of the smaller size of fine SiO_2 particles is lighter than the larger particles, fine SiO_2 particles having the size of 0.01 μm had superior dispersion and suspension in the lubricant to that having the size of 0.3 or 0.5 μm. Thus lubrication was enhanced with the smallest size of particles. There is a possibility to improve seizure resistance when the lubricant containing fine SiO_2 particles having the size of 0.01μm and the cermet die are utilised.

The effect of the size of fine SiO_2 particles mixed in the lubricant on an average ironing load with the cermet die for v=10 mm^2/s, W=5wt% and r=23% is shown in **Fig. 6.9**. The average ironing load increased as the particle size increased. Since the lubricant film thickness estimated for v=10 mm^2/s was thinner than 0.3μm [128]. The particle size of 0.3 and 0.5μm might stick and prohibit the sliding of die-cup interfaces increasing the ironing load. The particle size of 0.01 μm can flow and prevent the direct die-to-cup contact.

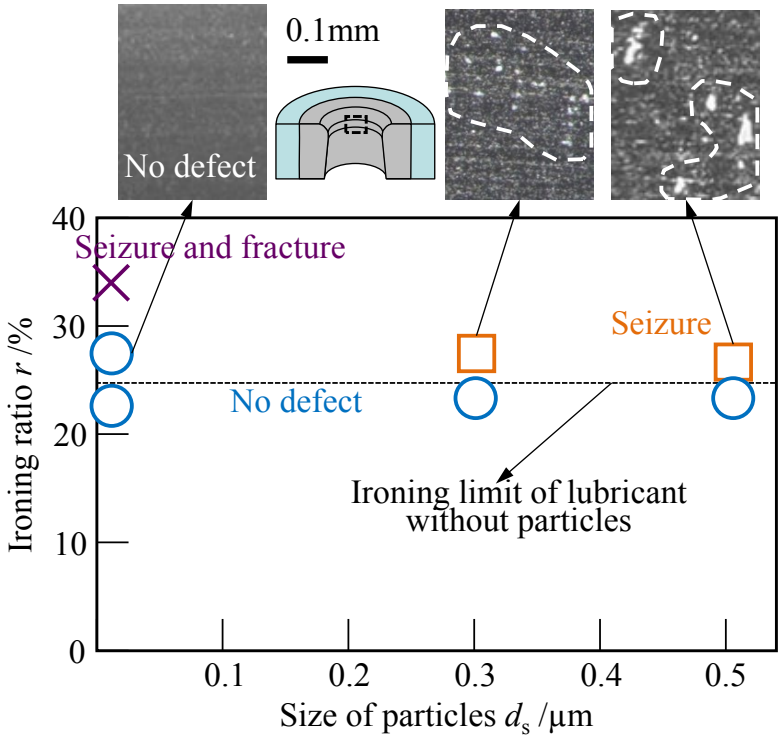

Fig. 6.8 Effect of size of fine SiO_2 particles mixed in lubricant on seizure resistance with cermet die for v=10 mm^2/s, W=5wt%.

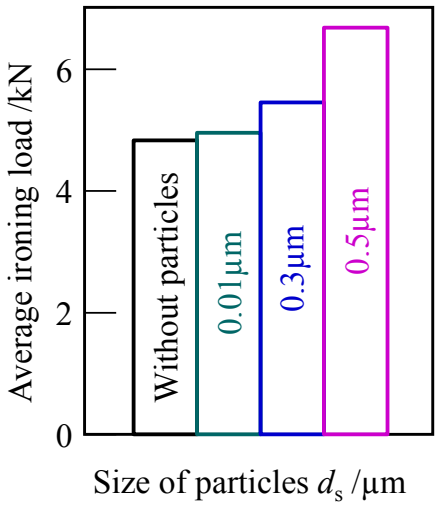

Fig. 6.9 Effect of size of fine SiO_2 particles mixed in lubricant on average ironing load with cermet die for v=10 mm^2/s, W=5wt%, r=23%.

The schematic diagram illustrating the effect of the size of fine SiO_2 particles mixed in the lubricant for v=10mm^2/s is shown in **Fig. 6.10**. The lubricant film thickness was thinner than 0.3μm for v=10 mm^2/s [128]. Therefore, only the particle size of 0.01 μm can flow

and can prevent the direct die-to-cup contact as shown in Fig. 6.10 (a). On the other hand in Fig. 6.10 (b), because of their large size of 0.3 or 0.5 μm, the particles cannot flow between the interfaces. Thus the die directly contacts to the cup initiating the seizure.

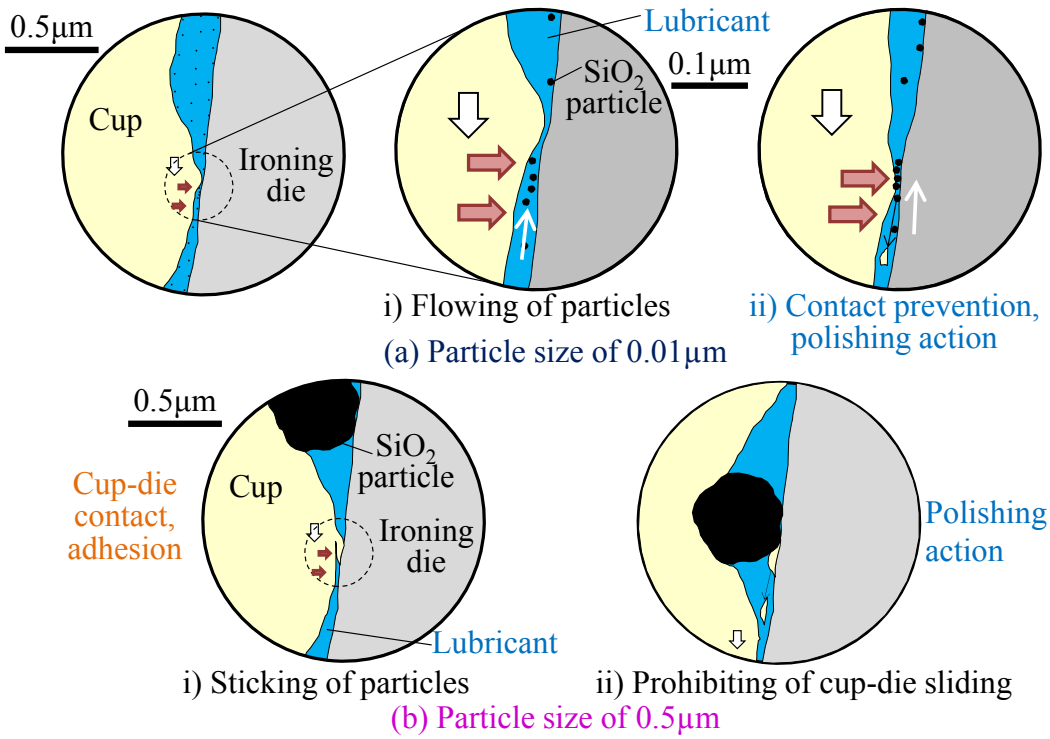

Fig. 6.10 Schematic diagram illustrating effect of size of fine SiO_2 particles mixed in lubricant for ν=10 mm^2/s

6.3.3 Effect of quantity of fine SiO_2 particles mixed in lubricant on seizure resistance

The ironed cups with the cermet die for d_s=0.01μm are shown in **Fig. 6.11**. For ν=10 mm^2/s and W=0.1 wt%, seizure early took place at a low ironing ratio. However, seizure was prevented when the mixing quantity was increased to 5 wt%. For ν=170 mm^2/s, although seizure was observed for W=0.5 wt%, the cup was successfully obtained with a smooth surface when the mixing quantity was 1 wt%. In comparison to the results for ν=10 mm^2/s, the increase in viscosity of the lubricant enhanced the performance of fine SiO_2 particles in the lubricant due to the formation of a thin film at the contact surface. Fine SiO_2 particles trapped in the thin film prevented the formation of local bonding among the

asperities at the contact surface. For v=500 mm^2/s, the results exhibit the same tendency as v=170 mm^2/s. The cup was obtained without the defect for W=1 wt%.

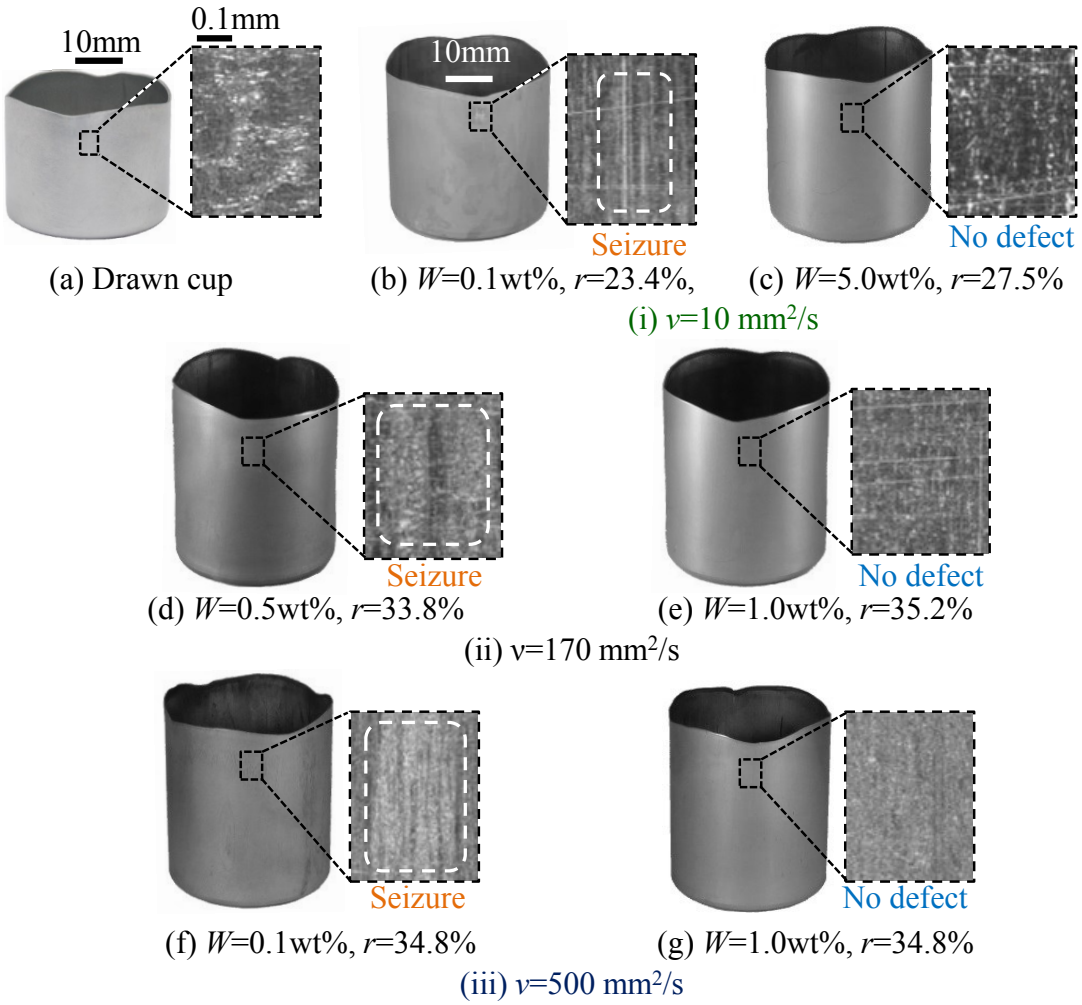

Fig. 6.11 Ironed cups with cermet die for d_s=0.01μm.

The effect of fine SiO_2 particles mixed in the lubricant on the ironing limit for v=10 mm^2/s is shown in **Fig. 6.12**. Fine SiO_2 particles had a little effect on increasing the ironing limit of the cups when the viscosity of the lubricant was low. The ironing limits of W=2 wt% and below quantity were almost the same as that of the lubricant without particles. However, the ironing limit was slightly increased for a high mixing quantity of 5 wt%. Seizure resistance was improved, because there were enough particles in the lubricant.

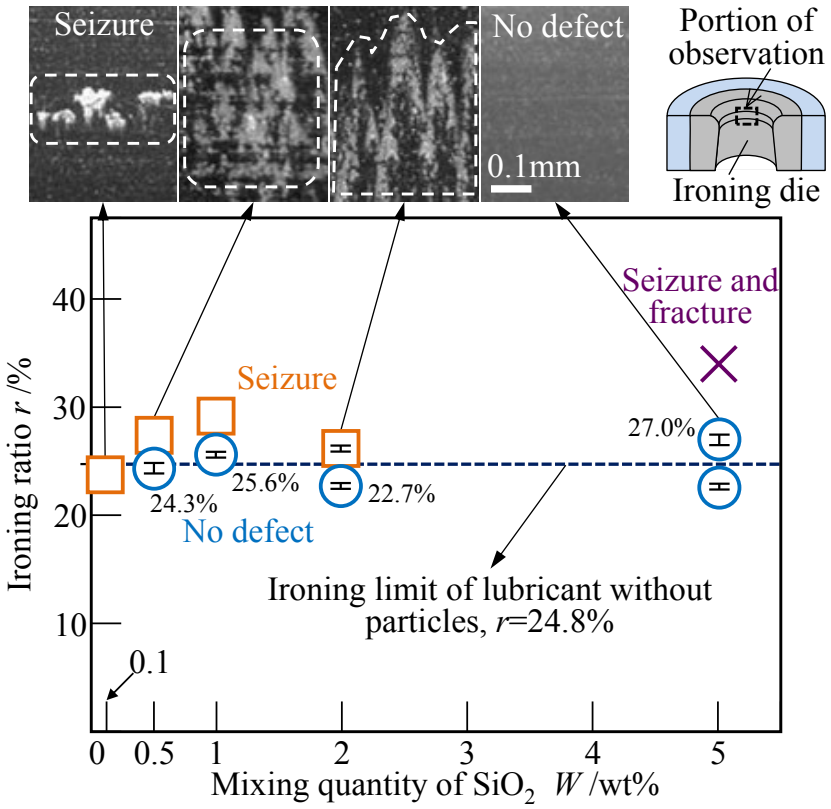

Fig. 6.12 Effect of fine SiO_2 particles mixed in lubricant on ironing limit for v=10 mm^2/s.

The effect of fine SiO_2 particles mixed in the lubricant on the ironing limit for v=170 mm^2/s is shown in **Fig. 6.13**. Although at r about 34%, there was seizure occur on the die for a mixing quantity of 0.5 wt%. At higher mixing quantities, seizure was prevented. The ironing limit for W=1 wt% exhibited the highest.

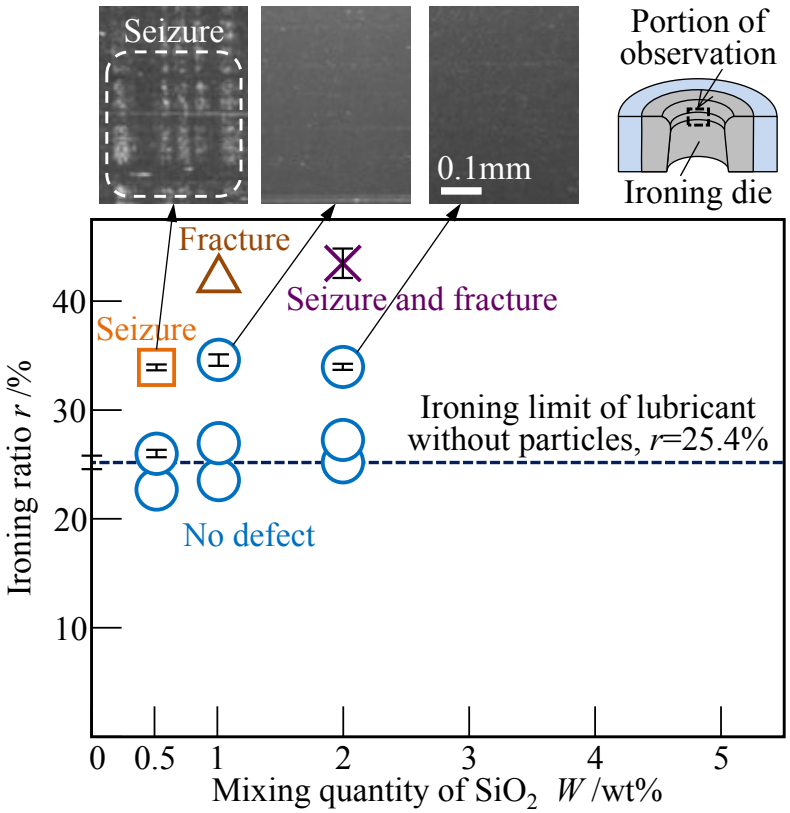

Fig. 6.13 Effect of fine SiO_2 particles mixed in lubricant on ironing limit for v=170 mm^2/s.

The effect of fine SiO_2 particles mixed in the lubricant on the ironing limit for v=500 mm^2/s is shown in **Fig. 6.14**. The ironing limits of all mixing quantities were significantly improved. The ironing limit for W=2 wt% was the highest. The increase in viscosity resulted in the better performance of the particles under high contact pressure. A lubricant having a high viscosity is essential for enhancing the performance of the SiO_2 at the contact surface. However, an excessive quantity of fine SiO_2 particles mixed in the lubricant lowered the ironing limit. This might be due to the ironing load increased when the lubricant containing a high quantity of fine SiO_2 particles were applied. Thus the fracture of the cup and seizure occurred.

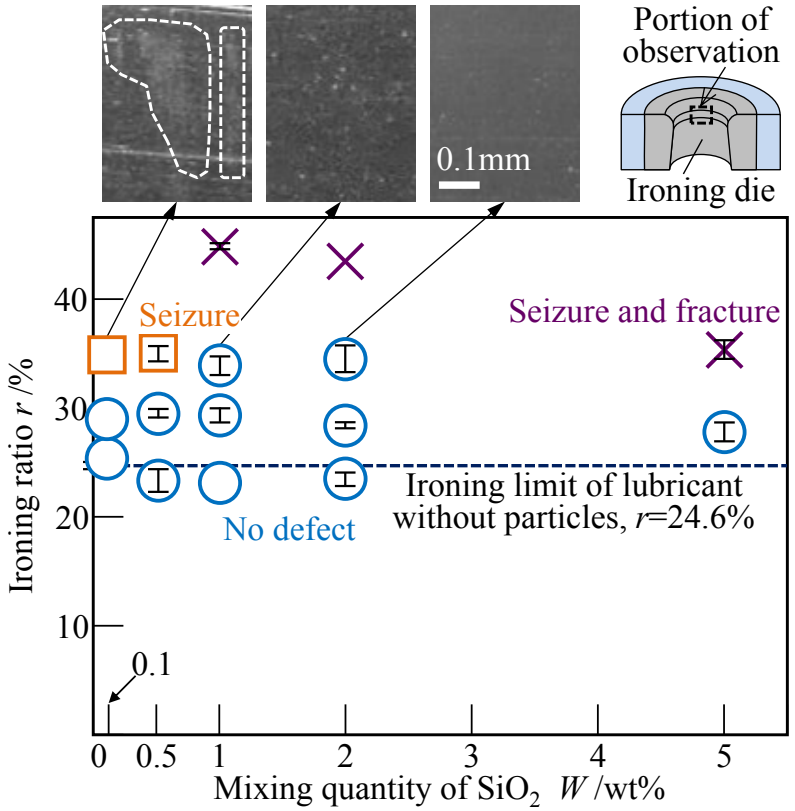

Fig. 6.14 Effect of fine SiO_2 particles mixed in lubricant on ironing limit for v=500 mm^2/s.

To better understand about the improvement on seizure resistance with the lubricant containing fine SiO_2 particles, the ironed cup surfaces were observed by using a scanning electron microscope (SEM). The SEM observation on ironed cup surfaces taken at a same height of 30 mm from the cup bottom for v=500 mm^2/s is shown in **Fig. 6.15**. There were some white particles remained at the ironed cup surface when the lubricant containing fine SiO_2 particles was applied. To assure that the particles remained on the cup surface after ironing were fine SiO_2 particles. The chemical analysis was further performed.

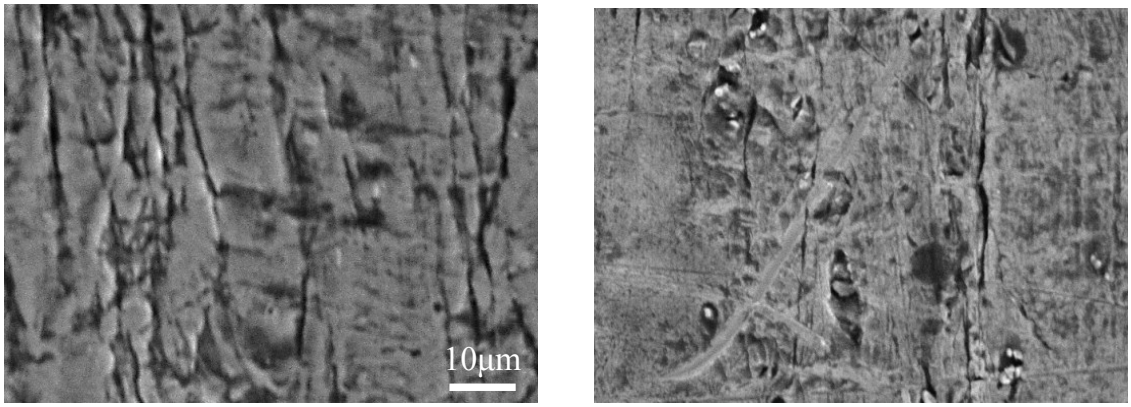

(a) W=0%, r =24.2%　　(b) W =1wt%, r =34.8%

Fig. 6.15 SEM observation on ironed cup surfaces taken at same height of 30 mm from cup bottom for v =500 mm^2/s.

It is difficult to directly observe fine SiO_2 particles having ten nanometers in size remaining on the sidewall surface of the ironed cups. Hence a quantitative elemental analysis of the Si element on the sidewall of the ironed cup surfaces was performed using a scanning electron microscope (SEM) equipped with energy dispersive X-ray spectroscopy (EDX). A quantification of the Si element on the sidewall of the ironed cups is shown in **Fig. 6.16**. Because an aluminium alloy A3003-O contains 0.1Si (wt%) in its composition, for a mixing quantity of 0 wt%, the Si element was also detected for both v=10 mm^2/s and 500 mm^2/s. The quantification of the Si element on the sidewall of the ironed cups increased when the mixing quantity of fine SiO_2 particles increased. Comparing the same mixing quantity, W=1 wt%, the quantification of the Si element on the sidewall of the ironed cups with a lubricant having a high viscosity was higher than that with a lubricant having a low viscosity. This might be due to fine SiO_2 particles were better retained by the lubricant having the high viscosity.

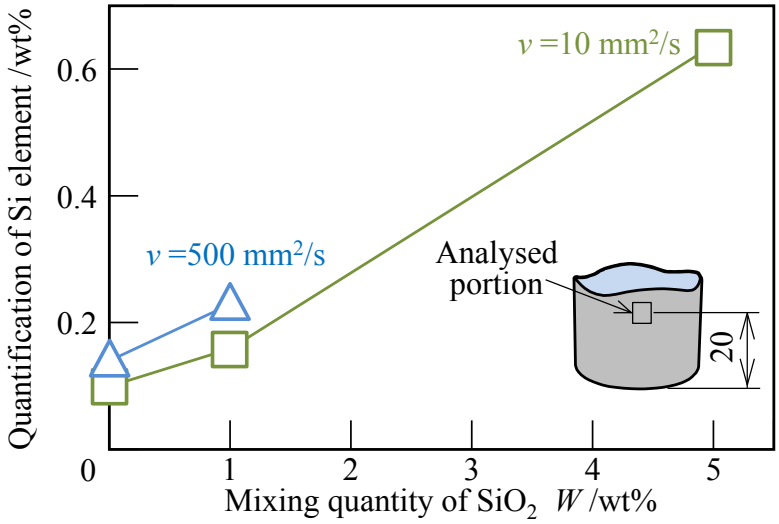

Fig. 6.16 Quantification of Si element on sidewall of ironed cup.

The comparison of hardness on the sidewall surface of the ironed cups between W=0 wt% and W=1 wt% for v=500 mm^2/s, d_s=0.01μm and r around 25% are shown in **Fig. 6.17**. Hardness of the ironed cup with the lubricant containing fine SiO_2 particles was slightly higher than with the lubricant without particles. This enhancement of hardness may cause by the formation of a boundary film mainly composed of Si on the cup surface.

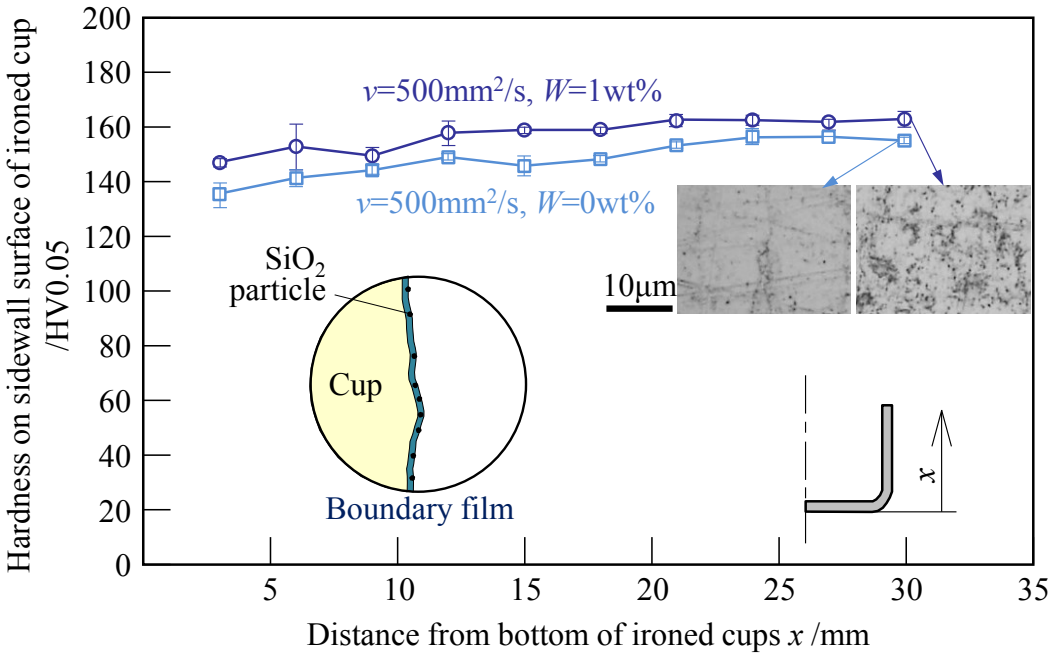

Fig. 6.17 Comparison of hardness on sidewall surface of ironed cups between W=0 wt% and W=1 wt% for v=500 mm^2/s, d_s=0.01μm and r around 25%.

The ironing load-stroke curves for d_s=0.01μm, r around 25% and different mixing quantities are shown in **Fig. 6.18**. The ironing loads increased when the viscosities of the lubricants were increased. With fine SiO_2 particles, the ironing loads are slightly higher than without particles for all viscosities.

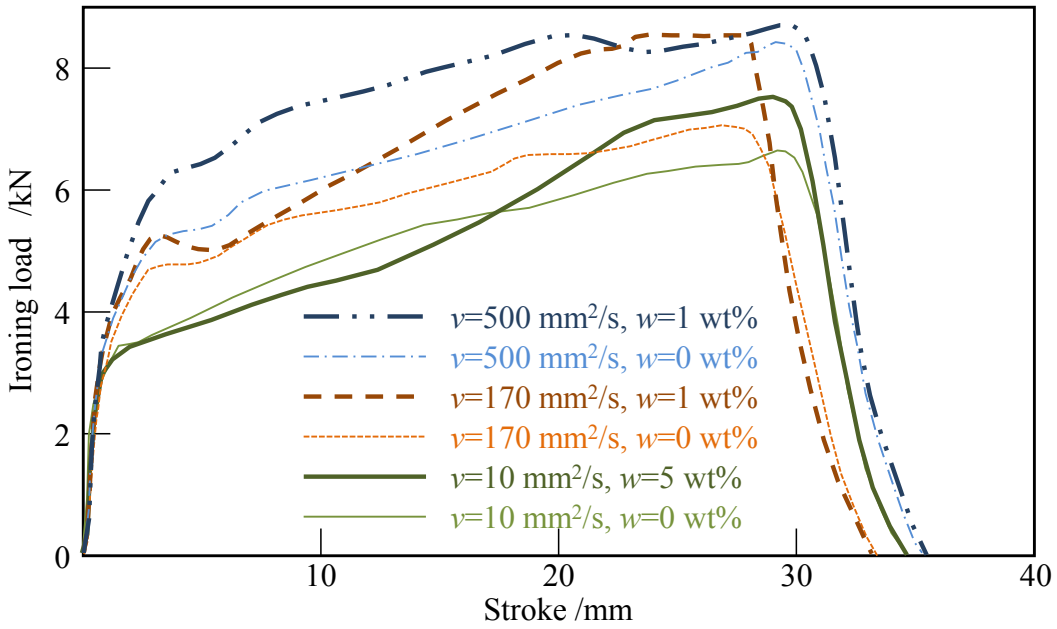

Fig. 6.18 Ironing load-stroke curves for d_s=0.01μm, r around 25% and different mixing quantities.

The surface profiles of the ironed cups in an axial direction for d_s=0.01μm, r around 25% and different mixing quantities are shown in **Fig. 6.19**. For all types of the lubricant, There was no a significant effect of fine SiO_2 particles on the average surface roughness of the ironed cups due to the nano-size and low mixing quantity of the particles.

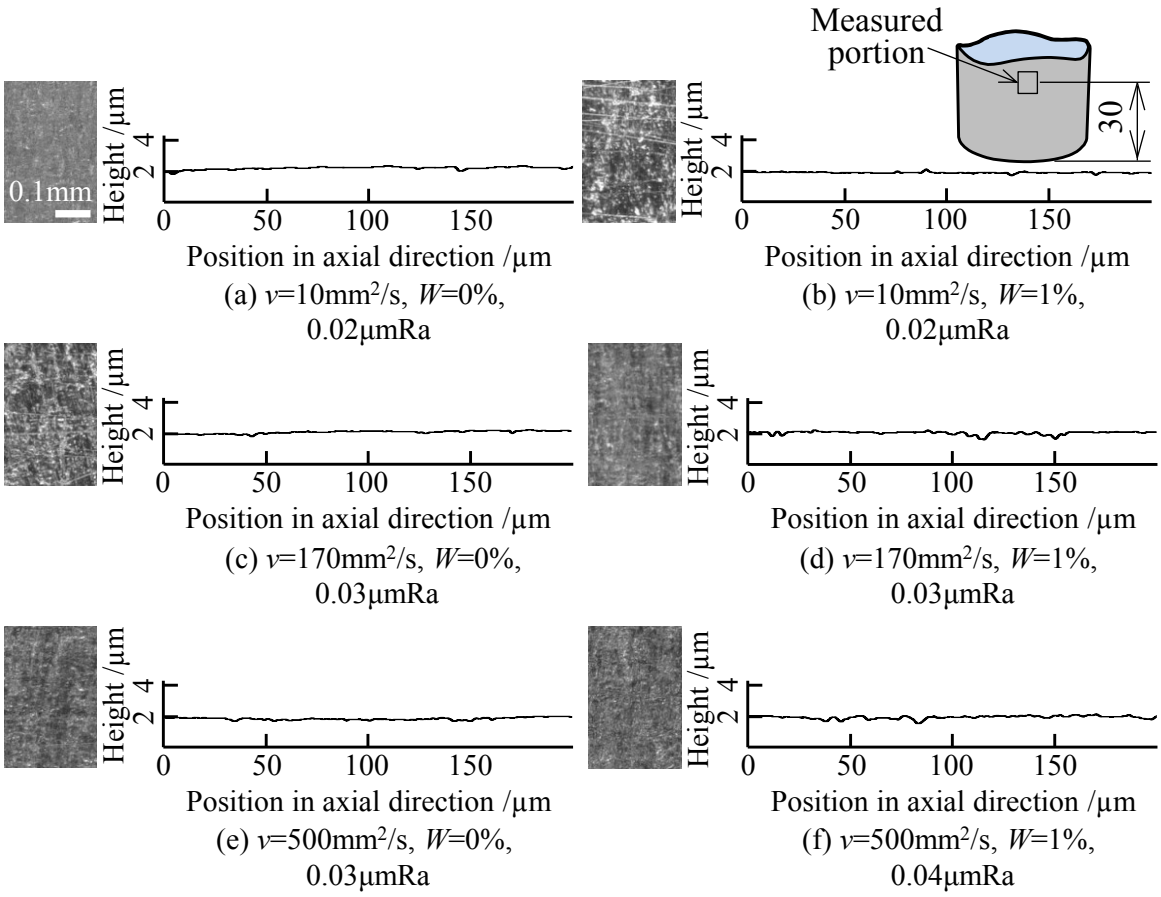

Fig. 6.19 Surface profiles of ironed cups in axial direction for d_s=0.01μm, r around 25% and different mixing quantities.

The surface roughness of ironed cups in circumferential direction for d_s=0.01μm, r around 25% and different mixing quantities is shown in **Fig. 6.20**. Before ironing, the surface roughness of the cup was 0.35μmRa. After ironing, surfaces of all cups became smooth. Ironing with the lubricant containing fine SiO_2 particles having the size of 0.01 μm had no a significant effect on the surface roughness around the circumferential direction of the ironed cup due to the nano-size and low mixing quantity of the particles.

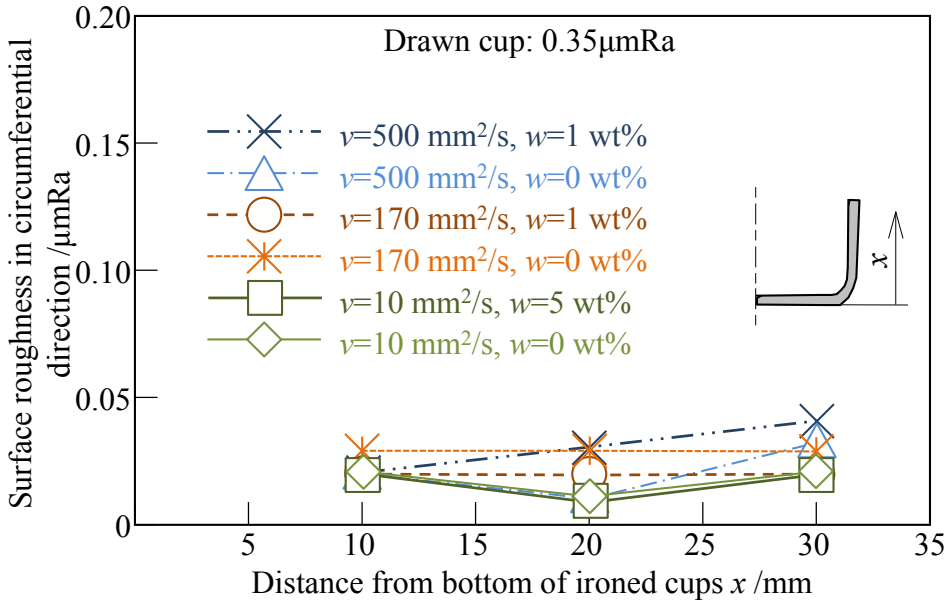

Fig. 6.20 Surface roughness of ironed cups in circumferential direction for d_s=0.01μm, r around 25% and different mixing quantities.

The comparison of the average ironing loads between v=10 mm^2/s and v=500 mm^2/s for W=0 wt% and W=1 wt% in repeated ironing is shown in **Fig. 6.21**. In this process, 20 samples of drawn cups were repeatedly ironed through the polished die with the ironing ratio r of 25% without re-polishing the die at the end of each process. The surface condition of the die was observed at the end of each test. The test was stopped once seizures were observed at the die surface and the number of trials, n was recorded. Although the average ironing load increased with the viscosity of the lubricant, the load of ironing using the lubricant with and without particles was not so different. For v=10 mm^2/s, seizure occurred at n=3. However the cups were successfully ironed until 20 strikes without the occurrence of seizure on the die for v=500 mm^2/s. Mixing of fine SiO_2 particles in the lubricant having the low viscosity had no effect on increasing the seizure resistance of the die.

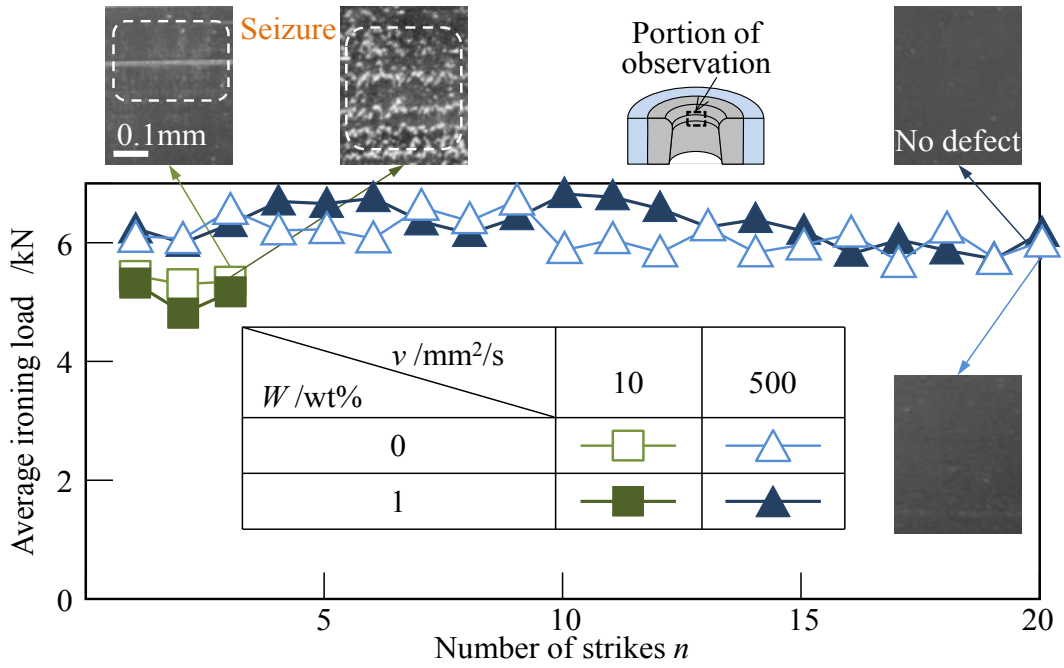

Fig. 6.21 Comparison of average ironing loads between v=10 mm^2/s and v=500 mm^2/s for W=0 wt% and W=1 wt% in repeated ironing.

The comparison of the coefficient of friction between v=10 mm^2/s and v=500 mm^2/s for W=0 wt% and W=1 wt% in repeated ironing is shown in **Fig. 6.22**. Although the coefficient of friction increased with the viscosity of the lubricant, the coefficient of friction of ironing using the lubricant with and without particles was not much different.

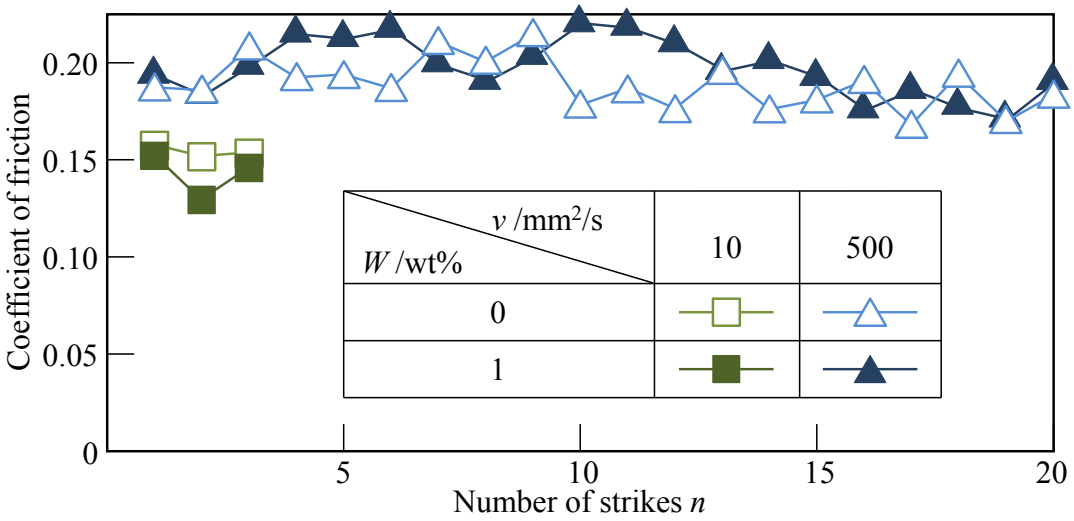

Fig. 6.22 Comparison of coefficient of friction between v=10 mm^2/s and v=500 mm^2/s for W=0 wt% and W=1 wt% in repeated ironing.

The prevention of the seizure growth with the SiO_2 particles having the size of 0.01 μm is shown in **Fig. 6.23**. As ironing progresses, (a) the cup contacts with the die and then (b) the particles flow between the interfaces. For (c) the low viscosity lubricant, the particles squeeze out with the flow of the lubricant, whereas for (d) the high viscosity lubricant, the particles are trapped and embedded between the contacting surfaces. The direct contact is prevented. If adhesion occurs, the adhered material on the die will be polished out by the particles.

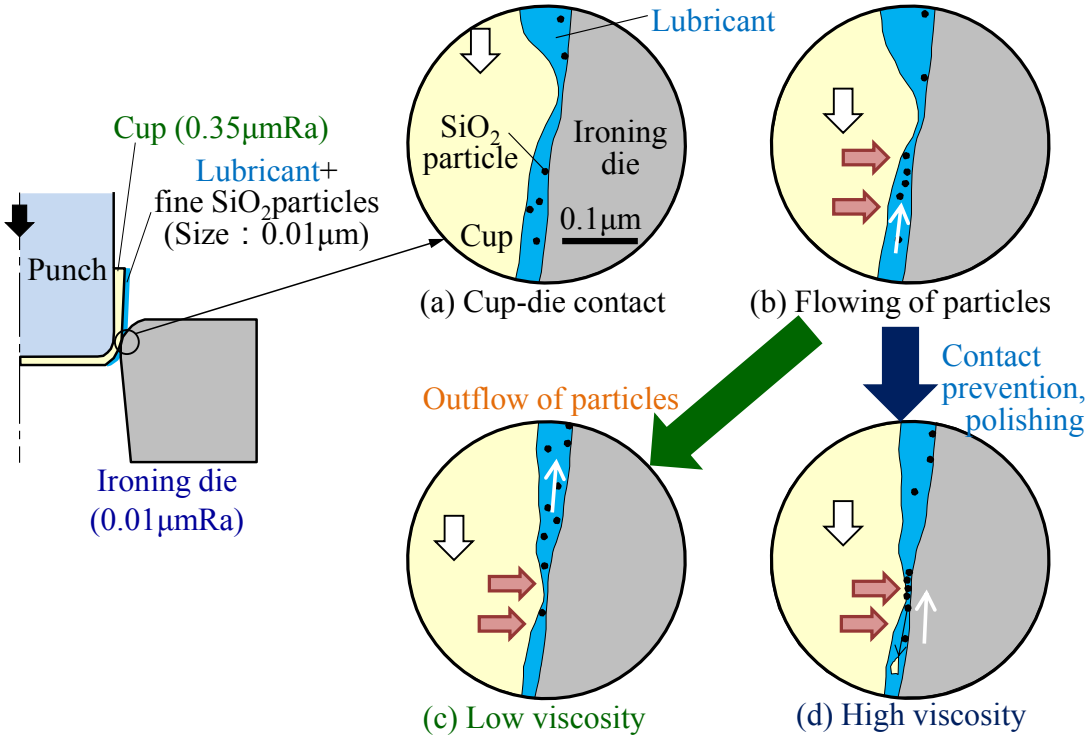

Fig. 6.23 Prevention of seizure growth with SiO_2 particles having size of 0.01μm.

6.4 Conclusions

The lubricants containing fine particles were utilised to improve seizure resistance in ironing of aluminium alloy cups. The results are summarized as follows:

1. Seizure resistance in ironing of the aluminium alloy cups was improved with the lubricant containing fine SiO_2 particles. For ZrO_2 or Al_2O_3 particles, seizure resistance was equal to or inferior to the lubricant without fine particles.
2. The lubricant containing fine SiO_2 particles having the size of 0.01 μm was effective in improving seizure resistance. There was no an improvement with the larger size of 0.3 μm and 0.5 μm.

3. For the low viscosity lubricant, fine SiO_2 particles had a little effect on increasing the ironing limit. The ironing limit was improved only with a large quantity of SiO_2.
4. Seizure resistance was effectively improved by applying the high viscosity lubricant with fine SiO_2 particles because the particles can be trapped and embedded for preventing the direct contact between the die and cup.
5. The improvement of seizure resistance caused by the formation of a protective film preventing the direct die-to-cup contact.
6. The surface roughness of the ironed cups was not affected by the presence of SiO_2.
7. The increase in ironing loads due to the presence of SiO_2 was not significant.

Chapter 7
Improvement of seizure resistance in ironing of aluminium alloy cup using titanium nitride coated die

7.1 Introduction

Aluminium alloys are widely used to produce lightweight components in automobiles [3]. Aluminium, however, has a tendency to induce an adhesive wear at the tool surface during forming hence lubricant is conventionally used to prevent the adhesion of aluminium alloys to the forming tools [33, 54]. Kawai et al. [27] showed that the metal adhesion in an ironing process of aluminium cups was prevented by using appropriate conditions of viscosity of lubricant and degree of reduction of Al thickness. However, a large amount of lubricant waste is a serious environmental issue.

To reduce the amount of lubricant used, low-adhesion tool materials such as ceramics and cermets as well as coatings by chemical and physical vapour deposition processes (CVD and PVD) are applied. Various types of tool material and coating combinations have been discussed in previous literature. Examples of these are presented here. Tamaoki et al. [42, 43] proposed the use of an electroconductive ceramic die for a dry deep drawing of a cold rolled mild steel sheet (JIS-SPCC), and the cups were successfully deep drawn for more than 10,000 times. MoB-based cermets had been shown to have an excellent anti-galling performance in aluminium sheet forming [103]. A TiCN-based cermet die was also studied and shown to exhibit a high seizure resistance in an ironing of stainless steel drawn cups [117].

Diamond-like carbon (DLC) has also been proven to successfully reduce the Al adhesion on metal forming dies. Murakawa et al. [105] demonstrated the effectiveness of DLC coating in preventing the adhesion of aluminium to a deep-drawing die for deep-drawing of aluminium sheets without lubrication. On an ironing die, a DLC coating also exhibited an excellent anti-galling performance for dry ironing of high strength steel sheets [108].

Other coatings were also studied. A CrN-coated die was demonstrated to be effective in a deep drawing of advanced high strength steel [111]. Podgonik et al. [104] indicated

that the galling resistance could be improved by using forming tools suitably coated for the type of the working material. For the forming of stainless steel, carbon-based coatings provided the best protection against the work material transfer. The forming of aluminium and aluminium alloys required nitride type coatings while titanium and titanium alloys required VN coatings to show improvement in galling performance. Amongst the nitride-based coatings, VN was shown to be less prone to galling as compared to TiN, for stainless steel [112].

In the present study, VN and TiN coatings deposited by a direct current (DC) magnetron sputtering PVD with optimum deposition parameters were utilised in an ironing process of Al alloy in order to reduce the metal adhesion. The objectives of this study were to improve the surface quality of ironed aluminium cups and to reduce the die polishing time for ironing operation by reducing the tendency of aluminium adhesion on the tool surface.

7.2 Experimental procedures

7.2.1 Tool and workpiece materials

JIS SKH51 high-speed steel with chemical composition (wt.%) of 0.8 C, 3.75 Cr, 4.73 Mo, 1.78 V and 5.50 W was employed as substrates for coating and as tool material for ironing dies. The substrates and dies were hardened to 63±2 HRC and finished by grinding followed by lapping prior to the coating process. The measurement of surface roughness is done by 2D stylus method using 8 mm measured length with 0.8 mm cut-off. The surface roughness of the substrates and dies are 0.01±0.003μm R_a and 0.02±0.01μm R_a, respectively. AA1050 H14 aluminium alloy rings with the dimensions as shown in **Fig. 7.1** and aluminium alloy sheets of the same grade having a thickness of 0.5 mm were used as the workpiece material. The chemical composition of AA1050 H14 alloy is shown in **Table 7.1** and the mechanical properties of SKH51 and AA1050 H14 are shown in **Table 7.2**.

Table 7.1 Chemical composition of AA1050 H14 alloy.

Element	Si	Fe	Cu	Mn	Zn	Ti	Other	Al
wt.%	0.25	0.4	0.05	0.05	0.05	0.03	0.03	Bal.

Table 7.2 Mechanical properties.

	Poisson ratio	Young's modulus [GPa]	Hardness [HV]
SKH51	0.29	207	772
AA1050	0.33	69	36

7.2.2 Coatings and deposition processes

VN and TiN coatings were deposited using PVD via DC magnetron sputtering technique. The substrates and dies were ultrasonically cleaned with methanol and acetone, then dried with hot air before being placed in the deposition chamber. Pure Ti (99.995%) and Pure V (99.5%) were used as sputtering targets for the deposition of TiN and VN respectively. Ar and N_2 were used as the working and reactive gases respectively. The base pressure of the chamber was below $5.0x10^{-6}$ mbar. The substrates and dies were etched for 15 mins in an argon plasma using the argon pressure of $7\ x10^{-3}$ mbar, a bias voltage of 600 V and a pulsed frequency of a dc power supply set at 200 kHz. Coating parameters of pressure, flow rate and DC pulse frequency were optimised to obtain stoichiometric phase compositions of TiN and VN. The resulting range of the deposition parameters of TiN and VN coatings in this study are given in **Table 7.3**.

Table 7.3 Magnetron sputtering PVD deposition parameters of TiN and VN coatings.

Parameter	**Specification**	
	TiN	VN
Target (50.8 mm. dia.)	Ti (99.995%)	V (99.5%)
Substrate	SKH51	SKH51
Target to substrate distance [mm]	90	90
Base pressure [mbar]	$5.0x10^{-6}$	$5.0x10^{-6}$
Sputtering pressure [mbar]	$5.0x10^{-3}$	$5.0x10^{-3}$
Ar flow rate [sccm]	4	6
N_2 flow rate [sccm]	1.03	1.7
Power [W]	225 and 265	225 and 265
DC pulse frequency [kHz]	50	75
Substrate temperature [°C]	390 ± 10	340 ± 10
Deposition time [min]	60	60

TiN coated samples via a cathodic arc technique typical of a commercial coating used on ironing dies were also prepared for comparison. The cathodic arc coating parameters are shown in **Table 7.4**.

Table 7.4 Cathodic arc PVD deposition parameters of TiN coating.

Parameter	
Target material (140 mm. dia.)	Ti
Substrate bias voltage [V]	24
Ar flow rate [sccm]	45
N_2 flow rate [sccm]	1,500
Substrate to target distance [mm.]	460
Base pressure [mbar]	$1.0x10^{-5}$
Arc current [A]	150
Substrate temperature [°C]	350 ± 10
Deposition time [min]	45

7.2.3 Coating characterization

The coatings were characterised for phase composition using X-ray diffraction (XRD). Crystallographic phases were deduced by comparing the experimental diffraction patterns with the Joint Committee on Powder Diffraction Standards (JCPDS) data. The hardness, coating adhesion and thickness of the coatings were characterised by nano-indentation, scratch testing and calotest, respectively. Surface roughness of coated and uncoated-surfaces was measured using a mechanical stylus profiler. The reported hardness, coating adhesion, thickness and surface roughness values are the averages of at least 3 measurements.

7.2.4 Ring-on-disc test

To evaluate the tribological properties of the coatings, sliding wear tests were conducted on a friction and wear test machine with a ring-on-disc type. The ring on disc rotation test imitates the sliding movement in the ironing process under normal pressure. Two types of sliding test with different purposes were conducted; a constant loading and a

step loading. The constant loading test used a small load in order to clearly observe the initial aluminium transfer from the ring to the disc. In practice, the transfer of aluminium onto the tool surface causes rough tool surface which, in turn, introduce deep scratches on the cup. The step loading, on the other hand, introduced a higher normal loading. However, the load employed was still significantly lower than that in the ironing process. This test was used to rank the specimens according to their resistance to aluminium adhesion at high normal load. The step loading test is also used to verify the relevancy of the standard ring-on-disc test by comparing the surface damages of the aluminium ring and the ironed aluminium cup. The coating showing the best performance was then applied onto a die for the ironing test in section 7.2.5. The ironing test assumed a high normal loading comparable to the industrial condition which cannot be achieved using a standard ring-on-disc test rig.

The ring on disc test was carried out at room temperature under a lubricated condition as illustrated in **Fig. 7.1.** The contacting couple is an aluminium alloy ring and a high-speed steel SKH51 disc. Both uncoated and coated discs were employed. The coated disc samples were cathodic arc TiN, 225W-TiN, 265W-TiN, 225W-VN and 265W-VN and the deposition parameters are shown in Table 7.3. The sample naming reflects the coating material and the voltage used during sample preparation. A liquid lubricant of highly refined mineral oil and commercial grade additives, namely Castrol ILOFORM PN232 with a kinematic viscosity of 9.94 cSt at 40 °C, was applied. Under an applied normal load, the ring slid against the disc rotating in opposite directions to one another.

In the constant loading test, the amount of aluminium adhered on the disc after test was evaluated in order to compare the effectiveness of each coating in resisting adhesion. The applied normal load, sliding speed and total sliding cycles were kept constant at 35 N, 0.014 m/s and 24 cycles, respectively. Due to the small mass of transferred aluminium, the discontinuity in aluminium coverage on the disc and the variation in its thickness, it was difficult to accurately quantify the amount of aluminium based on the weight gain or the adherence area. A quantitative elemental analysis was thus performed on four locations evenly spaced along the circumference of the wear track on a disc at x30 magnification. An "adherence index" was derived from the average weight percentage of aluminium from the four measurements. Imaging and chemical analysis of all wear areas were performed using

SEM equipped with an EDS instrument. The EDS analysis was taken at 15 kV voltage, 10 mm working distance and the probe current was 70 μA.

In the step loading test, the wear resistance was evaluated as a function of a normal load. The applied normal load was increased in 10 N steps for every 24 cycles while the sliding speed was fixed until severe damage from aluminium transferring is detected. 4 samples were tested for each condition. Typically, a significant amount of surface damage and the amount of material transfer to the counter surface can indicate the occurrence of severe wear. A coating was thus selected from this evaluation to deposit on the ironing die.

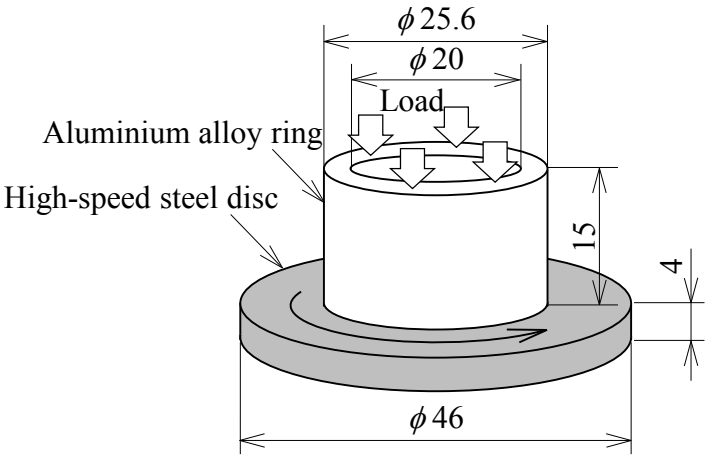

Fig. 7.1 Ring-on-disc test (scale in mm.).

7.2.5 Ironing test of aluminium cups

The ironing test utilised a 40-tonne mechanical press to simulate an industrial operating condition where the die surface is subjected to high normal loads. The test was conducted to evaluate the performance of the selected die coating on ironing of AA1050 H14 aluminium alloy cups in comparison with an uncoated SKH51 die. The surface roughness of the die was 0.02±0.01 μm R_a. The selected coating from the results of evaluation of the previous test was deposited on the die with an approximate thickness of 1 μm. Aluminium alloy drawn cups having a wall thickness of 0.5 mm were ironed as shown in **Fig. 7.2**. The number of strikes per minute was approximately 30. A Castrol ILOFORM PN232 liquid lubricant was applied. For each die, the ironing was done until a severe scratch detected by naked eye occurred on the ironed cup surface. The drawn cups were ironed with the ironing ratio, *r,* of 35%, which is typical of an industrial ironing process.

The ironing ratio was determined by a difference between the initial thickness of the blank and the average wall thickness of the ironed cup divided by the initial thickness.

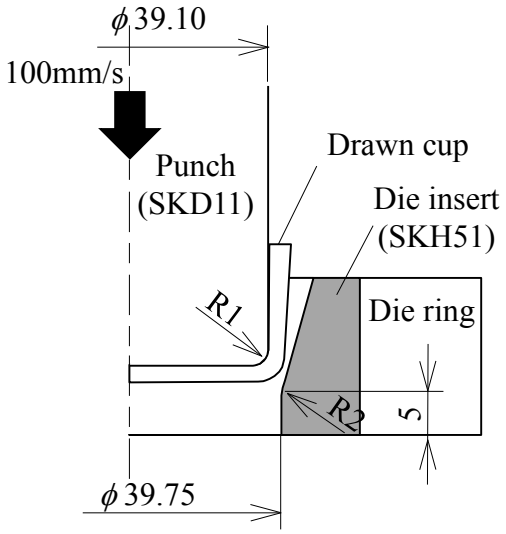

Fig. 7.2 Ironing of aluminium cups illustrated in half-section view (scale in mm.).

7.3 Results and discussion

7.3.1 Coating properties

The XRD patterns of 225W-TiN and 225W-VN coatings are shown in **Fig. 7.3**. The XRD results verified that the TiN phase was obtained when the argon-nitrogen flow rate ratio was 4/1.03 sccm and the VN phase was obtained when the flow rate ratio was 6/1.7 sccm. The TiN coating exhibits a golden color and the color of the VN coating is metallic gray.

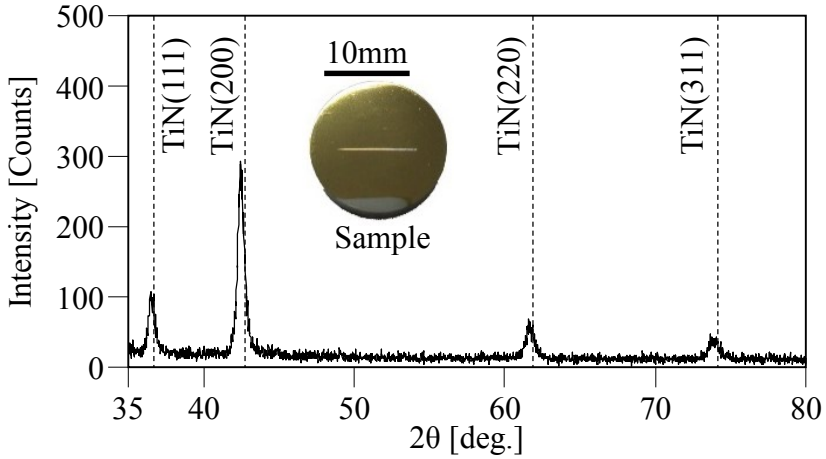

(a) 225W-TiN, Ar = 4 sccm, N_2 = 1.03 sccm

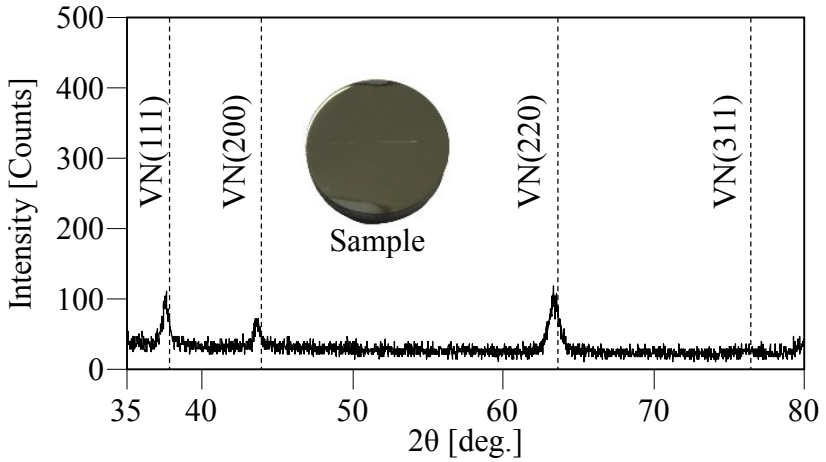

(b) 225W-VN, Ar = 6 sccm, N_2 = 1.7 sccm

Fig. 7.3 XRD patterns of coatings by DC magnetron sputtering technique.

The load-to-failure and the thickness of the coatings are shown in **Table 7.5**. The load-to-failure reflects the coating-substrate adhesion strength and is defined as the critical load as indicated by the scratch testing. The load under which a crack initiates on a coating is defined as critical load 1 (Lc_1) and the load under which the coating fails completely is determined as critical load 2 (Lc_2). In the ironing process, an occurrence of a small crack on a die coating can cause a scratch on the cup products. Therefore, Lc_1 becomes more significant for an ironing die. The cathodic arc TiN shows rather high Lc_1 of 63 N. The reason for this may partly be due to a thick coating layer of 4 μm. The Lc_1 of 265W-TiN and VN coated dies are higher than those of 225W-TiN and VN. The thickness of the four coatings is about 0.5 μm.

Table 7.5 Load-to-failure and thickness of coatings.

Coating	Load-to-failure [N]		Thickness [μm]
	Initial crack Lc_1	Coating Failure Lc_2	
Cat. arc-TiN	63	Above 100	4.10
225W-TiN	28.3	63.0	0.42
265W-TiN	50.1	71.0	0.56
225W-VN	22.6	66.5	0.57
265W-VN	29.0	61.1	0.64

The arithmetic mean surface roughness of the discs with different coatings is shown in **Fig. 7.4**. Prior to coating, the discs were finished by lapping to R_a of 0.01±0.003μm. After deposition, the TiN and VN coatings were polished to remove droplets by solution of 0.25μm diamond grit. There are indications that the surface roughness of all discs increases after coating. The cathodic arc TiN exhibits the highest surface roughness. The other coatings deposited using the DC magnetron sputtering PVD technique show a slight increase in their roughness.

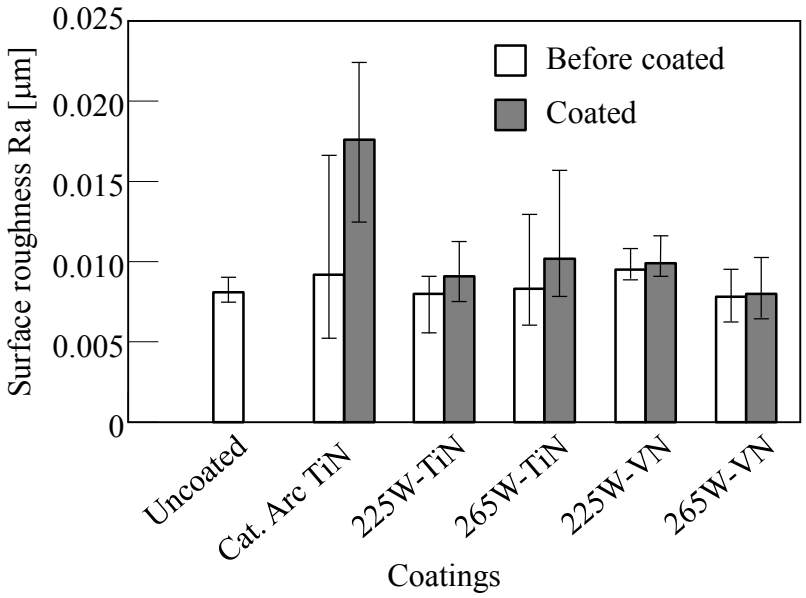

Fig. 7.4 Surface roughness of discs with various coatings.

The hardness of the discs measured by indentation test with 5 mN load with various coatings is shown in **Fig. 7.5**. The maximum penetration depth reached 20 - 25% of the coating thickness, therefore the hardness of coatings may show lower results than it should be due to the influence from the substrate, except for the cathodic arc TiN. However, in comparison, the hardness of the coated surfaces was enhanced as compared to the uncoated one. The two different sputtering powers showed slight differences in the hardness of TiN and VN coatings.

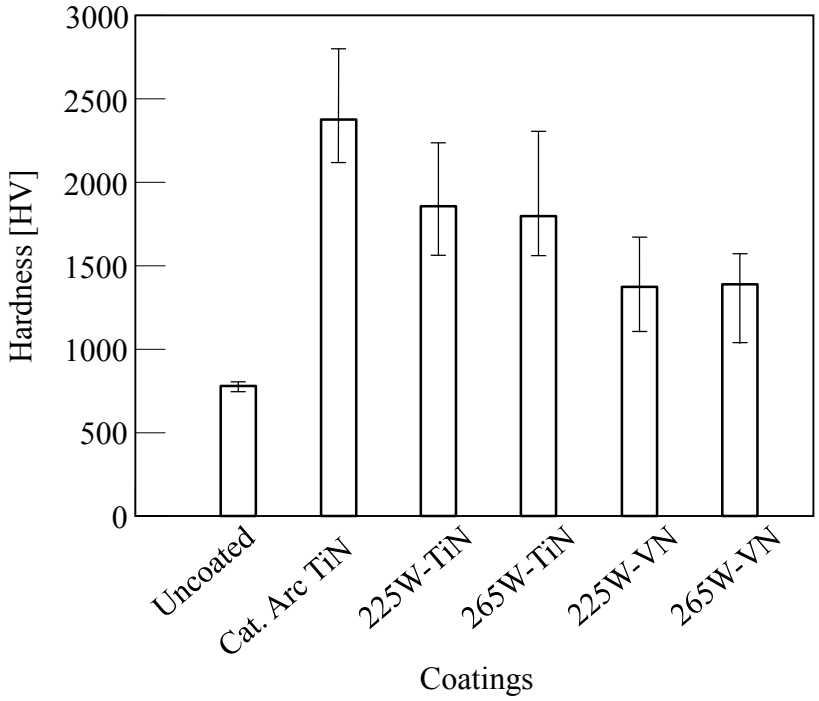

Fig. 7.5 Hardness of discs with various coatings.

7.3.2 Ring-on-disc test results

In the constant loading test, the amount of transferred aluminium on discs analyzed by SEM via EDS was used as an indicator for the coating's ability to resist aluminium transfer as shown in **Fig. 7.6**. Fig. 7.6 (b), (d) and (f) compare the wear surfaces after test using the back-scattered electron mode to exhibit the aluminium transfer more clearly. Aluminium is displayed as a darker phase.

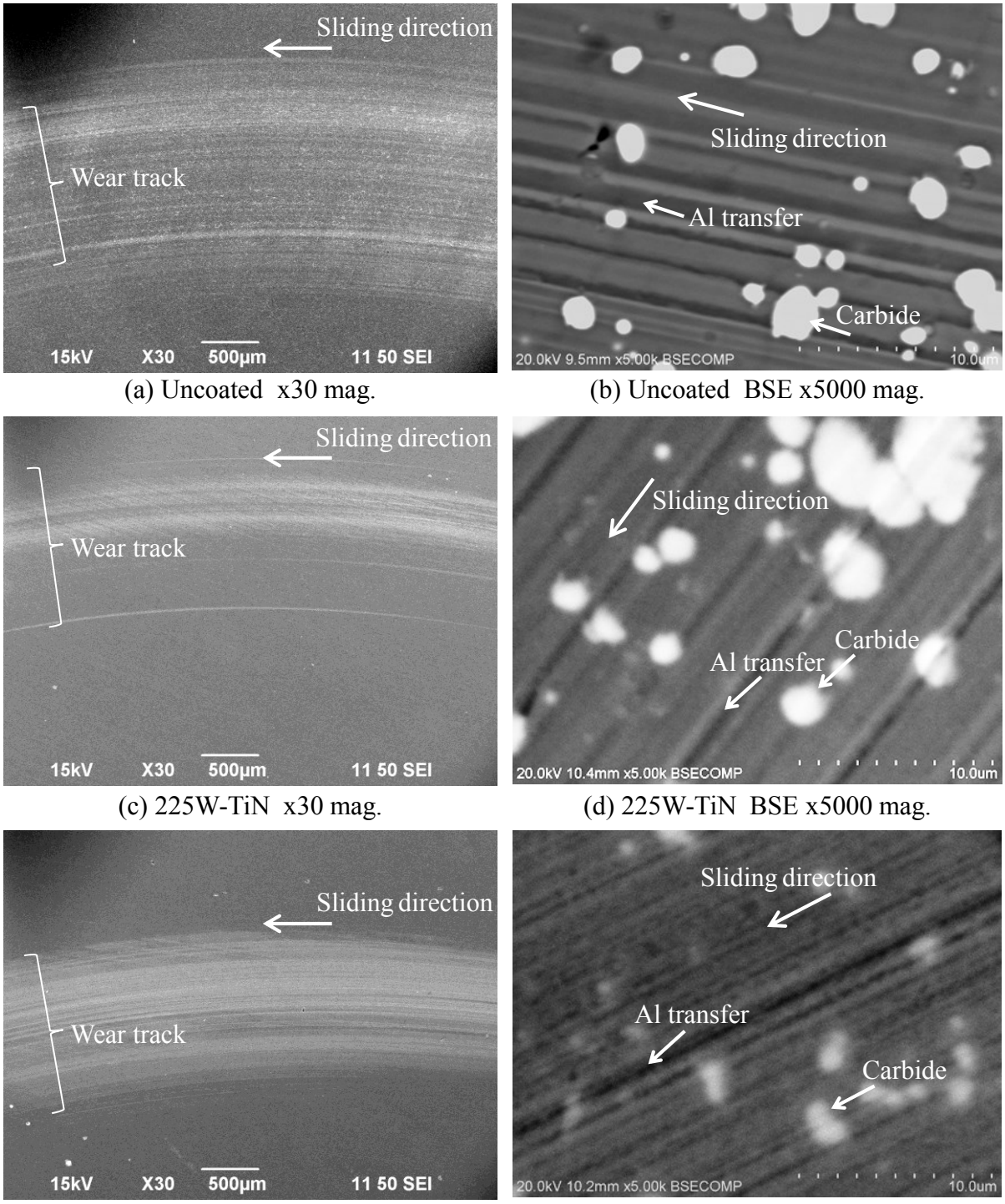

(a) Uncoated x30 mag. (b) Uncoated BSE x5000 mag.

(c) 225W-TiN x30 mag. (d) 225W-TiN BSE x5000 mag.

(e) 265W-TiN x30 mag. (f) 265W-TiN BSE x5000 mag.

Fig. 7.6 Severity of aluminium transfer in wear tracks of uncoated and coated discs in the constant loading test. Image (a), (c) and (e) were taken at x30 magnification using a secondary electron mode. Image (b), (d) and (f) were taken at x5000 magnification using a back-scattered electron mode.

Due to the difference in the thickness of the aluminium transfer layers, it was not possible to obtain a quantitative comparison from aluminium coverage areas. An "aluminium adherence index" was created to represent the average degree of transferred aluminium present along the wear track with no regards to the absolute mass or the area of coverage. A lower index value indicates a higher wear resistance. The adherence index of the discs coated with various coatings is shown in **Fig. 7.7**. The amounts of transferred aluminium on all coated disc surfaces are lower than that of the uncoated one. The 225W-TiN exhibits the lowest aluminium adherence index which indicates its minimum aluminium transferring. This in turn reflects its high aluminium adhering resistance.

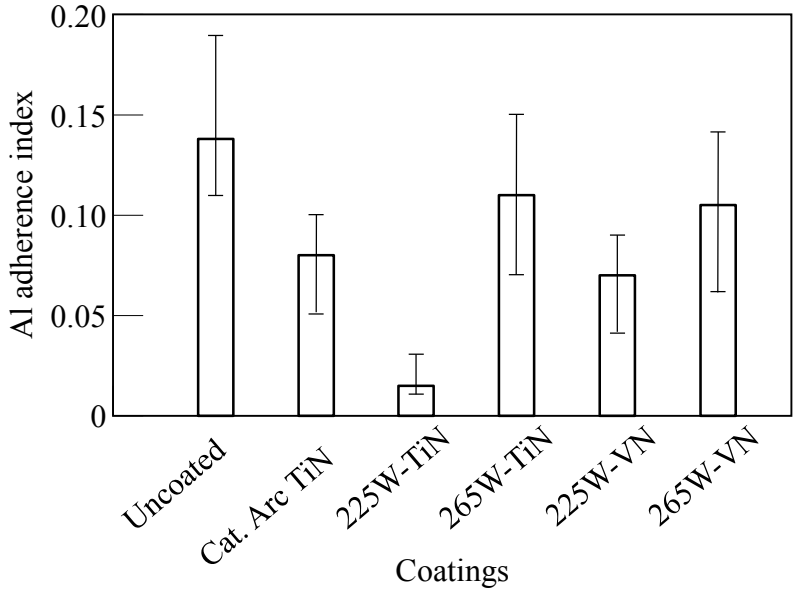

Fig. 7.7 Aluminium adherence index of discs with various coatings in constant loading test.

In the step loading test, when a certain level of applied normal load was exceeded, a transition from mild to severe wear occurs (referred to as the "transition load"). A significant surface damage on the ring and a large amount of aluminium transfer on the disc surface can be observed by the naked eye and then the observation by the optical microscope was performed to confirm. The higher transition load suggests higher adhesive wear resistance.

The transition load of the test specimen is shown in **Fig. 7.8**. The transition from mild to severe wear initiated early for an uncoated disc. On the other hand, all types of coating on the discs increased the transition load. Among three of the TiN coatings, the 225W-TiN

shows a higher transition load than other TiN coatings. This corresponds to the surface roughness result as shown in Fig. 7.4 in which the 225W-TiN exhibits the smoothest surface of the three TiN coatings. For VN coating, the smoother 265W-VN also demonstrates a higher transition load than that of the 225W-VN. Podgornik et al. [113] showed that the surface roughness has a crucial influence on the galling properties of a coating. The smoother the surface is, the higher the adhesive wear resistance becomes. Although the cathodic arc TiN exhibits the highest hardness (see Fig. 7.5), its galling resistance is not superior. It has been suggested in previous work that the hardness of the coating is not directly correlated to the galling resistance [114].

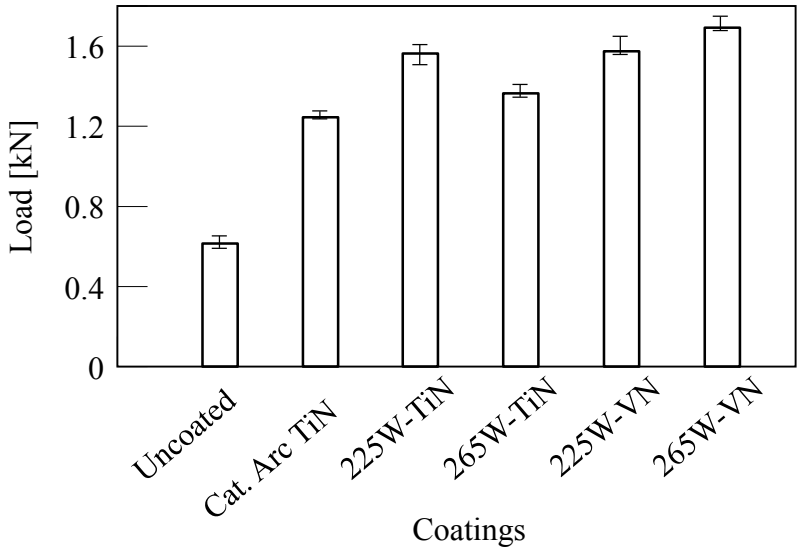

Fig. 7.8 Transition load of various coatings.

In order to clarify the dominant wear mechanisms on the uncoated and coated surfaces, the planar surfaces of the contacting couples were studied. The SEM observations on the ring and disc surfaces tested at 630 N load are shown in **Fig. 7.9**. In the case of the uncoated disc sliding against an aluminium ring, severe deformation, scratching and seizure occurred on the ring. Shallow craters can be observed scattered throughout the wear scar. This is likely to be due to a delamination of aluminium and transferred aluminium from the ring surface. The scratch and crater formation resulted in freshly exposed aluminium ring surface which contribute to the acceleration of wear. A large amount of aluminium was also transferred and adhered onto the disc surface. Whereas in the case of cathodic arc TiN- and sputtering TiN-coated discs sliding against the

aluminium rings, the ring surface was smoothened and plastically deformed following the sliding direction. Crater was not observed. The disc surface was partially covered by a thin aluminium layer.

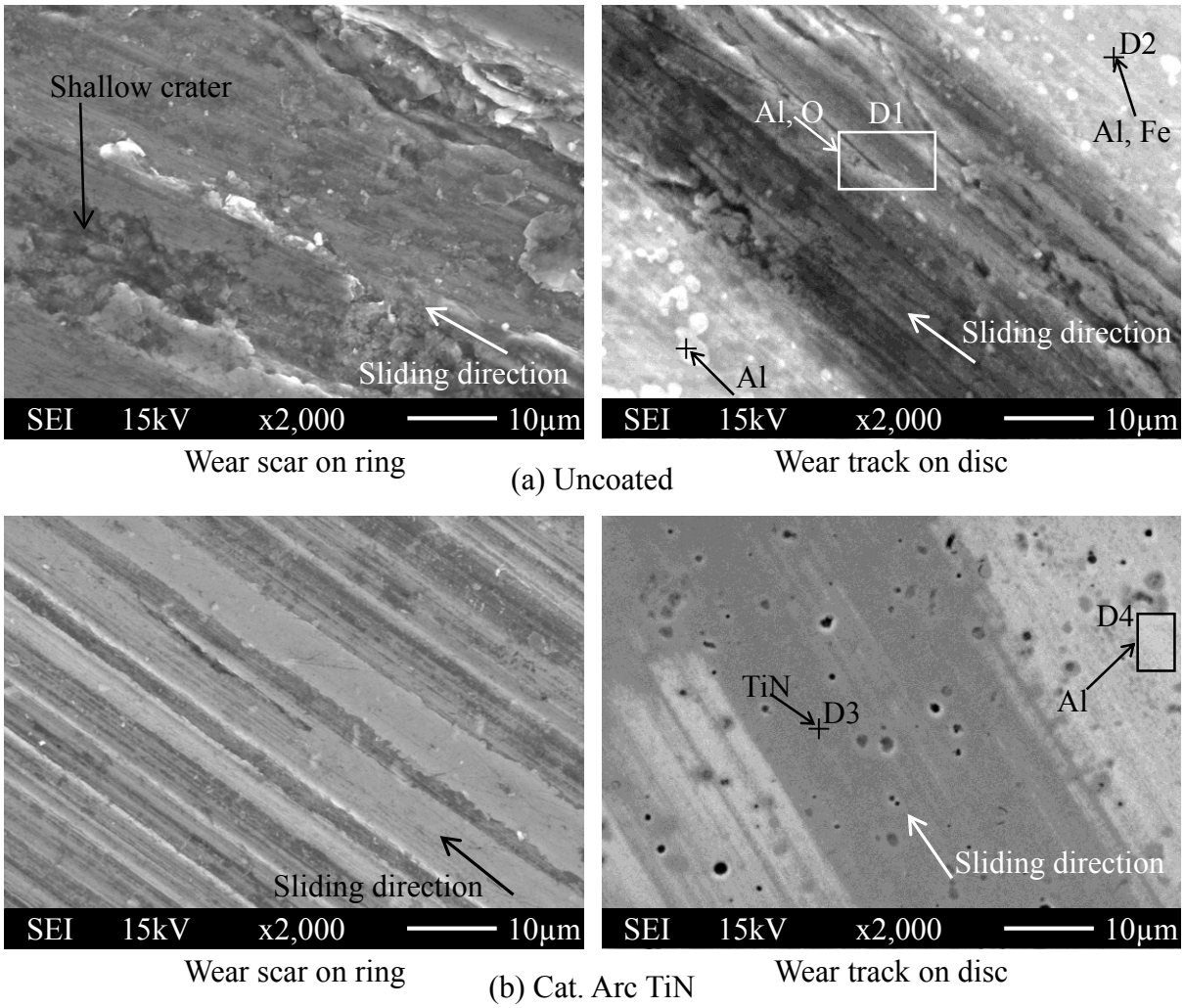

Fig. 7.9 SEM observation on the ring and disc surfaces tested at 630 N load in step loading test.

EDS spectra indicate the ring surfaces after test to consist mostly of Al with small amounts of O and C consistently across the surfaces. There is no evidence of transferring of the disc material to the ring surface. EDS spectra of the disc surfaces on the other hand exhibit appreciable amounts of Al to support the observation above, see **Fig. 7.10**.

For the uncoated disc, typical metal-to-metal adhesive wear [118] can be fittingly used to explain the material behaviour. The good compatibility of materials, in this case Al and

Fe, can induce Al to adhere onto the Fe-based disc surface easily due to the formation of metallic bonds. The adhesion commonly occurs at the protuberances of the disc due to a high contact pressure at these locations. For cathodic arc TiN- and sputtering TiN-coated discs however, the contacting surfaces were continuously covered with ionically bonded TiN. Thus the contact became a ceramic-to-metal contact. Al could not adhere onto the TiN film using the metallic bond due to the difference in the structure of the materials. Consequently, it was more difficult to form a transfer layer on the TiN disc surface.

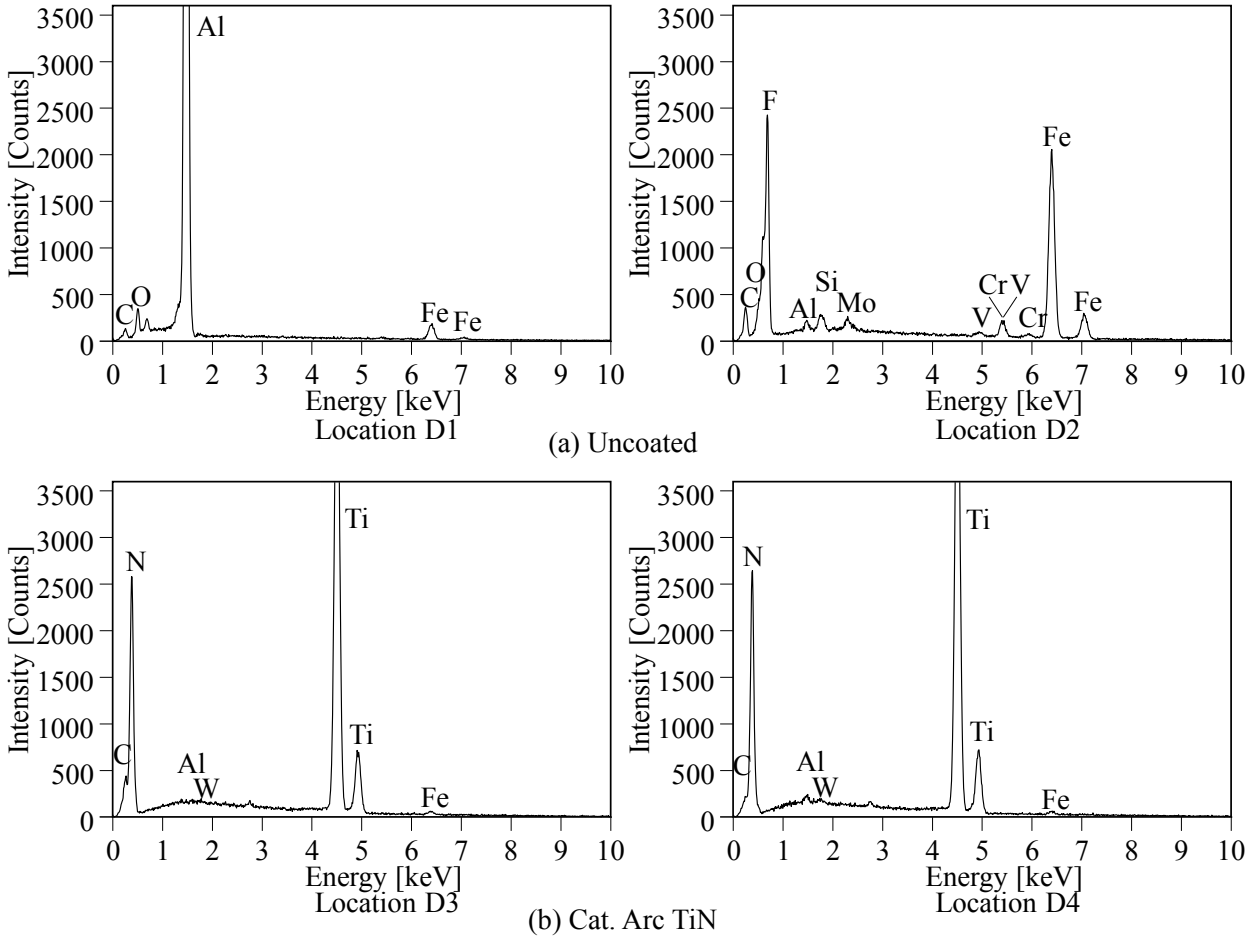

Fig. 7.10 EDS spectra of the disc surfaces tested at 630 N load in step loading test (locations as indicated in Fig. 7.9).

From the evaluation of tribological properties by the ring-on-disc test, the chemical analysis results of the wear tracks produced at a constant normal load show that aluminium did not adhere to the 225W-TiN surface as readily as to the other coated samples, as evidenced by the lowest aluminium adherence index, see Fig. 7.7. This is likely to be due

to the difference in the surface roughness of the coating. When comparing the 225W-TiN and the 265W-TiN coatings, even though the distinction in their surface roughness is not significant, the fluctuation in the roughness of the 265W-TiN is higher as shown in **Fig. 7.11**. This shows that the 265W-TiN is more likely to have regions of large protuberances. These protuberances create high contact pressure which breaks the oxide film on the aluminium ring and at the same time deform the aluminium surface to the contour of the disc. The deformed aluminium surface results in a larger contact area, particularly in the valley of the disc surface. As the ring and disc slide against one another, a tangential force acts to tear aluminium within the valley away from the bulk of the ring. Aluminium remaining on the disc surface then can act as an anchor for further aluminium-aluminium adhesion, accelerating the aluminium transferral to the disc surface. This phenomenon is referred to as junction growth [119]. Thus the aluminium adherence index increases for the 265W-TiN.

Results of the transition load for adhesion in Fig. 7.8 nevertheless reveal that all of the coatings improved the adhesive wear resistance compared with the uncoated surface. The 225W-TiN coating was selected for further evaluation in the cup ironing process.

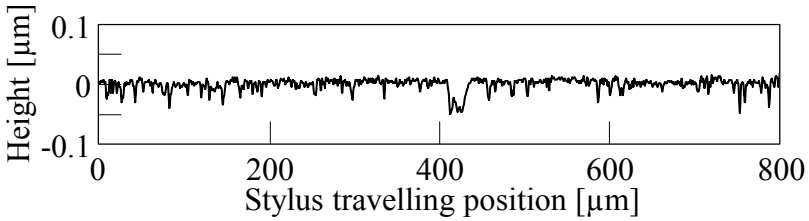

(a) 225W-TiN, Ra = 0.007µm, Rp = 0.021µm

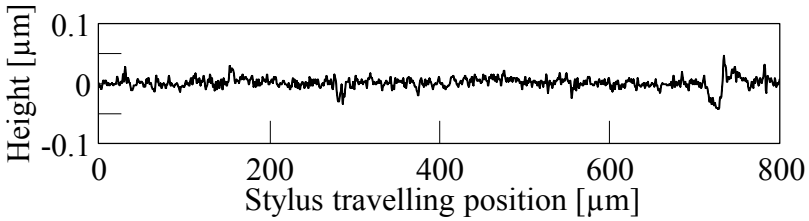

(b) 265W-TiN, Ra = 0.008µm, Rp = 0.037µm

Fig. 7.11 Surface roughness profile after coating, arithmetic mean roughness (Ra) and maximum profile peak height (Rp) of coated discs (a) 225W-TiN and (b) 265W-TiN.

7.3.3 Ironing tests

The appearances of ironed cups are shown in **Fig. 7.12**. Surface damage of deep scratch along sliding direction detected in the ironed cup was similar to that detected from the aluminium ring in ring on disc test (Fig. 7.9). For the tests carried out using the uncoated disc and uncoated die, possible delamination of aluminium on the cup surface can be seen as shallow craters in the wear scars. These craters were rarely observed in the tests using the coated discs and dies. This suggests the same wear mechanism between the ring-on-disc and the ironing tests. For the uncoated die, severe scratches on the ironed cup surface can be observed after 12 cycles. The 225W-TiN coated die, on the other hand, can successfully run for 60 cycles and still result in good appearance of the cup. Only small scratches can be observed. Cracking was not detected in all dies tested. Some aluminium transfer was evident on both coated and uncoated dies. The number of strikes cycles is denoted as *n*.

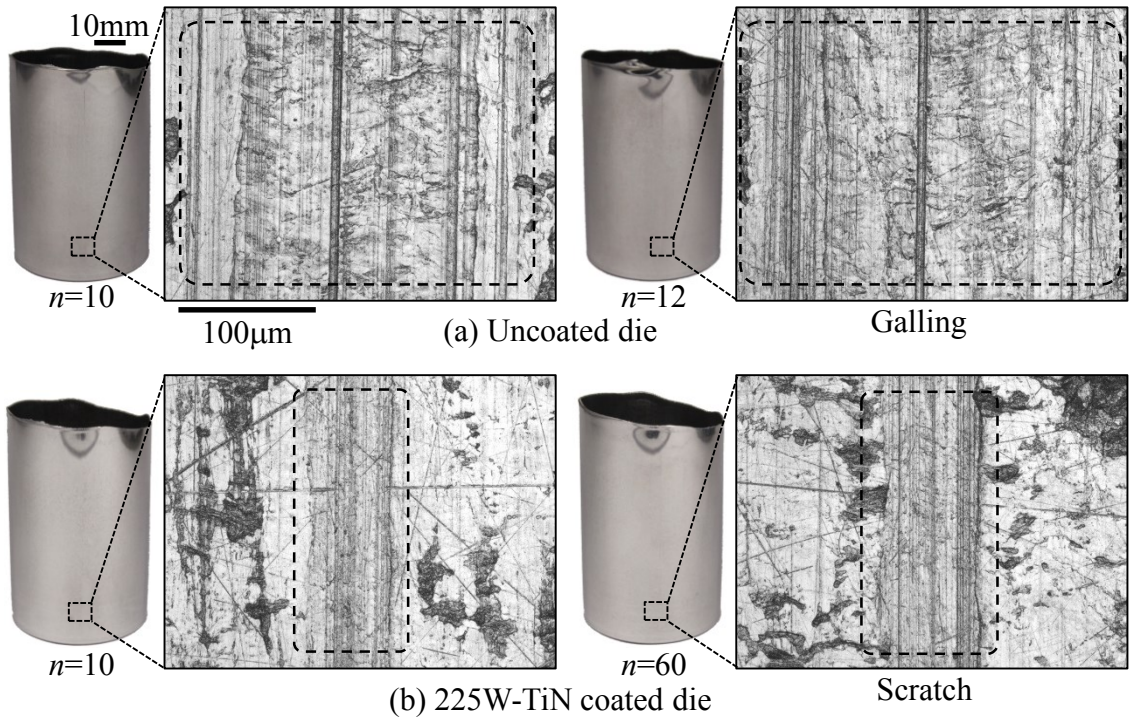

Fig. 7.12 Surface appearances of the ironed cups.

The surface roughness of the ironed cup was measured perpendicular to the ironing direction. **Fig. 7.13** shows the surface roughness of the ironed cups as a function of the

number of strikes. The cup surface was smoothened by ironing to a lower surface roughness than that of the drawn cup. Surface roughness values (R_a and R_t) of the ironed cups from both dies increase as the number of strikes increases. The arithmetic mean roughness, R_a, of the cups ironed by the uncoated die is higher than the R_a of the cups ironed by 225W-TiN-coated die. The maximum height roughness R_t of the cups produced by the uncoated die increased suddenly at n=12 due to an occurrence of galling and was higher than R_t of the initially drawn cup. R_t of the cups produced by 225W-TiN-coated die slightly increased after 40 cycles.

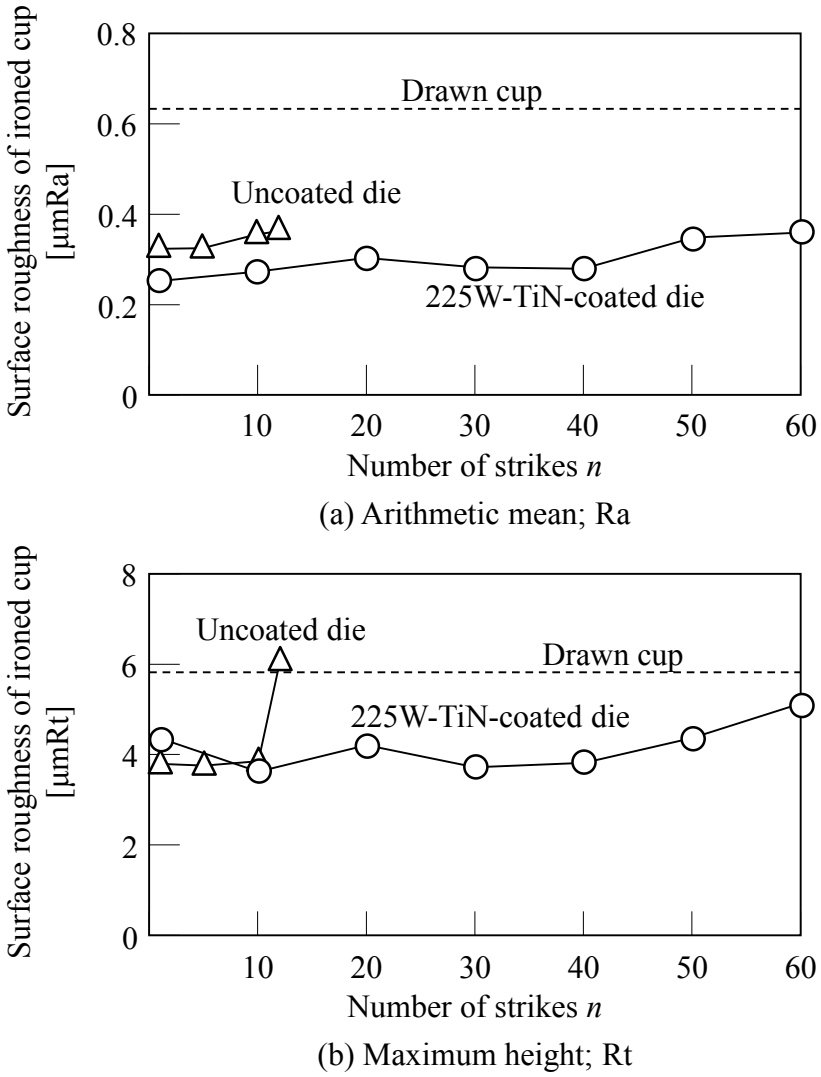

Fig. 7.13 Surface roughness of ironed cups.

The surface roughness profile of ironed cups at n=10 is shown in **Fig. 7.14**. Comparing the same number of strikes cycle, n=10, it was found that the size of scratch on the cup ironed by the uncoated die is larger than that by 225W-TiN-coated die. Therefore, ironing with 225W-TiN-coated die showed an improvement in ironed cup surface quality. The time interval between each die polishing can be extended, thus the ironing process efficiency can be increased.

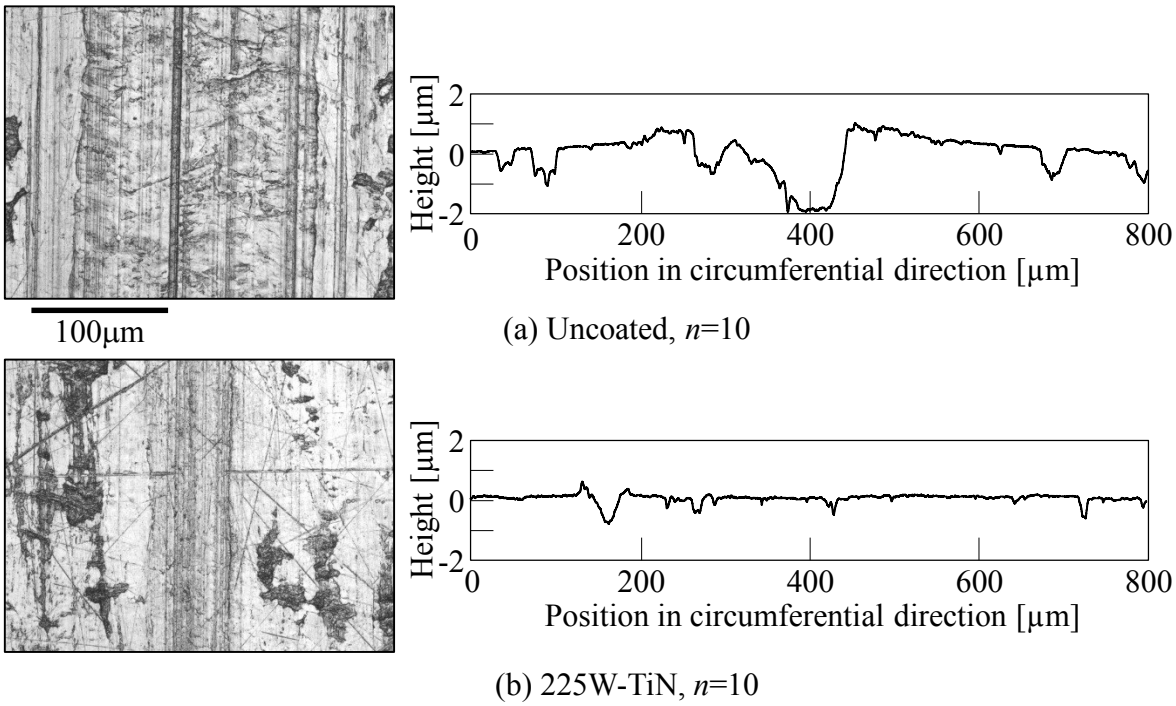

(a) Uncoated, n=10

(b) 225W-TiN, n=10

Fig. 7.14 Surface roughness profile of ironed cups.

7.4 Conclusions

The deposition parameters of VN and TiN coatings were optimised. The tribological properties of the coatings were evaluated. Ironing using the coated die was conducted and the following conclusions can be drawn from the results obtained in the present study:

1. Cathodic arc TiN coating exhibits the highest hardness and can withstand the highest critical load 1 (Lc_1) of all the coatings tested. This indicates the coating's ability to resist cracking.
2. The ring-on-disc test puts an emphasis on the material adhesion compatibility. All of the coatings tested were effective at reducing aluminium transferred to the coatings.

The result indicates that 225W-TiN coating exhibits the lowest amount of aluminium transfer.

3. The ironing test shows that the surface quality of the ironed aluminium cups were determined by scratches caused by aluminium transfer rather than cracking of the coating. 225W-TiN coating with a low degree of aluminium transfer thus performed well in the ironing test.

Chapter 8
Concluding remarks

8.1 Summary

8.1.1 Ironing of stainless steel and aluminium alloy drawn cups using TiCN-based cermet die

The TiCN-based cermet die was utilised to reduce friction in ironing of stainless steel and aluminium alloy drawn cups. Because cermets are combinations of a ceramic phase bonded with a metallic phase. They have high hardness and excellent wear resistance as well as high fracture toughness. In the TiCN-based cermet die, an additional surface coating is not required because it is made of hard TiCN having low friction. And thus peeling off as a coated die can be ignored. For comparison, TiC-coated WC-Co, non-coated WC-Co and tool steel dies were employed in ironing. For stainless steel and aluminium alloy drawn cups, the TiCN-based cermet die exhibited the largest ironing limit for single ironing due to its low friction. For repeated ironing of the ferritic stainless steel SUS430 and aluminium alloy A3003 cups using the TiCN-based cermet die, the SUS430 and A3003 cups were successfully formed up to 100 and 50 strikes, respectively, without the occurrence of seizure. The height of the cup increased as the elastic modulus of the die was large. With high Young's modulus for the TiC-coated WC-Co die and the TiCN-based cermet die, the height of the ironed cup became high due to a reduction in the extent of elastic deformation of the die.

8.1.2 Die having lubricant pockets for reduction in friction in ironing of stainless steel and aluminium alloy drawn cups

The TiCN-based cermet dies having fine lubricant pockets made by lapping of shot-peened surfaces was utilised to reduce friction in ironing of stainless steel and aluminium alloy drawn cups. Because of the surface having fine lubricant pockets consists of flat smooth portions and fine pocket portions for retaining the lubricant. Thus the ironing limit for the die having an appropriate surface shape of fine lubricant pockets became higher than that for a polished surface having very fine surface roughness. Friction was reduced

by the liquid lubricant being squeezed out from the pockets during ironing, and the ironing load became smaller. By applying a fluorescence powder-mixed lubricant and using ultraviolet rays in ironing, the areas in which the amount of the lubricant remained larger became brighter. The remaining lubricant on the sidewall of the ironed cup with the die having the lubricant pockets became greater than that with the polished die. For the die having the lubricant pockets, the large amount of the lubricant was able to be retained during the process.

8.1.3 Lubrication behaviours in ironing of stainless steel cup with die having lubricant pockets

The TiCN-based cermet die having fine lubricant pockets brought about a high ironing limit. To clarify the lubrication behaviours in ironing with this die, the measurement of the film thickness of the remaining lubricant on the sidewall of the ironed cup was employed. For the die having lubricant pockets, when the amount of the lubricant was sufficient and the ironing speed was high, the ironing load was lower than that of a die having a polished surface and greater thickness of the remaining lubricant on the sidewall of the ironed cup. In repeated ironing, the surface roughness of the ironed cup with the die having the polished surface increases with the number of strikes because of the growth of seizure. But with the die having the lubricant pockets, adhesion and peeling-off of micro-seizure have repeatedly occurred. The surface roughness of the ironed cups maintains the same level regardless of the number of strikes.

8.1.4 Improvement of lubrication in ironing of stainless steel cups by roughening of cup surface

The surface topography of the die or cup has an influence on the improvement of the lubrication. A rough surface is able to provide small pits for retaining, consequently, transporting of the trapped lubricant to the die-cup interface. The TiCN-based cermet die having fine lubricant pockets and roughening of drawn cup surface were utilised to improve lubrication for reducing friction in ironing of stainless steel drawn cups. During ironing, the lubricant was trapped with the cups sanded in the circumferential direction and the ironing limit was higher than with the cup sanded in the axial direction. The surface

roughness of the drawn cup can be increased for improving lubrication by employing deep drawing with large clearance or deep drawing and redrawing with a small die radius. Friction in ironing was lowered by roughening of cup surface because the lubrication was enhanced. The thickness of the remaining lubricant on the sidewall of the ironed cup increased as the surface roughness in the axial direction of a drawn cup increased.

8.1.5 Lubricant containing fine particles for improving seizure resistance in ironing of aluminium alloy cups

Aluminium alloys develop a thin, hard adherent film of oxide on their surface that protects the metal from corrosion. In ironing of aluminium alloy cups, because of extreme contact pressure, localized bonding is formed between the asperities of the die-cup interface. The asperity roots of the softer cup side are torn apart under the sliding motion leading to the formation of seizure. To improve seizure resistance in ironing of aluminium alloy drawn cups the lubricants containing fine particles were utilised. There was no a lubricating effect caused by Al_2O_3 or ZrO_2 particles because high density of these particles caused sedimentation of them in few minutes after ultrasonically mixing. The good dispersion and suspension of fine SiO_2 particles in the lubricant enhanced lubrication. The lubricant containing fine SiO_2 particles having the size of 0.01 μm was effective in improving seizure resistance. There was no an improvement with the larger size of 0.3 μm and 0.5 μm. For the low viscosity lubricant, fine SiO_2 particles had a little effect on increasing the ironing limit. The ironing limit was improved only with a large quantity of SiO_2. Seizure resistance was effectively improved by applying the high viscosity lubricant with fine SiO_2 particles because the particles can be trapped and embedded for preventing the direct contact between the die and cup.

8.1.6 Vanadium and titanium nitride coatings for improving seizure resistance in ironing of aluminium alloy cups

Seizure resistance could be improved by using forming tools suitably coated for the type of the working material. To improve seizure resistance, vanadium nitride (VN) and titanium nitride (TiN) coatings deposited by a direct current (DC) magnetron sputtering PVD with optimum deposition parameters were utilised in ironing of aluminium alloy cups.

The TiN coatings produced by the PVD process with different techniques; a DC magnetron sputtering deposition versus a cathodic arc deposition were compared. A cathodic arc TiN coating exhibited the highest hardness and the highest adhesion strength to the tool surface of all the coatings. This coating had high ability to resist cracking. However the coating obtained from this technique had high surface roughness. The tribological evaluation by the ring-on-disc test put an emphasis on the material adhesion compatibility. All of the coatings were effective in reducing aluminium transferred to the coatings compared to the uncoated one. A 225W-TiN coating produced by the DC magnetron sputtering deposition exhibited the lowest amount of aluminium transfer due to its low surface roughness. The smoother the surface was, the higher the adhesive wear resistance became. Although the cathodic arc TiN coating exhibited the highest hardness, its seizure resistance was not superior. The hardness of the coating was not directly correlated to seizure resistance. For the ironing test, the surface quality of the ironed aluminium cups were determined by scratches caused by aluminium transfer rather than cracking of the coating. The 225W-TiN coating with a low degree of aluminium transfer thus performed well in ironing.

8.2. Future perspectives

8.2.1 Determination of improvement of lubrication with die having fine lubricant pockets with respect to boundary lubrication

The ironing limit in the ironing of stainless steel cups was effectively improved when the cermet die having fine lubricant pockets was utilised with the lubricant containing the chlorine additive. Whereas, with the lubricant containing the sulphur additive, the ironing limit was the same as the conventional polished die. The improvement of the ironing limit not only depended on the enhancement of lubrication by the die having fine pockets but also depended on the formation of a boundary lubrication film by the chemical reaction between the work material and the additive in the lubricant. The lubrication regimes in ironing with the die having fine lubricant pockets were hydrodynamic lubrication and boundary lubrication. To gain knowledge and better understand about the improvement on seizure resistance with the die having fine lubricant pockets with respect to boundary lubrication, the experiment of the die having fine lubricant pockets for several work materials, different additives in the lubricant is interesting. The analysis of boundary

lubrication films formed by chemical reaction on the workpiece surface by the EDX can give the quantification of elements.

8.2.2 Determination of improvement mechanism of seizure resistance with lubricant containing fine particles

Nanoparticles have been widely used as additives to improve the tribology performance of some lubricants in load-bearing processes such as metal cutting, and sliding bearing. However, there have been still few applications of lubricants containing nanoparticles in ironing.

The lubricant containing fine SiO_2 particles which have lower hardness among three types of fine particles performed well for improving seizure resistance in the ironing of aluminium alloy cups, whereas seizure resistance for ZrO_2 or Al_2O_3 particles which have intermediate or highest hardness was equal to or inferior to the lubricant without fine particles, respectively. The seizure resistance performance related to the hardness of fine particles. Therefore, the application of fine particles which have lower hardness such as CuO and ZnO is possible to be able to improve the seizure resistance in ironing. However the use of CuO and ZnO as additives in ironing has not been investigated yet. In addition, the improvement of seizure resistance with the lubricant containing fine particles may depend on the types of particles and the cup material. Selecting a proper particle type for the cup material is important and needs to be examined.

The chemical analysis using a scanning electron microscope (SEM) equipped with energy dispersive X-ray spectroscopy (EDX) on the sidewall of the ironed cups with the lubricant containing fine SiO_2 particles showed the quantification of the Si element increased when the mixing quantity of fine SiO_2 particles increased. The improvement of seizure resistance may cause by the formation of a protective film preventing the direct die-to-cup contact. To confirm the improvement mechanism of seizure resistance that the protective film mainly composed of the Si element was formed on the cup surface, the EDX mapping need to be further performed.

References

[1] Romm, J., 2006. The car and fuel of the future. Energy Policy 34 (17), 2609-2614.

[2] Pistoia, G., 2014. Lithium-ion batteries: advances and applications. Elsevier, Amsterdam, the Netherlands, 84-85.

[3] Husain, I., 2011. Electric and Hybrid Vehicles: Design Fundamentals, Second Edition. CRC Press, New York.

[4] Jorgensen, K., 2008. Technologies for electric, hybrid and hydrogen vehicles: Electricity from renewable energy sources in transport. Electricity from renewable energy sources in transport, Utilities Policy 16 (2), 72-79.

[5] Mordike, B.L., Ebert, T., 2001. Magnesium properties-application-potential, Materials science and Engineering A302, 37-45.

[6] Furuya, H., Kogiso, N., Matunaga, S., Senda, K., 2000. Applications of magnesium-alloys for aerospace structure systems, Materials Science Forum 350-351, 341-348.

[7] Kleiner, M., Geiger, M., Klaus, A., 2003. Manufacturing of lightweight components by metal forming, CIRP Annals - Manufacturing Technology 52 (2), 521-542.

[8] Watari, H., Koga, N., Davey, K., Haga, T., Alonso Ragado, M.T., 2006. Warm deep drawing of wrought magnesium alloy sheets produced by semi-solid roll strip-casting process, International Journal of Machine Tools and Manufacture 46(11), 1233-1237.

[9] Mori, K., Tsuji, H., 2007. Cold deep drawing of commercial magnesium alloy sheets. CIRP Annals - Manufacturing Technology 56 (1), 285-288.

[10] Mori, K., Nishijima, S., Tan, C.J., 2009. Two-stage cold stamping of magnesium alloy cups having small corner radius. International Journal of Machine Tools and Manufacture 49 (10), 767-772.

[11] Schünemann, M., Ahmetoglu, M.A., Altan, T., 1996. Prediction of process conditions in drawing and ironing of cans. Journal of Materials Processing Technology 59 (1-2), l-9.

[12] Park, C.S., Ku, T.W., Kang, B.S., Hwang, S.M., 2004. Process design and blank modification in the multistage rectangular deep drawing of an extreme aspect ratio. Journal of Materials Processing Technology 153-154, 778-784.

[13] Kim, S.H., Kim, S.H., Huh, H., 2002. Tool design in a multi-stage drawing and ironing process of a rectangular cup with a large aspect ratio using finite element analysis. International Journal of Machine Tools and Manufacture 42 (7), 863-875.

[14] Ku, T.W., Kim, Y., Kang, B.S., 2007. Design and modification of tool to manufacture rectangular cup of Ni-MH battery for hybrid cars. Journal of Materials Processing Technology 187-188, 197-201.

[15] Zhang, X., Wierzbicki, T., 2015. Characterization of plasticity and fracture of shell casing of lithium-ion cylindrical battery. Journal of Power Sources 280, 47-56.

[16] Fukui, S., Hansson, A., 1970. Analytical study of wall ironing. CIRP Annals - Manufacturing Technology, 18 (1), 593-599.

[17] Odell, E.I., 1978. A study of wall ironing by the finite element technique. Transactions of the ASME Journal of Engineering for Industry 100 (1), 31-36.

[18] Danckert, J., 1994. The residual stress distribution in the wall of a deep-drawn and ironed cup determined experimentally and by FEM. CIRP Annals - Manufacturing Technology 43 (1), 249-252.

[19] Kampuš, Z., Kuzman, K., 1995. Analysis of the factors influencing the geometrical shape of workpieces produced by ironing. Journal of Materials Processing Technology 49 (3-4), 313-332.

[20] Baillet, L., Brunet, M., Berthier, Y., 1996. Experimental and numerical dynamic modelling of ironing process. Journal of Materials Processing Technology 60 (1-4), 677-684.

[21] Delarbre, D., Montmitonnet, P., 1999. Experimental and numerical study of the ironing of stainless steel cups. Journal of Materials Processing Technology 91 (1-3), 95-104.

[22] Danckert, J., 2001. Ironing of thin walled cans. CIRP Annals - Manufacturing Technology 50 (1), 165-168.

[23] Deneuville, P., Lecot, R., 1994. The study of friction in ironing process by physical and numerical modelling. Journal of Materials Processing Technology 45 (1-4), 625-630.

[24] Han, S.S., 1997. The influence of tool geometry on friction behavior in sheet metal forming. Journal of Materials Processing Technology 63 (1-3), 129-133.

[25] Yanran, Z., Wang, Z.R., Weimin, C., 1995. Numerical simulations for extrusion and ironing and die-optimization. Journal of Materials Processing Technology 55 (1), 48-52.

[26] Becker, P., Jeon, H.J., Chang, C.C., Bramley, A.N., 2003. A Geometric approach to modelling friction in metal forming. CIRP Annals - Manufacturing Technology 52 (1), 209-212.

[27] Kawai, N., Dohda, K., Saito, M., Hayashi, N., Wang, Z., 1992. Friction behavior in the cup ironing process of aluminum sheets. Journal of Engineering for Industry 114 (2), 175-180.

[28] Mori, K., Murao, T., Harada, Y., 2003. Multi-stage cold deep drawing of long pure titanium cups using coloured sheets for prevention of seizure. CIRP Annals - Manufacturing Technology 52 (1), 237-240.

[29] Abe, Y., Mori, K., Murao, T., Okubo, F., 2004. Improvement of roughness of inner surface in multi-stage deep drawn stainless steel cups by inner ironing. Steel Grip 2, 245-250.

[30] Schedin, E., Lehtinen, B., 1993. Galling mechanisms in lubricated systems: A study of sheet metal forming. Wear 170 (1), 119-130.

[31] Schedin, E., 1994, Galling mechanisms in sheet forming operations. Wear 179 (1-2), 123-128.

[32] Groche, P., Nitzsche, G., 2007. Influence of temperature on the initiation of adhesive wear with respect to deep drawing of aluminum-alloys. Journal of Materials Processing Technology, 191 (1-3) 314-316.

[33] Groche, P., Nitzsche, G., Elsen, A., 2008. Adhesive wear in deep drawing of aluminum sheets. CIRP Annals - Manufacturing Technology 57 (1), 295-298.

[34] Andreasen, J.L., Bay, N., Andersen, M., Christensen, E., Bjerrum, N., 1997. Screening the performance of lubricants for ironing of stainless steel with a strip reduction test. Wear 207 (1-2), 1-5.

[35] Andreasen, J.L., Bay, N., De Chiffre, L., 1998. Quantification of galling in sheet metal forming by surface topography characterisation. International Journal of Machine Tools and Manufacture 38 (5-6), 503-510.

[36] Petrushina, I.M., Christensen, E., Bergqvist, R.S., Møller, P.B., Bjerrum, N.J., Høj, J., Kann, G., Chorkendorff, I., 2000. On the chemical nature of boundary lubrication of stainless steel by chlorine- and sulfur-containing EP-additives. Wear 246 (1-2), 98-105.

[37] Kim, H., Sung, J.H., Sivakumar, R., Altan, T., 2007. Evaluation of stamping lubricants using the deep drawing test. International Journal of Machine Tools and Manufacture 47 (14), 2120-2132.

[38] Kim, H., Altan, T., Yan, Q., 2009. Evaluation of stamping lubricants in forming advanced high strength steels (AHSS) using deep drawing and ironing tests. Journal of Materials Processing Technology 209 (8), 4122-4133.

[39] Kalpakjian, S., Schmid, S.R., 2006. Manufacturing Engineering and Technology, 5th ed. Pearson Education South Asia Pte Ltd, Singapore.

[40] Tinga, T., 2013. Principles of Loads and Failure Mechanisms: Applications in Maintenance, Reliability and Design. Springer Series in Reliability Engineering, Springer-Verlag, London.

[41] Kataoka, S., Murakawa, M., Aizawa, T., Ike, H., 2004. Tribology of dry deep-drawing of various metal sheets with use of ceramics tools. Surface and Coatings Technology 177-178, 582-590.

[42] Tamaoki, K., Manabe, K., Kataoka, S., Aizawa, T., 2010. Electroconductive ceramic tooling for dry deep drawing. Journal of Materials Processing Technology 210 (1), 48-53.

[43] Tamaoki, K., Manabe, K., Kataoka, S., Aizawa, T., 2013. Continuous dry cylindrical and rectangular deep drawing by electroconductive ceramic dies. Journal of Manufacturing Science and Engineering 135 (3), 031010-1 to 031010-7.

[44] Klocke, F., Kuwer, C., 2007. Wear reduction in the sheet-metal forming of AISI 304. in Azushima, A., (Ed.) Proceedings of the 3rd International Conference on Tribology in Manufacturing Process, 207-212.

[45] Peng, Y., Miao, H., Peng, Z., 2013. Development of TiCN-based cermets: Mechanical properties and wear mechanism. International Journal of Refractory Metals and Hard Materials 39, 78-89.

[46] Jeon, E.T., Joardar, J., Kang, S., 2002. Microstructure and tribo-mechanical properties of ultrafine Ti(CN) cermets. International Journal of Refractory Metals and Hard Materials 20 (3), 207-211.

[47] Cardinal, S., Malchère, A., Garnier, V., Fantozzi, G., 2009. Microstructure and mechanical properties of TiC-TiN based cermets for tools application. International Journal of Refractory Metals and Hard Materials 27 (3), 521-527.

[48] http://www.mitsubishicarbide.net

[49] Russias, J., Cardinal, S., Aguni, Y., Fantozzi, G., Bienvenu, K., Fontaine, J., 2005. Influence of titanium nitride addition on the microstructure and mechanical properties of TiC-based cermets. International Journal of Refractory Metals and Hard Materials 23 (4-6), 358-362.

[50] Bellosi, A., Calzavarini, R., Faga, M.G., Monteverde, F., Zancolò, C., D'Errico, G.E., 2003. Characterization and application of titanium carbonitride-based cutting tools. Journal of Materials Processing Technology 143-144, 527-532.

[51] Fu, T., Yu, Q., Liu, B., Wu, Y., 2008. Development and application of cermet cutting tools material. Key Engineering Materials 375-376, 163-167.

[52] Chen, W., Li, W., Liu, N., Yang, H., 2008. Performance of Ti(C,N)-based cermets cutter and simulation technique of cutting process. Journal of Materials Processing Technology 197 (1-3), 36-42.

[53] Wilson, W.R.D., 1979. Friction and lubrication in sheet metal forming. Mechanics of sheet metal forming: Material behavior and deformation analysis. 157-177.

[54] Bay, N., Azushima, A., Groche, P., Ishibashi, I., Merklein, M., Morishita, M., Nakamura, T., Schmid, S., Yoshida, M., 2010. Environmentally benign tribo-systems for metal forming. CIRP Annals - Manufacturing Technology 59 (2), 760-780.

[55] Mizuno, T., Okamoto, M., 1982. Effects of lubricant viscosity at pressure and sliding velocity on lubricating conditions in the compression-friction test on sheet metals. Transactions of the ASME Journal of the Lubrication Technology 104 (1), 53-59.

[56] Kudo, H., Tsubouchi, M., Takada, H., Okamura, K., 1982. An investigation into plasto-hydrodynamic lubrication with a cold sheet drawing test. CIRP Annals - Manufacturing Technology 31 (1), 175-180.

[57] Azushima, A., Uda, M., Kudo, H., 1991. An interpretation of the speed dependence of the coefficient of friction under the micro-PHL condition in sheet drawing. CIRP Annals - Manufacturing Technology 40 (1), 227-230.

[58] Azushima, A., 1995. Direct observation of contact behaviour to interpret the pressure dependence of the coefficient of friction in sheet metal forming. CIRP Annals - Manufacturing Technology 44 (1), 209-212.

[59] Bech, J., Bay, N., Eriksen, M., 1998. A Study of mechanisms of liquid lubrication in metal forming. CIRP Annals - Manufacturing Technology 47 (1), 221-226.

[60] Sørensen, C.G., Bech, J.I., Andreasen, J.L., Bay, N., Engel, U., Neudecker, T., 1999. A basic study of the influence of surface topography on mechanisms of liquid lubrication in metal forming. CIRP Annals - Manufacturing Technology 48 (1), 203-208.

[61] Bech, J., Bay, N., Eriksen, M., 1999. Entrapment and escape of liquid lubricant in metal forming. Wear 232 (2), 134-139.

[62] Steinhoff, K., Rasp, W., Pawelski, O., 1996. Development of deterministic-stochastic surface structures to improve the tribological conditions of sheet forming processes. Journal of Materials Processing Technology 60 (1-4), 355-361.

[63] Hector, L.G., Shue, S., 1993. Focused energy beam work roll surface texturing science and technology. Journal of Materials Processing and Manufacturing Science 2, 63-117.

[64] Vermeulen, M., Scheers, J., 2001. Micro-hydrodynamic effects in EBT textured steel sheet. International Journal of Machine Tools and Manufacture 41 (13-14), 1941-1951.

[65] Bünten, R., Steinhoff, K., Rasp, W., Kopp, R., Pawelski, O., 1996. Development of a FEM-model for the simulation of the transfer of surface structure in cold-rolling processes. Journal of Materials Processing Technology 60 (1-4), 369-376.

[66] Geiger, M., Engel, U., Pfestorf, M., 1997. New developments for the qualification of technical surfaces in forming processes. CIRP Annals - Manufacturing Technology 46 (1), 171-174.

[67] Nilsson, MS., Olsson, DD., Petrushina, I., Andreasen, JL., Bay, N., Christensen, E. & Bjerrum, NJ. 2010. Strategic surface topographies for enhanced lubrication in sheet forming of stainless steel. International Journal of Surface Science and Engineering 4 (1), 68-79.

[68] Geiger, M., Popp, U., Engel, U., 2002. Excimer laser micro texturing of cold forging tool surfaces - influence on tool life. CIRP Annals - Manufacturing Technology 51 (1), 231-234.

[69] Popp, U., Engel, U., 2006. Microtexturing of cold-forging tools-influence on tool life. Proceed IMechE Part B Journal of the Engineering Manufacture 220, 27-33.

[70] Wagner, K., Putz, A., Engel, U., 2006. Improvement of tool life in cold forging by locally optimized surfaces. Journal of Materials Processing Technology 177 (1-3), 206-209.

[71] Wagner, K., Völkl, R., Engel, U., 2008. Tool life enhancement in cold forging by locally optimized surfaces. Journal of Materials Processing Technology 201 (1-3), 2-8.

[72] Vilhena, L.M., Sedlaček, M., Podgornik, B., Vižintin, J., Babnik, A., Možina, J.,·2009. Surface texturing by pulsed Nd:YAG laser. Tribology International 42 (10), 1496-1504.

[73] Vilhena, L.M., Podgornik, B., Vižintin, J., Možina, J.,·2011. Influence of texturing parameters and contact conditionson tribological behaviour of laser textured surfaces. Meccanica 46 (3), 567–575.

[74] Costa, H.L., Hutchings, I.M., 2009. Effects of die surface patterning on lubrication in strip drawing. Journal of Materials Processing Technology 209 (3), 1175-1180.

[75] Meng, F., Zhou, R., Davis, T., Cao, J., Wang, Q.J., Hua, D., Liu, J., 2010. Study on effect of dimples on friction of parallel surfaces under different sliding conditions. Applied Surface Science 256 (9), 2863-2875.

[76] Aramaki, M., Yamada, N., Furukimi, O., 2011. Effect of combined shot treatment and nitriding on galling property of die used for high strength steels. ISIJ International 51 (7), 1137-1141.

[77] Furukimi, O., Aramaki, M., Abe, K., Fukaura, H., Yamada, N., 2012. Improvement of die life with surface texture control and solid lubricant. HTM Journal of Heat Treatment and Materials 67 (2), 153-157.

[78] Podgornik, B., Jerina, J., 2012. Surface topography effect on galling resistance of coated and uncoated tool steel. Surface and Coatings Technology 206 (11-12), 2792-2800.

[79] Anderson, W., Jarzynski, J., Salant, R.F., 2000. Condition monitoring of mechanical seals: detection of film collapse using reflected ultrasonic waves. Proceedings of the Institution of Mechanical Engineers, Part C: Journal of Mechanical Engineering Science 214 (9), 1187-1194.

[80] Dwyer-Joyce, R.S., Drinkwater, B.W., Donohoe, C.J., 2002. The measurement of lubricant-film thickness using ultrasound. Proceedings of the Royal Society Series A: Mathematical Physical Engineering Sciences 459, 957-976.

[81] Dwyer-Joyce, R.S., Harper, P., Pritchard, J., Drinkwater, B.W., 2006. Oil film measurement in polytetrafluoroethylene-faced thrust pad bearings for hydrogenerator applications. Proceedings of the Institution of Mechanical Engineers, Part A: Journal of Power and Energy 220 (6), 619-628.

[82] Zhang, J., Drinkwater, B.W., Dwyer-Joyce, R.S., 2006. Acoustic measurement of lubricant-film thickness distribution in ball bearings. Journal of the Acoustical Society of America 119 (2), 863-871.

[83] Zhang, J., Drinkwater, B.W., Dwyer-Joyce, RS., 2007. Ultrasonic oil-film thickness measurement: an angular spectrum approach to assess performance limits. Journal of the Acoustical Society of America 121 (5), 2612-2620.

[84] Zhang, J., Drinkwater, B.W., 2008. Thin oil-film thickness distribution measurement using ultrasonic arrays. NDT & E International 41 (8), 596-601.

[85] Azushima, A., Miyamoto, J., Kudo, H., 1998. Effect of surface topography of work piece on pressure dependence of coefficient of friction in sheet metal forming. CIRP Annals - Manufacturing Technology 47 (1), 479-482.

[86] Azushima, A., 2005. In lubro 3D measurement of oil film thickness at the interface between tool and workpiece in sheet drawing using a fluorescence microscope. Tribology International 38 (2), 105-112.

[87] Azushima, A., 2006. In situ 3D measurement of lubrication behavior at interface between tool and workpiece by direct fluorescence observation technique. Wear 260 (3), 243-248.

[88] Xue, Q., Liu, W., Zhang, Z., 1997. Friction and wear properties of a surface-modified TiO_2 nanoparticle as an additive in liquid paraffin. Wear 213 (1-2), 29-32.

[89] Hernández Battez, A., González, R., Felgueroso, D., Fernández, J.E., del Rocío Fernández, M., García, M.A., Peñuelas, I., 2007. Wear prevention behaviour of nanoparticle suspension under extreme pressure conditions. Wear 263 (7-12), 1568-1574.

[90] Hernández Battez, A., González, R., Viesca, J.L., Fernández, J.E., Díaz Fernández, J.M., Machado, A., Chou, R., Riba, J., 2008. CuO, ZrO2 and ZnO nanoparticles as antiwear additive in oil lubricants. Wear 265 (3-4), 422-428.

[91] He-long YU, Yi XU, Pei-jing SHI, Bin-shi XU, Xiao-li WANG, Qian LIU, 2008. Tribological properties and lubricating mechanisms of Cu nanoparticles in lubricant. Transactions of Nonferrous Metals Society of China 18 (3), 636-641.

[92] Li, X., Cao, Z., Zhang, Z., Dang, H., 2006. Surface-modification in situ of nano-SiO_2 and its structure and tribological properties. Applied Surface Science 252 (22), 7856-7861.

[93] Jiao, D., Zheng, S., Wang, Y., Guan, R., Cao, B., 2011. The tribology properties of alumina/silica composite nanoparticles as lubricant additives. Applied Surface Science 257 (13), 5720-5725.

[94] Sarhan, A.A.D., Sayuti, M., Hamdi, M., 2012. Reduction of power and lubricant oil consumption in milling process using a new SiO_2 nanolubrication system. International Journal of Advanced Manufacturing Technology 63 (5), 505-512.

[95] Sayuti, M., Erh, O.M., Sarhan A.A.D., Hamdi, M., 2014. Investigation on the morphology of the machined surface in end milling of aerospace AL6061-T6 for novel uses of SiO2 nanolubrication system. Journal of Cleaner Production 66, 655-663.

[96] Sia, S.Y., Bassyony, E.Z., Sarhan, A.A.D., 2014. Development of SiO_2 nanolubrication system to be used in sliding bearings. International Journal of Advanced Manufacturing Technology 71 (5), 1277-1284.

[97] Wu, Y.Y., Tsui, W.C., Liu, T.C., 2007. Experimental analysis of tribological properties of lubricating oils with nanoparticle additives. Wear 262 (7-8), 819-825.

[98] Hu, Z.S., Lai, R., Lou, F., Wang, L.G., Chen, Z.L., Chen, G.X., Dong, J.X., 2002. Preparation and tribological properties of nanometer magnesium borate as lubricating oil additive. Wear 252 (5-6), 370-374.

[99] Liu, G., Li, X., Qin, B., Xing, D., Guo, Y., Fan, R., 2004. Investigation of the mending effect and mechanism of copper nano-particles on a tribologically stressed surface. Tribology Letters 17 (4), 961-966.

[100] Tao, X., Jiazheng, Z., Kang, X., 1996. The ball-bearing effect of diamond nanoparticles as an oil additive. Journal of Physics D: Applied Physics 29, 2932-2937.

[101] Lee, K., Hwang, Y., Cheong, S., Choi, Y., Kwon, L., Lee, J., Kim, S.H., 2009. Understanding the role of nanoparticles in nano-oil lubrication. Tribology Letters 35 (2), 127-131.

[102] Escher, C., Henke, T., 2002. New trends in thin coatings for sheet-metal forming tools. in: Proceedings of the Sixth International Tooling Conference on the Use of Tool Steels: Experience and Research, Karlstad, 771-784.

[103] Sato, T., Besshi, T., 1998. Anti-galling evaluation in aluminum sheet forming. Journal of Materials Processing Technology 83 (1-3), 185-191.

[104] Podgornik, B., Hogmark, S., Sandberg, O., 2006. Proper coating selection for improved galling performance of forming tool steel. Wear 261 (1), 15-21.

[105] Murakawa, M., Koga, N., Kumagai, T., 1995. Deep-drawing of aluminum sheets without lubricant by use of diamond-like carbon coated dies. Surface and Coatings Technology 76-77 (2), 553-558.

[106] Kim, H., Han, S., Yan, Q., Altan T., 2008. Evaluation of tool materials, coatings and lubricants in forming galvanized advanced high strength steels (AHSS). CIRP Annals - Manufacturing Technology 57 (1), 299-304.

[107] Sresomroeng, B., Premanond, V., Kaewtatip, P., Khantachawana, A., Koga, N., Watanabe, S., 2010. Anti-adhesion performance of various nitride and DLC films against high strength steel in metal forming operation. Diamond & Related Materials 19 (7-9), 833-836.

[108] Dohda, K., Kubota, H., Tsuchiya, Y., 2005. Application of DLC coating to ironing die. JSME International Journal. Series A, 48 (4), 286-291.

[109] Daodon, W., Premanond, V., Wongpisarn, W., Niranatlumpong, P., 2015. Vanadium nitride and titanium nitride coatings for anti-galling behavior in ironing of aluminum alloy cups. Wear 342-343, 279-287.

[110] Abe, Y., Ohmi, T., Mori, K., Masuda, T., 2014. Improvement of formability in deep drawing of ultra-high strength steel sheets by coating of die. Journal of Materials Processing Technology 214 (9), 1838-1843.

[111] Sresomroeng, B., Premanond, V., Kaewtatip, P., Khantachawana, A., Kurosawa, A.,Koga, N., 2011. Performance of CrN radical nitrided tools on deep drawing of advanced high strength steel. Surface and Coatings Technology 205 (17-18), 4198-4204.

[112] Wiklund, U., Casas, B., Stavlid, N., 2006. Evaporated vanadium nitride as a friction material in dry sliding against stainless steel. Wear 261 (1), 2-8.

[113] Podgornik, B., Hogmark, S. and Sandberg, O., 2004. Influence of surface roughness and coating type on the galling properties of coated forming tool steel. Surface and Coatings Technology 184 (2-3), 338-348.

[114] Heinrichs, J., Jacobson, S., 2010. Laboratory test simulation of aluminium cold forming - influence from PVD tool coatings on the tendency to galling. Surface and Coatings Technology 204 (21-22), 3606-3613.

[115] Basu, B., Kalin, M., 2011. Tribology of ceramics and composites: a materials science perspective. John Wiley & Sons, New Jersey, 353-361.

[116] S.H. Kim, S.W. Chung, S. Padmanaban, 2006. Investigation of lubrication effect on the backward extrusion of thin-walled rectangular aluminum case with large aspect ratio. Journal of Materials Processing Technology 180 (1-3), 185-192.

[117] Abe, Y., Fujita, T., Mori, K., Osakada, K., Shiba, T., Daodon, W., 2014. Improvement of formability in ironing of stainless steel drawn cups using low friction cermet dies. 11th International Conference on Technology of Plasticity, Procedia Engineering 81, 1896-1901.

[118] Rabinowicz, E., 1964. Friction and Wear of Materials. John Wiley & Sons, New York.

[119] Ovcharenko, A., Halperin, G., Etsion, I., 2008. In situ and real-time optical investigation of junction growth in spherical elastic–plastic contact. Wear 264 (11-12), 1043-1050.

[120] Sachs, G., Lubahn, J.D., Tracy, D.P., 1944. Drawing thin-walled tubing with a moving mandrel through a single stationary die. ASME Journal of Applied Mechanics 11, 119-210.

[121] Ragab, M.S., Orban, H.Z., 2000. Effect of ironing on the residual stresses in deep drawn cups. Journal of Materials Processing Technology 99 (1-3), 54-61.

[122] Li, Z., Mingjiang, Y., Liu, W., Zhong, M., 2006. Investigation on crater morphology by high repetitive rate YAG laser-induced discharge texturing. Surface and Coatings Technology 200 (14-15), 4493-4499.

[123] Wakuda, M., Yamauchi, Y., Kanzaki, S., Yasuda, Y., 2003. Effect of surface texturing on friction reduction between ceramic and steel materials under lubricated sliding contact. Wear 254 (3-4), 356-363.

[124] Costa, H.L., Hutchings, I.M., 2007. Hydrodynamic lubrication of textured steel surfaces under reciprocating sliding conditions. Tribology International 40 (8), 1227-1238.

[125] Basnyat, P., Luster, B., Muratore, C., Voevodin, A.A., Haasch, R., Zakeri, R., Kohli, P., Aouadi, S.M., 2008. Surface texturing for adaptive solid lubrication. Surface and Coatings Technology 203 (1-2), 73-79.

[126] Abe, Y., Mori, K., Hatashita, F., Shiba, T., Daodon, W., 2015. Improvement of seizure resistance in ironing of stainless steel cup with die having lubricant pockets. Journal of the Japan Society for Technology of Plasticity 56 (658), 972-978, in Japanese.

[127] Daodon, W., Abe, Y., Mori, K., Takahashi, N., 2016. Optimum lubrication conditions in ironing of stainless steel cup with die having lubricant pockets. Journal of the Japan Society for Technology of Plasticity 57 (660), 22-27, in Japanese.

[128] Mahdavian, S. M., He, D., 1998. Hydrodynamic lubrication of the ironing process. Lubrication Science 10 (4), 287-308.

List of publications

1. 安部洋平，森謙一郎，畑下文裕，柴孝志，**Witthaya Daodon**，“潤滑剤ポケットを有するダイを用いたステンレス鋼容器のしごき加工における耐焼付き性の向上－潤滑剤ポケットを有するサーメットダイを用いたしごき加工　第 1 報－”，塑性と加工，56-658 (2015), 972-978.
2. **Witthaya Daodon**，安部洋平，森謙一郎，高橋尚志，“潤滑剤ポケットを有するダイを用いたステンレス鋼容器のしごき加工における最適潤滑条件－潤滑剤ポケットを有するサーメットダイを用いたしごき加工　第 2 報－”，塑性と加工，57-660 (2016), 22-27.
3. **Witthaya Daodon**, Varunee Premanond, Witthawat Wongpisarn, Panadda Niranatlumpong, “Vanadium nitride and titanium nitride coatings for anti-galling behavior in ironing of aluminum alloy cups”, Wear 342-343 (2015), 279-287.
4. Chin Joo Tan, Yohei Abe, **Witthaya Daodon**, Naoyuki Takahashi, Ken-ichiro Mori, Judha Purbolaksono, “Increase in ironing limit of aluminium alloy cups with lubricants containing nanoparticles”, Journal of Materials Processing Technology 229 (2016), 804-813.

List of conferences

International conferences

1. Yohei Abe, Tomohiro Fujita, Ken-ichiro Mori, Kozo Osakada, Takashi Shiba and **Witthaya Daodon**, “Improvement of formability in ironing of stainless steel drawn cups using low friction cermet dies”. 11th International Conference on Technology of Plasticity, October 19-24, 2014, Nagoya, Japan.
2. **Witthaya Daodon**, Yohei Abe, Ken-ichiro Mori and Shingo Kato, “Improvement of seizure resistance in cold extrusion of alminium alloy billet using die having heterogeneous surface”. 7th JSTP International Seminar on Precision Forging, March 9-12, 2015, Nagoya, Japan.

Domestic conferences

1. **Witthaya Daodon**, Yohei Abe, Ken-ichiro Mori, Takashi Shiba, “Effects of ironing velocity and lubricant additive on ironing limit of stainless steel cups using heterogeneous surface die”. The 64th Japanese Joint Conference for the Technology of Plasticity, November 1-3, 2013, Osaka University Suita campus, Osaka, Japan.
2. **Witthaya Daodon**, Yohei Abe, Ken-ichiro Mori, Takashi Shiba, Naoyuki Takahashi, “Seizure growth on heterogeneous surface die in continuous ironing of stainless steel cups”. The 2014 Japanese Spring Conference for the Technology of Plasticity, June 6-8, 2014, Tsukuba, Japan.
3. **Witthaya Daodon**, Yohei Abe, Ken-ichiro Mori, Takashi Shiba, Naoyuki Takahashi, “Improvement of ironing limit of aluminium alloy cups using TiCN-based cermet die having heterogeneous surface”. The 65th Japanese Joint Conference for the Technology of Plasticity, October 11-13, 2014, Okayama, Japan.
4. **Witthaya Daodon**, Yohei Abe, Ken-ichiro Mori, Tan Chin Joo, Naoyuki Takahashi, “Improvement of seizure resistance in ironing of aluminum alloy cups using lubricant containing SiO_2 particles”. The 2015 Japanese Spring Conference for the Technology of Plasticity, May 29-31, 2015, Yokahama, Japan.

Acknowledgements

It would not have been possible to write this doctoral thesis without the help and support of the kind people around me, to only some of whom it is possible to give particular mention here.

First of all, I would like to express my deepest and sincere gratitude to my supervisor Professor Ken-Ichiro Mori, Toyohashi University of Technology for his help, support and patience throughout the course of my studies. His supports helped me tremendously in every stage of the research work. This dissertation is immeasurably better as a result of his precious comments.

I would like to express my appreciation Professor Takayuki Shibata for serving me as the committee member in my final defense. Thank you very much for valuable discussions, comments and suggestions for my thesis.

I would also like to express special gratitude to Associate Professor Dr. Yohei Abe and Associate Professor Dr. Tomoyoshi Maeno for the good advice and support, have been invaluable on both an academic and a personal level.

I would like to express my appreciations to Mr. Tomohiro Fujita, Mr. Fumihiro Hatashita, Mr. Takashi Shiba, Mr. Naoyuki Takahashi, Mr. Shingo Kato and Mr. Kai Sugiura who helped me during the experiments and discussions. I would also like to thank to Mr. Muhammad Hasnulhadi bin Mohammad Jaafar, Ms. Nur Liyana Binti Tajul Lile and other lab members from 2012 until 2016 for their kindness, friendship and support.

I would like to acknowledge the financial support of the Japanese government scholarship that provided the necessary financial support for this study. I would like to thank the Department of Mechanical Engineering, Academic Affairs and International Affairs Divisions of Toyohashi University of Technology for their support and assistance since the start of my postgraduate work in 2012.

I would like to express my sincere gratitude to Associate Professor Dr. Varunee Premanond, Dr. Panadda Niranatlumpong and Mr. Witthawat Wongpisarn for valuable assistance. And I greatly appreciate my friends whose names are not mentioned here for their support and encouragement.

I would like to describe my deepest love and sincere gratitude to my lovely mother, father, and sister who are always there for me when I need them and thank for their unequivocal support.

For any errors or inadequacies that may remain in this work, of course, the responsibility is entirely my own.

Witthaya Daodon

Toyohashi

January, 2016